

**MECHANICAL AND DURABILITY PROPERTIES OF
HIGH PERFORMANCE 100 MPA RICE HUSK ASH
CONCRETE**

SYAMSUL BAHRI

**FACULTY OF ENGINEERING
UNIVERSITY OF MALAYA
KUALA LUMPUR**

2017

**MECHANICAL AND DURABILITY PROPERTIES OF
HIGH PERFORMANCE 100 MPA
RICE HUSK ASH CONCRETE**

SYAMSUL BAHRI

**THESIS SUBMITTED IN FULFILMENT OF THE
REQUIREMENTS FOR THE DEGREE OF
DOCTOR PHYLOSOPHY**

**FACULTY OF ENGINEERING
UNIVERSITY OF MALAYA
KUALA LUMPUR**

2017

UNIVERSITY OF MALAYA
ORIGINAL LITERARY WORK DECLARATION

Name of Candidate: Syamsul Bahri

Passport No:

Matric No: KHA 070074

Name of Degree: Doctor of Philosophy

Title of Project Paper/Research Report/Dissertation/Thesis:

Mechanical and durability properties of high performance 100 MPa rice husk ash concrete

Field of Study:

Civil Engineering, Concrete Technology

I do solemnly and sincerely declare that:

- (1) I am the sole author/writer of this Work;
- (2) This Work is original;
- (3) Any use of any work in which copyright exists was done by way of fair dealing and for permitted purposes and any excerpt or extract from, or reference to or reproduction of any copyright work has been disclosed expressly and sufficiently and the title of the Work and its authorship have been acknowledged in this Work;
- (4) I do not have any actual knowledge nor do I ought reasonably to know that the making of this work constitutes an infringement of any copyright work;
- (5) I hereby assign all and every rights in the copyright to this Work to the University of Malaya ("UM"), who henceforth shall be owner of the copyright in this Work and that any reproduction or use in any form or by any means whatsoever is prohibited without the written consent of UM having been first had and obtained;
- (6) I am fully aware that if in the course of making this Work I have infringed any copyright whether intentionally or otherwise, I may be subject to legal action or any other action as may be determined by UM.

Candidate's Signature

Date:

Subscribed and solemnly declared before,

Witness's Signature

Date:

Name:

Designation:

ABSTRACT

This thesis deals with the development of high performance concrete (HPC) of 100 MPa incorporating rice husk ash (RHA) as a supplementary cementing material (SCM). Some constraints to produce HPC of 100 MPa incorporating RHA are related to appropriate average particle size of RHA to be used, percentage replacement of cement with RHA at low water to binder ratio (w/b) concrete, mixing method and to design such HPC. Most information available on the strength of RHA concrete is up to compressive strength of 80 MPa only.

In this study, three average particle sizes of RHA of 13.5, 20.43 and 29.92 μm were used in mortar mixes to find a suitable particle size to produce the highest compressive strength. In producing HPC, the homogeneity of mixing affects the mechanical properties of concrete. Conventional and two steps mixing method were examined in order to find which appropriate mixing method is more suitable. For 100 MPa HPC, the average particle size of RHA and suitable mixing method are 13.5 μm and the two step mixing method, respectively. This particle size and mixing method significantly improved the compressive strength of RHA concrete. Furthermore, the models based on five key factors, which are ratio of water to cement, binder content, percentages replacement of cement with RHA, ratio of fine aggregate to total aggregate and dosage of superplasticizer, were developed to design HPC containing RHA. The models were able to predict the value of slump as well as compressive strength at 1 day and 28 days. The optimum mix proportion of HPC of 100 MPa containing RHA was used for further study and compared with silica fume and OPC concretes. The fresh HPC was tested for slump, unit weight and air content. The hardened HPC was tested for compressive, tensile, flexural strengths, modulus of elasticity and ultrasonic pulse velocity. The effect of water curing and air drying on

compressive strength of the HPC were also studied. In durability tests, samples were tested for water absorption, total porosity, sorptivity, initial surface absorption and magnesium sulphate attack on compressive strength of HPC. The time dependent deformation tests such as drying shrinkage and restrained shrinkage at early age were also conducted.

Test results revealed that the mechanical and durability properties of HPC incorporating RHA were better than that of control concrete. The compressive strength and ultrasonic pulse velocity increased, whereas the water absorption and total porosity decreased with w/b of 0.25 and the percentages of cement replacement with RHA up to 20%. HPC incorporating RHA is less sensitive to curing as insignificant differences in compressive strength were observed. The RHA and silica fume were able to function as a filler and pozzolanic material so that the porosity and water absorption of these concrete decreased due to the concrete being less porous and denser. In general, these concretes indicated good durability. The HPC containing 10% RHA showed better compressive strength than HPC containing 10% silica fume or OPC. Another advantage of utilizing 10% RHA instead of 10% silica fume in HPC is its ability to delay the propagation of cracks under restrained shrinkage at early ages.

RHA, therefore, has the potential for contributing to the sustainable development and economic prosperity of the construction and agricultural industries of Malaysia as well as other rice growing countries of the world.

ABSTRAK

Tesis ini membentangkan pembangunan konkrit berprestasi tinggi (HPC) berkekuatan mampatan 100 MPa dengan abu sekam padi sebagai supplementary cementitious material (SCM). Terdapat banyak rintangan dihadapi dalam proses pembangunan HPC yang mempunyai kekuatan mampatan 100 MPa. Antara rintangan adalah mencari saiz partikel RHA yang sesuai, peratusan optimum penggantian RHA dengan simen apabila nisbah air-pengikat rendah, cara pencampuran konkrit dan kaedah merekabentuk HPC. Kebanyakan literature mengenai konkrit RHA adalah campuran setakat kekuatan mampatan 80 MPa

Pada peringkat awal kajian, 3 purata saiz partikel RHA 13.5, 20.43 dan 29.92 μm digunakan dalam pencampuran mortar. Saiz partikel optimum ditentukan dengan berpandukan kekuatan mampatan mortar. Kehomogenan adalah penting dalam penghasilan HPC kerana ia boleh menjejaskan sifat mekanikal konkrit. Kesesuaian antara cara pencampuran konvensional dan cara pencampuran dua peringkat dalam proses penghasilan campuran yang seragam telah dijalankan. Untuk HPC 100 MPa, purata saiz partikel RHA yang optimum adalah 13.5 μm dan pencampuran dua peringkat didapati paling berkesan untuk mencapai kehomogenan. Saiz partikel tersebut dan cara pencampuran dua peringkat didapati meningkatkan kekuatan mampatan konkrit. Tambahan pula, sebuah model berdasarkan 5 faktor iaitu nisbah air-simen, kandungan bahan pengikat, peratusan penggantian simen dengan RHA dan dos superplasticizer telah dihasilkan untuk merekabentuk HPC yang mengandungi RHA. Model tersebut dapat meramalkan turun konkrit dan kekuatan mampatan pada 1 dan 28 hari. Seterusnya campuran optimum HPC 100 MPa mengandungi RHA dibandingkan dengan konkrit mengandungi wasap silika dan konkrit biasa. Ujian yang dijalankan untuk konkrit segar adalah ujian turun, ketumpatan dan kandungan udara. Ujian untuk

konkrit terkeras adalah ujian kekuatan mampatan, ujian kekuatan ketegangan, ujian modulus keanjalan dan ujian kelajuan denyutan ultrasonik. Kesan pengawetan konkrit dalam air dan udara terhadap kekuatan mampatan turut dikaji. Dalam ujian ketahanan lesakan, spesimen konkrit telah diuji penyerapan air dan ujian serangan magnesium sulfat. Dua ujian berlandaskan masa adalah ujian pengerutan kering dan pengecutan terhalang. Kedua-dua ujian ini dijalankan ketika konkrit berumur muda.

Keputusan-keputusan ujian menunjukkan sifat mekanikal dan ketahanan lasakan HPC mengandungi RHA adalah lebih baik daripada konkrit kawalan. Kekuatan mampatan dan kelajuan denyutan ultrasonik meningkat, manakala sifat penyerapan air dan kandungan keliangan berkurangan apabila nisbah air dengan pengikat adalah 0.25 dan simen diganti dengan 20% RHA. Konkrit yang mengandungi RHA adalah kurang sensitif terhadap cara pengawetan dan ini dapat ditunjukkan antara hubungan kekuatan mampatan dengan cara pengawetan. RHA dan wasap silika dapat berfungsi sebagai pengisi dan bahan pozolanik. Kandungan udara dan penyerapan air konkrit ini berkurangan menunjukkan konkrit adalah tahan lasak. HPC mengandungi 10% RHA menunjukkan kekuatan mampatan yang lebih tinggi berbanding dengan konkrit yang mengandungi 10% wasap silika dan konkrit biasa. Selain itu kelebihan menggunakan RHA dalam konkrit berbanding dengan wasap silika berkebolehan untuk melewatkan propogasi retakan dalam ujian pengecutan terhalang.

RHA mempunyai potensi untuk menyumbang dalam pembangunan mampan dan membawa pendapatan kepada industri pembinaan dan sektor pertanian di Malaysia serta negara-negara pengeluar beras di seluruh dunia.

ACKNOWLEDGEMENTS

All praise is due to the Almighty Allah (SWT) and to the Great Prophet Muhammad S.A.W. the best model character for mankind, for the kindest blessings to make this piece of work done.

The author would like to take this opportunity to express his deepest appreciation and gratitude to his supervisors Prof. Dr. Hilmi Bin Mahmud, for his support, inspiration and valuable suggestions throughout this research. The author received valuable advice, encouragement and critical comments whenever necessary throughout the course of this research.

Most sincere appreciation goes to University of Malaya (UM), Kuala Lumpur, Malaysia for supporting financially through PPP (PS113/2008B) and UMRG (RP018/2012C) grants and excellent working environment for this research and Lhokseumawe State of Polytechnic (LSP), Lhokseumawe, Indonesia for allowing a leave of study for the research period.

Sincere gratitude and indebtedness are conveyed to Khamistan, ST, MT and Ir. Nahar, MT, Head Department of Civil Engineering and Director of LSP, for their inspiration in initiating the PhD research. The author is very grateful to his companions and best friends, **Moatasem, Omar, Ghazan, Arul, Abdus Salam, Rusel, Akhtar and Dr. Johnson**, and all friends. They have been always ready to help and provide advice; each one has a unique contribution in this thesis.

The author also would like to thank all members in the Department of Civil Engineering, University of Malaya; the author wishes them all to accomplish their goals successfully. Thanks go to the author's dearest parents, brothers and sisters and all those who cooperated and expressed best wishes for him; appropriate words could not be found to express sincere appreciation to his wife, daughter and sons for their

understanding, friendliness, absolute love, endless patience and encouragement in all difficulties in research and living.

Finally, the author is grateful to Bernas Sdn. Bhd., Sekinchan, Kuala Selangor, Malaysia for help in providing the raw rice husk. Sincere appreciation also goes to BSAF Sdn. Bhd., Malaysia for supplying chemical admixtures used in the research.

University of Malaya

TABLE OF CONTENTS

Abstract	iii
Abstrak	v
Acknowledgements	vii
Table of Contents	ix
List of Figures	xv
List of Tables	xxi
List of Symbols and Abbreviations	xxiv
CHAPTER 1: INTRODUCTION	1
1.1 RESEARCH BACKGROUND	1
1.2 PROBLEM STATEMENT	4
1.3 OBJECTIVES OF THE STUDY	5
1.4 RESEARCH SIGNIFICANCE AND NOVELTY	6
1.5 ORGANIZATION OF THE THESIS	7
CHAPTER 2: LITERATURE REVIEW	9
2.1 INTRODUCTION	9
2.1.1 Characteristics of HPC	9

2.1.2	Definition of high performance concrete.....	12
2.1.3	Curing of HPC	13
2.1.4	Advantages of HPC	15
2.1.5	The mixture proportion for HPC	15
2.2	POZZOLANIC MATERIALS USED IN HPC.....	18
2.2.1	Rice husk ash as a supplementary cementitious material.....	20
2.2.2	Characteristic of RHA	21
2.3	EFFECT OF RHA ON FRESH CONCRETE	26
2.3.1	Workability	27
2.3.2	Setting time.....	29
2.3.3	Effect of superplasticizer types.....	30
2.4	EFFECT OF RHA ON HARDENED CONCRETE	31
2.4.1	Compressive strength.....	31
2.4.2	Modulus of elasticity, flexure strength, and tensile strength	39
2.5	TIME DEPENDENT DEFORMATION	41
2.5.1	Effect of RHA on drying shrinkage.....	41
2.5.2	Restrained shrinkage.....	41
2.6	DURABILITY PROPERTIES OF RHA CONCRETE	44
2.6.1	Permeability.....	45
2.6.2	Chemical resistance	50
2.7	MIXING TECHNIQUE	53
2.8	MICROSTRUCTURE	55
	CHAPTER 3: MATERIALS AND EXPERIMENTAL PROGRAMS	57

3.1 INTRODUCTION	57
3.1.1 Cement.....	57
3.1.2 Rice husk ash (RHA).....	57
3.1.3 Superplasticizer.....	61
3.1.4 Water.....	61
3.1.5 Aggregates	62
3.2 MIXTURE PROPORTIONS.....	63
3.2.1 Optimizing composition of aggregates.....	63
3.2.2 Packing density	64
3.2.3 Surface area	66
3.2.4 Saturation dosage of superplasticizer	67
3.2.5 Mix design of mortar	68
3.2.6 Mix design of concrete	68
3.2.7 Box-Behnken design (BBD).....	69
3.2.8 Response surface methodology (RSM)	72
3.2.9 D-optimal designs	73
3.3 SAMPLE PREPARATION	74
3.3.1 Manufacturing of concrete.....	74
3.3.2 Size and curing of specimens	76
3.4 TESTING OF CONCRETE	77
3.4.1 Test for material properties.....	77
3.4.2 Test for fresh concrete	79
3.4.3 Test for mechanical properties of concrete.....	81
3.4.4 Drying shrinkage test.....	87
3.4.5 Durability tests.....	88
3.4.6 Restrained shrinkage test	91
CHAPTER 4: RESULTS AND DISCUSSION	95
4.1 INTRODUCTION	95

4.2	PROPERTIES OF CONSTITUENT MATERIALS.....	95
4.2.1	Chemical properties of OPC, RHA and SF	96
4.2.2	Physical properties of OPC, RHA and SF	98
4.2.3	Physical properties of aggregates	102
4.2.4	Quality of water	107
4.2.5	Dosages of high range water reducer (HRWR).....	107
4.3	MORTAR.....	109
4.3.1	Mix design of mortar	109
4.3.2	Effect of the percentage and fineness of RHA on workability of fresh mortar... ..	110
4.3.3	Effect of fineness and percentage of RHA on compressive strength of mortar	110
4.4	DETERMINE THE APPROPRIATE MIXING PROCEDURES BEING ADOPTED	112
4.4.1	Mix Proportion of concrete.....	113
4.4.2	Mixing procedures	113
4.5	OPTIMIZING THE COMPOSITION OF MIXTURE THROUGH A RESPONSE SURFACE METHOD.....	116
4.5.1	Statistical Analysis.....	122
4.5.2	Influence of w/b, binder, fa/ta, % RHA and Sp dosage on slump value of HPC ..	131
4.5.3	Influence of w/b, binder, fa/ta, RHA and % of Sp dosage on compressive strength of HPC at 1 day.....	132
4.5.4	Influence of w/b, binder, fa/ta, RHA and Sp dosage on compressive strength of HPC at 28 days	133
4.5.5	Optimization using the desirability function to get the mix proportion of HPC containing RHA	134
4.6	PROPERTIES OF HPC INCORPORATING RHA AND SF.....	136
4.6.1	Workability and density.....	137
4.6.2	Compressive strength of HPC	141
4.6.3	Flexural strength	157

4.6.4 Splitting tensile strength	163
4.6.5 Static modulus of elasticity.....	175
4.6.6 Ultrasonic pulse velocity (UPV).....	179
4.7 DURABILITY OF HPC.....	184
4.7.1 Porosity.....	184
4.7.2 Initial surface absorption (ISA)	187
4.7.3 Sorptivity	190
4.7.4 Sulphate attack.....	192
4.8 TIME DEPENDENT DEFORMATION	195
4.8.1 Shrinkage	195
4.8.2 Restrained shrinkage.....	201
4.9 COST ANALYSIS	213
CHAPTER 5: CONCLUSIONS AND RECOMMENDATIONS.....	215
5.1 CONCLUSIONS.....	215
5.1.1 Properties of RHA, aggregate blends and mixing method	215
5.1.2 Statistical models.....	215
5.1.3 The mechanical properties of HPC.....	215
5.1.4 The durability of RHA concrete	216
5.1.5 Time dependent properties	216
5.2 RECOMMENDATIONS FOR FUTURE STUDIES	217
References	219
List of Publications and Papers Presented	239
Appendix A: Response surface and contour plots of slump of HPC.....	240

Appendix B: Response surface and contour plots of compressive strength at 1 day of HPC	244
Appendix C: Response surface and contour plots of compressive strength at 28 day of HPC	248

University of Malaya

LIST OF FIGURES

Figure 2.1: Method for HPC mixture proportioning.....	16
Figure 2.2: XRD analysis of RHA at different calcination temperatures	22
Figure 2.3: Color changes of RHA at different calcination temperatures (the color change of all the RHA samples is black with some grey or white particles).....	23
Figure 2.4: Grading of the rice husk ash by laser	24
Figure 2.5: Variations of the median particle size (D50) and BET specific surface area due to grinding. (The X-axis equal to 0.1 refers to the AR-RHA –sample without grinding).....	25
Figure 2.6: Relationship between pozzolanic activity and Blaine specific surface area of ground RHAs	25
Figure 2.7: Effect of RHA replacement level on rheological parameters of plastic viscosity and yield stress.....	28
Figure 2.8: Effects of particle size of RHA on workability of concrete at different RHA contents	29
Figure 2.9: Initial and final setting times of RHA with different replacement percentages	30
Figure 2.10: Compressive strengths of wet-mixed specimens steamed at.....	34
Figure 2.11: Compressive strengths of wet-mixed specimens steamed at.....	35
Figure 2.12: Effect of fineness of RHA on the compressive strength for various mixes (a) Passing #325 and (b) passing #200.....	36
Figure 2.13: Effect of RHA on pore size distribution	46
Figure 2.14: Effect of RHA on total chloride content distribution.....	51
Figure 2.15: Rapid chloride penetrability at 28 days for various concrete mixes... 	52
Figure 2.16: Microstructure of RHA concrete	56
Figure 3.17: (a) Rice husk (b) ferrocement incinerator (c) rice husk after combustion..	58
Figure 3.18: The LA machine for grinding RHA	59
Figure 3.19: XRD of RHA	60

Figure 3.20: Particle size distribution of SCM	60
Figure 3.21: Particle distribution of fine aggregates	62
Figure 3.22: Particle distribution of coarse aggregate	63
Figure 3.23: Flow cone cross section	67
Figure 3.24: Response surface plots	72
Figure 3.25: Contour plot	72
Figure 3.26: Example of responses from suggested mix proportion from model ...	73
Figure 3.27 (a) Conventional mixing method sequences (b) Two steps mixing method sequences	75
Figure 3.28: (a) Slump test (b) Slump flow test	80
Figure 3.29: Air content of fresh concrete test	81
Figure 3.30: Compressive strength	82
Figure 3.31: Modulus of elasticity	83
Figure 3.32: Splitting tensile strength	84
Figure 3.33: Flexural tensile strength	85
Figure 3.34: Ultrasonic pulse velocity test (UPV)	86
Figure 3.35: Measurement of shrinkage test	87
Figure 3.36: ISA test	89
Figure 3.37: Sorptivity test set up	90
Figure 3.38: Schematics of magnesium sulphate cycling	91
Figure 3.39: Schematic diagram of restrained shrinkage test rig (all dimension in mm)	92
Figure 3.40: Restrained shrinkage test rig	93
Figure 3.41: Illustration of the strain in the restrained and free shrinkage test specimens	94
Figure 4.42: The burning temperature and duration for rice husk	97

Figure 4.43: The X-ray spectrum of RHA	98
Figure 4.44: Cycles of grinding RHA vs the density of RHA	100
Figure 4.45: Cycle of grinding RHA vs the Blaine fineness of RHA.....	100
Figure 4.46: Relationship between density and fineness of RHA	101
Figure 4.47: Particle size distributions of binder used in this research.....	102
Figure 4.48: Sieve analysis for the material used in this research	104
Figure 4.49: Comparing between theoretical packing density of Toufar and experimental.....	105
Figure 4.50: Packing density of combination fine aggregate and coarse aggregate	106
Figure 4.51: Total surface area of combination different fine aggregate and coarse aggregate	106
Figure 4.52: The effect of particle size of RHA and percentage replacement of RHA on superplasticizer dosage in paste incorporating different fineness of RHA	108
Figure 4.53: Compressive strength of mortar containing 10% replacement of RHA with variation of fineness of RHA	111
Figure 4.54: Compressive strength of mortar containing 15% replacement of RHA with variations of fineness of RHA.....	111
Figure 4.55: Compressive strength of mortar containing 20% replacement of RHA with variations of fineness of RHA.....	112
Figure 4.56: The effect of mixing method on compressive strength	115
Figure 4.57: The effect of mixing methods on tensile strength	116
Figure 4.58: Normal plots of residuals of responses.....	124
Figure 4.59: Plot of the experimental and predicted response of slump, compressive strength at 1 day and 28 days	131
Figure 4.60: Perturbation of slump on w/b of 0.25, Binder of 550 kg/m ³ , 10% of RHA, fa/ta of 0.4 and Sp dosage of 0.9%.....	132
Figure 4.61: Perturbation of compressive strength of concrete at 1 day on w/b of 0.25, Binder of 550 kg/m ³ , 10% of RHA, fa/ta of 0.4 and Sp dosage of 0.9%.....	133

Figure 4.62: Perturbation of compressive strength of RHA concrete at 28 days on w/b of 0.25, Binder of 550 kg/m ³ , 10% of RHA, fa/ta of 0.4 and Sp dosage of 0.9%.....	134
Figure 4.63: Desirability ramp for optimization	136
Figure 4.64: Comparing superplasticizer dosage of RHA and SF concrete to that of OPC concrete	140
Figure 4.65: Comparing fresh properties of RHA and SF concrete to that of OPC concrete	141
Figure 4.66: Compressive strength development of concrete for w/b of 0.22 subjected to water curing and air drying condition	143
Figure 4.67: Compressive strength development of concrete for w/b of 0.25 subjected to water curing and air drying condition	143
Figure 4.68: The predicted compressive strength using equation 1 base on compressive strength of HPC concrete at 28 days	151
Figure 4.69: The predicted compressive strength using equation 2 base on compressive strength of HPC concrete at 28 days	152
Figure 4.70: The compressive strength relation between OPC concrete and blended concrete subjected water curing	153
Figure 4.71: The compressive strength relation between OPC concrete and blended concrete subjected air curing.....	153
Figure 4.72: The compressive strength relation between 3rd day and 28th day concrete subjected water curing.....	155
Figure 4.73: The compressive strength relation between 7th day and 28th day concrete subjected air curing	155
Figure 4.74: The strength efficiency of cement on selected mixes at W/b ratio of 0.22	156
Figure 4.75: The strength efficiency of cement on selected mixes W/b ratio of 0.25 ..	157
Figure 4.76 The development strength of flexure strength w/b of 0.22.....	159
Figure 4.77 The development of flexure strength w/b of 0.25.....	159
Figure 4.78: Relationship between compressive strength and predicting modulus of rupture from available models	162

Figure 4.79: Relationship between compressive strength and predicting modulus of rupture for OPC, RHA and SF concrete.....	163
Figure 4.80: The curve of predicted splitting tensile strength by various formulas	169
Figure 4.81: The curve of predicted splitting tensile strength by various formulas of concrete containing RHA	170
Figure 4.82: The curve of predicted splitting tensile strength by various formulas of concrete containing RHA	171
Figure 4.83: The curve of relationship between the compressive strength and the ratio of splitting tensile and compressive strength for all mixes	173
Figure 4.84: The curve of Relationship between the compressive strength and the ratio of splitting tensile and compressive strength for RHA concrete.....	173
Figure 4.85: Relationship between Splitting tensile strength and modulus of rupture .	175
Figure 4.86: The development of static modulus of elasticity w/b 0.25 on water curing and air drying	177
Figure 4.87: Relationship between compressive strength and predicting modulus of elasticity from available models.....	179
Figure 4.88: Relationship between compressive strength and predicting modulus of elasticity from OPC, RHA and SF concrete	179
Figure 4.89: Evolution of UVP of concrete with age for w/b 0.22.....	181
Figure 4.90: Evolution of UVP of concrete with age for w/b 0.25.....	181
Figure 4.91: Relationship between compressive strength and UVP for all mixes.....	183
Figure 4.92: ISA value of concrete at 60 minutes at 7, 28 and 90 days for w/b 0.22...	188
Figure 4.93: ISA value of concrete at 60 minutes at 7, 28 and 90 days for w/b 0.25...	188
Figure 4.94: Relationship between ISA value and compressive strength.....	190
Figure 4.95: Development of compressive strength on sulphate condition	194
Figure 4.96: Development of compressive strength on sulphate condition	195
Figure 4.97: The shrinkage development of OPC, RHA10, RHA15 and SF10 at various ages (water curing)	198

Figure 4.98: The shrinkage development of OPC, RHA10, RHA15 and SF10 at various ages (air drying curing)	199
Figure 4.99: The rate of shrinkage due to water curing and air drying at w/b 0.25 up to 242 days	200
Figure 4.100: Free shrinkage during the age of one day	203
Figure 4.101: Temperature of concrete mixture after casting up to 60 hours	203
Figure 4.103 Mass losses after 24 hours	204
Figure 4.103: Free shrinkage of HPC.....	205
Figure 4.104: Elastic strain of HPC.....	206
Figure 4.105: Shrinkage and creep strain of HPC.....	207
Figure 4.106: Early age creep/free shrinkage	208
Figure 4.107: Early age creep factor	208
Figure 4.108: Stress versus strain in drying conditions.....	209
Figure 4.109: Tensile stress (σ) and tensile strength evolution with time	211
Figure 4.110: Ratio of tensile stress and tensile strength with time	212
Figure 4.111: Modulus of elasticity of HPC at early age	213

LIST OF TABLES

Table 2.1: C3A content in the types of cement.....	11
Table 2.2: Classification of concrete based on strength at 28 days (Pliskin, 1992).....	13
Table 2.3: Classification of pozzolans according to ASTM C618.....	19
Table 2.4: World rice paddy, potential husk and ash production (millions tons).....	21
Table 2.5: Chemical composition of RHA from various countries	26
Table 2.6: Effect of RHA ‘replacement’ on compressive strength.....	32
Table 2.7: Effect of curing types on compressive strength of RHA concrete.....	34
Table 2.8: Strength development for RHA concrete.....	36
Table 2.9: Compressive strength of BRHA for various mixes	38
Table 2.10: The mechanical properties of various RHA mixes (w/b = 0.32).....	39
Table 2.11: Mechanical properties for various RHA mixes (w/b = 0.32)	40
Table 2.12: Mechanical properties for various RHA mixes (w/b = 0.32)	40
Table 2.13: Permeability related properties of RHA blended concretes	48
Table 3.14: Chemical composition and physical properties of cement	57
Table 3.15: Chemical composition and physical properties of RHA and SF	59
Table 3.16: The physical properties of fine and coarse aggregate.....	63
Table 3.17: Calculated specific surface area of aggregates	66
Table 3.18: Mix proportion of mortar.....	68
Table 3.19: Level and code of variable chosen for Box-Behnken design	70
Table 3.20: BBD with five variables	71
Table 3.21: Size and curing of specimens.....	76
Table 4.22: Chemical compositions of RHA, SF and OPC	96
Table 4.23: Physical properties of RHA, SF and OPC	99

Table 4.24: The physical properties of fine and coarse aggregate.....	104
Table 4.25: Mix proportions of mortar	109
Table 4.26: Mix proportion of OPC and RHA concrete	113
Table 4.27: Properties of fresh concrete	114
Table 4.28: Factors, level and code for design expert.....	119
Table 4.29: Box-Behnken design with actual code and level of variables	120
Table 4.30: Mix proportions of forty six runs.....	121
Table 4.31: Responses of forty six mixtures.....	122
Table 4.32: Proposed models by the Design Expert software	126
Table 4.33: ANOVA for the complete combined quadratic model of slump responses	126
Table 4.34: ANOVA: for complete combined quadratic model of 1 d compressive strength response.....	127
Table 4.35: ANOVA: for complete combined quadratic model of compressive strength at 28 days	128
Table 4.36: Coefficients for the quadratic model.....	129
Table 4.37: Responses and predicted values from the quadratic model	129
Table 4.38: Experimental proportions versus optimized proportions	135
Table 4.39: The mixes involved in the mechanical properties test.....	137
Table 4.40: Mix proportion and workability for OPC, RHA and SF concrete	138
Table 4.41: The properties of fresh concrete	140
Table 4.42: Compressive strength of concrete.....	146
Table 4.43: Rate of compressive strength development	147
Table 4.44: Compressive strength ratio under air drying and water curing.....	150
Table 4.45: Coefficient and constant explored to find $f_{cm t}$	151
Table 4.46: The flexural strength.....	160

Table 4.47: The curing ratio of Air drying and Water curing	161
Table 4.48: Estimating equations of the different models	162
Table 4.49: Splitting tensile strength of OPC and RHA concrete subjected to water curing and air drying conditions	165
Table 4.50: Splitting tensile strength ratio of air drying and water curing	166
Table 4.51: The relationship between compressive and splitting tensile strength formula	168
Table 4.52: Statistical model used to predict the relationship between the compressive strength and the ratio of splitting tensile and compressive strength	172
Table 4.53: Static modulus of elasticity	176
Table 4.54: Relationship models between static modulus of elasticity and compressive strength	178
Table 4.55: The results of UPV on various RHA and SF concrete up to 90 days	182
Table 4.56: The porosity at different w/b, age and in various percentages of RHA and SF concrete	184
Table 4.57: Reducing porosity value from w/b 0.25 to w/b 0.22	186
Table 4.58: Reducing porosity value from OPC concrete to various percentages of RHA and SF concrete	186
Table 4.59: Initial surface absorption test for w/b 0.22 and 0.25 subjected water curing and air drying curing	189
Table 4.60: Relationship model between ISA value and compressive strength	190
Table 4.61: Effect of Rice husk ash and curing on sorptivity	192
Table 4.62: Drying shrinkage values for selected mixtures	197
Table 4.63: The ratio of shrinkage strain percentage of 242 days	201
Table 4.64: Expansion and shrinkage stress and age of cracking	211
Table 4.65: Comparison of cost analysis of OPC, RHA and Silica fume concrete	214

LIST OF SYMBOLS AND ABBREVIATIONS

NC	:	Normal concrete
HSC	:	High strength concrete
UHSC	:	Ultra-high strength concrete
HPC	:	High performance concrete
HPC	:	High strength high performance concrete
RHA	:	Rice husk ash
SCM	:	Supplementary cementitious materials
HSSCC	:	High strength self-compacting concrete
HRWR	:	High range water reducer
Sp	:	Superplasticizer
SF	:	Silica fume
POFA	:	Palm oil fly ash
SGA	:	Sugar cane ash
C2S	:	Di calcium silicate
C3S	:	Tri calcium silicate
C4AF	:	Tetra calcium alumino ferrite
C3A	:	Tri calcium aluminate
ACI	:	American Concrete Institute
OPC	:	Ordinary Portland Concrete
W/c	:	Water to cement ratios
PSD	:	Particle size distribution
RSM	:	Response surface methodology
CCD	:	Central composite design
ASR	:	Alkali silica reaction

CSH	:	Calcium silicate hydrate
W/c	:	Water to cement ratios
XRD	:	X-ray diffraction
BET	:	Brunauer–Emmett–Teller
PCE	:	polycarboxylic polyether
BRHA	:	Black rice husk ash
LOI	:	Loss on ignition
FA	:	Fly ash
ISAT	:	Initial surface absorption test
SEM	:	Scanning electron microscope
XRF	:	X-ray fluorescence spectrometry
UPV	:	Ultrasonic pulse velocity
MPa	:	Stress unit (N/mm ²)
BBD	:	Box-Behnken design
σ_t	:	Maximum tensile stress at failure
f_t	:	Splitting tensile strength
HRWR	:	High range water reduced
Sp	:	Superplasticizer
IAE	:	Integral absolute error

CHAPTER 1: INTRODUCTION

1.1 Research Background

Concrete is the most common construction material used nowadays and accounts for a large part of the infrastructure system. It is recorded as a second material being used after water in the world (Gambhir, 2006). Comparing to other construction materials, concrete is easy to form the shape and to cast in situ. Its basic ingredients are available in the local area of the construction site, such as fine aggregate, coarse aggregate, water and Portland cement.

Like other building material used in industries, concrete also experiences the development of qualities in order to support the need of concrete industries, which develop from normal concrete (NC) to high strength concrete (HSC) and up to ultra-high strength concrete (UHSC). However, the classification HSC is changing with time, depending mainly on the availability of raw materials and technical know-how and the demand from the construction industry. It could be classified as low or at most medium strength concrete now but it was considered HSC in the 1950s (Rashid et al., 2002). According to ACI-363 (1984), HSC is the concrete having a compressive strength of 6000 psi (41 MPa) or greater. The deterioration and premature failure of concrete structures such as marine structures, and concrete bridge deck, etc. has leads to the development of high performance concrete (HPC) which is the answer of weakness of normal concrete. The American concrete institute defines HPC as concrete that meets special performance and uniformity requirements that may not always be obtained using conventional ingredients, normal mixing procedures and typical curing practices. Mehta and Aïtcin (1990) defined HPC as concrete has better in strength, workability, and durability. The HPC can range the compressive strength from normal up to high strength concrete.

High strength concrete is often made with a high cement content, a very low water-cement ratio, a highly reactive pozzolan and then it is called as high-performance concrete. The concrete may not turn out to be durable and maintenance-free because these concrete mixtures may generate too much heat and are characterized by high autogenous and drying shrinkage, and therefore are prone to cracking due to restrained shrinkage at early age. A concrete structure containing interconnected cracks and micro cracks will not be durable under certain conditions and will award “low-performance” based on Mehta and Aitcin’s definition.

The history of new modern skyscrapers started in Chicago in 1884 as the city rebuilt due to a fire devastated the city. Those structures were designed with iron and steel frame to support its weight. Soon, skyscrapers started to appear in New York as well as Chicago and mostly they were built higher as competition with one another. In recent years, skyscrapers are also built in China, Malaysia, Taiwan, Saudi Arabia and the United Arab Emirates as economic growing on those countries. Building a skyscraper becomes validated if the buying price of the area is really high in order to decrease the expense of the area per the total floor area of a building. Hence the structure of skyscrapers is determined by its economics and benefits. On engineering views, skyscraper also must have fulfilled the requirement of foundation and construction materials. The location of bedrock determines the type of foundation and it is preferred near the surface which can save the cost of foundation. The skyscraper also needs the construction material that having high stiffness can reduce the drift due to either wind or earthquake and the high compressive strength concrete that can support the load. A few Examples of application of this special type of concrete are Twin tower in Kuala Lumpur and East Island Centre in Hong Kong used high performance concrete with compressive strength of 80 MPa and 100 MPa, respectively. To produce such a high

performance concrete (HPC), it is a necessity to apply a low w/b ratio and to include cementitious material and superplasticizer (Speare et al., 1999) in the ingredients.

Supplementary cementitious materials (SCM) such as fly ash, silica fume, slag and rice husk ash are applied successfully as partial replacement of cement in normal concrete. Most SCM now days used is silica fume due to capable to improve the strength and workability of concrete. The particle size of SF is 100 times finer than Portland cement and the content of SiO₂ is almost 90%. CaOH of cement hydration reacts with SiO₂ of SCM forming another CSH which create concrete denser and less permeability. Mazloom et al. (2004) investigated the influence of silica fume (0, 6, 10, and 15%) on the compressive strength of high performance concrete. They observed that the compressive strength of silica fume concrete was 21%, 26 % and 14 % stronger than that of control concrete at 28, 90 and 360 days, respectively. To cope with low workability of fresh concrete, they applied a certain dosage of superplasticizer in concrete mixture. (Sobolev, 2004a) studied the compressive strength of high performance concretes. It was observed that increase in superplasticizer dosage from 8 to 18% led to a reduction of w/c from 0.31 to 0.26 and improved the concrete compressive strength from 86 to 97 MPa.

In this study, RHA was used as SCM due to its chemical properties are similar with silica fume and its raw material is locally available. Rice husk is considered a waste material in rice mill in paddy producing countries such as Malaysia, Thailand and Indonesia and has a potential to be used as raw material for SCM in concrete. Paddy is a leading agricultural crop in Southeast Asia countries and Malaysia is one of paddy production with the production around 1.8 million MT which is 0.38% of the total world supply. There are more than 231 rice mills operating in Malaysia (Wong et al., 2010) and a significant amount of rice husk is produced as waste. Each ton of paddy

produces about 200 kg of husk, which on combustion yields approximately 40 kg of highly siliceous ash. In addition, mostly rice husk did not feed to the cattle due to the husk contains arsenic that could accumulate and cause a disease on cattle (Rahman et al., 2008). Some of rice husk are used in turbine for supplying electrical energy for rice milling operation and par boiling paddy. The rests are dumped and burn it in a landfill area, creating environmental pollution and health hazard. RHA has a high content of silica in the surface of the husk and it is possible to be used in concrete as partially replacement of cement. RHA is reactive amorphous silica if combustion of rice husk is less than 700⁰C. Research outcomes confirmed that finely ground RHA can be used successfully as an SCM for producing various types of concrete (Safiuddin, M. et al., 2011). The production of HPC will be cost-effective if RHA can be used in concrete as an SCM. Comparing with silica fume which its price is high due to imposed import duties; RHA is locally available and assumed cheaper than silica fume. Therefore, the use of RHA is more desirable to decrease the overall production cost of HPC while achieving substantial environmental benefits.

1.2 Problem Statement

The practical approach to produce HPC with 28 day compressive strength of 100 MPa is by reducing water to binder ratio of concrete mixture and incorporating SCM. As water to binder ratio is decreased, mixing water is reduced and at other side binder content increases. Reducing water induces low workability of fresh concrete and makes the mixture sticky. Furthermore, the incorporating cementitious materials on these concretes also impose more effect on workability of concrete due to SCM having high specific surface area so that SCM need more water. The specific surface area of RHA is higher than silica fume and fly ash due to porous of RHA so that RHA absorbs more water than other SCMs. Safiuddin, M. (2008) also reported that high strength self-compacting concrete (HSSCC) needs higher amount of binder and special ingredients to

get workability and strength requirement such as high range water reducer (HRWR) and SCM. HRWR is used to lessen the demand for water and to ensure sufficient workability of fresh concrete. However, the use of HRWR, SCM, and higher cement content than that of normal concrete increase the cost of HPC. The strategy to solve this problem is through optimizing the amount of binder, aggregate composition and use local available SCM, such as RHA. However, there is no a guideline to mix design of HPC up to compressive strength of 100 MPa. The guidelines for mix design of concrete are available up to compressive strength of 70 MPa, ACI and BS standard. This study will propose a model that can predict slump value and compressive strength at 1 and 28 days.

The sources of any SCMs are from wastes and thus their disposal in concrete generally saves environmental pollution. Silica fume, fly ash, blast-furnace slag, metakaolin have been used in concrete as SCM to improve properties of concrete. However, some of them are not cheaper than cement and therefore it may not be cost-effective. The cost of silica fume is higher than that of cement. The cost of blast-furnace slag is comparable or higher than that of cement but fly ash is cheaper than others. Metakaolin has the high manufacturing cost as it must be produced with high temperature with specific turbine. Thus, those SCMs increase the material cost in producing HPC. In comparison, the use of RHA is more desirable due to it can be produced with simple equipment and minimum cost involvement, which decrease the overall production cost of HPC.

1.3 Objectives of the study

The main objective of the present research is to develop high performance concrete grade 100 concrete incorporating rice husk ash (RHA) as a supplementary cementing material (SCM). The sub objectives of the study can be described as follows:

1. To determine the most suitable fineness of RHA that can produce mortar with compressive strength of 100 MPa, the optimum packing density with desired proportion of fine and coarse aggregates and mixing method that is applicable for HPC incorporating RHA.
2. To develop a statistical model based on Response Surface Method for predicting responses of slump and compressive strength at 1 and 28 days. Based on this model, an optimum proportion was proposed to get concrete compressive strength of 100 MPa at 28 days,
3. To determine the mechanical properties such as compressive strength, tensile strength, flexure strength and modulus of elasticity of RHA concrete based on the optimum proportion adopted.
4. To study the durability of RHA concrete such as initial surface absorption, water absorption, sorptivity and porosity.
5. To investigate drying shrinkage behavior as time dependent property of OPC and RHA concrete as well as restrained shrinkage behavior of OPC, RHA and silica fume concrete at early ages.

1.4 Research Significance and Novelty

HPC is a special type of concrete that needs cementitious materials (SCM) and HWRA to obtain sufficient workability and high strength. SCM can reduce bleeding and increase plastic viscosity, thus improving the segregation resistance of HPC. Moreover, SCM also can improve the hardened properties and durability of concrete. Those SCM such as silica fume, fly ash, ground-granulated blast furnace slag, and rice husk ash have been used successfully in producing HPC so that RHA has the potential to be used as a suitable SCM for producing grade 100 concrete, which is the significant of this research.

The novelties of this study are the usage of RHA as a supplementary cementitious material in producing high performance concrete of 100 MPa with less binder through utilizing the two steps mixing method for improving the homogeneity of concrete and mixing time. In addition, the Box–Behnken design (BBD) and response surface methodology (RSM) are being applied for the design of experiment and for optimization of mix proportion of high performance RHA 100 MPa concrete.

1.5 Organization of the Thesis

The present thesis consists of five chapters. The first chapter gives the overview of the study. At the outset of the introduction, the background of the research has been described. The problem statement, summary of the research approach, research significance and novelty, research contributions, and organization of the thesis are briefly presented in this chapter. The second chapter is review on the use of cementitious materials like RHA. The properties of constituent materials, the workability of HPC and its binder paste phase, and the different methods of mixing are described here. This chapter also describes the fresh and hardened properties, discusses several basic aspects of HPC, and identifies the research needs for the further study. The third chapter presents the experimental investigation of the research. This chapter describes the selection and testing of constituent materials including the processing and testing of RHA, and the preparation and testing of aggregate blends. The detailed experimental procedures for the fresh and hardened concretes are also presented in this chapter. The fourth chapter presents the detailed experimental results obtained from the research. This chapter describes the characteristics of constituent materials and the properties of aggregate blends. The choosing of particle size of RHA and mixing method suitable for HPC incorporating RHA are explained. The developed model for predicting HPC incorporating RHA is explained in this section. The optimum mix proportion of HPC 100 MPa and results of the binder of different proportion of RHA and 10% SF concrete

are described and discussed here. The test results for the fresh and hardened properties of HPC and the optimum content of RHA are discussed in this chapter. In addition, this chapter discusses the microstructures of different HPC. The conclusions based on the research findings are given in the fifth chapter. This chapter also gives several recommendations for future study.

University of Malaya

CHAPTER 2: LITERATURE REVIEW

2.1 Introduction

One of the major construction materials being used worldwide is concrete and one type of the concrete, which its demand increased, is high performance concrete (HPC). Since 1990 in the US, there has been a significant increase in the use of HPC in buildings and bridges. Nowadays, HPC with compressive strength of 100 MPa, mostly by incorporating silica fume as mineral admixture, is available with good workability due to the high quality of high range water reducer admixture (HRWR). Silica fume (SF) is a pozzolanic material from a waste of silicon industries. There are pozzolanic materials from agriculture wastes such as rice husk ash (RHA), palm oil fly ash (POFA), sugar cane ash (SGA), etc. There are available codes for fly ash and silica fume in ACI such as ACI 232.2 and ACI 234. Similarly those are in ASTM such as ASTM C 618 and ASTM C 1240, respectively. However, there is still a hesitant by designers and constructors of concrete structure in specifying and recommending HPC incorporating RHA in the construction projects due to the absence of standards, code and other reliable information concerning its use. In the near future, the body of knowledge of HPC incorporating RHA will increase then the confidence in the use of HPC and construction standards will develop to take full advantage of RHA as a potential replacement of silica fume in HPC.

2.1.1 Characteristics of HPC

The material constituents of HPC are water, cement, fine aggregate, coarse aggregate, mineral admixtures and one or two types of superplasticizer. HPC is characterized by special performances in term of workability, strength and durability. Gagne et al. (1992) mentioned two fundamental principles should be applied to get high compressive strength of HPC. There are low w/b ratio and high workability. Mostly it

is designed with very low water binder ratio (w/b), from 0.35 down to 0.2. The low w/b ratio will affect the cement particle being close to each other due to less free water and then particles of cement will be denser. Consequently, this concrete is less permeable and more resistant to aggressive solution (Aïtcin, P.C., 2001).

HPC usually contains about 450-550 kg/m³ of ordinary Portland cement (OPC) with the cementitious material ranged from 5% to 15%. By using superplasticizer, workability of concrete ranged from 200-250 mm slump with a very low w/c ratio can be achieved (Aïtcin, P.C., 2000; Neville, A.M., 1995). However, it is sometimes difficult to control the rheological properties of HPC, with a slump of 200 mm, and to maintain its workability at an hour or more after mixing (Aïtcin, P.C., 2001). The interaction between the cementitious materials and superplasticizers are more complex when incorporating some mineral admixtures such as blast furnace slag, fly ash, silica fume or natural pozzolans. Therefore, the selection of the compatible between pozzolanic material and superplasticizer requires further consideration (Hallal et al., 2010).

The information on the properties of cement needed in producing HPC are the fineness (Bentz, 2010), particle size distribution (Osbaeck & Johansen, 1989), and the chemical composition of cement (Sobolev et al., 2009). The amount of chemical compounds in cement also affects the rate strength development. Chemical compounds of cement are dicalcium silicate (C2S), tricalcium silicate (C3S), tricalcium aluminate (C3A), and tetracalcium aluminoferrite (C4AF). It will hydrate and gain early strength at a faster rate if the amounts of C3A and C3S contain is high in cements. Table 2.1 shows the approximate the C3A in various type of cement. The other hand the quality of water is also important. Impurity water is possibly to interfere the setting of the

cement, affect the strength of concrete and lead to the corrosion of the reinforcement (Neville, A.M. & Brooks, 1987).

Table 2.1: C3A content in the types of cement

Type of Cement	Purpose	Content
Type I	General	C3A < 8%
Type II	Moderate heat of hydration and sulphate resistance	C3A < 8%
Type III	High early strength	C3A < 15%
Type IV	Low heat	C3S < 35%, C3A < 7%, C2S > 40%
Type V	Sulphate resistant	C3A < 5%

Workability is an important part in HPC because concrete with low w/b in the range of 0.2 to 0.3 and including mineral admixture cannot be placed easily. Superplasticizer has to be added during mixing to achieve high workability for that type of concrete. Also aggregate could affect the workability of HPC since aggregate is the most dominant quantity, which is about 70% of concrete volume. Its properties such as the fineness modulus, the maximum size and the type of aggregate influence the characteristic of HPC. The fineness modulus of fine aggregate of 3, which is a coarse one, is more favourable for HPC because there is a huge part of finesse material already in mix proportion of HPC. By increasing the fine modulus of fine aggregate the surface area of the aggregate in the mixture is decreasing and free water is more available and increasing the workability (Neville, A.M., 1995).

Zia et al. (1991) explained that HPC having high strength can be produced with coarse aggregate size within the range of 20-25 mm. Yaqub and Bukhari (2006) observed high strength concrete with different maximum size of coarse aggregates, cement content and w/b ratio. They mentioned that aggregate size of 10 mm gave higher strength than that concrete used higher aggregate size. In addition, Aïtcin, P.C.

(2001) reported that the type of coarse aggregate is also a significant factor in producing high strength HPC. Concrete containing basalt or limestone as coarse aggregate exhibit about 10% to 20% higher strength compared to granite and when comparing to limestone, concrete containing basalt exhibited higher compressive strength.

Larrard (1992) produced HPC with compressive strength of 80 MPa at 28 days inclusion of ultra-fine particles and superplasticizer in concrete with the w/c ratio of 0.3. It is expected that some particles react with lime and the other fill the voids between the cement and the silica. This effect contributes to the strength development of concrete. Aïtcin, P.C. (1992) explained that compressive strength of concrete can be increased by decreasing w/c ratio, using efficiently cement/superplasticizer combination and using the best material.

2.1.2 Definition of high performance concrete

Since HPC was introduced, there are many developments of HPC around the world. At the beginning, HPC is related to high strength concrete. According to Aïtcin, P.C. (2001) some parts of them are true but do not represent a complete and accurate picture. A variety of characteristics and enhanced properties of concrete generally refers to high-performance concrete. There are also some definitions by institution related to concrete such as ACI, SHRP and experts.

American Concrete Institute (ACI) defined HPC as a concrete that meets special performance and uniformity requirements that cannot always be achieved routinely by using only conventional materials and normal mixing, placing, and curing practices (Zia et al., 1991). Pliskin (1992) classified HPC based on the compressive strength of concrete at 28 days as shown in Table 2.2.

Table 2.2: Classification of concrete based on strength at 28 days (Pliskin, 1992)

Type of concrete	Comp. Strength (MPa)
Ordinary Portland Concrete (OPC)	20 to 50
High Performance Concrete (HPC)	50 to 100
Very High Performance Concrete (VHPC)	100 to 150
Exceptional Concrete (RPC)	> 150

Mehta and Aïtcin (1997) defined HSC as a concrete which generally characterized by low water/cement (w/c) ratio, high cement content, presence of several chemicals such as superplasticizer, air entrance agent and mineral admixtures such as fly ash (FA), ground granulated blast-furnace slag (GGBFS) and silica fume (SF). Strategic Highway Research Program (SHRP) defined HPC as a concrete having strength characteristics greater than or equal to 70 MPa at 28 days, or 20 MPa at 4-hour, or 35 N/mm² at 24-hour with w/c ratio less or equal to 0.35 (Meeks & Carino, 1999). Its durability factor should be greater than 80% when the concrete is subjected to freezing and thawing for more than 300 cycles. Brandt and Kucharska (1999) defined HSC as a concrete resulted from better quality aggregate, careful selection of the grain distribution down to the small diameters and low w/c ratio.

2.1.3 Curing of HPC

Curing is a method of keeping satisfactory moisture content and temperature in concrete for a period of time immediately following placing and finishing. Desired properties such as strength and impermeability may be obtained if curing is maintained during the development of concrete. After placement, the factors that influence cement hydration of concrete are the water to cement (w/c) ratios, curing temperature, particle size distribution (PSD) and water-accessibility (Chen, W. & Brouwers, 2008). Sastry et al. (2012) reported that maximum moisture losses from HPC are during the first 24

hours after placement. Proper curing can maintain a satisfactory moisture content and temperature in concrete during its early stages so that the desired properties may develop (Meeks & Carino, 1999).

Curing duration and curing techniques are important in HPC because they significantly affect the strength and durability of concrete (Huo & Wong, 2006). The characteristics of pozzolanic concrete are sensitive to poor curing condition than that of OPC concrete. It is necessary for silica fume concrete to apply water curing for the initial 7 days to explore pozzolanic activity. However, for fly ash concrete it is imperative to cure with an extended period to utilize its full potential pozzolanic. ACI Committee 234 (Zia et al., 1991) reported that silica fume does not improve the 7-day compressive strength of concrete when cured at 50 °F (10 °C). However, when cured under temperatures exceeding 68 °F (20 °C), the 7-day compressive strength tends to improve significantly (Meeks & Carino, 1999). It was also indicated that the pozzolanic reaction is, in general, very sensitive to the temperature. With the continuation of moisture curing, at later ages it was observed that the rate in tensile and flexural strength concrete with increasing silica fume content was higher as compared to plain concrete. However, it is also important to note that additional water gets into the near-surface zone of the concrete for durability purposes.

RHA has mesoporous structure which can absorb more water and creates high capacity of water absorption (Van, V.-T.-A. et al., 2013). RHA is possible to act as an internal curing agent (Van, V.T.A. et al., 2014). The mechanism of RHA starts to release water in pores when the internal RH in RHA concrete drops below 98%, the absorbed water in these mesoporous will be released to compensate the self-desiccation during hydration.

2.1.4 Advantages of HPC

During the last two decades the development and application of high performance concrete (HPC) have greatly increased all over the world. The process involved is a combination of improved compaction, improved aggregate matrix bond and reduced porosity using special additives. However, there are always pros and cons in HPC.

Some advantages of choosing HPC are economic, early strength, durability and environmental reasons. First, HPC is estimated more economical in major concrete construction projects (Sobolev, 2004b). The size of primary structural members such as columns of high-strength concrete (HSC) can be reduced significantly. Some structural members may also be safely designed with less reinforcing steel, saving on both labor and material costs due to greatly increased strength and load carrying capacity. Second, due to its early strength is higher than normal concrete; HPC has practical implication when required for faster turnover of formwork, especially a concern for early applications of construction loads (Swamy & Mahmud, 1986). Third, it is well known that repairing concrete is costly. One of the reasons choosing HPC is due to its durability that could avoid water or solutions penetrating into the concrete initiating or accelerating stress in concrete. It affects to the increase of life cycle of concrete structure. Last, now, there is an increasing important to preserve the environment. The uniqueness of HPC is some amount of cement can be replaced by mineral admixture which mostly from industrial and agriculture wastes. By using of these wastes in HPC, it will reduce the CO₂ emission due to less clinker production and less burning those wastes in dumping fill area (Vanchai et al., 2010).

2.1.5 The mixture proportion for HPC

There are various methods for proportioning conventional concrete. These methods are based on fundamental functions: water-to-cement ratio, the constancy of water

demand as well as theory of optimum aggregate proportioning. All those methods are used to determine mixtures with the required properties. For HPC, which is mostly incorporating mineral additive such as fly ash, silica fume and rice husk ash, these methods can be used to yield concrete mixtures of HPC. However, the mix proportion for achieving compressive strength of 100 MPa incorporating RHA is not available yet. Furthermore, Sobolev (2004b) also presented a chart as a guideline in designing mix proportion of HPC (see Figure 2.1.).

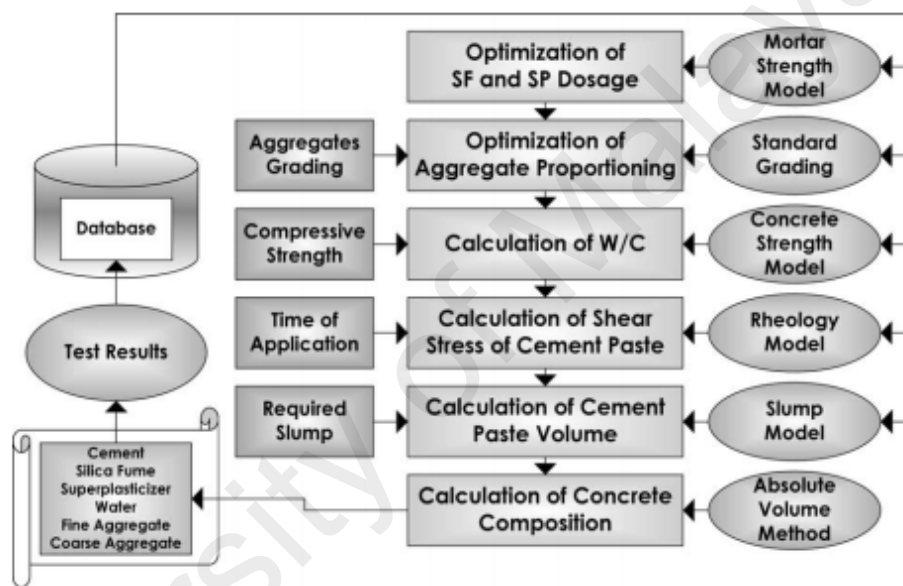


Figure 2.1: Method for HPC mixture proportioning
Adopted from (Sobolev, 2004b)

These steps can be elaborated as:

- a. Optimization of mineral additive and Sp dosage

Aïtcin, P.C. (1992) conducted optimization of Sp dosage on the binder of cement and silica fume. He found the saturation point of Sp dosage on the binder. Beyond that point, the time binder to flow the cone is almost similar even the dosage of Sp added. Compare to silica fume in similar percentage replacement, RHA needs more Sp dosage due to its higher specific surface area.

b. Optimization of aggregate proportioning

The proportion of fine and coarse aggregate affect the mechanical properties as well workability in fresh concrete. By optimizing the aggregate proportion it minimize the void in the aggregates and it can reduce the paste needed to cover all aggregates or increase workability. According to Domone and Soutsos (1994) the optimum proportion of fine and coarse aggregates depended on the surface area of the aggregates, the ratio of fine aggregate to total aggregate is in the range of 0.35-0.45.

c. Concrete composition

Aïtcin, P.C. (1997) proposed the absolute volume to find concrete composition for HPC but the formula was modified to incorporate superplasticizer. This method considers S_p in solid content and then the free water for mixing should be adjusted due to S_p also containing water.

d. Optimizing mix proportion

As the cost of materials increases, optimizing concrete mixture proportions for cost becomes more desirable. Furthermore, as the number of constituent materials increases, the problem of identifying optimal mixtures becomes increasingly complex. Not only are there more materials to consider, but there also are more potential interactions among materials. HPC is the concrete combined with several performance criteria, the number of trial batches required to find optimal proportions using traditional methods could become unreasonable. According to Domone and Soutsos (1994) the optimization of the material proportions was harder for HPC than for conventional concrete as many existing proportioning methods for concrete was based on data and knowledge of existing materials in a specific region or country, and generally are restricted to the type of Portland cement, aggregates and water.

Various statistical methods, such as Taguchi designs, designs for second order model, optimal designs, mixture designs, response surface methodology (RSM), etc., are satisfied in achieving desired concrete properties and mixture optimization for a given set of constituents. These methods are commonly used to optimize products and process in various industries (Simon, 2003). The method also have been applied in some researches to improve HPC (Nehdi, M.L. & Sumner, 2002), self-compacting concrete (SCC) (Alqadia et al., 2013) or general cement based material (Lawler et al., 2005). Islam et al. (2012) have utilized the static method to predict of strength and slump of HPC incorporating RHA with compressive strength in the range of 40-92 MPa. Another trend the statistical methods utilized in concrete is Response surface methodology (RSM), which is a tool of modern statistics to investigate the relative significance of multi variables in any complex form of interaction (Myers et al., 2004). Alqadia et al. (2013) used central composite design (CCD) and RSM to model the response of fresh and hardened concrete through mix proportioning of SCC. Bektas and Bektas (2014) investigated the effect of some critical concrete mix parameters on the alkali silica reaction (ASR) expansion and engineering properties by employing Box–Behnken and RSM. The results of the regression analysis showed that the fitted model explains over 85% of the variations for ASR expansion, compressive strength, flexural strength and modulus of elasticity.

2.2 Pozzolanic materials used in HPC

The utilization of pozzolanic materials were become establish especially in achieving a high strength and high performance concrete. ACI Committee 232 (1998) defined pozzolan “as a siliceous or siliceous and aluminous material, which itself possesses little or no cementitious value but will, in finely divided form and in the presence of moisture, chemically react with calcium hydroxide at ordinary temperatures to form compounds possessing cementitious properties”.

Pozzolans can be classified as natural or by-product materials. A natural pozzolan is one obtained from volcanic rocks and minerals. These pozzolan usually must be processed such as crushing, grinding and size separation. In some cases it may also involve thermal activation before use as mineral admixture. By-product materials are a waste from the industry and the use of these materials as mineral admixtures may or may not require any processing e.g., drying and pulverization (Mehta, P.K. & P.J.M. Monteiro, 1993). Table 2.3 shows the classification of pozzolan type based on chemical properties. The purpose of ASTM C618 is to classify different qualities of ash, especially for fly ash. The quality of fly ash is determined by the source of coal. Class F fly ash are pozzolanic in nature meanwhile Class C fly ash are pozzolanic and hydraulic material. Class F fly ashes have lower calcium contents and react slowly compared to Class C fly ashes. Differently from fly ash, RHA does not come by nature as a finely divided powder as one of the requirements to be a good pozzolan. The quality of RHA depends on combustion and grinding process. RHA can be classified as pozzolan type N as it has high content of SiO₂ and low SO₃. The contribution of the pozzolanic and cementitious material including in concrete are to fill-up void through producing additional products of calcium silicate hydrate (CSH) (Memeon et al., 2002). Calcium hydroxide (Ca(OH)₂) is reacted with SiO₂ from cementitious material is transformed into additional CSH gel and changed large pores into finer pores. This formed a basis for improvement of strength and durability of concrete (De Sensale, G. R. et al., 2008).

Table 2.3: Classification of pozzolans according to ASTM C618

Chemical properties	Type of Pozzolan		
	N	F	C
Minimum. SiO ₂ +Al ₂ O ₃ +Fe ₂ O ₃ (%)	70.0	70.0	50.0
Maximum Sulphur trioxide (SO ₃) (%)	4.0	5.0	5.0
Maximum Na ₂ O+0.658 K ₂ O (%)	1.5	1.5	1.5
Maximum loss on ignition (%)	10.0	6.0	6.0

2.2.1 Rice husk ash as a supplementary cementitious material

In concrete, the principal cementitious material is Portland cement. Nowadays, most concrete mixture contains supplementary cementitious material in concrete. RHA is natural pozzolan and also called as a supplementary cementitious material that makes up a portion of cementitious component in concrete.

RHA as a by-product from agriculture is understandable that its physical and chemical properties are related on the soil chemistry, and climatic condition varieties of paddy (Chandrasekhar et al., 2003). It could be that source of differences are also from fertilizer applied during the cultivation process (Maeda et al., 2001). However, the difference is a minor in chemical content and not harmful to characteristic of concrete.

To understand how RHA is reacted in concrete. Yu et al. (1999) examined the reaction of RHA to $\text{Ca}(\text{OH})_2$ solution at 40°C . They concluded that after adding RHA to the calcium hydroxide solution, the concentration of Ca^{2+} and OH^- were reduced with time. It was related to the reaction between $\text{Ca}(\text{OH})_2$ and RHA. Then, by using XRD test, it showed that CSH gel was formed. It meant that silica in RHA is stimulated by the $\text{Ca}(\text{OH})_2$ solution to form SiO_4^{4-} ions. By continuing stirring, these ions react with Ca^{2+} and OH^- ion in the solution to form CSH. The final effect gives an advantage in the mechanism of the strengthening i.e. CSH filled the pores and improve the strength of the concrete.

As mentioned that RHA as supplementary cementitious material, by using it as part of replacement cement will reduce the cement demand. In developing countries, as paddy fields are mostly available, it could save the cost of cement. As shown in Table 2.4, it was estimated that the world production of rice was 672 million tons or 132.1 million tons of husk and consequently about 26.4 million tons of RHA is potentially available as mineral admixture. Meanwhile the total cement production in 2010 was 3,310

million tons (Survey, 2012). Then the ash potentially produced was approximately 0.79 % of the annual cement production. On environment view, it will reduce CO₂ emission due to less clinker production and landfill area for dumping and burning those wastes.

**Table 2.4: World rice paddy, potential husk and ash production (millions tons)
(FAOSTAT, 2013)**

No.	Country	Rice paddy production in years		Average Potential husk/year	Average Potential ash/year
		2009	2010		
1	China	196.7	197.2	39.4	7.9
2	India	133.7	120.6	25.4	5.1
3	Indonesia	64.4	66.4	13.1	2.6
4	Bangladesh	47.7	49.4	9.7	1.9
5	Vietnam	40	40	8.0	1.6
6	Thailand	32.1	31.6	6.4	1.3
7	Rest of the word	170.2	166.8	33.7	6.7
8	World total	648.8	672	132.1	26.4

2.2.2 Characteristic of RHA

2.2.2.1 Physical properties of RHA

Rice husk contain a high proportion of lignin and about 20% of their outer surfaces are covered with silica, which is deposited onto this surface as monosilicic acid to form a silicon cellulose membrane (Juliano, 1985). Jauberthie et al. (2000) studied the properties of rice husks to identify amorphous silica. The silica content, by percentages of total weight, at external, interior and the internal surface of the husk was 45.2 %, 2.3% and 27.3%, respectively. It means that the external face of the husk has the highest concentration of silica. The internal face has much weaker and within the husk has practically non-existent silica.

Through further processing, by the combustion of husk, silica can undergo a structural transformation. Its properties are also affected by temperature and duration of combustion. (Xu et al., 2012) conducted several different temperature combustions of

RHA for two hours then they found out that there are transformations of silica from amorphous to crystalline form as can be seen on Figure 2.2.

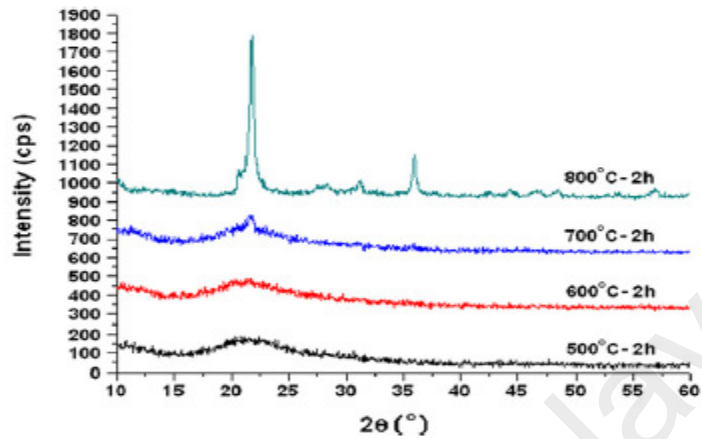


Figure 2.2: XRD analysis of RHA at different calcination temperatures
Adopted from (Xu et al., 2012)

Figure 2.2 shows the crystallographic structure of the silica in the powders. At 500 and 600 °C, it was observed that the RHA samples have the intense broad peak, which indicated that silica remained essentially amorphous and hardly any crystalline reflections occurred. However, at 700 °C, there are intense reflection started to confirm the formation of crystalline cristobalite but the diffraction peak is not sharp. Furthermore, at 800 °C the RHA samples show the diffraction peak is sharp, which can be assigned to cristobalite. The sharp peak of cristobalite phase represents the crystallization of silica. They suggested that to avoid any transformation of amorphous to crystalline form, the temperature of carbonization should preferably be below 700 °C

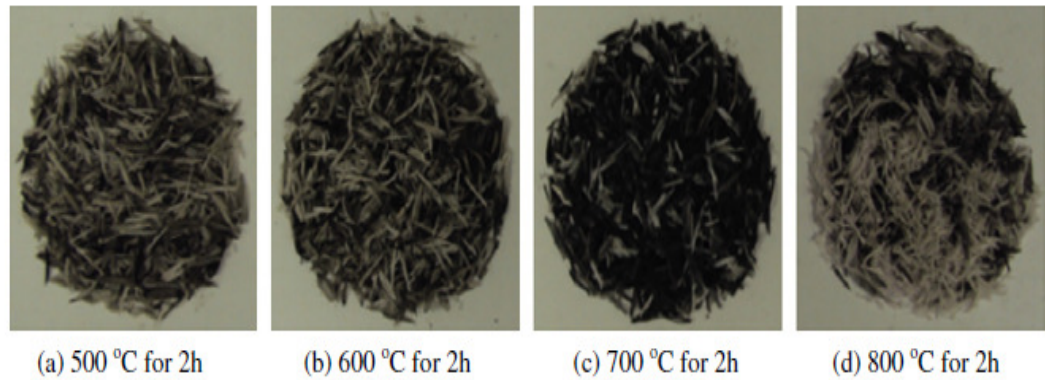


Figure 2.3: Color changes of RHA at different calcination temperatures (the color change of all the RHA samples is black with some grey or white particles)
Adopted from (Xu et al., 2012)

The transformations of combustion for different temperatures as well as the color changes taking place in RHA at different calcinations temperature are shown in Figure 2.3. It can be observed that the color of all RHA samples is black with some grey or white particles. The black particles are taken to represent the unburned fixed carbon in RHA. It can therefore be concluded that within the range of 500–800 °C, there are always some fixed black carbon particles and the extent of the black particles is decreasing with increasing in calcination temperature (up to 700 °C). At the calcination temperature of 800 °C, the number of black particles decreased while the number of white creamy silica particles represented by the bright appearance of ash increased.

Cisse and Laquerbe (2000) utilized grounded RHA in their research. Their grading analysis showed that 85% of the particles are smaller than 80 microns and then 34.46% of the particles are smaller than 7 microns (see Figure 2.4.). These particles appear to be responsible for the pozzolanic reactivity of the amorphous silica. However they did not mention the amount of hours of grinding that rice husk ash and the specification and type of grinding machine used. (Zhang, M. et al., 1996) reported that the particle size

and the specific surface area of RHA ranged from 5 to 1 μm and 20,000 to 50,000 m^2/kg , respectively, with specific gravity of around 2.06.

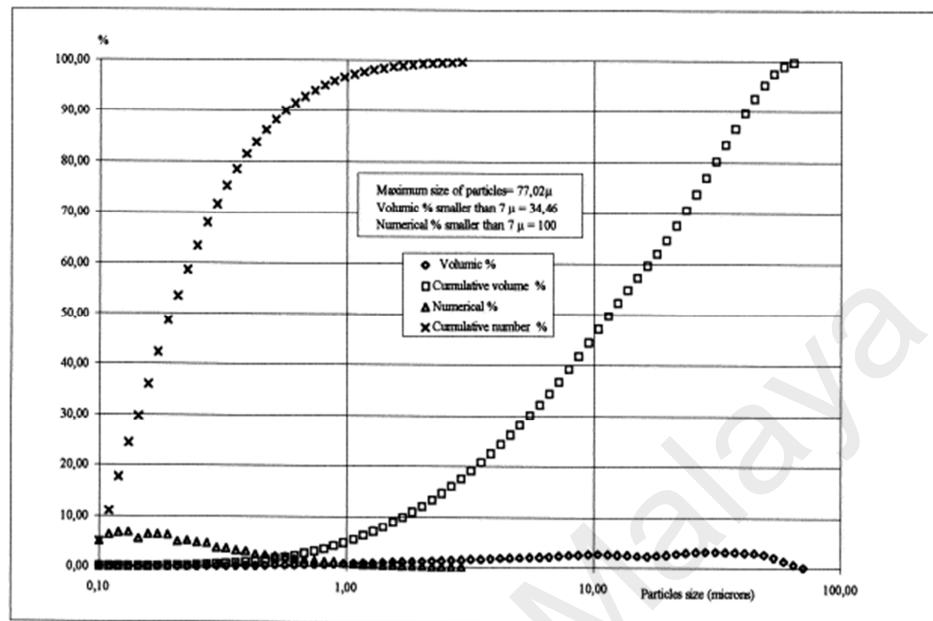


Figure 2.4: Grading of the rice husk ash by laser
Adopted from (Cisse & Laquerbe, 2000)

Cordeiro, G. C. et al. (2011) reported an interesting phenomenon on measuring the surface area of RHA grinding by BET and Blaine test. As seen in Figure 2.5, the particle size of RHA is reduced after grinding 8 minutes even after that it is increasing again. Measuring surface area of the BET show reduces the specific surface area but measuring by Blaine test increases as it is expected. The reason behind this is that the finer of RHA grinding filled the pores by submicron-size particles. The Blaine test detects surface area of the external pores but BET more detect surface area through internal pores.

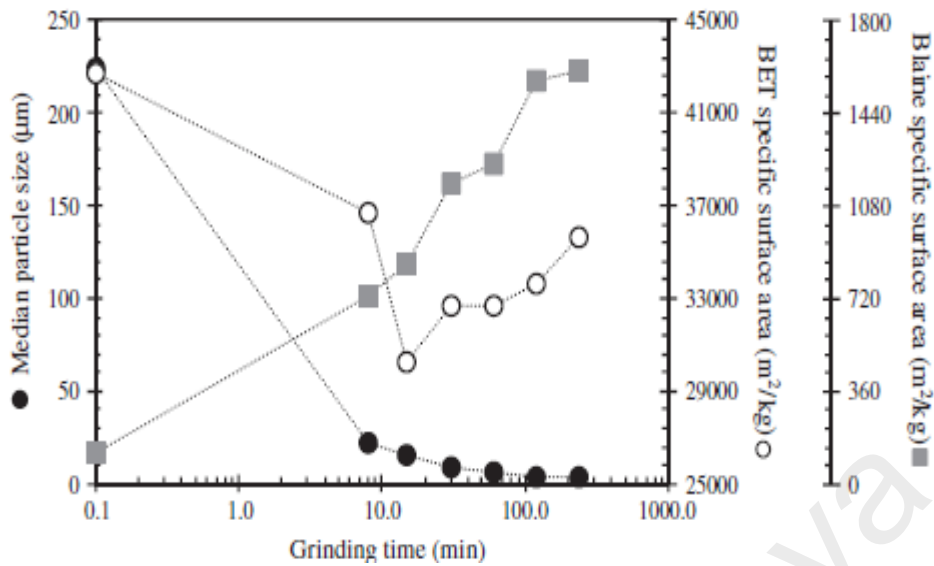


Figure 2.5: Variations of the median particle size (D50) and BET specific surface area due to grinding. (The X-axis equal to 0.1 refers to the AR-RHA – sample without grinding)
Adopted from (Cordeiro, G. C. et al., 2011)

Fig. 2.6 shows correlation Blaine specific surface area with pozzolanic activity index and Chappelle activity. The increment D_{50} of RHA affects to increase pozzolanic of RHA, significantly. Both curves show $R^2 > 0.9$. This figure also shows that using a Blaine specific surface test is more convenient than BET (Cordeiro, G. C. et al., 2011)

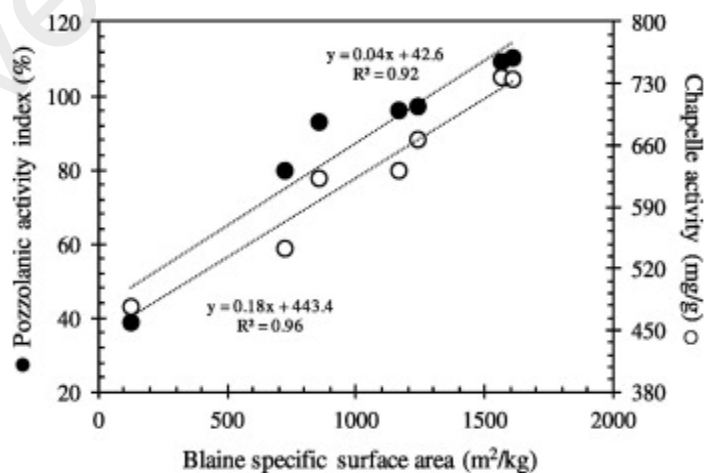


Figure 2.6: Relationship between pozzolanic activity and Blaine specific surface area of ground RHAs
Adopted from (Cordeiro, G. C. et al., 2011)

2.2.2.2 Chemical properties of RHA

The silica content of RHA is reported in Table 2.5. It is varying between 82.6 and 96 % (Stroeven et al., 1999) (Habeeb, G.A. & M.M. Fayyadh, 2009). The major impurity of the ash is formed by alkalis, of which potassium is predominant constituent. The presence and content of other metallic impurities such as phosphorus, iron, magnesium etc. are negligible and linked with fertilizer use. The lower value of SiO₂ could be the sample was incomplete-burnt. By presenting of large amounts of unburnt carbon in the ash it proportionally reduces the silica content. As mentioned earlier, the unburnt carbon content depends on the combustion methods by which rice husk is converted to ash. The chemical composition of RHA based on previous investigations is presented in Table 2.5.

Table 2.5: Chemical composition of RHA from various countries

(Paya et al., 2001; Stroeven et al., 1999; Yu et al., 1999) (Cordeiro, G. C. et al., 2009) (Habeeb, G.A. & M.M. Fayyadh, 2009)

Chemical composition (%)	Countries				
	Thailand	Brazil	Tanzania	Malaysia	Vietnam
Silicon dioxide (SiO ₂)	93.2	82.6	88.9	88.32	96.7
Aluminium oxide (Al ₂ O ₃)	0.4	0.4	0.3	0.46	0.08
Ferric oxide (Fe ₂ O ₃)	0.1	0.5	0.19	0.67	0.03
Calcium oxide (Cook et al.)	1.1	0.9	0.43	0.67	0.3
Magnesium oxide (MgO)	0.1	N/a	2.07	0.44	0.16
Potassium oxide (K ₂ O)	1.3	1.8	3.67	2.91	0.73

2.3 Effect of RHA on fresh concrete

RHA has very fine particles with high specific surface area and porosity compared to the OPC. RHA also can act as filler in the cement grains and improve the cohesiveness of concrete mixes. On the other hand, it affects the workability and setting time of fresh concrete

2.3.1 Workability

The most requirement of HPC in fresh form is workability. Damtoft et al. (1999) assumed concrete with good viscosity behave like a Bingham fluid. There are two parameters in the flow of Bingham model: yield stress and plastic viscosity. The quantitative measure of initial resistance of concrete to flow is related to yield stress. When it flows, it is related to plastic viscosity. Yield stress is the contribution of solid particles in concrete, and plastic viscosity is the contribution of suspending liquid in concrete (Wang et al., 1998). Recent research explained those terms with more simplify that yield stress close to the slump in concrete and plastic viscosity is related to stickiness, placeability, pumpability, mixing, segregation and finishability of concrete (ACI-363, 2002; Mbessa & Péra, 2001; Mehta & Aïtcin, 1997). The workability of concrete can be influenced by many factors such as water content, aggregate type and grading, aggregate to cement ratio, the presence of admixtures and fineness of cement as well as time and temperature (Paya et al., 2001).

Researchers (Mahmud, H.B. et al., 1997; Mahmud, H.B. et al., 2002) reviewed that there is a difference of need in superplasticizer for RHA replacement and RHA addition mixture. It was found that RHA addition need less Sp compared to RHA replacement. For example, 10% RHA addition mix consumed Sp about 1.8% of mass of cement content while about 2.2% was needed for replacement mix to produce similar workability at the same RHA content. However, there was no further explanation about that phenomenon. Later, they concluded that RHA concrete with slump value in the ranged of 150-200 mm with a w/b ratio of 0.31-0.32 can be produced by using superplasticizer. All concrete mixes incorporated either as an addition or cement replacement up to 15% RHA needed Sp in the range of 1.2% to 3.5% of the mass of cement content and about 24% of water content can be reduced. Duval and Kadri (1998) conducted a research related to rheology of HPC including RHA and FA in w/b

0.35. They reported that the yield stress decreases as the replacement level of RHA and FA increases. Reducing yield stress in fresh concrete is due to improve packing through the RHA particles filling in the spaces made by larger cement particles. It decreases frictional forces of the RHA-OPC system. The fineness and the shape of RHA play a critical role as interpreting the steep increase in plastic viscosity with the replacement levels shown in Figure 2.7. Fresh concrete is resistance to flow if the RHA more fineness, which means more the number of contacts among the particles. In addition, any deviation from a spherical shape implies an increase in plastic viscosity in the same phase volume.

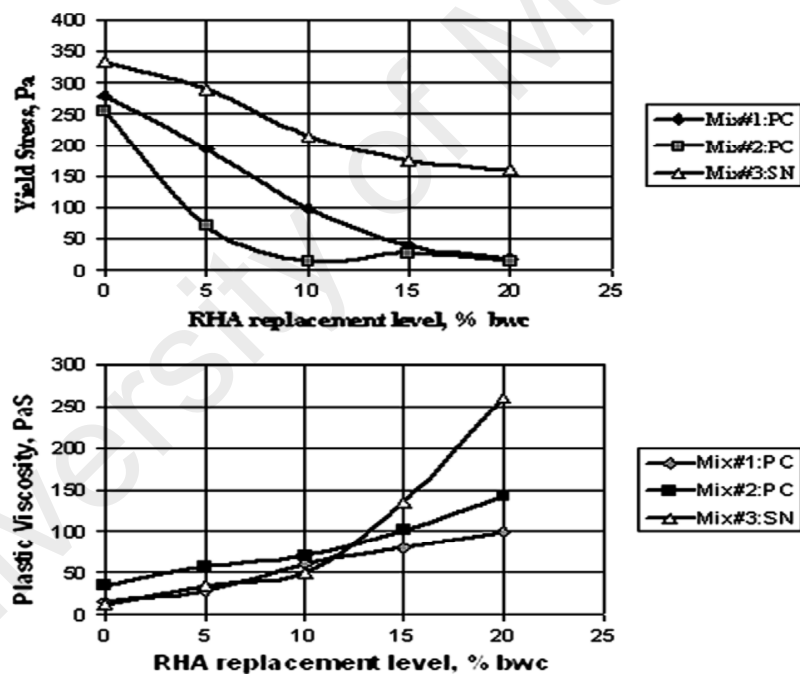


Figure 2.7: Effect of RHA replacement level on rheological parameters of plastic viscosity and yield stress

Adopted from (Laskar & Talukdar, 2008)

Givi et al. (2010) explained workability of RHA concrete with w/c of 0.4 and they used RHA with 95 μm and 5 μm sizes, with replacement of cement of 0, 5%, 10%, 15% and 20%. Figure 2.8 shows that the workability of concrete having RHA with particle size of 95 μm is better than that of 5 μm in all replacement comparing with OPC only.

They mentioned that these phenomena related to 5 μm of RHA having bigger specific surface area than that 95 μm of RHA. The increased specific surface of RHA particles needs more free water to cover all the surfaces of particles.

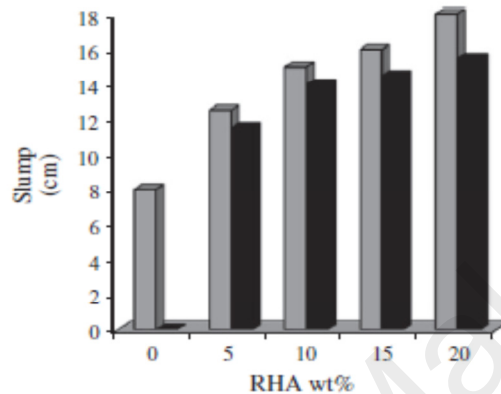


Figure 2.8: Effects of particle size of RHA on workability of concrete at different RHA contents

Adopted from (Givi et al., 2010)

Cordeiro, G. C. et al. (2009) conducted a research in HPC by utilizing RHA with high carbon content with replacement up to 20% of OPC. They could reduce the disadvantages of carbon content in RHA by grinding it to particle sizes in the range 1 μm to 1 mm, which 50% of that is 225 μm . The 20% of replacement with RHA showed better workability due to increased ratio volume of paste to aggregate as the density of RHA is less than OPC.

2.3.2 Setting time

As reported in previous investigations (Ismail, M.S., and Waliuddin, A.M., 1996; Paya et al., 2001) consistency of ordinary paste increase with increasing RHA content due to the higher specific surface area of RHA compare to OPC. They observed that initial and final setting time influenced by the percentage of RHA. Similar results were

also reported by Ganesan et al. (2008), Cook (1986) and Bhanumathidas et al. (2004) that RHA increases the setting time of pastes. Just like other hydraulic cement, the reactivity of RHA depends very much upon the specific surface area or particle size. The RHA with finer particles exhibits superior setting time behavior. El-Dakroury and Gasser (2008) pointed that it could be related the slower pace of heat induced evaporation of water from the RHA–cement (Figure 2.9).

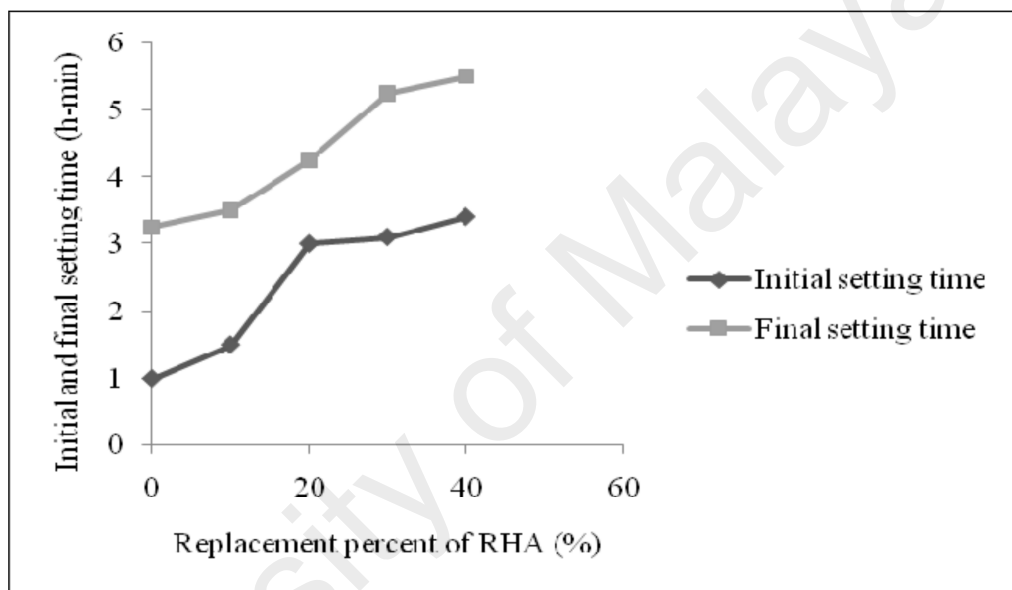


Figure 2.9: Initial and final setting times of RHA with different replacement percentages

Adopted from (El-Dakroury & Gasser, 2008)

2.3.3 Effect of superplasticizer types

Superplasticizer is one of the main constituent materials in HPC, especially, with low w/b ratio. Its dosage is related to the chemical content of cement used. The superplasticizer dosage is lower for cement with a small content of C3A compared with ordinary Portland cement. It was reported by Duval and Kadri (1998) that the dosage doubles when the percentage of C3A increases from 2% to 10%. According to them, the reason of this was the first minutes of mixing the superplasticizer is adsorbed by C3A phase and interferes with the early hydration of ettringite and C-S-H.

Furthermore, Zingga et al. (2009) mentioned the amount of C3A and on the presence of soluble alkali sulphate govern the superplasticizer adsorption occurred. Superplasticizer with a different family group exhibited different workability on fresh RHA concrete (Mahmud, H.B. et al., 2003). For example, to achieve slump of 150-200 mm, RHA concrete with the w/b ratio of 0.32 and 0.31 needed superplasticizer dosage based on sulphonated naphthalene formaldehyde condensed (Rheobuild 1000) in the range of 1-4% and 1.2-3.5% respectively. On the other hand, by using the new generation of Superplasticizer, workability of RHA concrete with a w/b ratio of 0.27 in the range of 200-240 mm slump can be obtained with Sp dosage less than 1.2%. Mahmud et al. (2004) examined the influence of four types of superplasticizer based on polycarboxylic on HSC containing 10 % RHA. The maximum strength was achieved in concrete containing superplasticizer based on polycarboxylic polyether (PCE). They reported that irrespective of the type of superplasticizer, concrete incorporating RHA can achieve strength of between 85-89 N/mm² at age of 28 days.

2.4 Effect of RHA on hardened concrete

It is well known that RHA has a contribution on mechanical properties and durability of HPC, irrespective of it is used as addition or replacement in concrete mixtures. RHA has a possibility to enhance properties of hardened concrete through reducing porosity, calcium hydroxide and improving interfacial transition zone (ITZ) on concrete

2.4.1 Compressive strength

The inclusion of RHA in concrete mix could be done either additional or replacement method. However the trend of research relating RHA has shown most research focused on replacement method in producing HPC. Table 2.6 shows that there are interesting information related to w/b of 0.32 and 0.31. The RHA concrete with 5% replacement shows higher strength compare to OPC concrete and by replacing of 10 % and 15%, the

compressive strength is lower than that of OPC concrete. For w/c of 0.3, in 10% replacement level its compressive strength is higher than OPC. However, there is inconsistency information as w/b ratio of 0.3 has lower strength than w/b ratio of 0.31 and 0.32. It can be seen in 20% replacement level the compressive strength of concrete can reach up to 98 MPa.

Table 2.6: Effect of RHA ‘replacement’ on compressive strength
(Mahmud, H.B. et al., 1997; Mahmud, H.B. et al., 2002; Stroeven et al., 1999; Zhang, M.H. et al., 1996)

Mix No.	Compressive strength (N/mm ²)			
	1d	3d	7d	28d
W/b = 0.40				
RHA 25R	-	-	53.5	72.3
RHA 43R	-	-	49.1	64.1
W/b = 0.35				
RHA 15R	-	-	64.6	82.2
RHA 20R	-	-	61.6	79.0
W/b = 0.32				
OPC	34.4	60.6	67.4	81.5
RHA 5R	40.6	65.9	75.3	93.0
RHA 10R	36.0	41.3	53.4	74.0
RHA 15R	32.4	38.0	51.0	78.0
W/b = 0.31				
OPC	35.2	60.9	66.3	81.8
RHA 5R	35.0	64.2	72.7	88.5
RHA 10R	34.0	46.6	57.3	75.3
RHA 15R	28.1	40.0	62.4	80.0
W/b = 0.30				
OPC	41.4	-	52.1	61.0
RHA 10R	41.4	-	57.9	70.8
W/b = 0.273				
RHA 20R*	-	-	81.1	98.8

*R = Replacement

RHA replacement mixes gave lower strength at early ages. This effect is due to RHA acts as filler in concrete and reduced cement content. These contribute to slowly strength development and hydration reaction of RHA. Due to the secondary pozzolanic reaction between silica and lime from cement hydration, the extra cementing compound to improve the strength of hardened concrete can be produced at later ages. It could be concluded that in that case the highest strength development was achieved at 5% cement

replacement and increasing the RHA content greater than 10% decrease the strength significantly (Mahmud, H.B. et al., 1997; Mahmud, H.B. et al., 2002).

2.4.1.1 Optimum replacement level of RHA in concrete

To get full benefit of using RHA, it needs to know the optimum of cement replacement with RHA which can be applied. Mehta and Aïtcin (1997) stated that RHA can be replaced with OPC for up to 50% and its compressive strength is considerably higher than that of OPC concrete. However, the disadvantage in Mehta's mixture was that the workability was very poor. Al-Khalaf and Yousif (1984) reported that RHA concrete has comparable strength to the control mix for up to 40%. In normal concrete, replacement of 5 % up to 10% RHA whether amorphous or crystalline, the concrete strength of 50 MPa could be achieved (Akasaki et al., 2005). The optimum replacement level of RHA in normal strength concrete is 25% (Muga et al., 2005; Saraswathy & Song, 2007)) and others (Ganesan et al., 2008), (Saraswathy & Song, 2007) claimed that for up to 30% of RHA may be replaced with cement and the strength is not affected.

To get the compressive strength of concrete is up to 70 MPa, the replacement level 5 up to 10% of the cement weight mostly shows higher strength compared to the control mix as shown by (Giaccio et al., 2007) and (Mahmud, H. B. et al., 2009). They found that the optimum replacement level of RHA for strength enhancement was 10% for achieving strength of 60 MPa, and the strength was increased for up to 70 MPa at the age of 180 days (Mahmud, H. B. et al., 2009). However, Muga et al. (2005) found that replacement RHA up to 12.5% would enhance the strength considerably. (Vanchai et al., 2007) investigated the use of RHA with 20% replacement and the result was comparable to the control. The possibility of variations in the optimum level of RHA replacement could be due to different characteristics of constituent material in concrete

such as particle size of cement, type of superplasticizer, particle size and reactivity of the RHA used in each study.

2.4.1.2 Effect of curing on compressive strength

Mahmud, H.B. et al. (2003) have studied the effect of type of curing regime on RHA concrete such as air drying and elevated temperature. They were conducted on addition and replacement RHA on concrete. Table 2.7 shows that there are no significant differences in compressive strength at 7 and 28 days. It means that different types of curing regimes did not impair the strength of RHA concrete significantly. It could be due to samples having initial water curing for 3 days. Before conducting those regimes curing, its compressive strength had reached 65-70% of 28 days compressive strength mostly in 3 days water curing.

Table 2.7: Effect of curing types on compressive strength of RHA concrete (Mahmud, H.B. et al., 2003)

Mix No.	Types of curing					
	Standard (moist)		Air-drying		High temp. (50°C)	
	7d	28d	7d	28d	7d	28d
OPC	66.3	81.8	63.7	80.5	64.0	79.8
RHA 10A	68.2	87.3	70.3	86.0	76.2	83.2
RHA 5R	72.7	88.5	73.8	82.8	75.0	88.5

A= addition; R= replacement

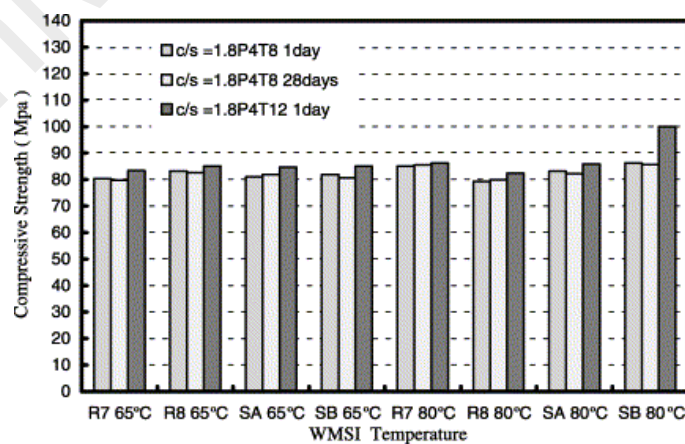


Figure 2.10: Compressive strengths of wet-mixed specimens steamed at low-temperatures for different delay times and ages

Adopted from (Wu & Peng, 2003)

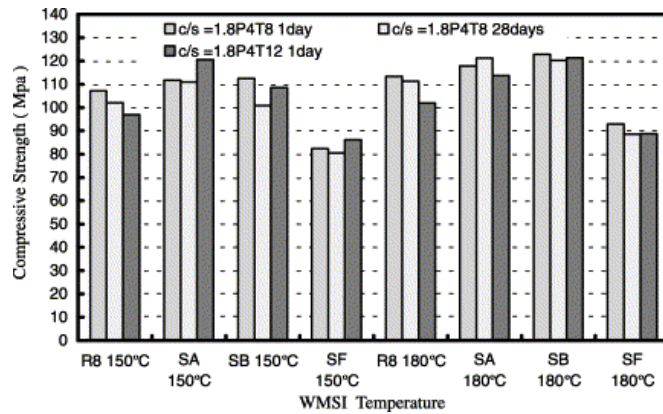


Figure 2.11: Compressive strengths of wet-mixed specimens steamed at high-temperatures for different delay times and ages
Adopted from (Wu & Peng, 2003)

Wu and Peng (2003) studied wet-mixed steam injection on cement pastes containing RHA with a low water/binder ratio of 0.27 and the test results are shown in Figures 2.10 and 2.11. Two types of RHA were used in their experiment, which RHA burned at 700 and 850 °C. Five different temperatures for wet-mixed steam injection were conducted in 65, 80, 120, 150 and 180 °C. The results indicate that the high-temperature steam curing contributes more to the strength compared to the low-temperature. The compressive strength of RHA concrete did not increase significantly at temperature in the range of 65-120 °C but increase in 180 °C. However, at normal temperature for 28 days did not increase the strength.

2.4.1.3 Effect of fineness of RHA on compressive strength

Ismail, M.S. and Waliuddin (1996) had studied two types of particle size of RHA in concrete, equivalent pass to sieve #200 and #325, were used to replace OPC at 10%, 20% and 30% with w/b ratio ranged from 0.24 to 0.34. The results indicated that all concrete mixes exhibited higher strength development from RHA with a fineness of pass #325, shown in Figure 2.12. Within this particle size, the optimum strength gain was obtained from 10% replacement and its strength can be obtained 70 MPa at 28

days. Nonetheless, both fineness of RHA exhibited lower strength when they were compared to the control concrete. It could be due to the w/b of mix proportion RHA concrete and OPC is different. The w/b ratio of OPC concrete was 0.24 and RHA concrete were 0.30 and 0.34. In addition, they did not also clearly mention the quality of silica form of RHA used.

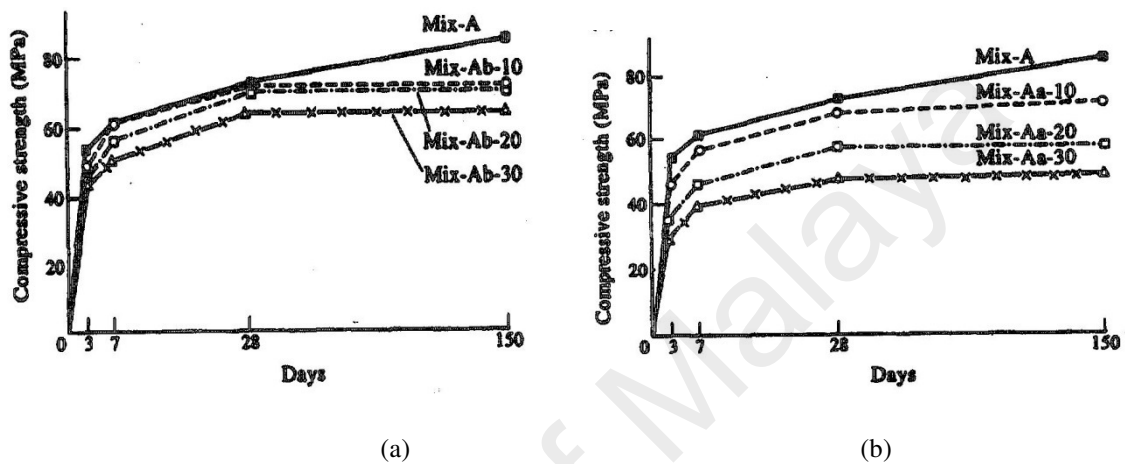


Figure 2.12: Effect of fineness of RHA on the compressive strength for various mixes (a) Passing #325 and (b) passing #200
Adopted from (Ismail, M.S. & Waliuddin, 1996)

Table 2.8: Strength development for RHA concrete
(Habeeb, G.A. & M.M. Fayyadh, 2009)

Mixture	RHA replacement	Compressive strength (MPa)					
		1 day	3 days	7 days	28 days	90 days	180 days
CM	0%	19.1	26.7	30.2	39.6	44.1	45.7
20F1	20%	17.3	24.5	29.8	40.6	45.2	46.9
20F2	20%	17.8	24.5	30.5	41.0	46.1	48.8
20 F3	20%	18.1	25.2	32.1	41.7	47.3	49.8

F1= RHA particle size of 31.3 μm ; F2= RHA particle size of 18.3 μm ; F3= RHA particle size of 11.5 μm

Habeeb, G.A. and M.M. Fayyadh (2009) also studied the influence of the particle size of RHA on compressive strength of a concrete with 40 MPa compressive strength and w/b of 0.53. The particle sizes of RHA used are 31.3, 18.3 and 11.5 μm and they were used to replace cement by 20 % of its weight (see Table 2.8.). At below 7 days, all

compressive strengths of RHA concrete exhibited lower than that of OPC. It could be the RHA not yet reacted with CaOH to form CSH. Up than 7 days, all compressive strengths of RHA concrete exhibited higher than that of OPC. They concluded that finer RHA giving better improvement in compressive strength of RHA concrete.

The effect of two types of particle size of RHA, 95 μm and 5 μm , in compressive strength of a concrete with w/b ratio of 0.4 was studied by (Givi et al., 2010). The replacement of cement with RHA was 5%, 10%, 15% and 20% by weight. The results indicated that the compressive strength of RHA concrete was improved with replacement of cement up to a maximum of 15% and 20% for RHA particle size of 95 and 5 μm , respectively. However, the ultimate strength of concrete was gained when applied 10% of RHA and 5 μm of particles size of RHA

2.4.1.4 Effect of combustion and types of RHA on compressive strength

It is well known that the form of crystal RHA produced depends on combustion methods. It could be either in amorphous or crystalline ash. From visual, the product of RHA can be distinguished by its color namely black, grey and white (Siddique, 2008). The black color shows that there are some parts of carbon in RHA and that silica is in amorphous form. The grey one which is the favorite one shows that there are fewer carbons in RHA. The white color shows that the silica in the surface of husk has been transformed to be crystalline form.

Paya et al. (2001) studied about characterization, pozzolanic activity determination and pozzolanic activation of RHA containing a high percentage of crystalline silica. They concluded that the RHA affected on compressive strength having similar quality with amorphous RHA but need additional mechanical treatment such as by more grinding and increasing of curing temperature. Nehdi, M. et al. (2003) have examined RHA produced based on different temperatures: 750°C (RHA-A), 830°C (RHA-B) and

750°C + air (RHA-C). The w/c ratio of concrete and RHA used to replace with OPC are 0.40, 7.5%, 10% and 12.5%, respectively. As control, beside OPC they also used silica fume. The results indicated that the temperature of combustion and types of RHA influenced the compressive strength development of RHA concrete. However, all concrete mixes exhibited higher strength than the control concrete at 28 days irrespective of the temperature and the types of RHA. They concluded that RHA, which depends on the percentage of inclusion, enhanced the strength by up to 40% at 56 days and was better than that of silica fume concrete.

Mahmud, H.B. et al. (2003) conducted a research on the effect of black rice husk ash (BRHA) as cement replacement or addition in percentage of 5, 10, 15% in a concrete with 28 days compressive strength of 80 MPa (seen in Table 2.9). They concluded that incorporating BRHA as a cementitious material at 5% replacement can provide strength of 80 MPa at 28 days. For 10% BRHA addition, strength of 77 MPa was obtained. The BRHA concrete mixes produce lower strength compared to the normal RHA (NRHA). It could be due to BRHA containing high carbon in the ash. LoI of BRHA in the study was 11.7%. BRHA still considered as pozzolanic material according to ASTM C618 which a powder could be considered as pozzolan if its loss of ignition (LOI) not exceeded 12% and the sum of chemical composition of SiO₂, Al₂O₃ and Fe₂O₃ was not less than 70%.

Table 2.9: Compressive strength of BRHA for various mixes
(Mahmud, H.B. et al., 2003)

Mix No.	Compressive strength (MPa)			
	1d	3d	7d	28d
OPC	34.4	60.6	67.4	81.5
BRHA5A	33.2	55.0	63.4	74.1
BRHA10A	26.1	47.6	61.0	76.9
NRHA 10A*	35.7	59.5	68.2	87.3
BRHA15A	23.6	42.4	59.0	69.6
BRHA5R	32.0	58.1	69.2	80.7

Table 2.9: Continue

Mix No.	Compressive strength (MPa)			
	1d	3d	7d	28d
NRHA 5R*	35.0	64.2	72.7	88.5
BRHA10R	26.9	51.9	62.1	77.9
RHA15R	26.2	43.3	54.3	69.1

2.4.2 Modulus of elasticity, flexure strength, and tensile strength

The other mechanical properties of concrete that need to know are modulus of elasticity, tensile strength, and flexural strength. Static modulus of elasticity is a significant property in concrete structural design. It determines the maximum allowable stress before the structural element would suffer permanent deformation. The pure elastic material is defined as that strain would appear and disappear immediately on application and removal of load (Neville, A.M., 1995).

On the structural design, most concrete elements are designed to resist compressive strength but not the tensile strength. However, tensile strength is mainly considered when concrete is designed for highways and airport pavement where bending is more concern and govern. Mahmud, H.B. et al. (2003) reported that the static and dynamic modulus of elasticity, RHA and SF addition gave similar or marginally superior properties than the control concrete. For a w/b ratio of 0.32, the tensile splitting strength of RHA and SF concrete mixes are marginally lower than the control concrete. The flexural strength and modulus of elasticity of RHA concrete are superior (see Table 2.10).

Table 2.10: The mechanical properties of various RHA mixes (w/b = 0.32)
(Mahmud, H.B. et al., 2003)

Mix No.	Tensile strength (MPa)		Flexural strength (MPa)		Static modulus (GPa)	
	7d	28d	7d	28d	7d	28d
	OPC	4.7	4.9	6.1	6.7	30.4
RHA15A	4.3	4.7	6.2	7.9	30.7	31.8
SF15A	4.4	4.7	6.6	8.2	31.0	33.9

According to Neville, A.M. (1995) the tensile strength of concrete is generally in the range of 7-11% of the compressive strength. The tensile and bond properties are shown to be improved by the addition of RHA up to 25% of cement replacement (Saraswathy & Song, 2007). In addition, Mahmud, H.B. et al. (2003) found that water curing provided the best mechanical properties compared to air-drying curing. Partial wet curing for three days exhibited better mechanical properties than the air-dried ones (see Table 2.11 and Table 2.12).

Table 2.11: Mechanical properties for various RHA mixes (w/b = 0.32)

(Mahmud, H.B. et al., 2003)

Mix No.	Types of Curing	Flexural strength (N/mm ²)				Splitting strength (N/mm ²)			
		7d	28d	90d	180d	7d	28d	90d	180d
OPC	Water	4.5	6.3	7.0	7.6	3.7	4.0	4.3	4.6
	Air	4.0	5.3	6.0	6.8	3.4	3.6	3.7	4.1
	Partial	4.3	6.0	6.4	7.2	3.6	3.8	4.0	4.3
RHA10A	Water	6.5	7.9	8.4	8.8	4.0	4.5	5.0	5.4
	Air	5.8	7.0	7.4	7.9	3.8	4.0	4.5	4.8
	Partial	6.4	7.7	7.9	8.3	3.9	4.4	4.7	5.3
RHA5R	Water	5.4	7.0	8.3	8.9	3.7	4.0	4.9	5.3
	Air	5.0	6.3	7.3	8.0	3.4	3.5	4.1	4.9
	Partial	5.2	6.8	7.6	8.4	3.6	3.7	4.5	5.1

Table 2.12: Mechanical properties for various RHA mixes (w/b = 0.32)

(Mahmud, H.B. et al., 2003)

Mix No.	Types of Curing	Static modulus of elasticity (GPa)				Dynamic modulus of elasticity (GPa)			
		7d	28d	90d	180d	7d	28d	90d	180d
OPC	Water	31.5	32.8	34.3	35.7	42	44.8	45	45.2
	Air	25.4	29.2	31.5	32.8	35.7	37.3	38.3	40.4
	Partial	30.6	32.7	33.1	35.2	40.1	41.1	42.5	42.8
RHA10A	Water	30.2	31.1	36.0	37.7	41.6	43.0	44.3	45.4
	Air	28.6	29.4	30.6	34.2	37.1	38.3	39.0	40.9
	Partial	30.0	30.6	34.4	36.8	41.0	41.9	42.7	42.8
RHA5R	Water	31.5	33.0	35.8	37.2	45.0	46.0	46.4	47.0
	Air	25.1	27.2	30.6	34.3	38.2	34.6	37.2	42.4
	Partial	30.9	32.0	34.1	35.4	40.7	43.0	44.2	45.3

2.5 Time dependent deformation

2.5.1 Effect of RHA on drying shrinkage

There is limited information about drying shrinkage regarding to mineral admixtures especially RHA. It is assumed that most of the mineral admixtures are found to behave similarly with regard to drying shrinkage. (Mahmud, H.B. et al., 2002) found the drying shrinkage of OPC, RHA and SF concrete are 241 $\mu\epsilon$, 308 $\mu\epsilon$ and 338 $\mu\epsilon$, respectively, at 180 days. (Zhang, M.H. et al., 1996) reported drying shrinkage on concrete containing 10% RHA, and 10% SF concrete. After 448 days, the result shows that their shrinkage is similar, about 640 $\mu\epsilon$. Sugita et al. (1992) reported that mortar containing either RHA or SF showed larger shrinkage than the control. The drying shrinkage increased with increasing amounts of RHA. The final shrinkage of 5 % RHA concrete was 1767 $\mu\epsilon$ but increasing RHA content up to 15% increase its shrinkage to 2397 $\mu\epsilon$. It is believed that regardless of the type of mineral admixtures used, the shrinkage values are considerably dependent on the fineness of the admixture. It has been reported that the shrinkage would increase by increasing the fineness of the filler (Cochet & Sorrentino, 1993; Mindess, S. et al., 2003; Nehdi, M. et al., 2003).

2.5.2 Restrained shrinkage

Restrained shrinkage in concrete can cause cracking which is a major durability problem for pavements and restrained structures (Tongaroonsri & Tangtermsirikul, 2009). The ingress of water and aggressive chemicals allow through cracks in concrete leading to accelerated corrosion of reinforcing steel. Cracking may cause unnecessary deflections which may limit the serviceability of structures. Although, high performance concrete can offer high strength and low permeability, it may develop considerable autogenous shrinkage due to self-desiccation at early age.

The behavior of shrinkage cracking observed through free shrinkage tests do not present sufficient information because all concrete elements are restrained in some ways, such as by reinforcement, by their boundary or even within the elements. Restrained shrinkage test has been developed to measure the shrinkage cracking behavior of concrete (Wiegrink et al., 1993). Test methods commonly used for evaluating restrained shrinkage cracking of concrete are ring test, plate test and bar test (Wiegrink et al., 1993). The disadvantage of ring test is that the restrained strain cannot be directly calculated like the restrained shrinkage of bar specimen. However, the ring test is widely used to assess the potential of shrinkage cracking due to its simplicity and versatility (Cusson & Hoogeveen, 2007; Tao & Weizu, 2006). The plate test provides a biaxial restraint that depends on geometry and boundary conditions. Several studies utilized linear specimen geometries due to the advantage of straightforward data interpretation, to assess the potential of shrinkage cracking. In their research, the measurements of shrinkage, tensile creep, tensile elastic modulus and tensile strength in the early ages of the concretes were made. These measurements were carried out in two specimens, one subjected to a simulated fully restrained condition and other free shrinkage conditions. The tests were carried out using a test rig developed for these tests based on a similar concept by Kovler.

Altoubat and Lange (2001) conducted restrained concrete at early age by using restrained uniaxial test. They studied on effects of fibre reinforcement (steel and polypropylene), water-cement ratio (w/c), drying conditions, and curing conditions on restrained shrinkage behaviour of normal concrete (De Sensale, Gemma Rodríguez, 2006) and high-performance concrete (HPC). They found that tensile creep relaxed shrinkage stresses by 50% and doubled the failure strain capacity. Both the magnitude and time history of the shrinkage stress influenced the time of cracking, which in this study occurred at approximately 80% of the static tensile strength. Steel fibres

substantially delay the shrinkage cracking, but without influencing the stress at failure. Finally, they found that sealing of the concrete specimens did not eliminate the early age shrinkage, and that wet curing effectively relaxed shrinkage stresses.

Tarek and Sanjayan (2008) investigated all the factors contributing to early age shrinkage cracking in concrete, namely, shrinkage, tensile creep, tensile elastic modulus, tensile strength of concretes, and studied the effect of slag as a binder on these factors. The above-mentioned factors were measured in early age concretes made with 0, 35, 50 and 65% level replacement of ordinary Portland cement by slag. All the concretes studied were moist cured for 7-days. They found that at lower stage replacement levels of 0, 35 and 50% the tensile strength decreased with increasing slag replacement. There was no significant change found in tensile creep with the changing slag levels. The study shows that the influence of the tensile elastic modulus is a major consideration for early age cracking of slag concretes. Later Tarek and Sanjayan (2008) also studied four types of concrete mixes: concretes made with ordinary Portland cement (OPC) and slag-blended cements with 35%, 50% and 65% replacement of OPC. Two identical specimens of each mix were tested: one subjected to fully restrained conditions and the other allowed to shrink freely, both under the drying conditions of 23°C and 50% relative humidity at the age of 24 h. Indirect tensile tests were also performed in the same concretes to monitor the tensile strength development. It was found that the tensile creep played a significant role in relieving the tensile shrinkage stresses developed in all restrained concrete specimens. Creep strain compensated for approximately 50% of the shrinkage strains. They concluded that increasing slag contents decreased the tensile strength, which is detrimental to crack resistance. However, with increasing slag contents, the elastic modulus also decreased, which is beneficial to crack resistance.

Tongaroonsri and Tangtermsirikul (2009) studied on cracking behavior at the medium age of uniaxial restrained specimens containing different types of mineral admixture, namely fly ash and limestone powder. The study of the potential of cracking of concrete under restrained shrinkage condition was utilizing the uniaxial restrained shrinkage, free shrinkage and strength tests. They investigated the influences of water to binder ratio, mineral admixtures and curing period of concrete on cracking behavior. The results showed that cracking age and cracking strain of restrained specimens vary with mix proportion, mineral admixture and curing period. In addition to cracking strain and amount of shrinkage, shrinkage rate and tensile creep also influence the potential of shrinkage cracking. Mixture with lower water to binder ratio ($w/b = 0.35$) shows shorter cracking age than the mixture with higher water to binder ratio ($w/b = 0.55$). Fly ash and limestone powder significantly increase cracking age of concrete. The cracking age increases with the increase of the replacement ratio of fly ash. They concluded that the rate of shrinkage is higher when exposed to drying and the concrete with longer curing period leads to shorter cracking age.

2.6 Durability properties of RHA concrete

Most mineral admixtures have a favourable influence on the strength and durability of concrete. ACI Committee 201 defined durability of Portland cement concrete as its ability to resist weathering action, chemical attack, abrasion, or any other process of deterioration. Durable concrete will retain its original form, quality, and serviceability when exposed to its environment. Thus, concrete durability is strongly related to the quality of its cover, which corresponds to the first few centimetres of material below the surface of the structure. Porosity and permeability are widely recognized durability indices, since they quantify the resistance of the material against penetrating agents. Current tests on site absorption and permeability are based on measurements of liquid or air flow. They include capillary suction, initial surface absorption test (ISAT) and Figg

test (Mahmud, H.B. et al., 1997). The presence of RHA in OPC concrete will enhance deterioration resistance such as chloride, freeze-thaw, and alkali-silica reaction.

2.6.1 Permeability

It is known that the permeability controls deteriorations of concrete in the aggressive environment (Damtoft et al., 1999; Mehta, 2002), because the process of such deteriorations as carbonation, chloride and sulphate attack are governed by the fluid transportation in concrete. The addition of fillers and pozzolanic materials are introduced to improve the strength and other properties of concrete for necessary conditions. A study on compressive strength and water permeability of concrete containing a new material is therefore of considerable interest. Previous investigation showed that inclusion of RHA decreased permeability of concrete (Coutinho, 2003; Maeda et al., 2001; Speare et al., 1999).

2.6.1.1 Absorption

Speare et al. (1999) showed that absorption characteristic of RHA concrete such as absorption by immersion, initial surface absorption (ISA) and sorptivity decreased compared to the control concrete. They show that, after 1 hour, the ISA value of the control concrete was about 0.083 ml/m²/s while 10% RHA concrete decreased the ISA value up to 50%. (Coutinho, 2003) reported that sorptivity values for concrete with 10%, 15% and 20% replacement by RHA are lower than the control concrete. Compared to the SF concrete, the sorptivity of these mixes was also lower.

Givi et al. (2010) studied the effect of two types of particle size of RHA, 95 µm and 5 µm, in water absorption in concrete with w/b ratio of 0.4. The replacement of cement with RHA was 5%, 10%, 15% and 20% by weight. They concluded that the percentage,

velocity and coefficient of water absorption significantly decreased with 10% cement replacement by the 5 μm particle size of RHA.

2.6.1.2 Porosity

Maeda et al. (2001) reported that the total porosity of concrete containing 5% and 10% RHA was about 72% to 90% lower than the control concrete, respectively. About 68% to 82% of its porosity had pore radius more than 50 nm. However, the pore size distribution of concrete tended to shift towards the smaller range of pores (Figure 2.13).

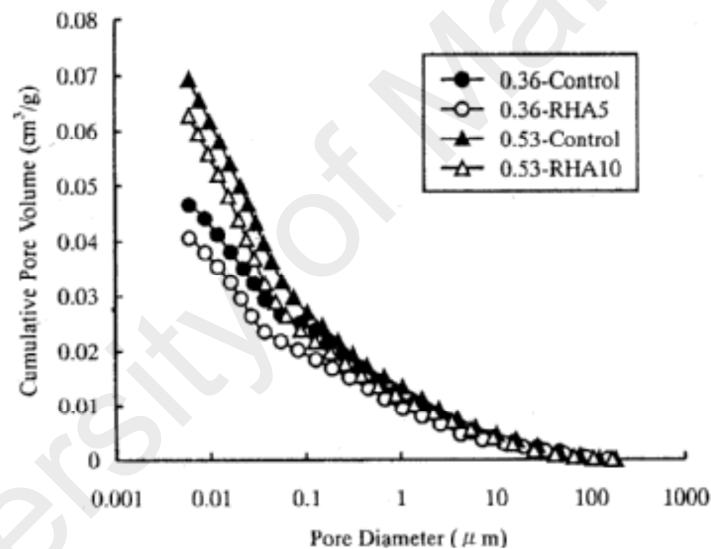


Figure 2.13: Effect of RHA on pore size distribution
Adopted from (Maeda et al., 2001)

Chindaprasirt and Rukzon (2008) studied porosity of mortar containing RHA and fly ash at 7, 28 and 90 days age. The results show that at the age of 7 days, the porosities of mortar containing 10% and 20% of pozzolans and the blend of pozzolans are lower than that of the control at all ages. This results in pore refinement and a reduction of calcium hydroxide in paste. The mortar containing FA gives slightly less porosity than that of RHA. In other word, FA is slightly more effective in modifying pore and reducing the

porosity of mortar. The porosity of 20% FA mortar is 17.3% in comparison with 17.8% of both OPC and 20% RHA mortars. The addition of fine particles of FA and RHA causes segmentation of large pores and increases nucleation sites for precipitation of hydration products in cement paste (Aïtcin, P.C., 2001).

However, at high replacement level of 40%, the porosities of the mortars containing pozzolans increase in comparison with that of the control. At the age of 7 days, the porosities of 40% FA, 40% RHA and 20%FA+20% RHA mixes are 21.0%, 21.8% and 19.4%, respectively, which are significantly larger than 17.8% of the OPC mortar. The increases in porosity with a relative large amount of pozzolans are resulted from the reduced amount of OPC. These results showed that in less hydration products especially at the early age the pozzolanic reaction is small. It should be pointed out here that although the porosity is increased, the beneficial effect of pore refinement as a result of the incorporation of pozzolan exists. Cordeiro, G. C. et al. (2009) reported utilizing RHA with high carbon content in concrete. They concluded that there are slightly refinements in the pores in present of RHA in concrete. The amount of pores less than 0.02 μ m increased from 3.7% to about 5%. Also there is no substantial different in the pores distribution since the proportion of concrete mixtures applied maximum packing density.

2.6.1.3 Sorptivity

Sorptivity is a measure of the capillary forces exerted by the pore structure causing fluids to be drawn into the body of the material (Hall, 1989). Ganesan et al. (2008) reported the sorptivity values on RHA blended concrete specimens after 28 and 90 days of curing. As seen in Table 2.13, sorptivity progressively decreases with increasing in RHA content up to 25% at 28 days of curing. However, there is an increase in sorptivity at 30% and 35% RHA but still lower than that of control concrete. At 90 days of

curing, the sorptivity of concrete containing 10% up to 35% RHA reduced almost 50% than that at 28 days and all sorptivity of RHA concrete was lower than that of control concrete. It showed that prolonged curing to RHA concrete affected reduction in pore space.

Table 2.13: Permeability related properties of RHA blended concretes

(Ganesan et al., 2008)

Mix designation	RHA (%)	Sorptivity x 10 ⁻⁶ (m/s ^{1/2})	
		28 Days	90 Days
RO(control)	0.00	10.50	9.76
R1	5.00	10.60	7.09
R2	10.00	9.16	4.86
R3	15.00	7.37	4.09
R4	20.00	6.00	3.61
R5	25.00	5.53	2.28
R6	30.00	6.08	3.38
R7	35.00	10.30	4.04

The relationship between sorptivity and compressive strength was reported by (De Schutter & Audenaert, 2004) (Al-Amoudi et al., 2009) (Bozkurt & Yazicioglu, 2010) They observed that there is good correlation between the coefficients of sorptivity and the values of compression strength. As the compressive strength of concretes increased due to hydration, meanwhile the sorptivity significantly decreases indicating a denser microstructure. Saraswathy and Song (2007) performed water absorption test according to ASTM C642-97 for concrete containing RHA up to 30 %. They reported that the coefficient of water absorption reduced by incorporating RHA in concrete in all percentages replacement level. Givi et al. (2010) reported that the water absorption coefficient lower for ultrafine RHA (average particle size of 5 µm) replaced concrete compared to control concrete up to 20%. However, RHA (average particle size of 95 µm) concrete showed greater water absorption value than OPC.

2.6.1.4 Initial surface absorption (ISA)

Initial surface absorption test (ISAT) is variedly used to measure the durability of concrete which is important for a long life of structures to resist chemical attacks, and physical impacts. Initial surface absorption value is the rate of flow of water per unit area into a concrete surface with a constant head of 200 mm. Paulini (2012) explained that the degradation mechanism of concrete mostly begins from surface planes and the ingress of harmful material to concrete which gradually affect to reinforcement. Near surface concrete has higher porosities and coarser pore system than core concrete due to insufficient hydration and water evaporation during fresh concrete. The mechanical properties and durability of concrete mainly depend on the refinement of microstructure of the hardened cement paste and improvement of paste aggregate interface zone (Nili et al., 2010). According to the Concrete Society that ISA values at 10 min that are greater than $0.50 \text{ ml/m}^2/\text{s}$ can be considered as high and values smaller than $0.25 \text{ ml/m}^2/\text{s}$ can be considered as low. Furthermore, the ISA values at 120 min that are greater than $0.15 \text{ ml/m}^2/\text{s}$ can be considered as high and values smaller than $0.07 \text{ ml/m}^2/\text{s}$ can be considered as low.

Kartini and Mahmud (2010) reported the improvement of microstructures on near surface RHA concrete as they compared RHA and SF concrete and OPC concrete. It shows that pozzolanic materials reduce the permeability of concrete as SiO_2 from pozzolanic material reacted to CaOH on capillary and the product of reacted material blocked and segmented the capillary. In the interfacial zone of aggregate and cement paste, such modification of microstructure by RHA produces more dense concrete with fewer pores. Kartini and Mahmud (2010) reported the ISA values of a concrete containing 20% RHA as well as a concrete containing 30 % RHA along with superplasticizer. The results showed that ISA values of these concretes are lower than OPC concrete mixes. Their reason on improving RHA concrete on ISA value is it

might be due to reduction in the average pore radius of concrete due to the formations of C-S-H gel from primary hydration and secondary pozzolanic reaction that gradually fill the original water filled space.

2.6.2 Chemical resistance

The enhancement of the resistance to chloride penetration is one of the benefits of incorporation of pozzolans. It is generally accepted that incorporation of a pozzolan improves the resistance to chloride penetration and reduces chloride-induced corrosion initiation period of steel reinforcement. The improvement is mainly caused by the reduction of permeability/diffusivity, particularly to chloride ion transportation of the blended cement concrete (ACI-363, 2002; Mbessa & Péra, 2001; Mehta & Aïtcin, 1997).

2.6.2.1 Chloride resistance

Sugita et al. (1992) reported that loss of weight of RHA mortar subjected to 2% HCl solution was decreased in comparison to the control mortar. This indicated that the addition of RHA in mortar improved its resistance to the acid attack. Maeda et al. (2001) also studied the effect of RHA concrete on the chloride diffusivity with w/b ratio of 0.30, 0.36 and 0.53. The specimens were subjected to chloride solution by using the accelerated chloride method. The results showed that at 10% addition of RHA, the chloride diffusion is lower than the control concrete (Figure 2.14).

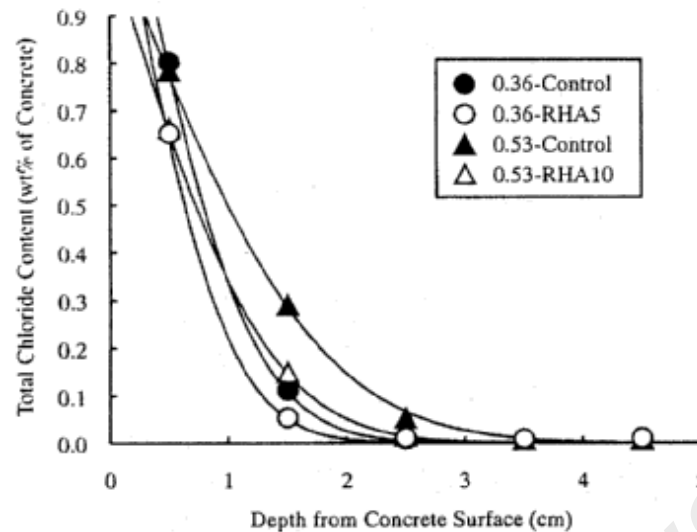


Figure 2.14: Effect of RHA on total chloride content distribution
Adopted from (Maeda et al., 2001)

Speare et al. (1999) reported that increasing RHA content up to 12.5% decrease its rapid chloride penetrability from low rating to the very low rating at 28 days. Compared to the water cured, chloride penetrability of RHA concrete subjected to 10% sodium chloride solution for nine months was about 95% of the control. Its strength reduction was minimal in comparison to the control concrete (Speare et al., 1999). This result indicated that the strength change of RHA mixes under prolonged exposure to chloride was not significant. Nehdi, M. et al. (2003) concluded that rapid chloride penetrability of RHA concrete reduced significantly (see Figure 2.15).

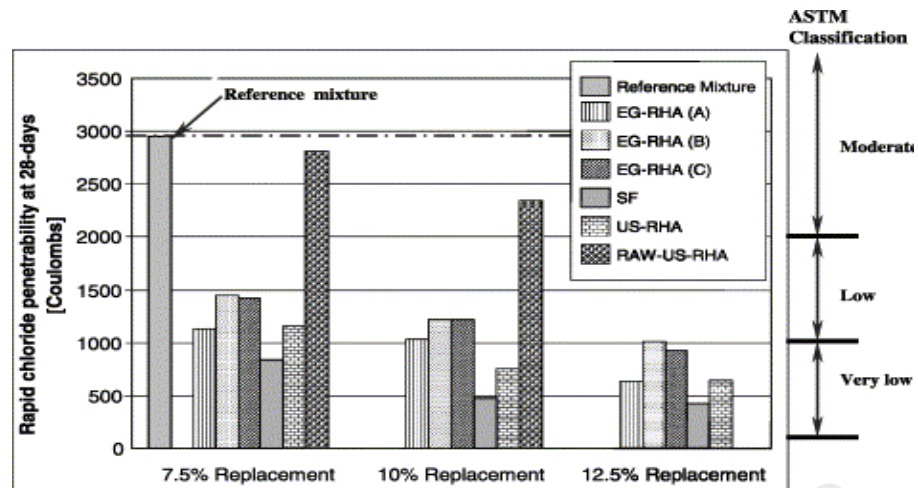


Figure 2.15: Rapid chloride penetrability at 28 days for various concrete mixes
Adopted from (Nehdi, M. et al., 2003)

2.6.2.2 Sodium sulphate resistance

Mazlum and Uyan (1992) studied the effect of RHA on the durability of mortar with a w/b ratio of 0.57. RHA was used as a cement replacement at 10%, 20% and 30% by weight. After 28 days of water curing, samples were subjected to 0.35 M $\text{Na}_2\text{SO}_4 \cdot 10\text{H}_2\text{O}$ solution and tested up to 12 weeks. The result showed that the flexural strength of the control mortar stored in sulfate solution decreased. On the other hand, RHA mortar still produced greater values of flexural strength than the control mortar. For example, after 12 weeks of immersion, the relative flexural strength of the control mortars was about 64% while the 30% RHA mortars exhibited in the range of 135% to 140%. Moreover, they concluded that RHA can be used in sulfate environments successfully.

2.6.2.3 Magnesium sulphate resistance

To maintain durability of concrete it should be concern also on sulphate attack. The sulphate ions in the solution, which come from soil, ground water, and seawater, are found in combination with other ions such as sodium, potassium, magnesium and calcium ions. According to the Durability Guide of ACI 201 Committee, they classified

the aggressiveness of sulphate environments based on the concentration of SO_4^{2-} (g/l) and suggest MgSO_4 is more aggressive. MgSO_4 reacts with all cement compounds, including C-S-H, thus decomposing cement, and subsequently forming gypsum and ettringite. The sulphate ions react with C3A and $\text{Ca}(\text{OH})_2$ to produce expansive and softening types of deterioration. Under sulphate attack, mechanical properties of concrete were changed due to the enhancement effect of delayed ettringite crystal and weakening effect of damage evolution (Yimazt, 1997 ; Marchan, 2002). In the first stage of sulphate attack, the nucleation and growth of delayed ettringite crystal fills the pores of samples which lead to decrease of the porosity of concrete. It causes the surface hardness of samples increases. In further stage, the damage on surface of concrete due to the expansion force of the delayed ettringite decrease the surface hardness. Ramezaniapour et al. (2009) reported that blended cements prepared with RHA reduced the potential for the formation of ettringite due to the reduction in the quantity of calcium hydroxide and C3A, and thus improved the resistance of specimens to sulphate attack. (Chindaprasirt & Rukzon, 2008) also revealed that concrete mixed with RHA and immersed in 5% magnesium sulphate and 5% sodium sulphate had good resistance to sulphate attack. Chewan et al. (2014) reported the usage of RHA on sulphate attack in wet and dry cycling and show that the incorporation of RHA as cement replacement significantly improved the resistance to sulphate penetration of concrete.

2.7 Mixing technique

The main purpose of concrete mixing is to achieve a uniform mixture of all materials. Mixing is especially important for high performance concrete (HPC) of low binder content. Poorly mixed concrete not only fails to meet the requirement of workability, but also affects its engineering properties. Khalaf (1995) has collected and analyzed concrete mixing methods in various countries. He concluded that the method of first

mixing the binder and then followed by the addition of aggregate can reduce the amount of water and cement needed in the process and at the same time lead to an increase in strength of about 10-20%. However, the result was related to normal concrete. In addition, the type of mixer used also has a large influence on the mixing efficiency and uniformity of concrete. The drum type concrete mixer is most commonly used.

The effects of a two-step mixing method upon the properties of concrete mixtures containing superplasticizer admixtures have been investigated by (Rejeb, 1996). The processes of this method are described as the materials and machines employed. The properties of the two-step mixed concrete and conventional concrete are compared. At 28-day age, concrete mixed by the two-step mixing method showed about 8 to 17% higher compressive strength than the concrete mixed by the normal method, depending upon the water to cement ratio, the mixing process and the type of mixer. Further, he explained that concrete mixed by the premixing of grout process gave higher strengths than the concrete mixed by the premixed cement paste process.

Chen, C.T. and Struble (2009) have studied cement pastes containing a high-range water-reducing admixture and prepared using various mixing sequences by using dynamic rheology. Samples were prepared using delayed admixture addition, delayed water addition, double mixing, and vigorous mixing techniques. The effects of the mixing sequence varied with cement composition, admixture dosage, and time of addition. In these mixing sequences, delayed admixture addition was the most effective way to enhance the dispersion. A delay time of 2.5 minutes was sufficient to disperse all the cement-admixture combinations. With delayed water addition, there exists an optimum amount of delayed water. With double mixing, pastes with longer time intervals between the mixing were dispersed more. With vigorous mixing, the pastes were, in general, dispersed by the admixture. The dispersing effect, however, was not

apparent at low admixture dosages. The results of this study demonstrate that the batching sequence and mixing procedure must be taken into account when comparing different concrete batches, even though they have same mixture proportions and raw materials.

2.8 Microstructure

Nowadays the trends to study concrete through microstructure get more attention due to its reliability. The porosity and pore size distribution and the crystal shape form in concrete are mostly be a focus of research in concrete. The microstructure of concrete can be studied through Scanning electron microscope (SEM). Chopra, D. and Siddique (2015) studied RHA concrete through SEM images of unblended SCC (100% OPC), 10% RHA, 15% RHA and 20% RHA. They observed that micro pores have decreased due to hydration progress. C-S-H gel is more widely spread in this case giving a uniform dense structure than unblended concrete and pore structure is improved to a greater extent. Through SEM, they show in Figure 2.16 that 15% RHA is better in performing CSH and show more homogeneous and dense. In 10% RHA and 20% RHA, the RHA concrete show some voids and cracking. In 20% RHA replacement, it was observed that concrete has started crumbling as the amount of RHA is increased and it reduced strength and degraded durability.

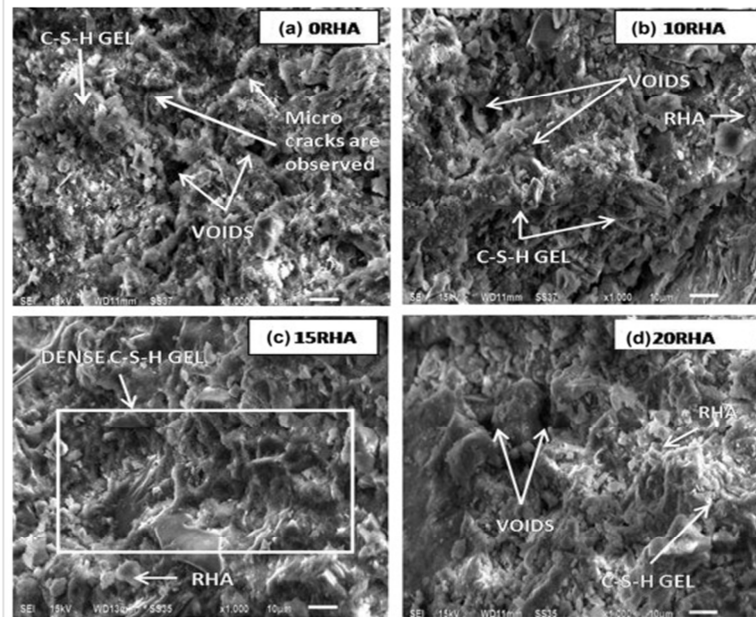


Fig. 6.

Figure 2.16: Microstructure of RHA concrete
Adopted from (Venkatanarayanan & Rangaraju, 2015)

Venkatanarayanan and Rangaraju (2015) studied the effect of grinding of low carbon RHA through the change of microstructure in concrete pores. He reported that fine RHA has better effect on microstructure of concrete compared to the coarse size. For the coarse RHA, the internal porosity created in the matrix and their inability to completely participate in pozzolanic reaction may be the reasons the matrix pores still higher than fines one.

CHAPTER 3: MATERIALS AND EXPERIMENTAL PROGRAMS

3.1 Introduction

This chapter describes the material used and various experimental programs in this study. The standards adopted for justified materials and test procedures in this study are BS and ASTM standards.

3.1.1 Cement

Local cement product, Tasek cement, was used and classified as Ordinary Portland Cement (OPC) which is fulfilled ASTM C 150 type I (ASTM-C150, 2004). The specific gravity (SG) of cement was determined according to British Standard (BS 1377, 1990) using the small pycnometer method. For the specific surface area analysis, the Blaine test was conducted in the laboratory according to (ASTM-C150, 2004). Its chemical composition and physical properties are presented in Table 3.14.

Table 3.14: Chemical composition and physical properties of cement

Chemical composition		Tasek Cement (%)
Silicon dioxide	SiO ₂	21.54
Aluminum oxide	Al ₂ O ₃	5.32
Ferric oxide	Fe ₂ O ₃	3.63
Calcium oxide	CaO	63.66
Manganic oxide	Mn ₂ O ₃	1.08
Carbon dioxide	CO ₂	N/a
Sulphur trioxide	SO ₃	2.18
Physical properties		
Loss on ignition (%)	LOI	2.5
Blaine fineness (cm ² /g)		3050
Specific gravity (kg/m ³)		3140

3.1.2 Rice husk ash (RHA)

3.1.2.1 Combustion of RHA

Rice husk was collected from a dump site at a rice mill in Kuala Selangor. Then rice husk ash was produced by burning rice husk in a ferrocement incinerator in the

University of Malaya (UM) laboratory, which its capacity is 50-60 kg of rice husk each time. There are some holes in the bottom of incinerator for ventilation and starting fire. To start burning rice husk waste papers are fired at the bottom of incinerator and then the rice husk would slowly burn for about a day. After another day the ash was cool down inside incinerator, the ash is ready to take out. The rice husk before and after combustion and ferrocement incinerator are shown in Figure 3.17.



Figure 3.17: (a) Rice husk (b) ferrocement incinerator (c) rice husk after combustion

3.1.2.2 Grinding of RHA

To grind the RHA to be a certain average particle size, a Los Angeles (LA) machine was used, see Figure 3.18. The machine consists of a rotating drum with an opening at the top of the middle of the drum. Forty mild steel-rods of 10 mm diameter and 500 mm in length were placed into the rotating drum together with about 5 kg of ash. This machine can be set to rotate for 5000 cycles/set using an electric motor speed of 33.3 rpm and by this machine the ash was ground for 15000 cycles, which its duration closed to 360 min. Three types of grinding cycles were conducted to get different average particle size of RHA. F1-RHA, F2-RHA and F3-RHA were grinding on 5000, 15000

and 30000 cycles, respectively. The grounded RHA was tested for particle size analysis and surface area to get the average particle size and specific surface area.



Figure 3.18: The LA machine for grinding RHA

To determine the silica form in the RHA, XRD (the X-Ray diffraction) analyses were performed and the chemical composition of the RHA was determined using the XRF (X-ray fluorescence spectrometry), see Table 3.15. RHA samples were also scanned using electron microscope to show the RHA's particles texture.

Table 3.15: Chemical composition and physical properties of RHA and SF

Chemical composition (%)		RHA (%)	SF (%)
Silicon dioxide	SiO ₂	90.82	92.06
Aluminum oxide	Al ₂ O ₃	0.46	0.48
Ferric oxide	Fe ₂ O ₃	0.67	2.11
Calcium oxide	CaO	0.67	0.40
Sodium oxide	Na ₂ O	0.12	0.63
Potassium oxide	K ₂ O	0.44	0.28
Magnesium oxide	MgO	N/a	N/a
Sulphur trioxide	SO ₃	N/a	N/a
Physical properties (%)			
Loss on ignition	LOI	4.5	N/a

They were scanned with an X-ray diffractometer using *CuK_α* radiation at 40 kV/20 mA, CPS=1 k, width 2.5, speed 2 °/min and scanning from 2θ = 3-70°. The XRD of RHA is shown in Figure 3.19. The specific surface area of RHA was determined by the

nitrogen adsorption test (Muga et al.). Both tests were conducted at the Nanocem laboratories, Institut Pengajian Siswazah, UM. The specific gravity of RHA was determined using the small pycnometer method according to British Standard (BS-1881-1377, 1990). Its particle size analyses were done using the Master Sizer Laser Particle Analyzer with obscuration of 12.3% and beam length of 2.40 mm. Particle size distributions of several cycles of grinding RHA are shown in Figure 3.20.

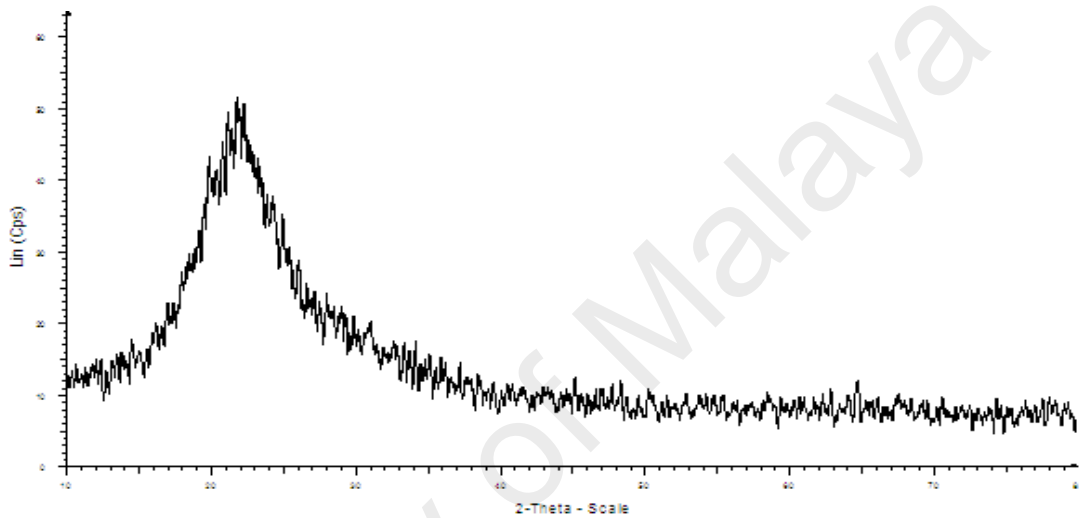


Figure 3.19: XRD of RHA

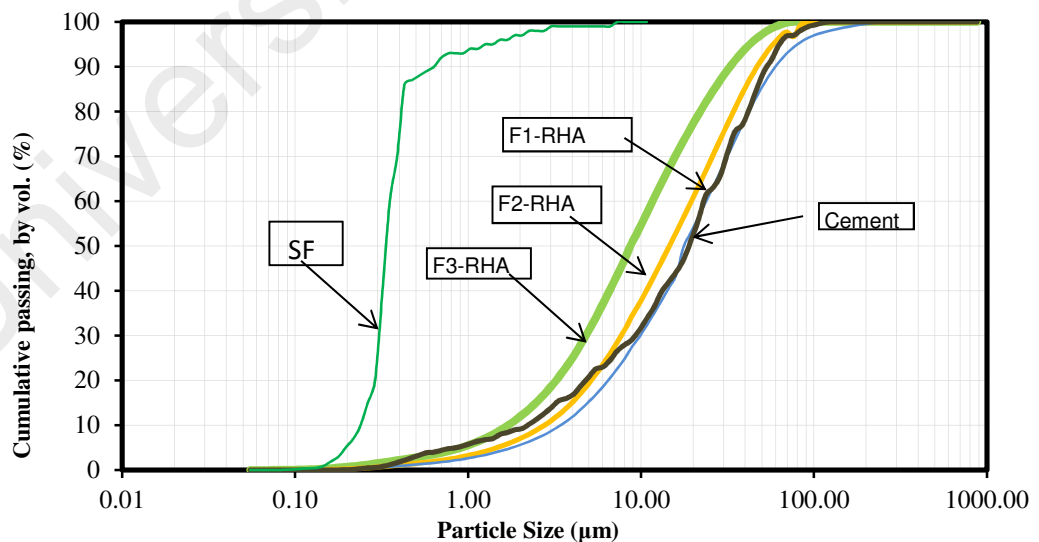


Figure 3.20: Particle size distribution of SCM

3.1.3 Superplasticizer

The usage of high range water reducers is necessary in the low w/b ratio of high performance concrete. High range water reducers, also known as superplasticizer, are chemicals used as admixtures where well-dispersed particle suspension is required. The type of superplasticizer used in this research is polycarboxylate ether-based superplasticizers (PCEs), which is the new generation of this kind of admixtures. Their addition to concrete or mortar allows the reduction of the water to cement ratio, meanwhile not affecting the workability of the mixture, and enables to produce a high performance concrete.

The specific gravity of Superplasticizer is 1.09 and its solid content is 40%. In this study, the dosage of superplasticizer used based on a percentage of the solid content to the binder. The dosage of superplasticizer is adjusted to keep similar workability of mortar mixtures. The new generation of polycarboxylic ether superplasticizer (Speare et al.), Glenium ACE 388 and Viscocrete 2044, was used and classified as a (ASTM-C494, 2004) type F and G admixture, respectively. Type F is water-reducing, high range admixtures and type G is water-reducing, high range, and retarding admixtures. It was supplied by BASF Sdn. Bhd. and Sika Kimia Sdn Bhd., respectively. The recommended Sp dosage of Glenium ACE 388 and Viscocrete 2044 is 0.75-1.2 liters per 100 kg of cement or binder. Specific gravity and solid content of Glenium ACE 388 and Viscocrete 2044 are 1.1, 40% and 1.09, 30%, respectively.

3.1.4 Water

Water is an important constituent in producing concrete and it is required that water is free from organic material and suspended solids which may affect the properties of fresh and hardened concrete. Tap water was used for mixing and curing of concrete and its temperature was about 27°C. Water was visually checked for any dirt that may be

present due to corrosion in the pipeline. The curing water was kept clean from excessive dirt and changed once every two months.

3.1.5 Aggregates

Aggregate is a major constituent in concrete, 70-80% of concrete is aggregate. The Fine aggregate used was mining sand which passed the 4.75 mm sieve. To create three different of fine modulus of fine aggregates, the fine aggregate was then sorted to be three categories of fine modulus by eliminated some part of particle passing sieve #200. Then, the fine moduli of the fine aggregates are 2.64, 2.81 and 3.15. The Coarse aggregate used was crushed granite with angular shape and rough surface texture and its size ranged from 4.75 – 19 mm. It was washed to eliminate the dust and dirt on its surface and air dried before using. The sieve analysis and fineness modulus of fine aggregate was conducted according to the (BS 882:1992) while the specific gravity as well as absorption tests for both coarse and fine aggregate were done as specified in (ASTM-C127, 2004); (ASTM-C128, 2004), respectively. Particle distributions of fine and coarse aggregate are shown in Figure 3.21 and Figure 3.26, respectively. The physical properties of fine and coarse aggregates are shown in Table 3.16.

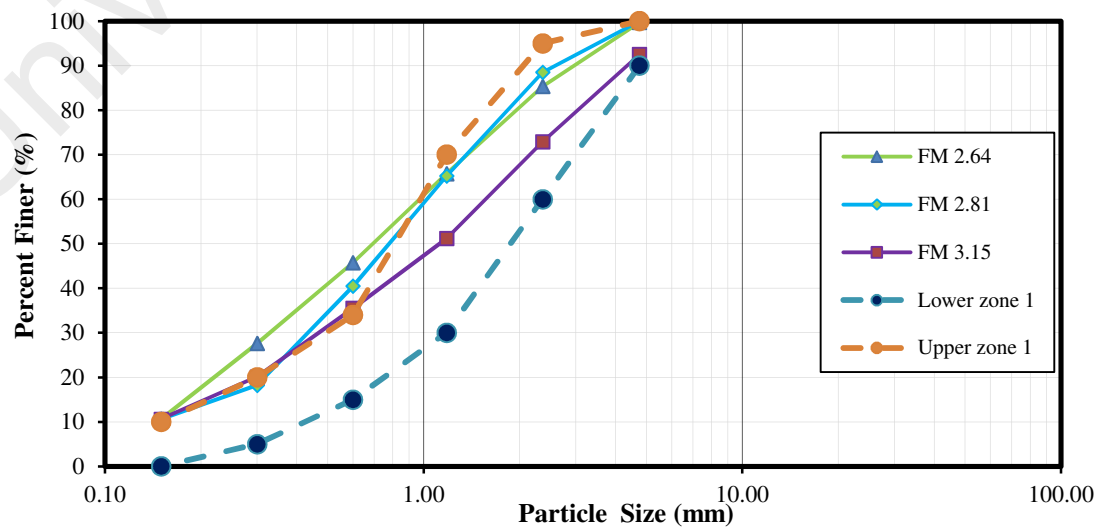


Figure 3.21: Particle distribution of fine aggregates

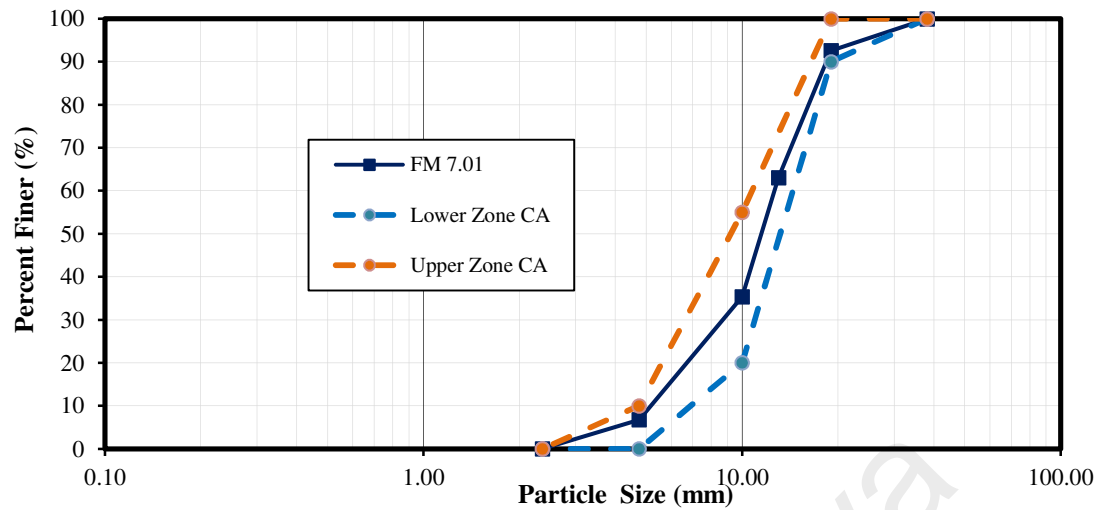


Figure 3.22: Particle distribution of coarse aggregate

Table 3.16: The physical properties of fine and coarse aggregate

Aggregate	Fine modulus	Water absorption (%)	Specific gravity	Max particle size (mm)
Mining sand A	2.64	0.96	2.69	0-4.75
Mining sand B	2.81	0.89	2.68	0-4.75
Mining sand C	3.15	0.82	2.68	0-4.75
Crushed granite	7.02	0.65	2.65	4.75-19

3.2 Mixture proportions

3.2.1 Optimizing composition of aggregates

The composition between coarse aggregate and fine aggregate has effect to minimize using paste in concrete. Various aggregate blends were conducted using air-dry basis fine and coarse aggregate to determine compact and loose bulk densities. The target is to find the optimum ratio of fine aggregate to total aggregate (f_a/t_a) in producing maximum bulk density.

That blended aggregated was prepared by mixing fine aggregate and coarse aggregate with hand and shovel. The amount of 20 kg blended aggregates was used in

this test. This weight was 125% more than the weight of blended aggregate in measured cylinder used for determining bulk density. According to (ASTM-C29/C29M, 2004) the quantity of sample should be in range of 125% to 200% of the quantity to fill the cylinder measurement.

3.2.2 Packing density

3.2.2.1 Modified Andreassen model

The modified Andreassen model was adopted to justify the packing density of mortar incorporating different average particle sizes of RHA. The formula of modified Andreassen model (Funk & Dinger, 2013) is:

$$CPFT = \left(\frac{(d-d_0)}{(D-d_0)} \right)^q 100 \quad \text{Eq. 3.1}$$

Where:

CPFT = the cumulative (volume) percent finer than

d= the particle size

d₀= the minimum particle size

D= the maximum particle size

q= the distribution coefficient, it was adopted = 0.27

In this study, the software adopted in this study is LISA which developed based on Andreassen model.

3.2.2.2 The modified Toufar model

For calculating packing density in aggregates, the modified Toufar model is adopted to calculate the packing of binary mixtures for diameter ratios of $0.22 < d_1/d_2 < 1.0$ (Toufar et al., 1976). The packing density should depend on the diameter ratio of the two particle classes. The concept of the model is that for diameter ratios > 0.22 the

smaller particles with diameter d_1 will actually be too large to be situated within the interstices between the larger particles with diameter d_2 . Therefore, Toufar et al. (1976) considered the statistical probability of the number of interstices between the coarser particles that are free from smaller particles. It was assumed that each of the fine particles is placed between exactly four of the coarse particles, which led to the factor. The total packing density is described by Equations 3.2 (Goltermann et al., 1997).

$$\phi = \frac{1}{\left[\frac{y_1 + y_2}{\phi_1 + \phi_2} - y_2 \cdot \left(\frac{1}{\phi_2} - 1 \right) \cdot k_d \cdot k_s \right]} \quad \text{Eq. 3.2}$$

$$k_d = \frac{(d_2 - d_1)}{(d_1 + d_2)} \cdot k_0$$

$$k_s = \left(\frac{x}{x_0} \right) \cdot k_0 \quad \text{for } x < x_0$$

$$k_s = 1 - \frac{(1 + 4 \cdot x)}{(1 + x)^4} \quad \text{for } x \geq x_0$$

$$x_0 = 0.4753$$

$$k_0 = 0.3881$$

$$x = \frac{\left(\frac{y_1}{y_2} \right) \left(\frac{\phi_2}{\phi_1} \right)}{(1 - \phi_2)}$$

Where:

ϕ = packing degree of combined gradation

y_1, y_2 = volume fraction of fine and coarse aggregates, respectively

ϕ_1, ϕ_2 = packing degree of fine and coarse aggregates, respectively

k_d = diameter ratio factor

d_1, d_2 = characteristic diameter of the fine and coarse aggregates, respectively

k_s = statistical factor

For ternary blending, the first process is by blending two aggregate materials with the highest diameter ratio (fine/coarser) and then blend with the rest.

3.2.3 Surface area

The aggregates used in the study are mining sand and crushed granite as coarse aggregate. To simplify the calculation process for the specific surface area of aggregate particles, we assume that the aggregates used are close to the spherical configuration of different Feret's diameters (Hinds, 2012), which is taken as the average value of the two opening sizes that aggregates passed or held on the sieve. The sieve analyses were performed to assess the particle sizes and percentage, R_i , retained on each sieve. From the obtained particle dimension and weight percentage of each sieve size throughout the entire particle distribution, the specific surface area, S_j , of each aggregate size can be reasonably estimated. Table 3.4 reveals the calculated specific surface areas.

Table 3.17: Calculated specific surface area of aggregates

Sieve size (mm)	Specific surface area (m ² /m ³)
19.1-12.7	378
12.7-9.5	540
9.5-4.75	840
4.75-2.36	1641
2.36-1.18	3361
1.18-0.60	6742
0.60-0.30	13529
0.30-0.15	26906
0.15-0.074	53812

Adopted from (Yen, T. et al., 2000)(Yen et al., 2000)

$$\sum S_j = V_a (R_1 S_1 + R_2 S_2 + \dots + R_n S_n) \quad \text{Eq. 3.3}$$

$$V_a = \frac{\rho_a}{\gamma_a}$$

Where

S_i = the total surface area of aggregates

V_a = the void volume of packed aggregates

ρ_a = bulk unit weight

γ_a = the specific gravity of aggregate

3.2.4 Saturation dosage of superplasticizer

It is important to find the proper dosage of high-range water reducer in order to minimize the amount of its usage and to avoid excess workability and also retardation in concrete. The grout composition used was from the concrete mixture proposed with minus coarse aggregate. The grout was added with high-range water reducer with certain dosage and started with low dosage. Then the grout was put in a trim, see Figure 3.23, and recorded time needed to fill a 200 ml container. There was a point of saturation dosage and beyond this point the addition of dosage of high-range water reducer did not change the time of pouring grout containing high-range water reducer into the trim.

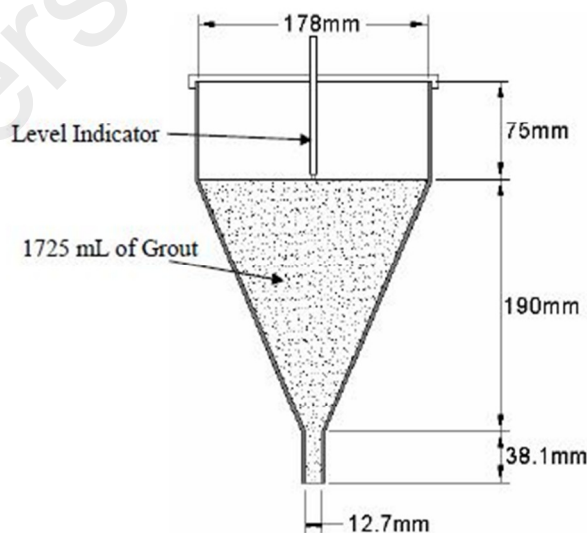


Figure 3.23: Flow cone cross section
Adopted from (Agullo et al., 1999)

3.2.5 Mix design of mortar

To find the average particle size of RHA being used in this study, there are needed to justify through incorporating three different particle size of the RHA on the mortar with similar mix proportion. The labels for three average particle sizes of RHA are F1, F2 and F3 with average particle size of 29.92 μm , 20.43 μm and 13.5 μm , respectively. The cube of 50 mm x 50 mm x 50 mm is adopted as mentioned in (ASTM-C109, 2007). The mortar is placed and compacted through vibrator table. The mortar is demolded after 24 hour and curing in water tank. The sample is tested at 1, 3, 7 and 28 days. The RHA that being chosen is based on the high compressive strength of mortar incorporating RHA. Table 3.18 shows the mix proportion of mortar to be used in justifying the average particle size of RHA used.

Table 3.18: Mix proportion of mortar

Constituent	W/b	Sp (%)	Water (kg/m ³)	Cement (kg/m ³)	RHA (kg/m ³)	Fine aggregate (kg/m ³)
OPC	0.25	0.5	137.5	550	0	733.91
RHA10-F1	0.25	1	137.5	495	55	707.35
RHA10-F2	0.25	1.1	137.5	495	55	707.35
RHA10-F3	0.25	1.2	137.5	495	55	707.35
RHA15-F1	0.25	1.1	137.5	467.5	82.5	692.59
RHA15-F2	0.25	1.2	137.5	467.5	82.5	692.59
RHA15-F3	0.25	1.3	137.5	467.5	82.5	692.59
RHA20-F1	0.25	1.7	137.5	440	110	671.95
RHA20-F2	0.25	1.85	137.5	440	110	671.95
RHA20-F3	0.25	2	137.5	440	110	671.95

3.2.6 Mix design of concrete

To find the optimum mix proportion for concrete having compressive strength of 100 MPa, the response surface methodology (RSM) is applied and design of experiments used is Box-Behnken design (BBD) method. The main factors are water to binder ratio (w/b), binder content, percentages of RHA, ratio of fine to total aggregate and the

percentages of superplasticizer. In BBD, the level of each factor is three. The ranges of each factor are w/b of 0.22-0.28, binder of 500-600 kg/m³, percentage of RHA of 0-20 %, ratio of fa/ta of 0.35-0.45 and superplasticizer of 0.5-1.3 %. The number of mix proportion should be run in this method are 46 mixes. Then, those mixture proportions are based on the Sherbrook mix design method, which adopted absolute volume method and considering solid content of superplasticizer in calculation of mix proportion. The slump of each mix proportion and compressive strength at the age of 1 day and 28 days are being the responses of each mix proportions. By utilizing RSM, the optimum mix proportion considered the response will be found. Then this mix proportion will be used for further study. For comparative study, 10 % silica fume will be used as substitute 10% RHA.

3.2.7 Box-Behnken design (BBD)

In statistics, BBD developed by George E. P Box and Donald Behnken in 1960 is an experimental design for response surface methodology. The parameters involved were carefully selected to carry out this method as it requires at least two factors with exactly three levels of each factor. In this study, five factors at three levels were used to evaluate each factor of the relevant HPC properties. The levels of variables were coded according to equation 3.4. Table 3.6 show the factors and their each level adopted.

$$x_i = \frac{X_i - X_0}{\Delta X} \quad \text{Eq. 3.4}$$

Where:

x_i = Coded at i

X_i = Uncoded at i
 X_0 = Uncoded at 0
 ΔX = The step change value

Five key parameters that have a significant influence on the mix characteristics of HPC were selected to derive the mathematical models for evaluating relevant properties. The modelled experimental region consisted of concrete mixes ranging between the coded variables of -1 to +1 as given in Table 3.19. The derived statistical models are valid for concrete mixes with w/b ranging from 0.22 to 0.28, binder ranging from 500 to 600 kg/m³, RHA percentages ranging from 0 up to 20%, ratio of fine aggregate to total aggregate ranging from 0.35 to 45% and dosages of SP ranging from 0.5 to 1.3 % solid content of binder.

Table 3.19: Level and code of variable chosen for Box-Behnken design

Variables	Symbol		Coded levels		
	Uncoded	Coded	-1	0	+1
W/b	X_1	x_1	0.22	0.25	0.28
Binder	X_2	x_2	500	550	600
%RHA	X_3	x_3	0	10	20
fa/ta	X_4	x_4	0.35	0.4	0.45
%Sp	X_5	x_5	0.5	0.9	1.3

Table 3.20 present the BBD with $k = 5$ and $j = 3$. The design consists of 40 factorial points and 6 additional centers point. It is recommended to add 6 center points for runs. Runs are a series of tests conducted in experiment in order to identify the reasons for changes in the output due to change in the input variables.

Table 3.20: BBD with five variables

Run number	BBD with 5variables				
	X ₁	X ₂	X ₃	X ₄	X ₅
1-4	±1	±1	0	0	0
5-8	±1	0	±1	0	0
9-12	±1	0	0	±1	0
13-16	±1	0	0	0	±1
17-20	0	±1	±1	0	0
21-24	0	±1	0	±1	0
25-28	0	±1	0	0	±1
29-32	0	0	±1	±1	0
33-36	0	0	±1	0	±1
37-40	0	0	0	±1	±1
40-43	0	0	0	0	0
42-46	0	0	0	0	0

For predicting the optimal point, a second-order polynomial model was fitted to correlate relationship between independent variables and response. For HPC in this study, responses (Y) were modelled for slump of fresh concrete, compressive strengths at 1 day and 28 days. In each of the models, the coefficients of the response surface equation were determined by using Design Expert ver.8. The models are given in Eq. 3.5 (Auta & Hameed, 2011).

$$Y = \beta_0 + \sum_{i=1}^k \beta_i X_i + \sum_{i=1}^k \beta_{ii} X_i^2 + \sum_{i < j}^k \beta_{ij} X_i X_j + e(X_1, X_2, \dots, X_3) \quad \text{Eq. 3.5}$$

Where

Y = Response

X_i = variables

i = the number of factors

j = the number of levels

3.2.8 Response surface methodology (RSM)

The goal of the investigation in mixture proportion of concrete is to find the optimum response due to the change of input variables. By utilizing the graph generated by software, it is helpful to see the shape of a response surface through the Eq. 3.6 that can be plotted versus the level of x_1 and x_2 , called as response surface plot, as shown in the Figure 3.24. The plot of response can also be more simplified through two dimensions called contour plot, as shown in Figure 3.25.

$$y = f(x_1, x_2) + \varepsilon \quad \text{Eq. 3.6}$$

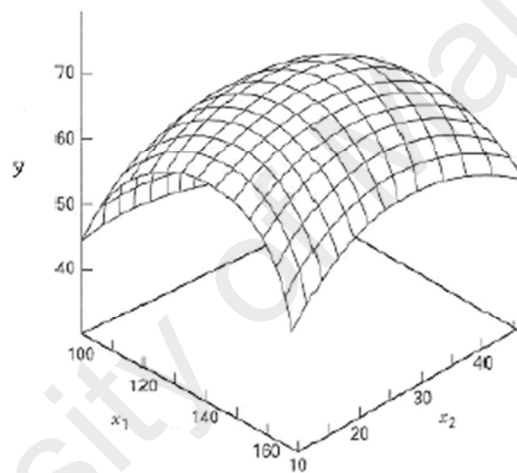


Figure 3.24: Response surface plots
Adopted from (Montgomery, 2005)

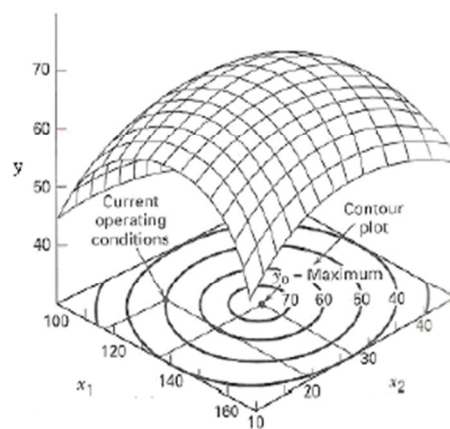


Figure 3.25: Contour plot
Adopted from (Montgomery, 2005)

3.2.9 D-optimal designs

Software Design Expert ver. 8 provides the menus on how to find the optimum response based on the range of variables and then it will provide the relevant values to that response. The D-optimality criterion states that the best set of points in the experiment maximizes the determinant $|X^T X|$. "D" stands for the determinant of the $X^T X$ matrix associated with the model. From a statistical point of view, a D-optimal design leads to response surface models for which the maximum variance of the predicted responses is minimized. This means that the points of the experiment will minimize the error in the estimated coefficients of the response model. Figure 3.26 shows the optimum responses of the mix proportion got from the model.

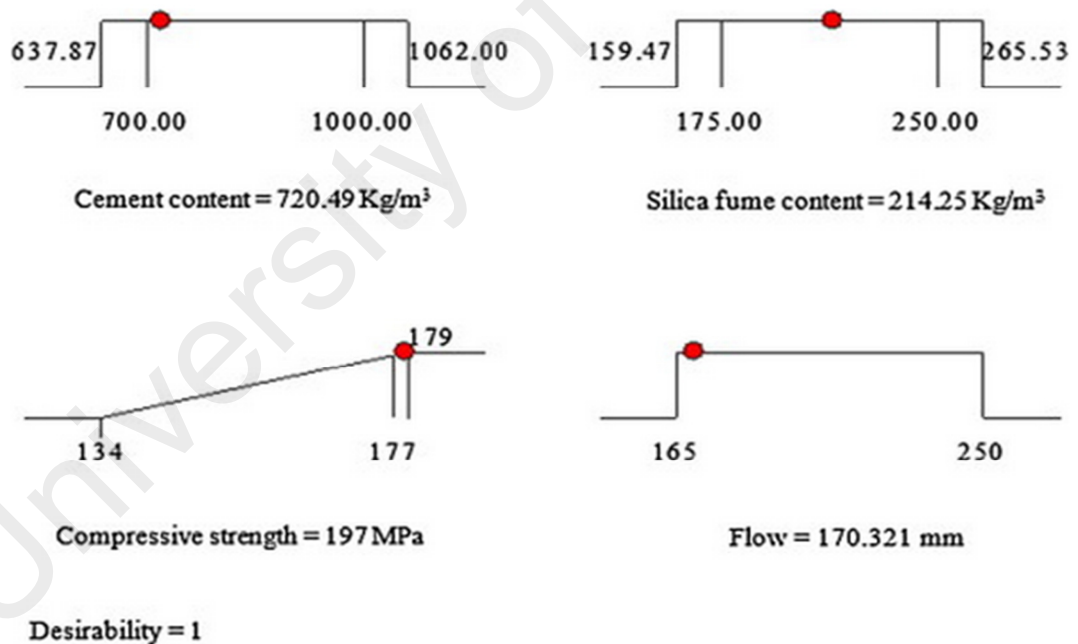


Figure 3.26: Example of responses from suggested mix proportion from model
Adopted from (Aldahdooh et al., 2013)

3.3 Sample preparation

Concrete of 0.2 m³ capacity was mixed in a laboratory concrete mixer, pan mixer, for maximum of 10 minutes. Workability of fresh concrete was measured using the slump test and slump flow. All test specimens, such as standard cubes (100 mm and 150 mm); cylinders (150 mm dia. x 300 mm length and 100 mm dia. x 200 mm length), prism (100 x 100 x 500 mm) and dog bone were cast using steel moulds (75 mm x 75 mm x 1100 mm) and filled in two layers. Each layer was compacted using a vibrating table for 5 seconds except for dog bone was compacted by 25 striking for two layers. The specimens were de-moulded after 24 hours and were cured both in water and air-drying. The specimens for chemical resistant test were immersed in magnesium sulphate solution either without curing (air-drying) or after 7 days initial water curing.

3.3.1 Manufacturing of concrete

In this study, the batching was done by weight and all ingredients of the concrete mixes were prepared according to the calculated mix design proportions. In phase I, the specimens were prepared using 100 mm steel moulds cube. For phase II, five types of specimens were prepared and they were 100 mm cubes, 150 mm cubes, 100 mm x 200 mm length cylinder, 150 mm dia. x 300 mm length cylinders and 100 x 100 x 500 mm prisms.

Before casting, a thin layer of mineral oil was applied at the interior surface of the moulds to ease demolding. In phase I, due to the small amount of concrete i.e. about 0.02 m³, mixing is carried out using a small pan mixer (capacity of 120 kg fresh concrete). For phase II, mixing was done using a pan mixer with the larger capacity of 500 kg. Before filling any material the interior of the pan mixer was wetted with water to prevent mixing water from being absorbed to the side of the mixer. The manufacture of concretes was conducted with two methods such as conventional mixing and two

steps mixing method. The procedures for conventional mixing and two steps mixing methods are shown in Figure 3.27 (a) and Figure 3.27 (b), respectively.

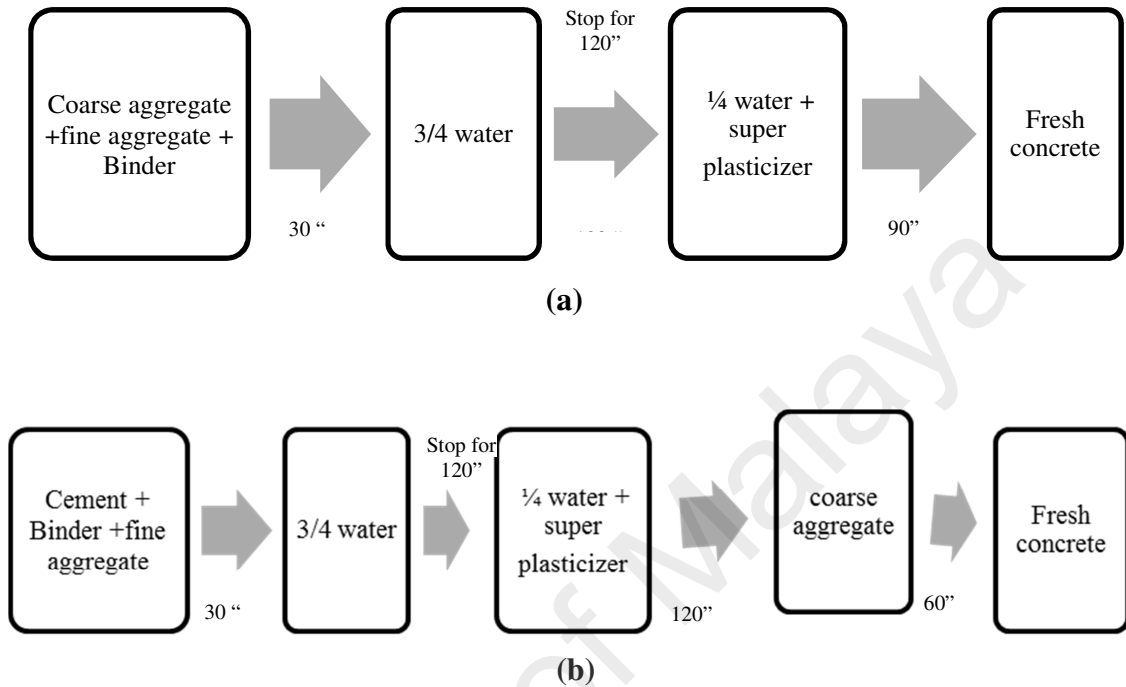


Figure 3.27 (a) Conventional mixing method sequences (b) Two steps mixing method sequences

The moulds were filled with fresh concrete in two equal layers. For each layer, the moulds were vibrated on a vibrating table for about 3 minutes and 5 minutes for phase I and II respectively. After casting, the fresh concrete were covered with the burlap (gunny) sacks to prevent the evaporation of water from fresh concrete. The moulds were demolded after about 24 hours and the specimens labelled. In phase I, all the specimens were subjected to water curing. For phase II, both water curing and air-drying were used until the age of testing.

3.3.2 Size and curing of specimens

To study the effect of curing on the mechanical properties and chemical resistant of concrete mixes, two types of curing i.e. water curing and air-drying were used. For water curing regime, after demolding at 1 day, the specimens were left in water tank until age of test. This type of curing was conducted in accordance to (BS-1881-111, 1983) (BS-1881-111, 1983). For air-drying condition, the samples were left inside the laboratory after demolding at 1 day, until age of test. Details of curing methods for different types of test that were used in this research are presented in Table 3.21.

Table 3.21: Size and curing of specimens

Phase	Type of test	Size of specimen	Types of curing	Age of test (day)	Amount of samples
I	Compressive strength	100 mm cube	water curing	1, 3, 7 and 28	12
II a.	Mechanical properties				
	Compressive strength	100 mm cube	Water curing/air-drying	1, 3, 7, 28, 56, 90 and 180	36
	Static modulus of elasticity	150 mm dia. x 300 mm cylinder	Water curing	28, 90 and 180	6
	Splitting tensile strength	100 mm dia. x 200 mm cylinder	Water curing	28, 90 and 180	6
	Modulus of rupture	100 x 100 x 500 mm	Water curing	28, 90 and 180	6
	Ultrasonic pulse velocity	100 mm cube	Water curing/air-drying	28, 90 and 180	-
b.	Durability				
	Initial surface absorption	150 mm cube	Water curing/air-drying	28, 90 and 180	4
	Sulphate resistance	100 mm cube and 150 mm dia. x 300 mm cylinder	7 days initial water curing/air-drying	* Cycle 1, 2 and 3	9 2
	Sorptivity	Cyl 100x200	water curing/air-drying	28,90 and 180	6

Table 3.21: Continue

Phase	Type of test	Size of specimen	Types of curing	Age of test (day)	Amount of samples
c.	Time dependent deformation				
	Drying shrinkage	150 mm dia. x 300 mm cylinder	7 days initial water curing/air-drying	7, 28, 58, 90 and 180	4
	Restrained shrinkage	Dog bone 100x100x750 Cyl 100x200	Water curing/air-drying	1,2,4,5,6, 7	2 14
	Temperature	100 x 100 x 500 mm		1,2,4,5,6, 7	1

* Each cycle consisting of 30 days of immersion in sulphate solution followed by 7 days of air-drying

3.4 Testing of concrete

3.4.1 Test for material properties

3.4.1.1 Test for cement

The specific gravity of cement was determined by using the small Pycnometer Method according to (BS-1881-1377, 1990); determination of partial density. The value of specific gravity was determined using Eq. 3.7.

$$\text{Specific gravity } (G) = \frac{\rho_L(m_2 - m_1)}{(m_4 - m_1) - (m_3 - m_2)} \quad \text{Eq. 3.7}$$

Where G = Specific gravity of cement or pozzolanic material

m_1 = mass of density bottle, g

m_2 = mass of bottle and cement or pozzolanic material (dry), g

m_3 = mass of bottle, cement or pozzolanic material and kerosene, g

m_4 = mass of bottle when full of kerosene only, g

ρ_L = density of kerosene, Mg/m³

3.4.1.2 Test for RHA

The specific gravity of RHA was determined using Eq. 3.7. Its fineness was obtained according to (BS-3892, 1982); specification for pulverized-fuel ash for use as a cementitious component in structural concrete. X-ray fluorescence (XRF) was employed in this study to determine the chemical composition of RHA. To determine the specific surface area and average diameter of RHA, the test was conducted at the Department of Chemical Engineering, University of Malaya, using ASAP2010, manufactured by Micrometrics Instrument Corporation, USA.

3.4.1.3 Test for fine aggregate

Sieve analysis according to (BS-882, 1992) was performed to obtain the particle size distribution, fineness modulus and grading zone of the fine aggregate. The specific gravity and water absorption was determined using Eq. 3.8 and 3.9, respectively, according to (ASTM-C128, 2004).

$$\text{Bulk specific gravity (saturated-surface dry)} = \frac{A}{[A - (B - C)]} \quad \text{Eq. 3.8}$$

$$\text{Water absorption (\%)} = [(A - D) / D] \times 100 \% \quad \text{Eq. 3.9}$$

Where

A = Weight of saturated-surface dry test sample in air, g

B = Weight of pycnometer containing sample and filled with water, g

C = Weight of pycnometer filled with water only, g

D = Weight of oven dried ($110 \pm 5^\circ\text{C}$) test sample in air, g

3.4.1.4 Test for coarse aggregate

The specific gravity and water absorption of coarse aggregate was obtained according to (ASTM-C127, 2004). The value of specific gravity and water absorption can be calculated as follows:

$$\text{Bulk specific gravity (saturated-surface dry)} = \frac{A}{[A - (B - C)]} \quad \text{Eq. 3.10}$$

$$\text{Water absorption (\%)} = [(A - D) / D] \times 100 \% \quad \text{Eq. 3.11}$$

Where A = Weight of saturated-surface dry test sample in air, g

B = Apparent weight in water of basket and saturated surface dry sample, g

C = Apparent weight in water of empty basket, g

D = Weight of oven dried ($110 \pm 5^\circ\text{C}$) test sample in air, g

3.4.2 Test for fresh concrete

3.4.2.1 Workability

The workability of fresh concrete was measured using the slump test according to (BS-1881-111, 1983) The test consists of a tamping rod and truncated cone i.e. 300 mm height, 100 mm dia. at the top and 200 mm dia. at the bottom. Concrete was filled into

the cone in three height layers. Each layer was tamped with 25 strokes using a 16 mm tamping steel rod (Figure 3.28 (a) and (b)).



(a)



(b)

Figure 3.28: (a) Slump test (b) Slump flow test

When the filling was completed, the top surface was levelled and the mould was lifted vertically with no lateral or twisting motion. The slump was measured by taking the average distance between the top of the mould and lowest points of the concrete surface. The entire testing process was completed within 150 seconds.

3.4.2.2 Air content

The air content of fresh concrete was measured using air content measurement according to (BS-1881-111, 1983), see Figure 3.29. The fresh concrete is gently put into container in three layers and each layer was stroke 30 times distributed in that layer. There should no dirt at the rim of junction of top and bottom of apparatus to provide air tight connection between two halves of the apparatus. After meter was mounted on the container, the contained was stroke by mullet at side of container to release any air.

Water is added through side apparatus until emerge at other side then the tap was clamp down. Air content was read by pushing the green button.



Figure 3.29: Air content of fresh concrete test

3.4.3 Test for mechanical properties of concrete

3.4.3.1 Compressive strength

The compressive strength test of 100 mm cube specimens was determined according to (BS-1881-116, 1983), see Figure 3.30. In phase I, the samples were tested at 1, 3, 7, and 28 days under water curing. For phase II, the specimens were tested at 7, 28, 56 and 180 days, under water or air-drying curing regime. An ELE (Engineering Laboratory Equipment) testing machine with a load capacity of 2000 kN was used. The sample was placed with the cast faces in contact with the platens of the testing machine and loading at the rate of 2.4 kN/s until failure. The compressive strength was calculated by dividing the load at failure by surface area of sample.



Figure 3.30: Compressive strength

3.4.3.2 Static modulus of elasticity

This test was conducted according to (BS-1881-121, 1983) on cylinder specimens (150 mm dia. x 300 mm length) at 7, 28 and 180 days. The test specimen, with the strain measuring apparatus attached axially, was placed centrally in ELE compression testing machine, see Figure 3.31. A basic stress (σ_b) of 0.5 MPa was applied and the strain gauge reading was recorded. The stress was steadily increased at a constant rate of 0.6 MPa.s^{-1} until an upper loading stress equaled to one-third of cylinder compressive strength reading (σ_a) was reached and the strain gauge reading was taken. The cylinder compressive strength (f_{cyl}) was estimated based on the compressive strength of cube (f_c) using the Eq. 3.12.

$$f_{cyl} = 0.85 \times f_c \quad \text{Eq. 3.12}$$

The static modulus of elasticity E_c (N/mm²) was determined as the average value taken from two specimens using the following equations (BS-1881-121, 1983):

$$\text{Strain coefficient} = \frac{0.002}{150} \times 0.5$$

ϵ = Gauge division x strain coefficient

The static modulus of elasticity in compression E_c (GPa) is calculated as follows:

$$E_c = \frac{\Delta\sigma}{\Delta\epsilon} = \frac{\sigma_a - \sigma_b}{\epsilon_a - \epsilon_b} \quad \text{Eq. 3.13}$$

Where σ_a = upper loading ($\sigma_a = f_{cyl}/3$) (MPa)

σ_b = basic stress (0.5 MPa)

ϵ_a = strain under upper loading stress

ϵ_b = strain under basic stress



Figure 3.31: Modulus of elasticity

3.4.3.3 Splitting tensile strength

The splitting tensile strength test was carried out on cylinder specimen (150 mm dia. x 300 mm length) according to (BS-1881-117, 1983), see Figure 3.33. The specimens were tested at 7, 28 and 180 days.

In the test, the specimen was positioned on the center of jig with packing strips placed along the top and bottom. Hardboard packing strips made of plywood i.e. 15 mm width by 4 mm thick were used to prevent local failure. Load was applied and increased continuously at a rate of 1.767 kN/s or 0.025 N/(mm².s⁻¹) until failure.

The splitting tensile strength f_{sp} (MPa) is calculated as follows:

$$f_{sp} = \frac{2F}{\pi \times L \times d} \quad \text{Eq. 3.14}$$

Where F = maximum load (N)

L = length of specimen (mm)

d = diameter of specimen (mm)



Figure 3.32: Splitting tensile strength

3.4.3.4 Flexural tensile strength

The flexural tensile strength test was carried out on 100 x 100 x 500 mm prism specimens according to (BS-1881-118, 1983) at 7, 28, 56 and 180 days. The flexural strength was determined by means of a constant moment in the central zone of the specimen using a two-point loading using the EL 33-6090 flexural testing machine manufactured by ELE Ltd, see Figure 3.33. Load was then applied steadily and continuously at rate of 0.067 kN/s or $0.06 \pm 0.04 \text{ N}/(\text{mm}^2 \cdot \text{s}^{-1})$ until failure. The flexural tensile strength, also known as the modulus of rupture f_r (MPa) can be calculated as follows:

$$f_r = \frac{F \times L}{b \times d^2} \quad \text{Eq. 3.15}$$

Where F = breaking load (N)

L = distance between the supporting roller (mm)

b = width of cross section (mm)

d = depth of cross section (mm)



Figure 3.33: Flexural tensile strength

A pulse of longitudinal vibrations was produced by an electro-acoustical transducer, held in contact with the surface of the specimen. After traversing a known path length in specimen (i.e. 100 mm), the pulse of vibrations was converted into an electrical signal by a second transducer. The time interval for the pulse to travel between the two transducers is measured by the time of the digital indicating device, see Figure 3.34. To ensure that the vibration of the transducer was transmitted to the concrete by close contact, grease was applied on the faces of the concrete and the transducers were pressed hard against the surface. The pulse velocity V (km/s or m/s) is given by

$$V = \frac{L}{T} \quad \text{Eq. 3.16}$$

Where L = path length 100 mm

T = time taken by the pulse to traverse that length (sec.)



Figure 3.34: Ultrasonic pulse velocity test (UPV)

3.4.4 Drying shrinkage test

Drying shrinkage testing was conducted in accordance with (ASTM-C531, 1985). The test method involves measuring the length change (shrink) of 150 mm dia. x 300 mm length concrete cylinders (Figure 3.35). The specimens were air dried for 2-3 hours before the demec discs were applied to the concrete surface using epoxy resin 'Araldite'. An initial reading was taken after 4 hours by using a 200 mm demec gauge (manufactured by W.H. Mayers & Son LTD, England) with 8 μ m accuracy. The specimens were stored in the room at temperature of about 30°C and relative humidity about 80%.

Subsequent length change was conducted at 7, 28, 58, 90, and 120 days. Before each measurement, the length of the demec gauge was calibrated against an invar rod. The drying shrinkage was determined by averaging six sets of readings measured from the two specimens.



Figure 3.35: Measurement of shrinkage test

3.4.5 Durability tests

3.4.5.1 Initial surface absorption test (ISAT)

The purpose of the ISA test was to obtain the time of water flow into concrete per unit area after a stated interval from the start of the test. This test was carried out according to (BS-1881-5, 1970) (Figure 3.36). 150 mm concrete cube specimens were used and tested at the ages of 28, 90, and 180 days of both water and air drying curing regimes. After placing the specimens under the appropriate curing conditions, the samples were conditioned in an oven at $105 \pm 5^\circ \text{C}$ for 3 x 24 hours i.e. to obtain constant moisture, then cooled at ambient room temperature of approximately 27°C for 24 hours before performing the ISA test.

Test procedure can be summarized as follows. The reservoir was filled with distilled water up to standard level i.e. 200 mm above the concrete. At the start of test, the tap from the reservoir was closed and the water flow through the capillary tube. Time in units was recorded for about 30 deviations. Then, the tap was opened and water level of reservoir was maintained at 200 mm. Reading was taken after 10 min, 30 min, 60 min and 120 min. The volume of infiltrated water f (millimetres/m²/second) in concrete surface can be calculated as follows:

$$f = \frac{60}{t} \times D \times 0.01 \quad \text{Eq. 3.17}$$

Where D = no. of scale divisions during the period t

t = test point time period (second)



Figure 3.36: ISA test

3.4.5.2 Sorptivity

The sorptivity test was done on a 100 mm diameter and 50 mm length concrete disk at the ages of 28, 90, and 180 days of both water and air drying curing regimes. The apparatus consists of 5 mm diameter steel rods, tray, paper towels and stop watch. Specimens were prepared by cutting the 100x200 mm length cylinder into three 100x50 mm length disks, after seven days of casting. Each time the test was conducted; three specimens were selected from different cylinders. They were oven dried at a temperature of $105 \pm 5^\circ$ for 72 hours after which they were allowed to cool-down in an airtight container for 24 hours. The oven-dried weight and the diameter of specimen were recorded to the nearest 0.01 gm and 0.1 mm respectively.

The disk surface was placed on the steel rods immersed in the tray. Water level was kept at 1-2 mm above the disk's bottom surface. Figure 3.37 shows the specimen setup for the test. The uptake of water by capillary was recorded through the mass increase in the specimen at a time interval of 5, 10, 30, 120, and 180 minutes. Before weighing the specimen, the wet surface was dried by a paper towel in order to remove any excess water. Water absorption in (mm^3/mm^2) was then calculated using the following equation (Fook, 2004).

$$a_s(t) = \frac{a_t - a_d}{N} \times 10^3 \quad \text{Eq. 3.18}$$

a_t = Weight at time t (gram)

a_d = Weight of oven dried specimen (gram)

N = Cross sectional area of bottom surface (gram)

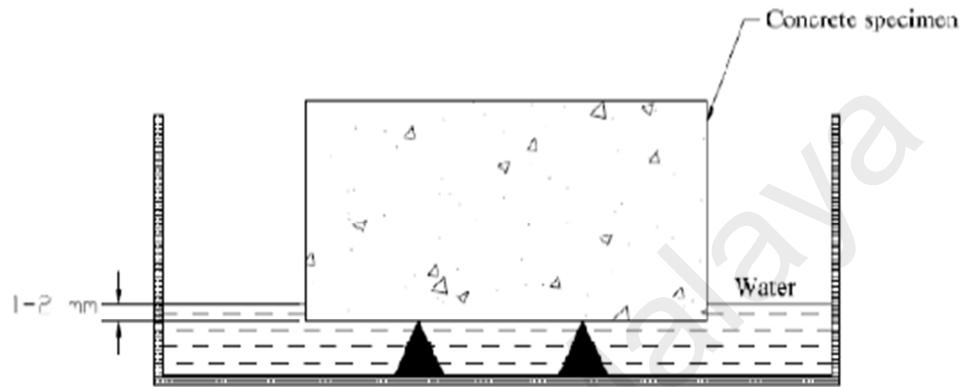


Figure 3.37: Sorptivity test set up
Adopted from (Fook, 2004)

The data $a_s(t)$ was plotted against the square root of time (\sqrt{t}). The sorptivity coefficient was then taken as the slope of line $a_s(t)$ against (\sqrt{t}). The relation between these two variables is summarized in the equation below.

$$a_s(t) = sor(\sqrt{t}) \quad \text{Eq. 3.19}$$

3.4.5.3 Resistance to Magnesium Sulphate Attack

The external sulphate salt attack is considered one of the major problems affecting concrete durability. The effects of sulphate attack on compressive strength, weight

reduction were studied. The salt used in the study was magnesium sulphate hydrate dissolved in water by 3% concentration. All specimens subjected to sulphate attack were initially cured in water for seven days of demolding and then they were immersed in the sulphate solution. The sulphate treatment was done in three cycles; each cycle consists of 30 days of sulphate immersion followed by seven days of air drying. Tests were conducted by the end of each cycle. The sulphate solution was changed every 15 days for each cycle. The schema of cycling is presented in Figure 3.38.

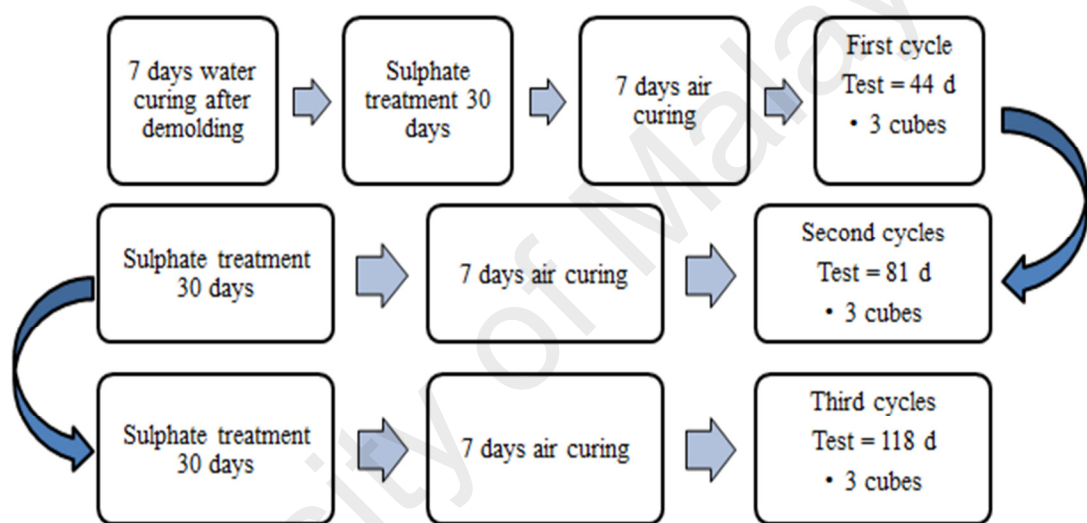


Figure 3.38: Schematics of magnesium sulphate cycling

3.4.6 Restrained shrinkage test

Two identical dog-bone specimens of 1100 mm long and 75 x 75 mm were used in a single test. One of the specimens was subjected to a fully restrained strain condition while the other specimen was allowed to shrink freely. A schematic diagram of the test rig developed for this purpose is shown in Figure 3.39 and Figure 3.40. The test rig contains two springs each with stiffness of 0.12 kN/mm. Each time, when the specimen shrinks by a predetermined target amount, this shrinkage is recovered manually by rotating the gear box, which increases the restraining force on the specimen. This

recovery is an instantaneous or elastic strain (ϵ_e) applied to the specimen. The specimen is then allowed to shrink in this state until it shrinks again by the target amount and then this strain again is fully recovered. This process is repeated until the specimen cracks. In the present study, target shrinkage of between 4 and 8 micro-strains (10^{-6} mm/mm) was used. During the periods between the manual strain recoveries (by rotating the gear box), the specimen is allowed to shrink between 4 and 8 micro-strains. During this shrinkage period, there is no increase in the force being applied to the specimen. This is achieved by allowing the flexible springs to absorb the shrinkage strain without increasing the force on the specimen. Load cell readings during these periods confirm that the force indeed remains constant. Figure 3.41 shows the step-by-step elastic strain recovery curve. As a result of the force being constant between recoveries, the elastic strain between recoveries remains constant in this curve. This is the key to the workings of this test rig.

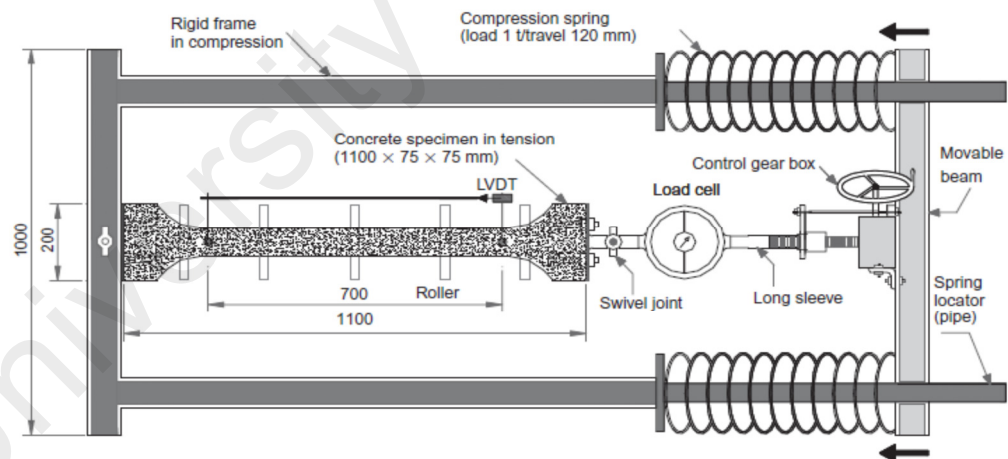


Figure 3.39: Schematic diagram of restrained shrinkage test rig (all dimension in mm)
Adopted from (Aly et al., 2008)



Figure 3.40: Restrained shrinkage test rig

Since the force is increased only when the strains are recovered (not when the specimen shrinks), the amount of elastic strain experienced by the specimen is known (by addition of all the recovered strains). The accompanying identical specimen undergoing free shrinkage provides the free shrinkage strains (ϵ_{sh}). Since the re-strain condition imposed is ‘fully restrained’—that is, all shrinkage strains are fully recovered. The total strain in the restrained test specimen is zero. Therefore

$$\epsilon_e + \epsilon_{sh} + \epsilon_{cr} = 0 \quad \text{Eq. 3.20}$$

Where ϵ_e is the cumulative elastic strain (from recovery strains), ϵ_{cr} is the creep strain and ϵ_{sh} is the free shrink- age strain obtained from the accompanying specimen. From this, the creep strain experienced by the specimen can be calculated by

$$\epsilon_{cr} = -(\epsilon_e + \epsilon_{sh}) \quad \text{Eq. 3.21}$$

This process of calculating elastic and creep strains is illustrated in Figure 3.41. The force in the load cell is measured during the test. By dividing the force by the cross-sectional area, the tensile stress is calculated.

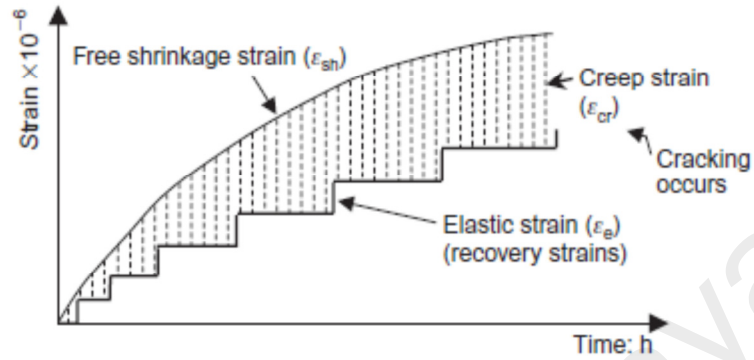


Figure 3.41: Illustration of the strain in the restrained and free shrinkage test specimens

Adopted from (Aly et al., 2008)

University of Malaya

CHAPTER 4: RESULTS AND DISCUSSION

4.1 Introduction

In this research some preliminary works were conducted in order to determine the optimum mix proportion and mixing method to achieve 100 MPa of high strength high performance concrete (HPC) incorporating RHA. This induces the determination of appropriate fineness of RHA to be used in HPC. The appropriate fineness of RHA is required to produce the highest compressive strength of RHA mortar. Different mixing methods were carried out to achieve the required slump value of 150-200 mm and to obtain optimum mechanical properties of hardened concrete. The compressive strength of RHA mortar and concrete was conducted at 1, 3, 7 and 28 days. The next stage of investigation involves the use of statistical method to find the optimum composition of concrete mixtures to study the behavior of that particular concrete mix on the workability, mechanical, durability and time dependent deformation property.

4.2 Properties of Constituent Materials

The main constituents of materials in concrete are cement, water and aggregate. Aggregate is a granular material such as sand, gravel and crushed stone that usually occupies approximately 60 to 75% of the volume of concrete. Due to its higher proportion in concrete, it significantly influences the performances of fresh, hardened and cost of concrete (Kosmatka & Panarese, 2002). The only exception from normal concrete is the additional constituents, which are supplementary cementitious material (CSM) and superplasticizer. The type of cement used in this study was ordinary Portland cement (OPC) type I and CSMs used were rice husk ash (RHA) and silica fume (SF).

4.2.1 Chemical properties of OPC, RHA and SF

Ordinary portland cement (OPC) is hydraulic cement composed primarily of hydraulic calcium silicates. The cement type used was “Cap Buaya” produced by Tasek cement Sdn. Bhd. The quality of cement is influenced directly by the chemistry of the raw materials used (Taylor, 1997). Two major compounds of cement are calcium oxide (Cook et al.) and silica dioxide (SiO_2) are from sources of limestone and clayey raw material, respectively. Table 4.22 shows that the compound of MgO and SO_3 in Tasek cement is in the range of ASTM C 150 of 6% and 3%, respectively. Total alkalis (Na_2O and K_2O) contents are 0.05% and the ASTM C150 required limit of those alkalis is 0.6%.

Table 4.22: Chemical compositions of RHA, SF and OPC

Oxide composition (%)		Tasek Cement (%)	ASTM C 150 Type I	RHA (%)	SF (%)
Silicon dioxide	SiO_2	21.28		90.82	92.06
Aluminum oxide	Al_2O_3	5.60	6 % max	0.46	0.48
Ferric oxide	Fe_2O_3	3.38	6 % max	0.67	2.11
Calcium oxide	CaO	64.64		0.67	0.40
Sodium oxide	Na_2O	N/a		0.12	0.63
Potassium oxide	K_2O	N/a		0.44	0.28
Magnesium oxide	MgO	2.06	6 % max	N/a	N/a
Sulphur trioxide	SO_3	2.14	3 % max	N/a	N/a
Total Alkalis	N/a	0.05	-	N/a	N/a
Insoluble residue	N/a	0.22	0.75 % max	N/a	N/a
Loss on ignition	LOI	0.64		4.5	N/a

RHA used in this research was produced through burning rice husk in a concrete furnace in concrete laboratory, University of Malaya. Meanwhile, SF used was supplied by a local supplier and it was ready to be used in concrete without further processing. During combustion processing of the rice husk in concrete furnace, the peak temperature was around $700\text{ }^\circ\text{C}$ at 7th hour as shown in Figure 4.42. According to Chopra, S.K. et al. (1981) and Ramezani pour et al. (2009), if the peak temperature of combustion of rice husk is below $700\text{ }^\circ\text{C}$, silica content of the RHA produced could be

amorphous, which is more reactive than crystalline silica. With uncontrolled combustion in concrete furnace, it took 30 hours to cool down before RHA is ready for use. Furthermore, it is important to identify the mineralogy of RHA to ensure the type of silica is formed.

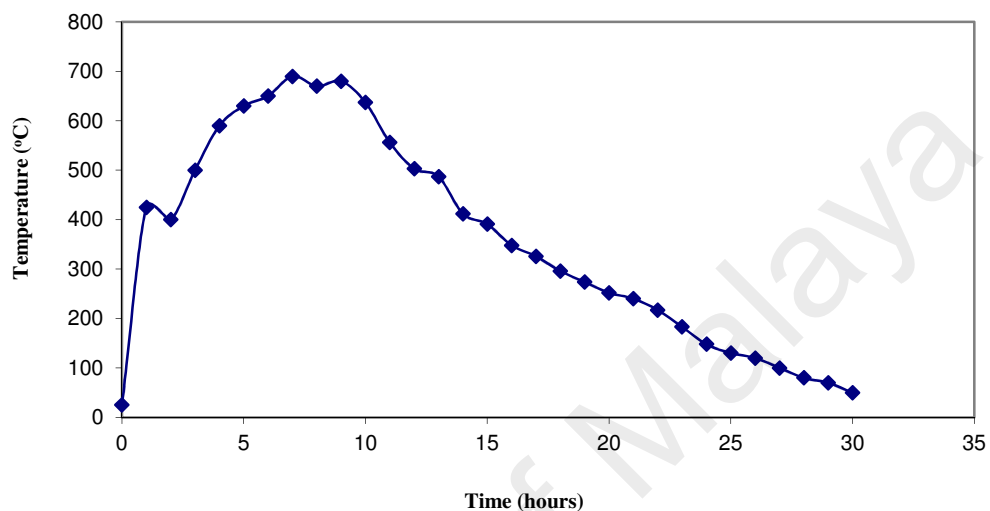


Figure 4.42: The burning temperature and duration for rice husk

The mineralogy of RHA was determined through the X-ray diffraction (XRD). Figure 4.43 shows the particles of RHA scatter, which is gradually towards a diffused peak of 125 counts at angle of 2θ equal to 22° . It means that the silica content of RHA is amorphous. In addition, the figure shows that there are no crystalline phases such as quartz, tridymite and cristobalite, which are less reactive than amorphous silica. The oxide compositions of RHA and SF used in this research were obtained by conducting XRF analysis and are shown in Table 4.22. The main compounds in RHA and SF are SiO_2 and their amount is almost five times higher than that of OPC. The RHA and SF used satisfy the ASTM C618-2003 requirement, which mention that the SiO_2 and loss on ignition (LOI) in a pozzolan should be a minimum of 70% and a maximum of 6%, respectively. The RHA and SF can be classified as artificial pozzolan of siliceous material class F. However, the content of SiO_2 in RHA is differently reported by

researchers due to the compound existing in rice husk id dependent on the variety of paddy, soil and fertilizer used (Dingyuan & Liqun, 1989).

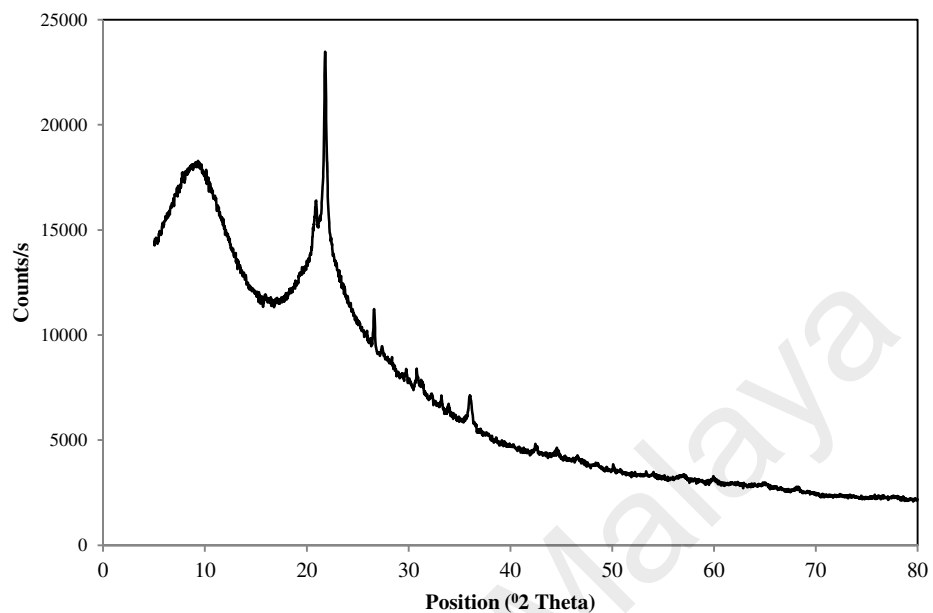


Figure 4.43: The X-ray spectrum of RHA

4.2.2 Physical properties of OPC, RHA and SF

Table 4.23 shows the physical properties of OPC considered in this research, which are median particle size (MPS), specific surface area (Hussain & Ishida, 2011) and specific gravity (SG). In addition to median particle size, particle size distribution is also an important parameter in mix design of concrete as it can determine the packing density of mixture (Fennis et al., 2008). Those parameters affect the properties of fresh and hardened concrete. The density and median particle size of cement are 3.16 and 22.1 μm . Meanwhile, the value of surface area of cement is depended on the measurement technique used. The technique measurements of BET are through utilizing gas absorption and Blaine tests are through air permeability. As cement particles have a rough, irregular surface with internal cracks and pores (Taylor, 1997), it is obvious that the value of BET is higher than that of Blaine test. The Blaine specific surface area of OPC was 351 m^2/kg whereas the BET specific surface area was 3046 m^2/kg . The average Blaine specific surface area of OPC is accepted as it complies with ASTM

C150, which it should be greater than 280 m²/kg. Furthermore, the relative density of OPC was 3.15, which the limit is 3.10 up to 3.25 as specified by (Kosmatka et al., 2002). In addition, the compressive strength of the cement is 42.5 MPa based on the data sheet of Tasek cement Sdn. Bhd. Therefore, the chemical and physical properties of selected OPC were suitable to produce HPC.

Table 4.23: Physical properties of RHA, SF and OPC

Material	F1-RHA	F2-RHA	F3-RHA	SF	OPC
Average particle size (μm)	29.92	20.43	13.5	0.50	22.1
BET's Nitrogen absorption (m ² /kg)	27,400	29,100	30,400	26,250	1,060
Blaine's surface area (m ² /kg)	8,100	11,000	12,200	-	351
Specific gravity	2.18	2.20	2.22	2.31	3.15
LoI (%)	4.5	4.5	4.5	2.54	-

Not a like SF, RHA needs to grind to a certain median particle size to be used to certain purposes. Giaccio et al. (2007) utilized RHA with 10% replacement and median particle size of RHA of 8 μm in w/b ratio of 0.5, 0.4, 0.32 and 0.28 produced compressive strength of 38, 49, 56 and 63 MPa. It ranges from normal concrete to high strength concrete by varying w/b ratios and binder content from 340 up to 515 kg/m³. Meanwhile Tuan et al. (2011) used RHA with median particle size of 5.6 μm to develop ultra-high strength concrete with compressive strength of 150 MPa, it required a low w/b of 0.18 and cement content 900 kg/m³.

From Figure 4.44, the densities of RHA are changed as the cycles of grinding are increasing. The first 5000 cycles of grinding increase the density almost 15 % and the other 5000 cycles only increase less than 5%. However, above 15000 cycles of grinding is almost not change the density of RHA.

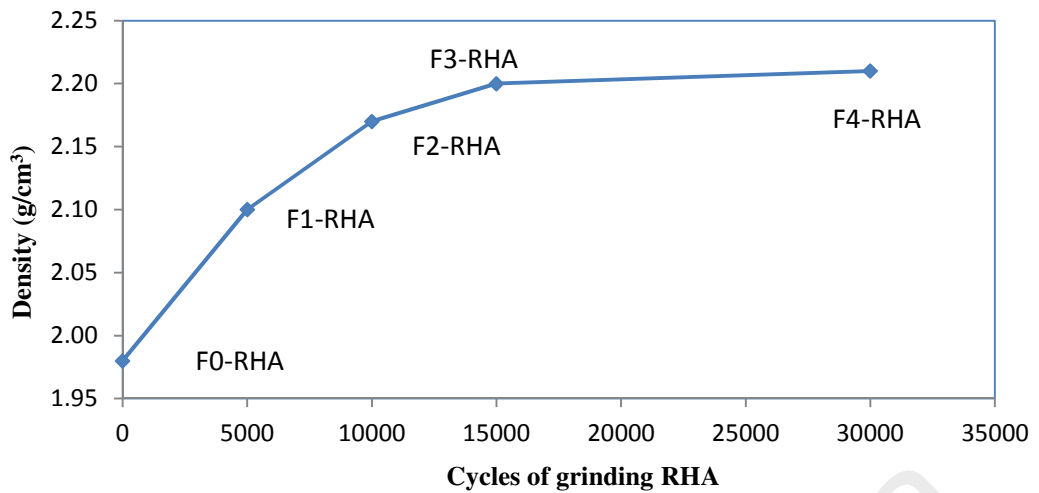


Figure 4.44: Cycles of grinding RHA vs the density of RHA

Figure 4.45 shows that Blaine fineness of RHA produced below 15000 cycles increased almost linear with the increasing cycles of grinding. Figure 4.47 shows that Blaine surface area increased when density increased. In addition, the differences densities and Blaine fineness of RHA between grinding of 15000 cycles and 30000 cycles, respectively, are insignificant. However according to Mehta (1992) the grinding of RHA too much reduces the reactivity of pozzolan of RHA.

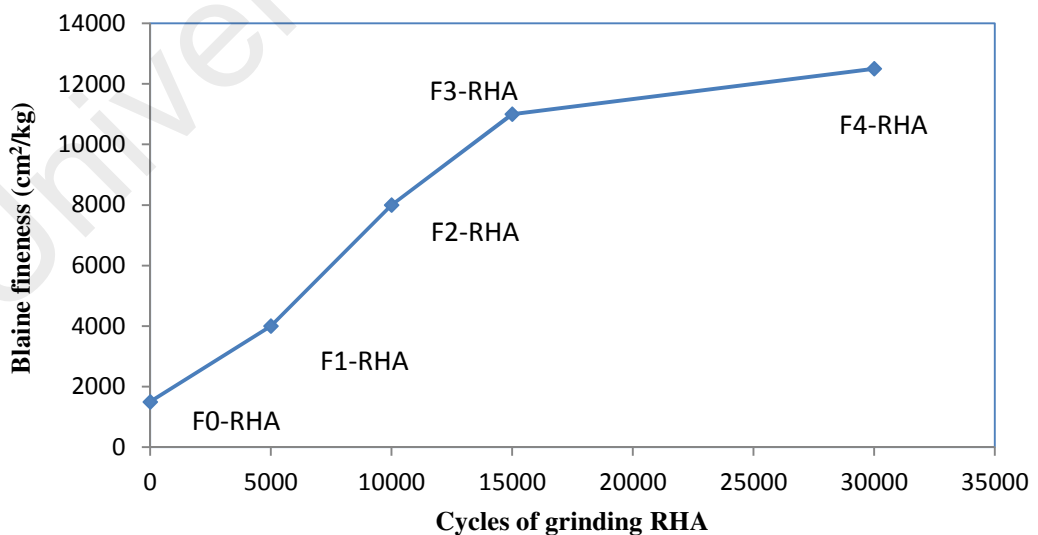


Figure 4.45: Cycle of grinding RHA vs the Blaine fineness of RHA

The RHA was grinding in three groups. The RHA was grinding with 10000 cycles (F1), 15000 cycles (F2) and 30000 cycles (F3), and produced the median particle sizes of RHA were 29.92 μm , 20.435 μm and 13.5 μm , respectively. Figure 4.46 shows the particle size distribution of cement, RHA-F1, RHA-F2, and RHA-F3. It can be seen that the grinding above 15000 cycles can achieve the particle size of RHA less than that of cement. However, the particle size of SF is significantly less than that of RHA. This is a weakness of agricultural waste ash compared to industrial waste ash which does not need to be ground as the ash naturally fineness and spherically shape. The purpose to grind the ash beyond the particle size of cement is to give the opportunity the ash be pozzolanic or filler effect. Hwang and Chandra (1996) have suggested that the particle size of RHA in the 10–75 μm range exhibits satisfactory pozzolanic behavior. Cordeiro, G.C. et al. (2008) mentioned that normally filler effect is defined as the packing characteristics of the mixture, which depend on size, shape and texture of the particles and also chemically inactive.

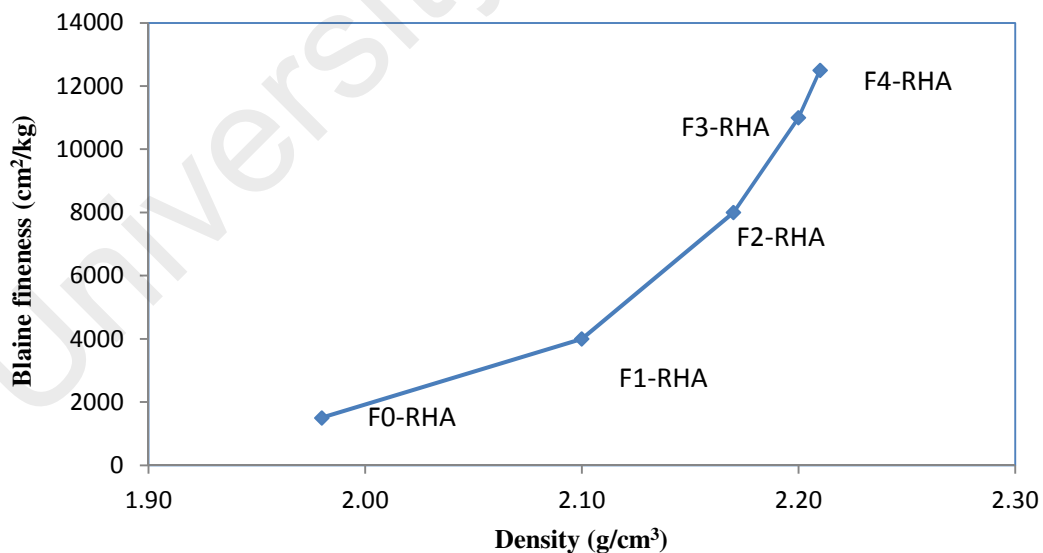


Figure 4.46: Relationship between density and fineness of RHA

The particle size distribution of OPC is presented in Figure 4.47. From PSD of cement, the coefficient of curvature $C_g = (d_{30})^2 / (d_{60} \times d_{10})$ equals to 1.6 and the

coefficient $C_u = (d_{60}/d_{10})$ equals to 10.45. It means that PSD of cement is in well-graded powders and uniform due to the C_g in the range 1-3 and C_u greater than 4. The particle size distributions of RHA and SF are presented in Figure 4.48. From PSD of RHAs, the coefficient of curvature C_g of RHA-F1, RHA-F2 and RHA-F3 equal to 1.22, 1.53 and 1.14, respectively. The coefficients of C_U of RHA-F1, RHA-F2 and RHA-F3 equal to 8.59, 10.45 and 6.61, respectively. Meanwhile the coefficient of curvature C_g and C_U of SF equal to 0.31 and 2.94, respectively. All PSD of RHAs were well-graded powders and uniform due to the C_g in the range 1-3 and a coefficient C_U greater than 4. For SF, the PSD of SF is gap graded due to the coefficient of curvature and uniformity less than 1 and 4, respectively.

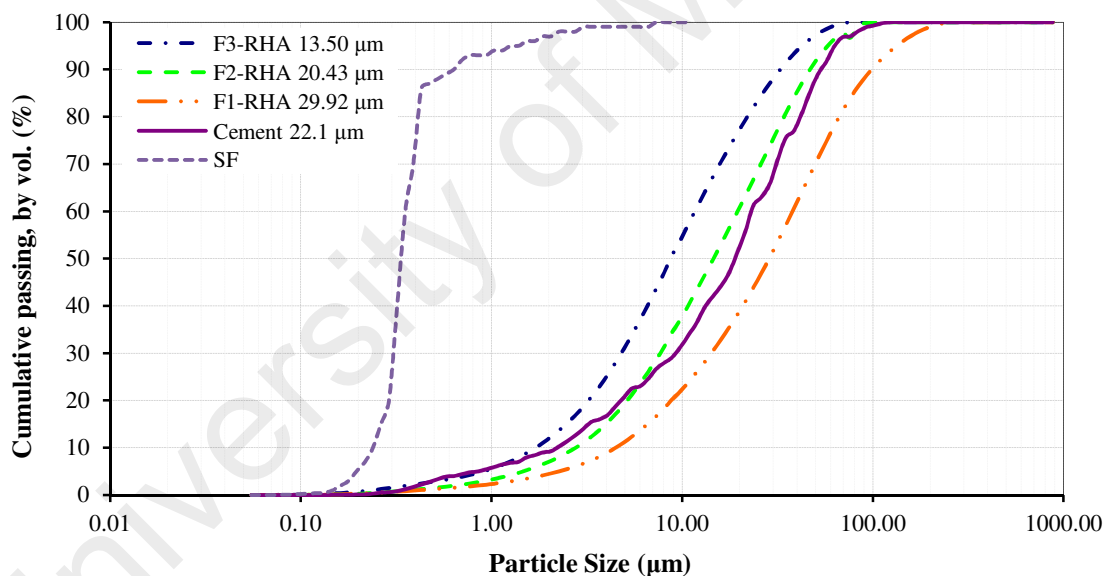


Figure 4.47: Particle size distributions of binder used in this research

4.2.3 Physical properties of aggregates

The sand used in this study was mining sand, which is a common type of sand used in construction building in surrounding Kuala Lumpur. It is well known that the fine aggregate is used to fill the voids in the coarse aggregate and to act as a workability agent (Kala, 2013). Coarse aggregate used in this research was crushed granite, and this aggregate is mostly available in Malaysia.

4.2.3.1 Particle size distribution of coarse and fine aggregate

Coarse aggregate is a material that passed the 3/4-inch screen and retained on the sieve of # 4. In order to withstand the designed loads and the effects of weathering aggregate, must be equal to or better than the hardened cement (Hussain & Ishida, 2011). The use of the largest permissible maximum size of coarse aggregate allows a reduction in cement and water requirements because of larger pieces offering to less surface area of the particles than an equivalent volume of small pieces (Ibragimov, 1989). Based on the optimum density theory, an economical mix and a strong structure can be achieved by using good gradation, which results in a dense mass of concrete with a minimum volume of voids. Optimum strength, water tightness, and durability of the hardened concrete required careful control of aggregate gradation (Safiuddin, M. et al., 2009). The physical properties of aggregate determine the fresh, hardened and time dependent of concrete behavior (Makani et al., 2010). The physical properties that important to know are the fine modulus, specific gravity, particle size distribution, moisture content and water absorption of aggregate. Table 4.24 shows the physical properties of aggregate. There are three types of mining sand available in mining sand industries: fine, mild and coarse. The first is finer than the second one as shown by their fine modulus of 2.64, 2.81 and 3.15. Figure 4.49 show that the particle size distributions of mining sand are categorized as zone 2 for FM of 2.64 and zone 1 for FM 2.81 and 3.15. From three types of mining sand, the fine aggregate adopted in this study was coarser mining sand, FM of 3.15, due to the coarser one has less specific surface area than that of finer ones. Although the coarser one has less porosity than the finer one, it will be substituted with less its specific area as in HPC finer material has higher amount of specific area (ACI-363R, 1992). Figure 4.48 shows the particle size distributions of aggregate are in the range of BS 812-103.1:1985. Maximum particle size of coarse aggregate being used in HPC was suggested by many researchers less

than 10 mm to get higher compressive strength of concrete (Safiuddin, M. et al., 2009). However, in this research, the coarse aggregate size used was in the range of 4.75-19 mm, and the aggregate grading was accepted by BS 882:1983. In addition, the flakiness index and elongation index of coarse aggregate were 10.8 % and 18%, respectively, and it was accepted by BS 882:1983.

Table 4.24: The physical properties of fine and coarse aggregate

Aggregate	Fine modulus	Water absorption (%)	Specific gravity	Particle size
Mining sand fine	2.64	0.96	2.69	0-4.75 mm
Mining sand mild	2.81	0.89	2.68	0-4.75 mm
Mining sand coarser	3.15	0.82	2.68	0-4.75 mm
Crushed granite	7.02	0.65	2.65	4.75-19 mm

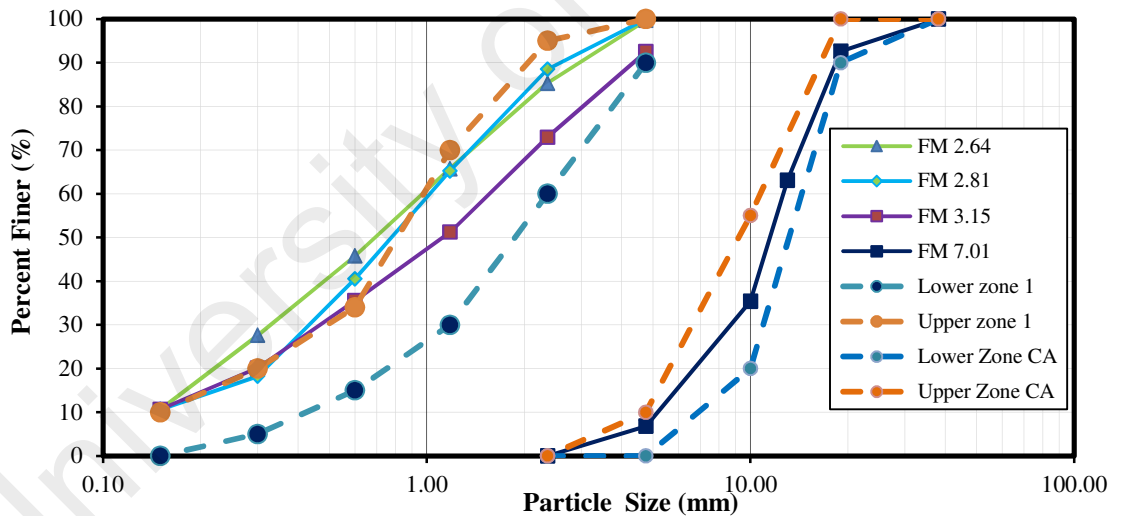


Figure 4.48: Sieve analysis for the material used in this research

4.2.3.2 Effect aggregate fraction on packing density of aggregate

To find packing density through experiment in the lab is time consuming. There are some models that can be used to find packing density of aggregate. In this study, the Toufar model is used to find packing density of aggregate. The model was examined through the experimental data and the result is shown in Figure 4.49. The experimental

data is close to the curve of the model so that in this study Toufar model was applied to find the packing density of fraction aggregate. Mohammed et al. (2012) mentioned that Toufar method is better predicted packing density of aggregate in binary mix proportion.

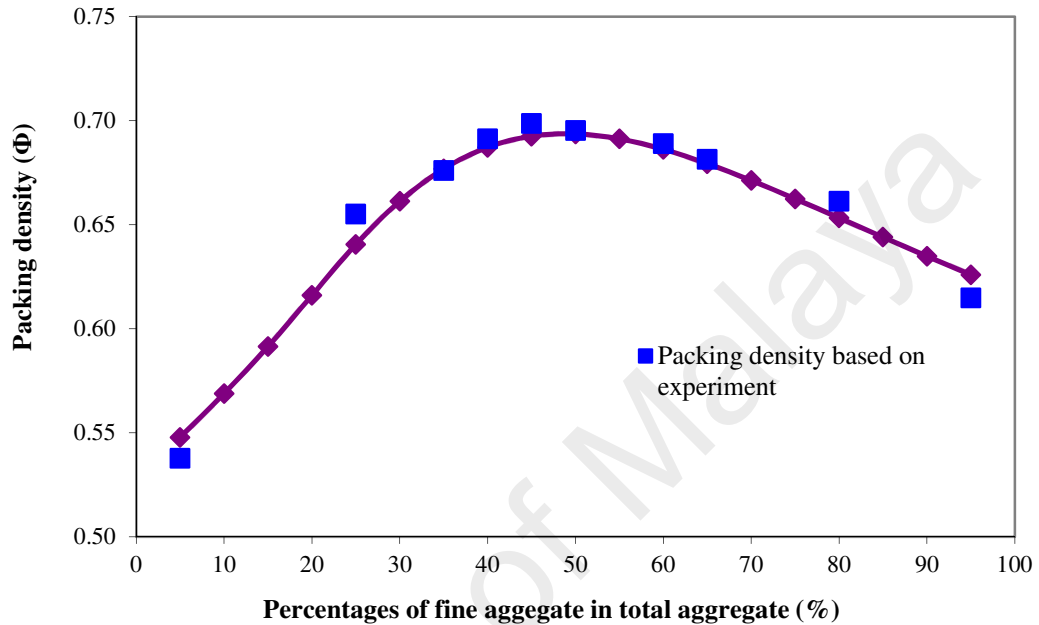


Figure 4.49: Comparing between theoretical packing density of Toufar and experimental

Figure 4.50 shows the graphs of every combination of fine aggregate with coarse aggregate and if the proportion of aggregate is changed, the packing density of aggregate also changed. The packing density is close to maximum with percentages of fine aggregate around 35-45% of total aggregate. Jeenu et al. (2012) reported similar result through experiment on proportion of HPC. However, they suggested taking the proportion slightly out of the maximum packing density value due to the workability on that point tend too harsh.

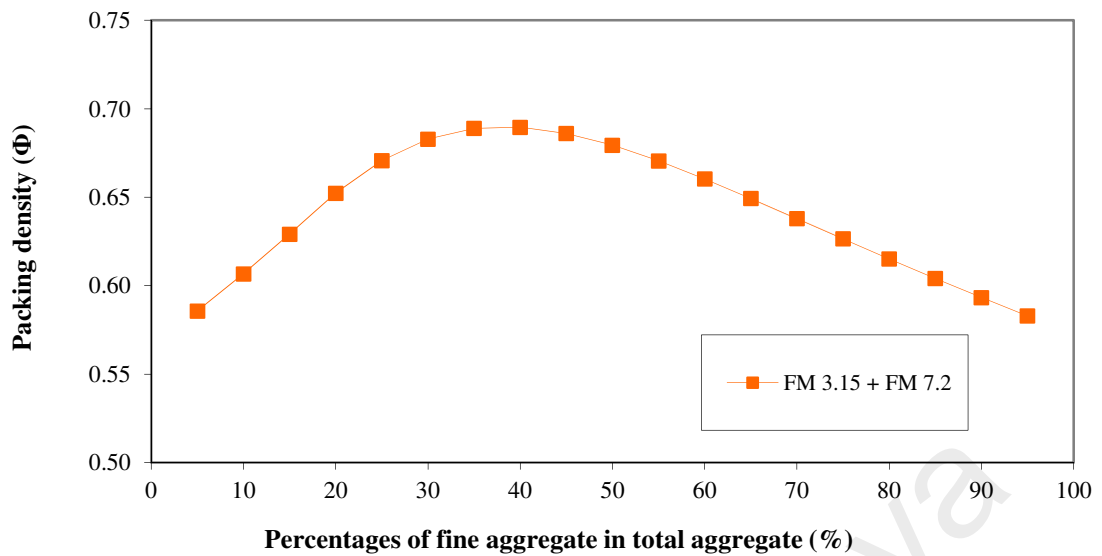


Figure 4.50: Packing density of combination fine aggregate and coarse aggregate

4.2.3.3 Effect aggregate fraction on specific surface area of aggregate

The previous result showed that proportion of fine aggregate to total aggregate affects to the packing density of aggregates. Another parameter that needs to consider is the specific surface area of total aggregate in the mixture. The total of specific surface area of aggregates affect to the thickness of paste to cover the aggregates (Kosmatka et al., 2002). Figure 4.51 shows that total surface area of combination aggregate is changed if the proportion is changed. Total surface area affected the water needed to cover all surface area of aggregates.

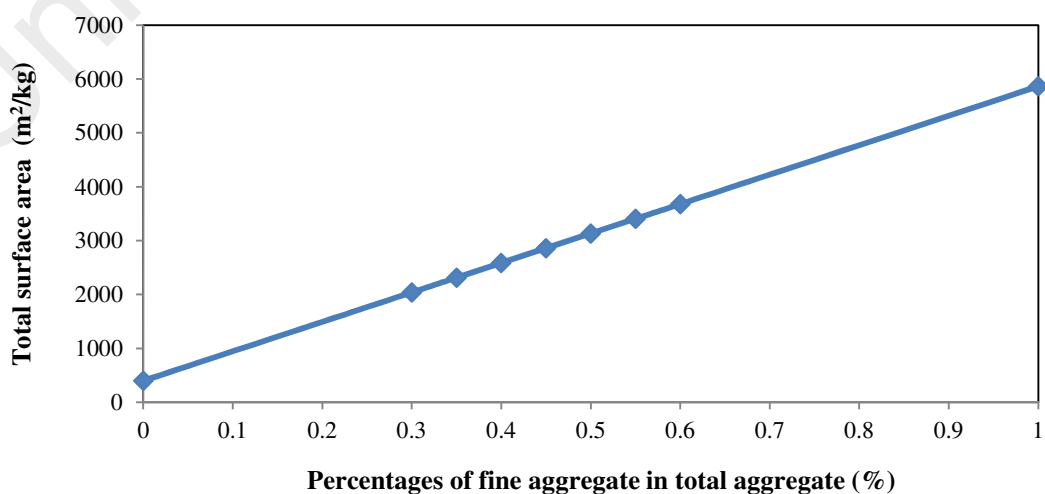


Figure 4.51: Total surface area of combination different fine aggregate and coarse aggregate

4.2.4 Quality of water

In concrete, the single most significant influence on most or all of the properties is the amount of water used in the mix. The normal tap water used for mixing and curing of HPC was aesthetically in excellent condition. It was free from dirt and organic matter that may cause bad odor. The water used in this study was satisfied according to BS 3148.

4.2.5 Dosages of high range water reducer (HRWR)

A modified polycarboxylate-based HRWR, commercially known as Glenium ACE 388, was used to produce different HPC. It was a liquid with off white color. The selected HRWR greatly reduced the water demand of binder and provided a superior workability of fresh concrete. The relative density and solid content of HRWR are 1.05 and 30 %, respectively.

4.2.5.1 Effect of fineness of RHA on saturation point

Three types of paste incorporating average particle sizes of RHA were examined to find the saturation point for Sp dosage, see Figure 4.52. The results show that the average particle size affected the dosage of Sp needed to reach the saturated point. The coarser particle size of RHA needed higher Sp dosage. Even though the finer RHA has higher surface area than coarser one, the coarser one still high porosity compare to finer one. It could be the porosity of coarser RHA absorbs more mixing water so that coarser RHA need more Sp than finer one. The similar result also found by (Habeeb, G.A & M.M Fayyadh, 2009) that decreasing mean particle size (MPS) of RHA from 31.3 to 11.5 μm increases the water demand or the SP dosage to reach a given workability when a partial cement content is replaced by 20 wt.% RHA. Also (Le et al., 2015) mentioned that increasing MPS of RHA increased the pore volume and the water demand of RHA. Incorporating the coarse RHA, which has a coarser than cement, will lower the free

water and the packing density of granular mixture of the paste in mortar. In this study, the dosage of SP for RHA with particle size in range of 13.5 up to 29 μm for level of replacement in the range of 5% up to 20% need Sp dosage in the range 0.5% up to 1.8%.

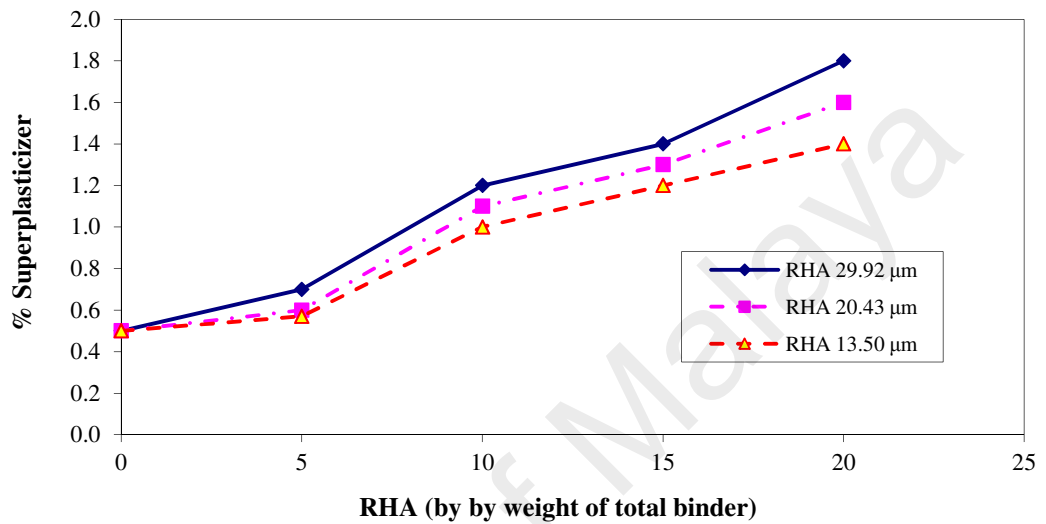


Figure 4.52: The effect of particle size of RHA and percentage replacement of RHA on superplasticizer dosage in paste incorporating different fineness of RHA

4.2.5.2 Effect of level replacement RHA on saturation point

Figure 4.53 shows that higher level replacements of RHA need more Sp dosages to reach a saturation point. The increase of level replacement of RHA also increases the volume of finer material as specific gravity of RHA is less than that of cement. As mention earlier, RHA has naturally porous on its cellular. (Safiuddin, Md, 2008) reported that the results of their study reveal that the increase in RHA content increases the flow time of paste and SCHPC, and decreases the slump flow of mortar, particularly at lower w/b ratios.

4.3 Mortar

In order to understand the effect of fineness of RHA in concrete, the trail mix in the mortar was conducted to study its effect to superplasticizer dosage and compressive strength. The w/b and the binder content were 0.25 and 550 kg, respectively. The mining sand with FM of 3.15 was adopted. The levels of replacement of cement with RHA were 0, 10, 15 and 20% and three types of median particle sizes of RHA, which are 13.50 μm (F3), 20.43 μm (F2) and 22.92 μm (F1), were involved.

4.3.1 Mix design of mortar

The water to binder (W/B) ratio of all the mixtures in this study was adopted to be 0.25. The dosage of Sp was based on previous study and adjusted to maintaining the mortar mixes with similar slump flow of 290-300 mm. Mix proportion of mortar is shown in Table 4.25.

Table 4.25: Mix proportions of mortar

Constituent	W/b	Sp (%)	Water (kg/m ³)	Cement (kg/m ³)	RHA (kg/m ³)	RHA (%)	Fine aggregate (kg/m ³)
OPC	0.25	0.5	137.5	550	0	0	733.91
RHA10-F1	0.25	1.2	137.5	495	55	10	707.35
RHA10-F2	0.25	1.1	137.5	495	55	10	707.35
RHA10-F3	0.25	1.0	137.5	495	55	10	707.35
RHA15-F1	0.25	1.3	137.5	467.5	82.5	15	692.59
RHA15-F2	0.25	1.2	137.5	467.5	82.5	15	692.59
RHA15-F3	0.25	1.1	137.5	467.5	82.5	15	692.59
RHA20-F1	0.25	2.0	137.5	440	110	20	671.95
RHA20-F2	0.25	1.85	137.5	440	110	20	671.95
RHA20-F3	0.25	1.7	137.5	440	110	20	671.95

F1= The APS of RHA=29.92 μm ; F2= The APS of RHA= 20.43 μm ; F3= The APS of RHA= 13.5 μm

4.3.2 Effect of the percentage and fineness of RHA on workability of fresh mortar

Previous Table 4.25 shows the dosage of superplasticizer needed in mixtures for achieving a constant flow value of mini slump cone in the range of 290 mm to 300 mm, which was adopted from (Tregger et al., 2008) who successfully studied on relationships between viscosity and flow-time measurement from mini slump tests. It can be seen the mortar containing 20 % RHA need more dosage of superplasticizer compared to that of 10% and 15% RHA. This could be due to the effect of total surface area mortar containing 20% RHA is higher than that of 10% and 15%. Similar results were reported that increasing replacement of SF increased Sp dosage (Tuan et al., 2011). Furthermore, it also shows that the amount and the median average particle sizes of RHA influence the workability of RHA mortar. The dosage of superplasticizer in mortar increases with the increase of RHA replacement, but with the same amount of RHA, the dosage of superplasticizer decreases when incorporating less median particle size of RHA. The dosage of Sp in mortar is slightly higher than that in paste. It could be the effect of fine aggregate need more fluid to cover its surface.

4.3.3 Effect of fineness and percentage of RHA on compressive strength of mortar

Figure 4.53 shows that the OPC mortar reaches the compressive strength below 100 MPa and RHA mortar reach above 100 MPa at 28 days. It means that pozzolanic reactions occurred in the RHA concrete at 28 days. With 10% RHA cement replacement, the highest compressive strength of HPC was achieved with incorporating MPS of 13.50 and 20.43 μm .

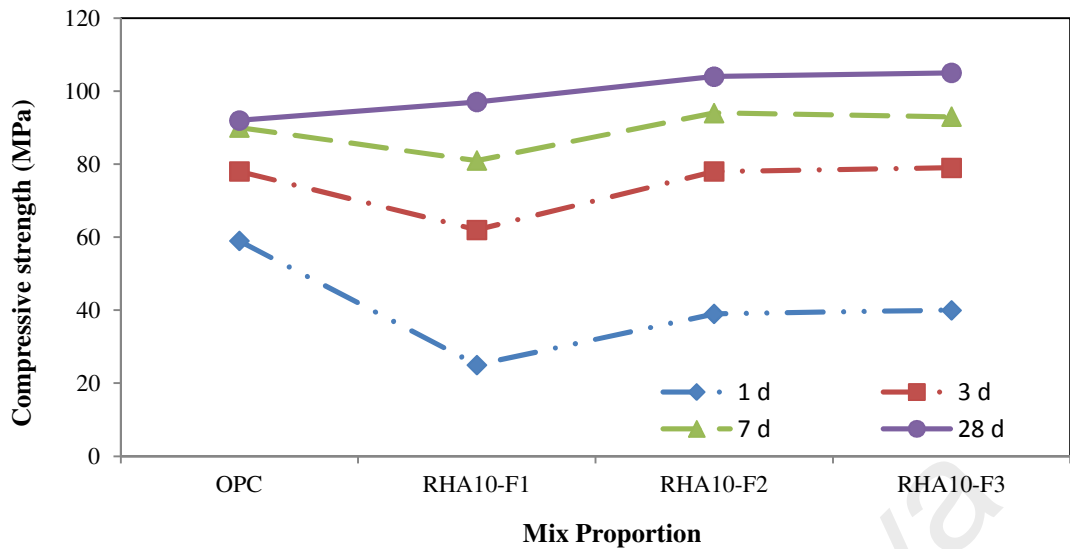


Figure 4.53: Compressive strength of mortar containing 10% replacement of RHA with variation of fineness of RHA

Figure 4.54 shows that 15% RHA with APS=13.50 μm was provided the highest compressive strength gain at 28 days. Incorporating MPS of RHA greater than 13.50 μm induced a reduction in compressive strength. Based on this result, it is clearly that RHA, which depends on its median particle size, can be used as partial cement replacement at 10% and 15%, to produce HPC 100 MPa.

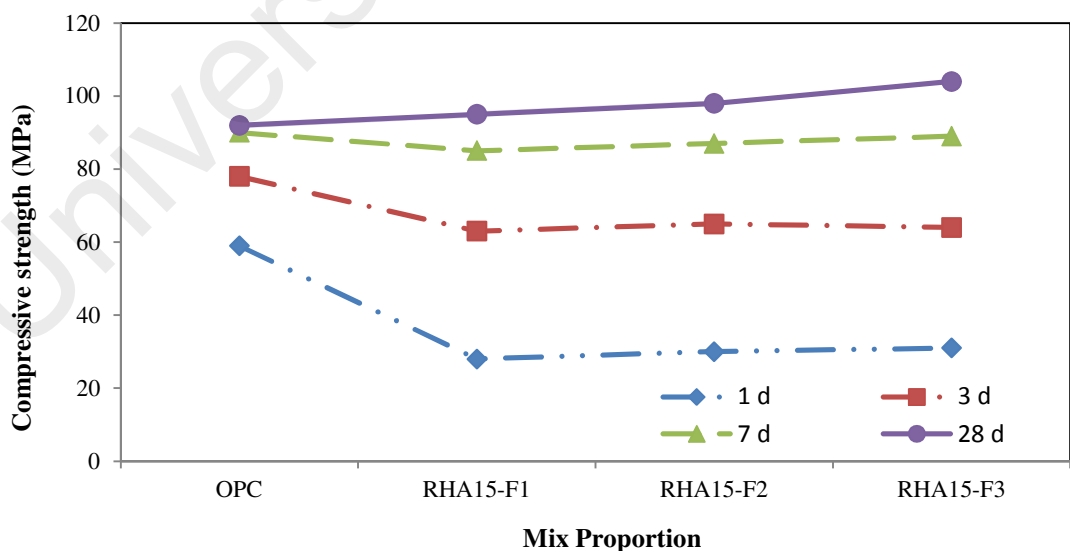


Figure 4.54: Compressive strength of mortar containing 15% replacement of RHA with variations of fineness of RHA

Furthermore, Figure 4.55 shows 20% replacement of cement with RHA. The compressive strength of RHA concrete at 28 days is similar to that of OPC concrete but low than that of 10% and 15% RHA concrete. Based on results, it is clearly that the fineness of RHA affects the compressive strength. However, utilizing the finer RHA was slowly affected the early pozzolanic reaction compared to the coarser one. It could be that the finer material acts more as a filler than as pozzolan. Grinding of RHA to a high degree of fineness should be avoided due to its pozzolanic activity derives mainly from the internal surface area of the particles (Mehta, 1979). Therefore, from results of this investigation, RHA with particle size of 13.5 μ m was chosen for further study in this research work.

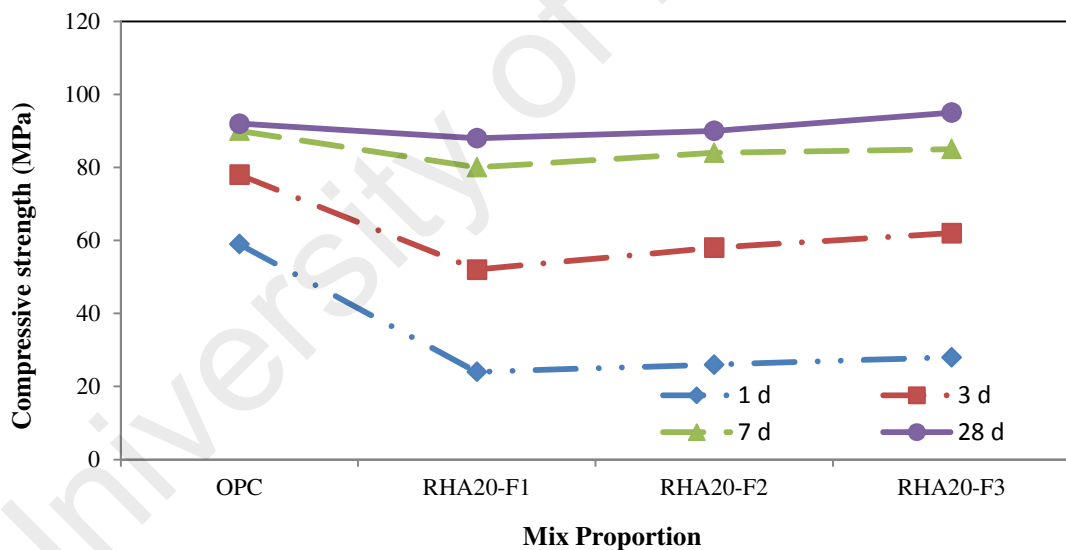


Figure 4.55: Compressive strength of mortar containing 20% replacement of RHA with variations of fineness of RHA

4.4 Determine the Appropriate Mixing Procedures Being Adopted

The cementitious material used in this study was ordinary Portland cement (OPC), classified as ASTM Type I of Grade 42.5, and the supplementary cementitious material used was rice husk ash (RHA). Silicon dioxide (SiO_2) content in OPC and RHA was

20.99 and 90.82 %, respectively. Calcium oxide (Cook et al., 1989) (Cook et al.) in OPC was 65.95%. The surface area of cement was tested using the Blaine test according to ASTM C 204-94a and that of RHA was tested by nitrogen absorption method. The surface area of cement and RHA was 0.351 and 29.1 m²/g, respectively. The 15% replacement of cement with RHA was adopted in this study due to 10% up to 20% replacements was planned on further study so that 15% replacement was assumed to represent those replacements. The specific gravities (SG) of cement and RHA were determined according to BS 1377: part 2:1990 which were 3.14 and 2.12 g/cm³ respectively. For fine aggregate, mining sand with specific gravity 2.63, and fineness modulus of 3.1 was used. Coarse aggregate used was granite with maximum size of 19 mm and fineness of modulus of 7.2. The water absorptions of fine and coarse aggregates were 2.38 and 2.65%

4.4.1 Mix Proportion of concrete

The proportions of OPC and RHA15 concrete mixtures are shown in Table 4.26. Water to binder ratio (W/b) of all mixtures in this research was adopted to be 0.25. SP content was adjusted to maintaining the fresh concrete with a slump in the range of 150-200 mm. Mix proportion of mixtures for both mixing methods was similar.

Table 4.26: Mix proportion of OPC and RHA concrete

Constituents	OPC	RHA15
W/b	0.25	0.25
RHA (kg/m ³)	0.00	82.5
Sp (%)	0.5	1.2
Water (kg/m ³)	137.5	137.5
Cement (kg/m ³)	550.0	467.5
FA (kg/m ³)	712.5	681.5
CA (kg/m ³)	1050	1050

4.4.2 Mixing procedures

Two mixing procedures namely conventional and two- step mixing methods were used. For the conventional mixing method (CMM), similar to that of the ACI mixing

method, coarse aggregate, sand and cement were mixed for 30 seconds in a normal mixer; then water and superplasticizer were added and mixed for three minutes. For the two-step mixing method (TSM), premixing of mortar was completed by mixing the water, superplasticizer, cement, and fine aggregate in a normal mixer for two minutes. The coarse aggregate was then added to the mortar and mixed for a further two minutes. For mixing all materials, a 100 liter pan mixer with adjustable speeds was used. The volume of each batch was 56 l.

4.4.2.1 Effect of mixing procedures on fresh concrete

Table 4.27 shows that mixing method affected the properties of fresh concrete. It can be seen that slump and slump flow of the two-step mixing was higher than the conventional mixing. The slump and slump flow of the two step mixing was 13% and 6% higher than the conventional mixing, respectively. The two-step mixing provided better workability than the conventional mixing due to the fine materials in the two steps mixing has the ability to distribute the aggregate more homogenous. (Punkki et al., 1996) reported the increasing slump and also higher slump loss on the two steps mixing applied on normal concrete.

Table 4.27: Properties of fresh concrete

Mix Id	Mixing Procedures	Slump (mm)	Slump flow (mm)
OPC-CM	Conventional	185	390
OPC-TSM	Two step	210	415
RHA15- CMM	Conventional	180	380
RHA15-TSM	Two step	205	400

4.4.2.2 Effect of mixing procedures on compressive strength

Figure 4.56 presents the variation of strength with age of concrete mixing method and percentage replacement of cement with RHA. The compressive strength of concrete in the two-steps mixing at early age was significantly higher than that of concrete produced using the conventional mixing. It was also observed that

compressive strength continued to increase with age in both mixing methods. In addition, the RHA concrete with the conventional mixing exhibited lower strength than OPC with the conventional and the two-steps mixing. However, the RHA concrete with two-step mixing was higher than OPC with the conventional and the two-steps mixing. In the two-steps mixing, the concrete achieved compressive strength above 100 MPa at 28 days. However, the previous study showed that incorporating 15% RHA gave lower than the control concrete (Kishore et al., 2011). But, in this study the compressive strength of 15% RHA concrete at 28 days was higher 16% than OPC concrete produced with conventional mixing and 2% than OPC concrete produced with two-steps mixing method. The compressive strength of 15% RHA and OPC concrete at 28 days was 19% and 14 % higher when it was produced in the two steps mixing method than that of conventional mixing method, respectively. It could be the concrete produced with two-stage mixing operation more homogeneous and workable mixture (Rupnow et al., 2007). Furthermore, it indicated that the two- step mixing method seems to be better in terms of ultimate strength gain than that of the conventional mixing method.

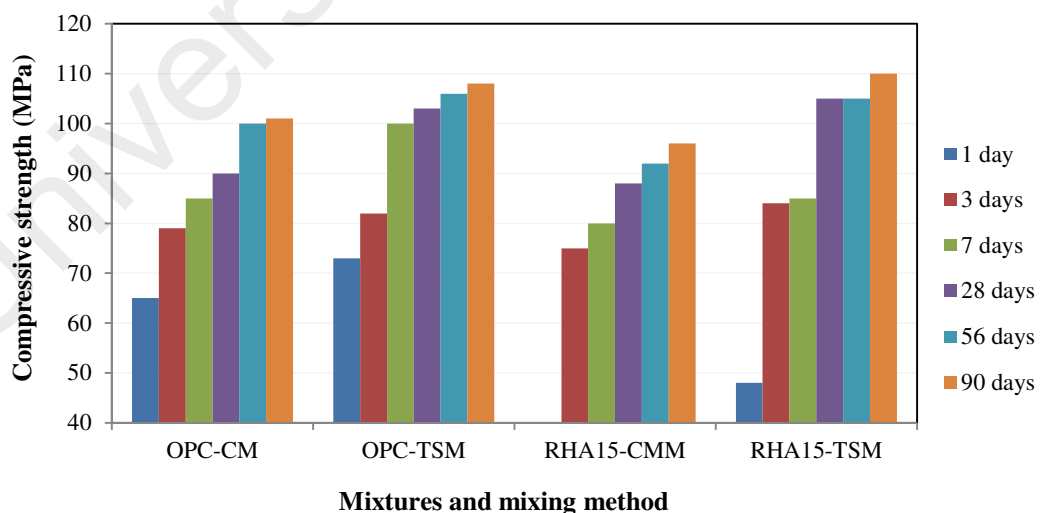


Figure 4.56: The effect of mixing method on compressive strength

4.4.2.3 Effect of mixing procedures on tensile strength

The tensile strength at 7, 28 and 90 days was found to be lower for RHA concrete than OPC under both mixing methods (Figure 4.57). The tensile capacities of OPC and RHA concrete under TSM method are higher than that of under CMM method. However, there are no significant improvements, less than 5%, in splitting tensile strength of concrete between two mixing methods.

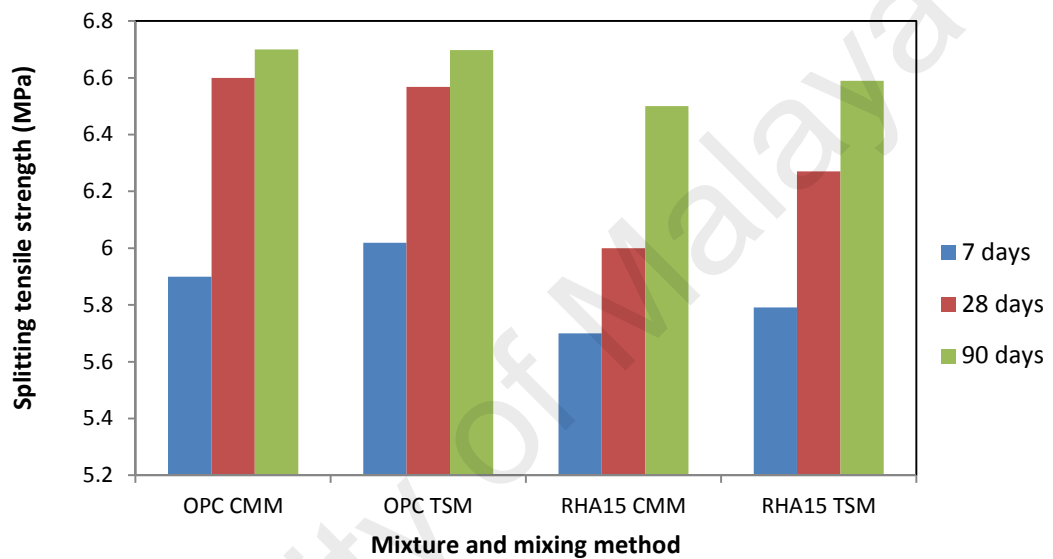


Figure 4.57: The effect of mixing methods on tensile strength

4.5 Optimizing the Composition of Mixture through a Response Surface Method

The results from previous section show that the average particle size of RHA around 13 μm can be used to achieve compressive stress 100 MPa mortar at 28 days. That average particle size of RHA was adopted on this study of high performance concrete, however, there are some parameters need to be consider to get high performance concrete 100 MPa incorporating RHA. Those parameters are w/b, the amount of binder, the percentages of RHA replacement, the ratio of fine aggregate to total aggregate, and

the dosage of Sp. To achieve high strength concrete is common to utilize a lower w/b ratio. The evaporation and desiccation on concrete make the amount of water left after the hydration process creates pores and capillary in concrete (Meddah & Tagnit-Hamou, 2009). So it is logic to utilize the lower w/b ratio to get high strength due to less porous and capillary. On the other side, the water cement ratio of 0.42 is enough to make cement hydration (Sari et al., 1999) and it imply that the concrete mixture of w/b lower than 0.42 needs superplasticer to make concrete workability. In this study, w/b ratios in the range of 0.22 and 0.28 were adopted to be optimized to achieve the compressive strength of 100 MPa at 28 days. The amount of cement also needs to be limited due to high temperature rise during the hydration process can create tension stress and then crack at early age. Also the environment reason, by optimizing the usage of cement it reduces the CO₂ released on the air during clinker is produced. Also, there is a certain limit that increases the amount of cement in concrete mixtures did not guarantee a linear increase of compressive strength of concrete. In this study, the optimum amount of binders in the range of 500 up to 600 kg/m³ were used to get compressive strength of 100 MPa. The aggregate is the main part of concrete mixture due to the high volume of aggregate used, almost 70%. Fine aggregate plays important role in the concrete mixture due to its high surface area compared to coarse aggregate. It needs to optimize the ratio or fine aggregate to total aggregate. The ratios in the range of 0.35 up to 0.45 were utilized in concrete mixing to find the good workability and high compressive strength. The percentages of cement replacement with RHA were in the range of 0 up to 20%. For dosage of Sp, based on solid content calculation, were in the range of 0.5 up to 1.3 %.

In order to determine the effects of various factors on the results of experiment, there are several different methods and approaches used in the experimental study. The fundamentals of methods mostly applied are full factorial design and fractional design.

In full factorial design, the experiments are performed for each condition, which consist of all factors. The full factorial design is applicable when the experiment consists of the number of factor and levels are few, otherwise it will consume of time due to a lot of experiment should be run and costly. Factorial design is a method that allowed the number of experiment conducted is a part of full factorial design. However, those methods cannot predict the interaction between their factors. In HPC, there is a wide range of variability of material should be considered to achieve the target requirement. It needs a lot of experiments are required if adopting the full factorial. The number of experimental conducted is the number of levels exponential of the factors and it is time consuming and high cost to pursue the experiment. There is one of methods that can substantially decrease the number of experiments and feasible to study the effect of factors and interaction of the considered factors, the Box-Behnken design (BBD). The BBD is applied only three-level design of every factor for fitting the response surface which the minimum factors applied should be two factors.

Five factors that affected properties of concrete are considered in this research which are w/b, the amount of binder, percentage of RHA, the ratio of fine aggregate to total aggregate and the dosage of Sp. By using statistical software, design expert version 9, BBD was adopted to find the effect of these factors to the responses of slumps and compressive strength of concrete 1d and 28 d. Table 4.28 shows the factors and the level considered in this study. In software, there are several models available to perform response surface method (RSM) such as linear, two factor interactions (2FI), quadratic and cubic. The suitable of the model was chosen by some criteria which satisfy the effects of the mixture components and their interaction on slump (R1), compressive strength at 1 d (R2) and at 28 d (R3) responses. With five factors and three levels, the number of central point suggested to adopt was 6 runs. The number of experiments in BBD can be calculated as $N=2k(k-1)+C_0$, where k is the number of

factors and co is the number of central points applied, and then the totals of run are 46 runs. The central points were provided to estimate pure error and lack of fit error.

Table 4.28: Factors, level and code for design expert

Levels	Code	Factors				
		W/b	Binder (kg/m ³)	RHA content (% binder)	*fa/ta	Dosage of Sp (% of cement)
1	-1	0.22	500	0	0.35	0.4
2	0	0.25	550	10	0.40	0.85
3	+1	0.28	600	20	0.45	1.30

*fa/ta= ratio of fine aggregate to total aggregate

It is well known that the volume concrete designed is always in 1m³. The ingredients of concrete in this study are cement, RHA as cementitious material, fine aggregate, coarse aggregate, water and superplasticizer. (Meddah et al., 2010) suggested the assumption of air content adopted in fresh concrete was $1.5 \pm 0.5\%$. In this investigation the mixing procedure adopted was two-steps mixing method. As already mention in previous section, this type of mix can improve homogenous of concrete. Treatment condition and test methods were kept in similar procedures to all the mixes. As mention earlier, the purpose of this study is to develop HPC containing RHA having compressive strength 100 MPa. As previous study in RHA concrete, (Mahmud, H.B. et al., 2005) reported the compressive strength of 80 MPa was achieved successfully by utilizing a low w/b of 0.27 and cement content of 550 kg/m³ by the conventional mixing. The level replacement cement by RHA up to 30% could be advantageously RHA concrete without adversely affecting the strength and permeability properties of concrete (Ganesan et al., 2008). The ratio of fine aggregate to total aggregate influenced the packing density of aggregate but Domone and Soutsos (1994) mentioned the better performance of fresh concrete if the ratio fine aggregate to total aggregate used was slightly lower than the optimum one. The use of Sp is crucial in HPC with low w/b ratio and containing pozzolan material and low w/b ratio. The usage proper of Sp dosage improved workability and compressive strength of harden concrete (Alsadey,

2012). The random run in this study and their mix proportions detailed are shown in Table 4.29 and 4.30.

Table 4.29: Box-Behnken design with actual code and level of variables

Run	A: W/b	B:Binder (Kg/m ³)	C:RHA (% binder)	D:fa/ta	E:Sp (%)
1	0	0	-1	-1	0
2	0	-1	0	+1	0
3	0	0	+1	0	+1
4	0	0	0	0	0
5	0	+1	0	-1	0
6	0	+1	0	+1	0
7	0	0	0	0	0
8	0	-1	0	0	+1
9	+1	-1	0	0	0
10	0	+1	0	0	+1
11	+1	0	+1	0	0
12	0	0	+1	0	-1
13	+1	+1	0	0	0
14	0	0	0	0	0
15	-1	0	0	0	-1
16	+1	0	0	0	-1
17	0	0	0	0	0
18	0	0	0	+1	-1
19	0	0	-1	0	+1
20	0	0	0	-1	-1
21	0	0	+1	-1	0
22	-1	0	0	-1	0
23	-1	0	-1	0	0
24	+1	0	0	-1	0
25	-1	0	+1	0	0
26	-1	0	0	0	+1
27	+1	0	-1	0	0
28	0	+1	0	0	-1
29	-1	+1	0	0	0
30	0	0	0	0	0
31	0	-1	+1	0	0
32	0	0	+1	+1	0
33	0	-1	0	-1	0
34	0	+1	+1	0	0
35	0	-1	-1	0	0
36	0	0	-1	0	-1
37	+1	0	0	+1	0
38	-1	-1	0	0	0
39	0	0	0	0	0
40	0	0	-1	+1	0
41	0	-1	0	0	-1
42	0	0	0	-1	+1
43	0	+1	-1	0	0
44	-1	0	0	+1	0
45	+1	0	0	0	+1
46	0	0	0	+1	+1

$$V_{Cr} = V_w + V_C + V_{RHA} + V_{CA} + V_{FA} + V_{SP} + V_A = 1 \text{ m}^3 = 1000 \text{ l}$$

$$X = \frac{M_{FA}}{M_{TA}}$$

$$V_m = 1000 - (V_w + V_c + V_{RHA} + V_{sp} + V_a)$$

$$M_{FA} = \frac{V_m}{\left(\frac{1}{\rho_{FA}} + \frac{(1-X)}{(X * \rho_{CA})}\right)}$$

$$M_{CA} = \left(V - \frac{M_{FA}}{\rho_{FA}}\right) \rho_{CA}$$

Table 4.30: Mix proportions of forty six runs

Run	A: W/b	B:Binder (kg/m ³)	C:RHA (%)	D:fa/ta (%)	E:Sp (%)	RHA (kg/m ³)	FA (kg/m ³)	CA (kg/m ³)
1	0.25	550	0	0.35	0.85	0	596	1107
2	0.25	500	10	0.45	0.85	50	781	955
3	0.25	550	20	0.4	1.3	110	657	986
4	0.25	550	10	0.4	0.85	55	668	1003
5	0.25	600	10	0.35	0.85	60	562	1043
6	0.25	600	10	0.45	0.85	60	714	873
7	0.25	550	10	0.4	0.85	55	668	1003
8	0.25	500	10	0.4	1.3	50	697	1045
9	0.28	500	10	0.4	0.85	50	683	1025
10	0.25	600	10	0.4	1.3	60	636	954
11	0.28	550	20	0.4	0.85	110	642	964
12	0.25	550	20	0.4	0.4	110	661	992
13	0.28	600	10	0.4	0.85	60	620	930
14	0.25	550	10	0.4	0.85	55	668	1003
15	0.22	550	10	0.4	0.4	55	687	1031
16	0.28	550	10	0.4	0.4	55	654	981
17	0.25	550	10	0.4	0.85	55	668	1003
18	0.25	550	10	0.45	0.4	55	750	917
19	0.25	550	0	0.4	1.3	0	676	1014
20	0.25	550	10	0.35	0.4	55	590	1095
21	0.25	550	20	0.35	0.85	110	580	1077
22	0.22	550	10	0.35	0.85	55	603	1119
23	0.22	550	0	0.4	0.85	0	694	1042
24	0.28	550	10	0.35	0.85	55	573	1065
25	0.22	550	20	0.4	0.85	110	676	1014
26	0.22	550	10	0.4	1.3	55	683	1025
27	0.28	550	0	0.4	0.85	0	661	991
28	0.25	600	10	0.4	0.4	60	641	961
29	0.22	600	10	0.4	0.85	60	657	985
30	0.25	550	10	0.4	0.85	55	668	1003
31	0.25	500	20	0.4	0.85	100	690	1035
32	0.25	550	20	0.45	0.85	110	737	901
33	0.25	500	10	0.35	0.85	50	614	1141
34	0.25	600	20	0.4	0.85	120	628	942
35	0.25	500	0	0.4	0.85	0	707	1060
36	0.25	550	0	0.4	0.4	0	680	1020
37	0.28	550	10	0.45	0.85	55	729	891
38	0.22	500	10	0.4	0.85	50	714	1070
39	0.25	550	10	0.4	0.85	55	668	1003
40	0.25	550	0	0.45	0.85	0	758	927

Table 4.30: Continue

Run	A: W/b	B:Binder (kg/m ³)	C:RHA (%)	D:fa/ta (%)	E:Sp (%)	RHA (kg/m ³)	FA (kg/m ³)	CA (kg/m ³)
41	0.25	500	10	0.4	0.4	50	700	1050
42	0.25	550	10	0.35	1.3	55	586	1089
43	0.25	600	0	0.4	0.85	0	649	973
44	0.22	550	10	0.45	0.85	55	767	937
45	0.28	550	10	0.4	1.3	55	650	975
46	0.25	550	10	0.45	1.3	55	746	911

The actual code from Box-Behnken design was transformed to be uncode base on Table 4.29. So for w/b, binder, level of RHA replacement, ratio of fine aggregate to coarse aggregate and dosage of superplasticizer directly can be found. However for fine aggregate and coarse aggregate must be calculated separately based on 1 m³ volume of concrete.

4.5.1 Statistical Analysis

The 46 mix proportions of HPC in Table 4.9 were casted. The fresh concrete and harden properties of concrete were tested and recorded as responses. The slump of fresh concrete, the compressive strength at 1 day and 28 days were named as R1, R2 and R3, respectively. The responses of 46 mixes are presented in Table 4.31.

Table 4.31: Responses of forty six mixtures

Run	Responses		
	Slump (mm)	1 day-Compressive strength (MPa)	28 day- Compressive strength (MPa)
1	216	64.2	99.3
2	219	32.8	87.9
3	218	35.7	94.2
4	198	50.6	108.0
5	164	42.4	100.3
6	165	42.9	101.3
7	199	52.1	109.0
8	224	33.1	88.8
9	222	29.5	75.1
10	219	47.2	116.3
11	197	35.4	83.5

Table 4.31: Continue

Run	Responses		
	Slump (mm)	1 day-Compressive strength (MPa)	28 day-Compressive strength (MPa)
12	71	23.2	59.7
13	202	43.3	102.6
14	197	50.1	107.0
15	82	26.0	75.3
16	125	32.4	76.0
17	195	51.2	108.6
18	96	34.7	76.2
19	223	65.5	103.5
20	95	34.4	75.4
21	163	30.8	81.2
22	174	37.8	104.5
23	205	69.7	106.6
24	215	41.3	96.7
25	150	25.1	78.3
26	220	42.2	115.9
27	225	54.6	76.4
28	69	30.7	75.6
29	148	38.5	98.2
30	192	53.6	109.8
31	202	31.1	72.9
32	165	31.1	82.1
33	216	32.4	87.0
34	145	31.8	81.6
35	226	41.2	73.6
36	139	50.4	77.8
37	215	41.7	97.7
38	215	34.0	90.8
39	200	54.0	111.0
40	215	64.8	100.3
41	139	25.5	68.4
42	218	49.8	111.9
43	202	73.8	105.3
44	176	38.2	105.6
45	226	42.1	98.7
46	219	50.3	113.1

The responses of experimental data need to be identified whether there are substantive departure from normality or not through identifying outliers, skewness and kurtosis (<http://www.itl.nist.gov/div898/handbook/pri/section2/pri24.htm>). Otherwise it needs more steps to be normalized through transformation and mixtures. In this study, normal probability plots were made of residual from model fits and estimated parameters. A histogram is not suggested to be used due to the sample sizes are less than 50 so that the normal probability plot is more sensitive than the histogram

(<http://www.itl.nist.gov/div898/handbook/pri/section2/pri24.htm>). Through graphs shown in Figure 4.58, the normal distribution of responses can be checked whether the models are reasonable and appropriate. The normal probability plot should produce an approximately straight line if the points come from a normal distribution. (<http://www.itl.nist.gov/div898/handbook/pri/section2/pri24.htm>) mentioned that small departures from the straight line in the normal probability plots are common. The normal plots of residual from slump, compressive strength at 1 day and 28 days show that all residual are dominant closed to strike line which means that the responses are normally distributed. It means the model chosen is appropriate.

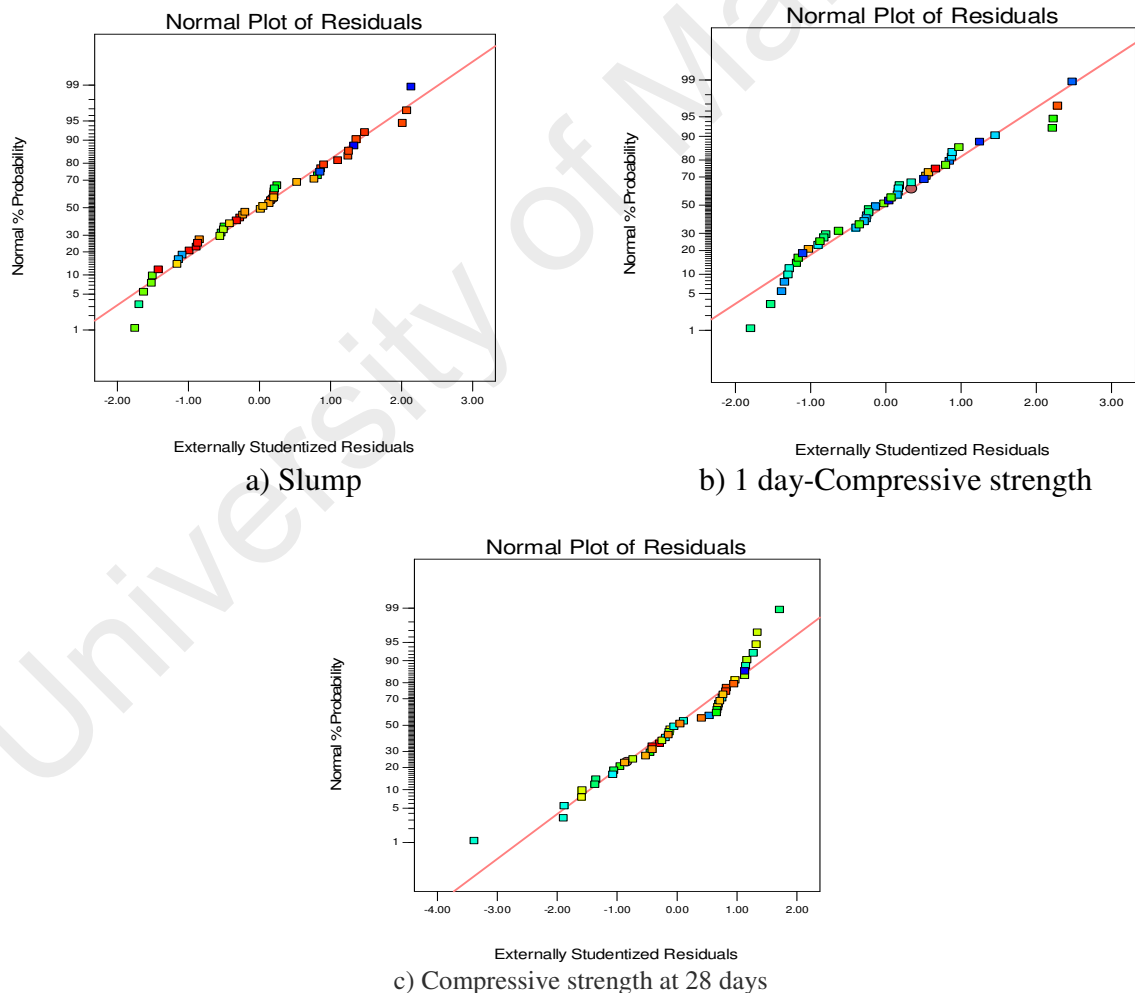


Figure 4.58: Normal plots of residuals of responses

Table 4.32 shows the summary of model analyzed by software, which are linear, two-way factor interaction, quadratic and cubic. To choose the best model, it can be used a formula of the predicted residual sum of squares (PRESS), which the lowest of the PRESS value is the best model among the models proposed. In Table 4.11, it shows that the responses of slump, compressive strength at 1 day and 28 days exhibited the model suggested by software are quadratic models. Those quadratic models are suggested based on the lowest values of PRESS, which are 1985.50, 499.07 and 549.12 for slump, compressive strength at 1 day and 28 days, respectively. Even their standard deviations of quadratic and R squares are higher than cubic one. The cubic is not suggested to be used in the model due to it shows some data are aliased in that model.

The coefficient of determination (R^2) of the models was 0.9943, 0.9810 and 0.9858 for response of slump, compressive strength 1 day and 28 days, respectively, which indicated a good fit between predicted values and the experimental data points (Fig. 4.18). In addition, this implies that 99.43%, 98.10% and 98.58% of the variations for slump, compressive strength at 1 day and 28 days, respectively, can be explained by the independent variables. Predicted R^2 is a measurement of how good the model predicts a response value. The adjusted R^2 and predicted R^2 should be within less than 0.20 of each other to be in reasonable agreement. If they are not, maybe there is a problem with either the data or the model (Sereshti et al., 2014). In Table 4.11, it shows in all cases that the differences between the adjusted R^2 and predicted R^2 are less than 0.2. Furthermore, adequate precision measures the signal to noise ratio and compares the range of the predicted values at the design points to the average prediction error. The value greater than 4 is desirable and indicates adequate model discrimination. In this work, as shown in Table 4.32, the value of the adequate precision for the models are found to be greater than 4 which indicates the reliability of the experiment data.

Table 4.32: Proposed models by the Design Expert software

Response	Model	Std. Dev.	R-Squared	Adjusted R-Squared	Predicted R-Squared	Adeq. Precision	PRESS
Slump	Linear	19.54	0.8322	0.8112	0.7740		20578.27
	2FI	19.91	0.8694	0.8041	0.6642		30577.76
	Quadratic	4.55	0.9943	0.9898	0.9784	53.775	1965.58
	Cubic	3.11	0.9989	0.9952	0.9611		3544.11
1 day-Compressive strength	Linear	7.19	0.7045	0.6676	0.6217		2647.83
	2FI	7.15	0.7807	0.6710	0.5400		3219.58
	Quadratic	2.31	0.9810	0.9658	0.9287	31.862	499.07
28 day-Compressive strength	Cubic	2.47	0.9913	0.9609	0.5585		3090.53
	Linear	9.65	0.6311	0.5850	0.5443		4601.22
	2FI	9.96	0.7054	0.5580	0.4546		5507.47
	Quadratic	2.40	0.9858	0.9744	0.9456	36.451	549.12
	Cubic	1.90	0.9964	0.9840	0.8325		1690.99

Furthermore, ANOVA for slump (Table 4.33), compressive strength at 1 day (Table 4.34) and compressive strength at 28 days (Table 4.35) indicated the “*P*-value” of models to be less than 0.0001, which implies that all the models are significant. The “Lack of Fit Test” compares the residual error to the pure error from replicated design points. Then the Table 4.33, 4.34 and 4.35 also show the “lack of fit *F*-value” of those models, which are 2.83, 2.83 and 3.41, respectively. All *p*-values for lack of fit of models are greater than >0.05, which implies that the lack of fit is insignificant. The insignificant lack-of-fit showed that the model was valid for this study. The models have high R^2 value, significant *F*-value, low standard deviation and insignificant lack-of-fit *P*-values. These results indicate the high precision in predicting the slump and compressive strength of HPC containing RHA at 1 day and 28 days. Therefore, the models were used for further analysis.

Table 4.33: ANOVA for the complete combined quadratic model of slump responses

Source	Sum of Squares	df	Mean Square	F Value	p-value Prob > F	Remark
Model	90528.20	20	4526.41	218.32	< 0.0001	significant
A-W/b	4117.36	1	4117.36	198.59	< 0.0001	
B-Binder	7615.29	1	7615.29	367.30	< 0.0001	

Table 4.33: Continue

Source	Sum of Squares	df	Mean Square	F Value	p-value Prob > F	Remark
E-Sp	56800.30	1	56800.30	2739.57	< 0.0001	
AB	552.25	1	552.25	26.64	< 0.0001	
AC	179.73	1	179.73	8.67	0.0069	
AD	0.88	1	0.88	0.042	0.8385	
AE	361.00	1	361.00	17.41	0.0003	
BC	267.46	1	267.46	12.90	0.0014	
BD	0.25	1	0.25	0.012	0.9134	
BE	1046.12	1	1046.12	50.46	< 0.0001	
CD	2.25	1	2.25	0.11	0.7446	
CE	974.61	1	974.61	47.01	< 0.0001	
DE	3.90E-03	1	3.906E-003	1.884E-04	0.9892	
A ²	5.26	1	5.26	0.25	0.6188	
B ²	4.99	1	4.99	0.24	0.6279	
C ²	38.18	1	38.18	1.84	0.1869	
D ²	199.61	1	199.61	9.63	0.0047	
E ²	9893.60	1	9893.60	477.18	< 0.0001	
Residual	518.33	25	20.73			
Lack of Fit	476.24	20	23.81	2.83	0.1261	not significant
Pure Error	42.09	5	8.42			
Cor Total	91046.53	45				

Table 4.34: ANOVA: for complete combined quadratic model of 1 d compressive strength response

Source	Sum of Squares	df	Mean Square	F Value	p-value Prob > F	Remark
Model	6866.70	20	343.33	64.54	< 0.0001	significant
A-W/b	5.00	1	5.00	0.94	0.3416	
B-Binder	476.26	1	476.26	89.53	< 0.0001	
C-RHA	3713.26	1	3713.26	698.05	< 0.0001	
D-fa/ta	0.73	1	0.73	0.14	0.7135	
E-Sp	736.32	1	736.32	138.42	< 0.0001	
AB	21.22	1	21.22	3.99	0.0568	
AC	162.18	1	162.18	30.49	< 0.0001	
AD	3.616E-04	1	3.616E-04	6.797E-05	0.9935	
AE	10.56	1	10.56	1.98	0.1712	
BC	317.38	1	317.38	59.66	< 0.0001	
BD	3.024E-03	1	3.024E-03	5.686E-04	0.9812	
BE	19.83	1	19.83	3.73	0.0649	
CD	0.029	1	0.029	5.460E-03	0.9417	
CE	1.65	1	1.65	0.31	0.5824	
DE	7.963E-03	1	7.963E-03	1.497E-03	0.9694	
A ²	457.80	1	457.80	86.06	< 0.0001	
B ²	762.86	1	762.86	143.41	< 0.0001	
C ²	2.26	1	2.26	0.43	0.5201	
D ²	145.82	1	145.82	27.41	< 0.0001	
E ²	550.91	1	550.91	103.56	< 0.0001	
Residual	132.99	25	5.32			
Lack of Fit	120.14	20	6.01	2.34	0.1760	not significant
Pure Error	12.84	5	2.57			
Cor Total	6999.69	45				

Table 4.35: ANOVA: for complete combined quadratic model of compressive strength at 28 days

Source	Sum of Squares	df	Mean Square	F Value	p-value Prob > F	Remark
Model	9953.78	20	497.69	86.67	< 0.0001	significant
A-W/b	292.21	1	292.21	50.89	< 0.0001	
B-Binder	1168.29	1	1168.29	203.46	< 0.0001	
C-RHA	746.64	1	746.64	130.03	< 0.0001	
D-fa/ta	3.74	1	3.74	0.65	0.4270	
E-Sp	4161.77	1	4161.77	724.78	< 0.0001	
AB	101.11	1	101.11	17.61	0.0003	
AC	314.00	1	314.00	54.68	< 0.0001	
AD	1.571E-003	1	1.571E-03	2.736E-004	0.9869	
AE	79.78	1	79.78	13.89	0.0010	
BC	132.62	1	132.62	23.10	< 0.0001	
BD	4.586E-03	1	4.586E-03	7.987E-004	0.9777	
BE	102.83	1	102.83	17.91	0.0003	
CD	0.012	1	0.012	2.148E-003	0.9634	
CE	19.22	1	19.22	3.35	0.0792	
DE	0.038	1	0.038	6.578E-003	0.9360	
A ²	344.99	1	344.99	60.08	< 0.0001	
B ²	1050.49	1	1050.49	182.94	< 0.0001	
C ²	1988.42	1	1988.42	346.29	< 0.0001	
D ²	82.19	1	82.19	14.31	0.0009	
E ²	1034.28	1	1034.28	180.12	< 0.0001	
Residual	143.55	25	5.74			
Lack of Fit	133.75	20	6.69	3.41	0.0889	not significant
Pure Error	9.80	5	1.96			
Cor Total	10097.33	45				

Table 4.36 is related to ANOVA in Table 4.33, 4.34 and 4.35. Some of coefficients in the complete models shown in Table 4.36 are insignificant and could be eliminated (i.e. values of “prob>F in Table 4.33, 4.34 and 4.35 less than 0.005 indicate the model terms are insignificant). However, in this case, there is no advantage to reduce model because the adjusted R square is only slightly changed. Moreover, the interaction should not be removed in the combined mixture process model, especially with the combined quadratic model. Therefore, the complete models in Table 4.36 were used. The predicted data and the ratios between predicted and experimental data are also given in Table 4.37. The values of the ratios of responses to prediction are close to 1 and it indicates the fitness of the complete models. Figure 4.59 shows the results and predicted value of slump, compressive strength 1 d and 28 days. It shows that the predicted value is close enough to straight line, which means the model is suitable to predict the slump, compressive strength at 1 day and 28 days of mix proportion.

Table 4.36: Coefficients for the quadratic model

Variables	Coefficients		
	Slump (mm)	1 day-Compressive strength (MPa)	28 days-Compressive strength (MPa)
Intercept	+952.25268	-1746.94666	-1478.20700
x W/b	-3705.33340	+3085.24033	+1498.11514
x binder	-2.46924	+3.92857	+4.07849
x RHA	-1.84707	+3.05644	+0.91658
x fa/ta	+1661.8765	+1304.68001	+984.99999
x Sp	+161.54438	+58.06252	+79.39616
x W/b x binder	+7.83333	+1.53568	+3.35183
x W/b x RHA	+22.34375	+21.22485	+29.53318
x W/b x fa/ta	-312.50000	+6.33833	-13.21333
x W/b x Sp	-703.70370	-120.33934	-330.81481
x binder x RHA	-0.016354	-0.017815	-0.011516
x binder x fa/ta	-0.10000	+0.010999	+0.013544
x binder x Sp	+0.71875	+0.098967	+0.22534
x RHA x fa/ta	+1.50000	-0.17042	-0.11106
x RHA x Sp	+3.46875	-0.14278	+0.48716
x fa/ta x Sp	-1.38889	+1.98300	+4.31904
x (W/b) ²	+862.86588	-8047.44900	-6985.85929
x binder ²	-0.00030	-0.0003739	-0.0004388
x RHA ²	-0.020915	+0.00509306	-0.15094
x (fa/ta) ²	-1912.97939	-1635.01675	-1227.53930
x Sp ²	-166.26964	-39.23509	-53.75957

Table 4.37: Responses and predicted values from the quadratic model

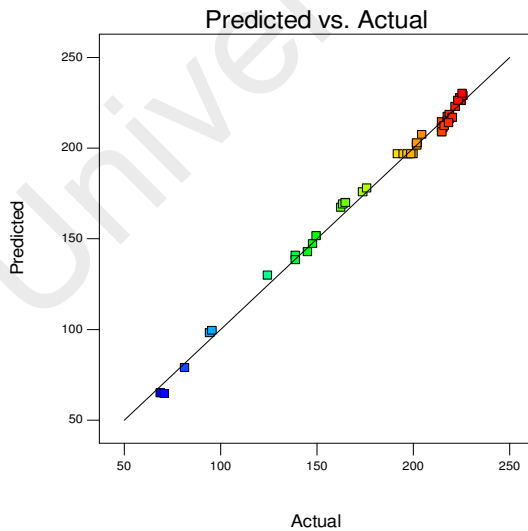
Run	Responses			Predicted			Ratios of responses to predicted		
	R1	R2	R3	R1*	R2*	R3*	(R1/R1*)	(R2/R2*)	(R3/R3*)
1	216	64.2	99.3	211	63.3	97.0	1.02	1.01	1.02
2	219	32.8	87.9	214	33.2	86.8	1.02	0.99	1.01
3	218	35.7	94.2	215	35.4	94.4	1.01	1.01	1.00
4	198	50.6	108.0	197	51.9	108.9	1.00	0.97	0.99
5	164	42.4	100.3	169	43.7	102.9	0.97	0.97	0.97
6	165	42.9	101.3	170	44.2	103.9	0.97	0.97	0.97
7	199	52.1	109.0	197	51.9	108.9	1.01	1.00	1.00
8	224	33.1	88.8	228	33.8	89.6	0.99	0.98	0.99
9	222	29.5	75.1	223	28.2	73.8	1.00	1.05	1.02
10	219	47.2	116.3	216	49.1	116.8	1.01	0.96	1.00
11	197	35.4	83.5	197	36.9	85.3	1.00	0.96	0.98
12	71	23.2	59.7	65	23.1	57.8	1.10	1.00	1.03
13	202	43.3	102.6	203	43.7	101.0	1.00	0.99	1.02
14	197	50.1	107.0	197	51.9	108.9	1.00	0.96	0.98
15	82	26.0	75.3	79	27.8	75.4	1.04	0.94	1.00
16	125	32.4	76.0	130	32.2	75.8	0.96	1.01	1.00
17	195	51.2	108.6	197	51.9	108.9	0.99	0.99	1.00
18	96	34.7	76.2	99	33.3	79.2	0.96	1.04	0.96
19	223	65.5	103.5	226	67.2	103.7	0.99	0.98	1.00
20	95	34.4	75.4	98	33.0	78.4	0.96	1.04	0.96
21	163	30.8	81.2	167	33.0	83.5	0.97	0.93	0.97

Table 4.37: Continue

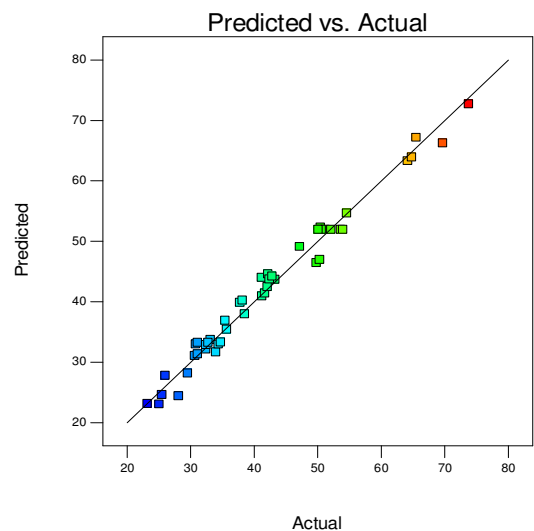
Run	Responses			Predicted			Ratios of responses to predicted		
	R1	R2	R3	R1*	R2*	R3*	(R1/R1*)	(R2/R2*)	(R3/R3*)
22	174	37.8	104.5	176	39.9	103.3	0.99	0.95	1.01
23	205	69.7	106.6	207	66.3	107.5	0.99	1.05	0.99
24	215	41.3	96.7	209	41.0	94.8	1.03	1.01	1.02
25	150	25.1	78.3	151	23.1	76.1	0.99	1.09	1.03
26	220	42.2	115.9	217	44.6	116.6	1.02	0.95	0.99
27	225	54.6	76.4	226	54.6	81.2	1.00	1.00	0.94
28	69	30.7	75.6	65	31.1	74.4	1.07	0.99	1.02
29	148	38.5	98.2	147	37.9	99.4	1.01	1.02	0.99
30	192	53.6	109.8	197	51.9	108.9	0.98	1.03	1.01
31	202	31.1	72.9	203	31.3	73.2	1.00	0.99	1.00
32	165	31.1	82.1	170	33.3	84.3	0.97	0.94	0.97
33	216	32.4	87.0	212	32.9	85.9	1.02	0.99	1.01
34	145	31.8	81.6	143	24.4	78.8	1.02	1.30	1.04
35	226	41.2	73.6	229	44.0	75.4	0.99	0.94	0.98
36	139	50.4	77.8	138	52.3	75.8	1.01	0.96	1.03
37	215	41.7	97.7	209	41.4	95.7	1.03	1.01	1.02
38	215	34.0	90.8	214	31.6	92.4	1.00	1.07	0.98
39	200	54.0	111.0	197	51.9	108.9	1.02	1.04	1.02
40	215	64.8	100.3	211	63.9	98.1	1.02	1.01	1.02
41	139	25.5	68.4	141	24.6	67.5	0.99	1.03	1.01
42	218	49.8	111.9	217	46.4	110.5	1.00	1.07	1.01
43	202	73.8	105.3	202	72.7	104.0	1.00	1.02	1.01
44	176	38.2	105.6	178	40.3	104.3	0.99	0.95	1.01
45	226	42.1	98.7	230	42.5	99.1	0.98	0.99	1.00
46	219	50.3	113.1	218	47.0	111.7	1.00	1.07	1.01

R1=Slump (mm); R2=Compressive strength at 1 day (MPa); R3=Compressive strength at 28 day (MPa)

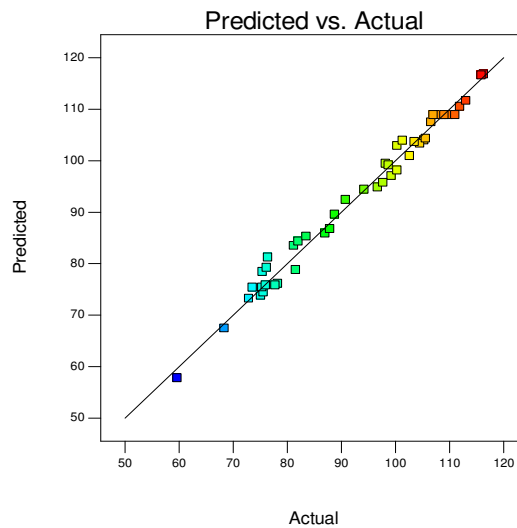
R1*=predicted slump (mm); R2*= predicted compressive strength at 1 day (MPa); R3*=predicted compressive strength at 28 day (MPa)



a) Slump



b) Compressive strength at 1 day



c) Compressive strength at 28 days

Figure 4.59: Plot of the experimental and predicted response of slump, compressive strength at 1 day and 28 days

4.5.2 Influence of w/b, binder, fa/ta, % RHA and Sp dosage on slump value of HPC

Figure 4.60 shows the perturbation of slump on w/b of 0.25, binder 550 kg/m^3 , 10% RHA, fa/ta of 0.4 and Sp dosage of 0.9%. Through this graph, the changing quantity of a variable can predict the affect to slump of fresh concrete. Increasing w/b (A) or Sp dosage (E) affect the increase of slump. However, increasing the RHA (C) or binder content (B) reduces the slump. Increasing fa/ta ratio (D) in the range of 0.35 up to 0.45 is not much change the slump of HPC. At the high Sp dosage of 1.3%, the slump is almost double compared to dosage of 0.5%. Three dimensions of response surface and contour plots to interpret the interaction two selection variables to the slump are shown in Appendix A.

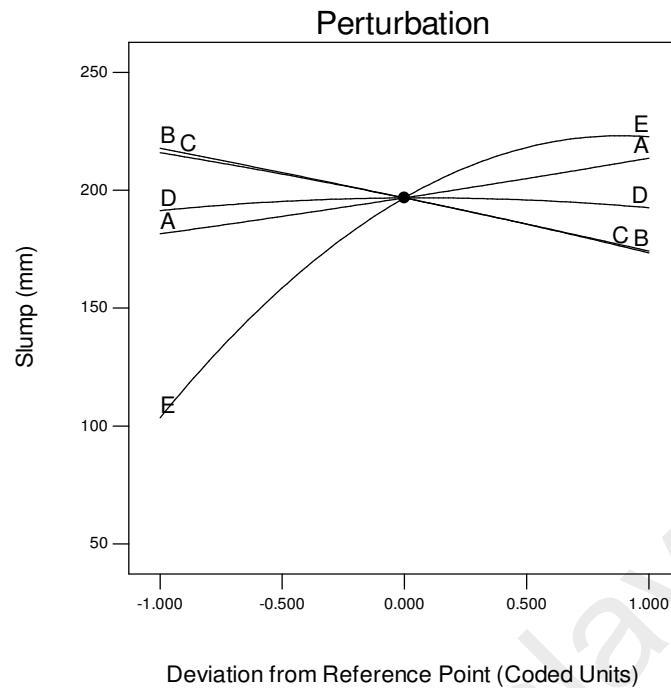


Figure 4.60: Perturbation of slump on w/b of 0.25, Binder of 550 kg/m³, 10% of RHA, fa/ta of 0.4 and Sp dosage of 0.9%

4.5.3 Influence of w/b, binder, fa/ta, RHA and % of Sp dosage on compressive strength of HPC at 1 day

Figure 4.61 shows the perturbation of compressive strength at 1 day on w/b of 0.25, binder 550 kg/m³, 10% RHA, fa/ta of 0.4 and Sp dosage of 0.9%. Increasing w/b (A) or binder (B), RHA content and Sp dosage (E) affect the increase of compressive strength at 1 day. However, increasing the RHA content (C) reduces the compressive strength at 1 day and increasing fa/ta ratio (D) in the range of 0.35 up to 0.45 is not much change the compressive strength at 1 day. At the high Sp dosage of 1.3%, the compressive strength at 1 day is higher 40% than that of dosage of 0.5%. Three dimension of response surface and contour plots to interpret the interaction two selection variables to the compressive strength at 1 day are shown in Appendix B.

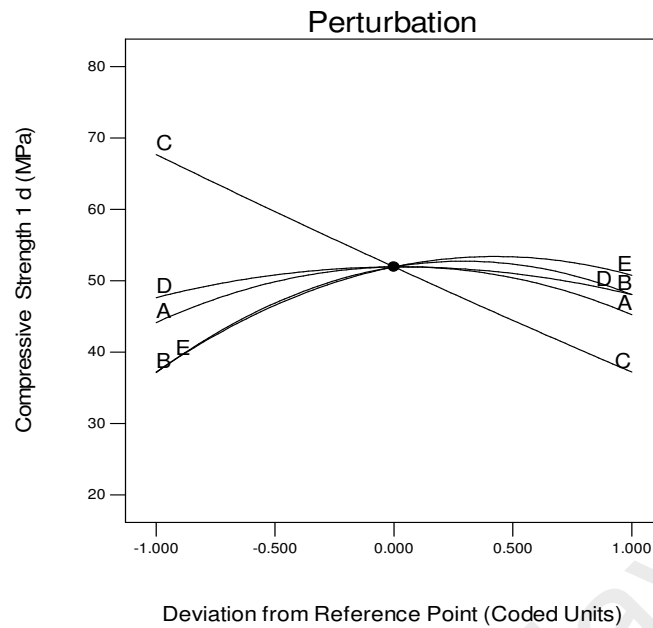


Figure 4.61: Perturbation of compressive strength of concrete at 1 day on w/b of 0.25, Binder of 550 kg/m³, 10% of RHA, fa/ta of 0.4 and Sp dosage of 0.9%

4.5.4 Influence of w/b, binder, fa/ta, RHA and Sp dosage on compressive strength of HPC at 28 days

Figure 4.62 shows the perturbation of compressive strength at 28 day on w/b of 0.25, binder of 550 kg/m³, 10% of RHA, fa/ta of 0.4 and Sp dosage of 0.9%. Decreasing W/b (A), increasing binder (B) or Sp dosage (E) significantly affects the increase of compressive strength at 28 days. However, decreasing w/b (A) or the increasing RHA content (C) more than 10% reduces the compressive strength at 28 days. Increasing fa/ta ratio in the range of 0.35-0.45 is not much change the compressive strength at 28 days. At the Sp dosage of 1.3%, the compressive strength of RHA concrete at 28 days is higher than that of dosage of 0.5%. At Sp dosage of 1.3 %, there was no sign of bleeding and segregation of fresh RHA concrete. According to (Chang, 2004) the proper dosage of Sp improves the flowability of concrete at low w/b ratios due to the friction between packed granular materials are reduced. As mentioned previously that saturation point of SP dosage for 10% RHA was around 1.3% and it means that the

dosage can reserve available mixing water and fulfill the required workability. Then, the compressive strengths of RHA concrete are improved due to the RHA concrete is denser which related to hydration produced CaOH and then reacted with SiO₂ from RHA created more CSH. Three dimension of response surface and contour plots to interpret the interaction two selection variables to the compressive strength at 28day are shown in Appendix C.

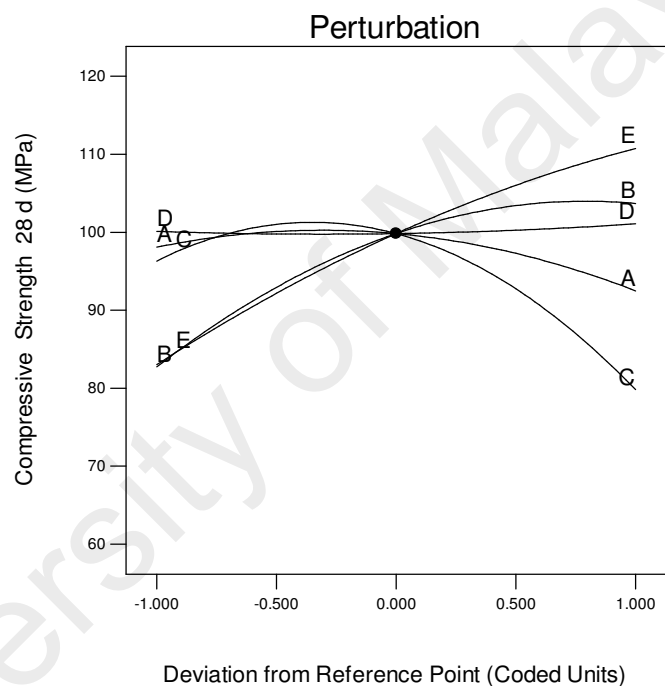


Figure 4.62: Perturbation of compressive strength of RHA concrete at 28 days on w/b of 0.25, Binder of 550 kg/m³, 10% of RHA, fa/ta of 0.4 and Sp dosage of 0.9%

4.5.5 Optimization using the desirability function to get the mix proportion of HPC containing RHA

By using numerical optimization provided by software, a desirable value for each input factor and response can be selected. For optimizing output values, it was given a

set condition such as the range, maximum, minimum, and target of variables in the model.

In this study, the input variables were given target and specific ranged values, whereas the response was designed to achieve a maximum value. Using these conditions, the target of achieved slump, was 200 mm (see Table 4.38 and Figure 4.63). The inputs in the target of w/b, binder, RHA replacement, the range ratio of fa/ta, and the range of Sp dosage were 0.25, 550 kg/m³, 10%, 0.35 up to .045 and 0.5 up to 1.3%, respectively. The output values interested were the slump in the range of 80-230 mm, the compressive strength at 1 day of 23-73 MPa and the compressive strength at 28 days of 64-116 MPa. The confirmatory experiment showed slump of 195 mm, compressive strength of 50.2 MPa at 1 day, and 109 MPa at 28 days. Meanwhile, the results from equations of model of the slump, compressive strength at 1 day and 28 days are 200 mm, 48.1 MPa and 107.1 MPa, respectively. This indicates the suitability and accuracy of the model. Based on this study, for further study the optimum mixture that proposed by model is utilized to reach the compressive strength of 100 MPa of HPC incorporating RHA and to study mechanical properties, durability and time dependent deformation.

Table 4.38: Experimental proportions versus optimized proportions

Material	Variables	Goal	Constrains	Selected	Unit	The mix proportions having the highest strength	
						Design expert	Experimental
W/b	A	Target	0.23-0.28	0.25	-	0.25	0.25
Binder	B	Target	500-600	550	kg/m ³	550	550
RHA	C	Target	0-20	10	%	10	10
fa/ta	D	In range	0.35-0.45	0.35-0.45	-	0.43	0.43
Sp	E	In range	0.5-1.3	0.5-1.3	%	1.15	1.15
Slump		Target	80-230		mm	200	195
1 day-Comp. strength		Maximum	23-73		MPa	47.72	50.2
28 days-Comp. strength		Maximum	64-116		MPa	107.85	109

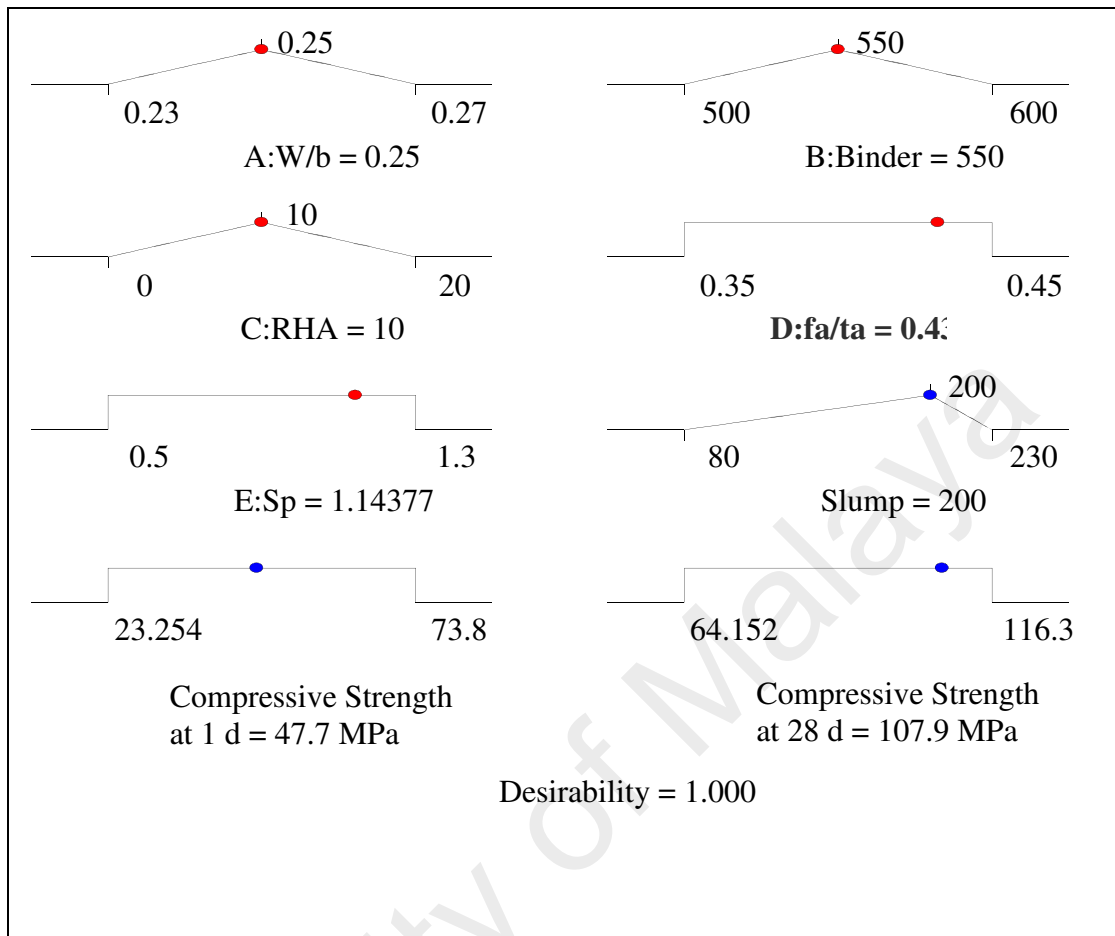


Figure 4.63: Desirability ramp for optimization

4.6 Properties of HPC Incorporating RHA and SF

This section discusses further detail on mechanical properties of the optimum proportion of HPC incorporating RHA based on previous optimum mix proportion by the response surface method of Box-Behnken design. It was found on previous section that HPC incorporating 10% RHA and W/b of 0.25 had a good workability and could achieve the compressive strength of 100 MPa at 28 days. However, for comparison reason, the composition was extended to make comparison for replacement 0, 10%, 15% and 20% of replacement cement with RHA and 10% of cement with SF for w/b ratio of 0.22 and 0.25.

In this research the mechanical properties included were compressive strength, splitting tensile strength, flexural strength and static modulus of elasticity. There were ten series mixes involved to elaborate the replacement of RHA and the effect of curing on those mixes. The mixes with w/b of 0.22 are denoted as OPC-22, RHA10-22, RHA15-22, RHA20-22 and SF10-22 and other mixes w/b of 0.25 are denoted as OPC-25, RHA10-25, RHA15-25, RHA20-25 and SF10-25. While RHA10, RHA15 and RHA20 denotes to replacement 10%, 15% and 20% replacement cement with RHA and SF10 denotes to replacement 10% cement with SF. There were two types of tests conducted to find mechanical properties: destructive test and non-destructive test. The tests of mechanical properties are shown in Table 4.39.

Table 4.39: The mixes involved in the mechanical properties test

Mechanical properties test	OPC	RHA10	RHA15	RHA20	SF10
Destructive test					
Compressive strength	√	√	√	√	√
Split tensile strength	√	√	√	√	√
Flexural strength	√	√	√	√	√
Static modulus of elasticity	√	√	√	√	√
Non-Destructive test					
UVP	√	√	√	√	√

4.6.1 Workability and density

Workability of fresh concrete can be defined as the fresh concrete which is easy to be transported, placed and consolidated without either segregation or excessive bleeding (Afiniwala et al., 2013). High performance concrete is the concrete designated having a high workability and enough cohesiveness without causing segregation and bleeding. According to Aïtcin, P.C (1998) if selected mixing water selected is very low, the mix could rapidly become sticky and a high amount of superplasticizer had to be used to achieve the required slump. It was possible to get retardation in some cases as well. To check or to control the workability of fresh concrete the slump test is the most common test used in concrete industry (Tam, 2003). The dosage of superplasticizer used for the

mixes was found from previous trial mixes and it was to maintain the slump of 200-210 mm. According to Bonikowsky et al. (1992) a concrete that can be cast into a mold with no excessive bleeding water, settlement and segregation has a slump around 190 mm. Then these dosages were applied to final mixes in order to get similar results on the workability of fresh concrete and mechanical properties of harden concrete. Table 4.40 shows the mix proportions of high performance concrete incorporated RHA and SF. As can be seen, the increasing percentages of RHA and SF as replacement cement in the mixes affects to the total volume of mixture due to the specific gravities of RHA and SF are lower compared to that of cement. The specific gravity of cement is 3.14 and that of RHA and SF are 2.15 and 2.22 respectively. To maintain a unity volume of mixture, the portion of fine aggregate is adjusted to achieve similar unity of the volume of the concrete mixes, 1 m³. However, the differences of fine aggregate to control mix are in the range of 1.7-3.1 %, which is insignificant. Meanwhile, the coarse aggregate was kept constant.

Table 4.40: Mix proportion and workability for OPC, RHA and SF concrete

Mix ID	W/b	Ingredient (kg/m ³)						
		Sp	Water	Cement	RHA	SF	Aggregate	
							Fine	Coarse
OPC-22	0.22	2.41	121	550	0	0	719	1050
RHA10-22	0.22	3.93	121	495	55	0	708	1050
RHA15-22	0.22	4.37	121	467.5	82.5	0	703	1050
RHA20-22	0.22	4.80	121	440	110	0	697	1050
SF10-22	0.22	3.49	121	495	0	55	710	1050
OPC-25	0.25	2.38	137.5	550	0	0	702	1050
RHA10-25	0.25	3.49	137.5	495	55	0	690	1050
RHA15-25	0.25	3.93	137.5	467.5	82.5	0	685	1050
RHA20-25	0.25	4.15	137.5	440	110	0	681	1050
SF10-25	0.25	3.13	137.5	495	0	55	692	1050

OPC = ordinary Portland cement; RHA = rice husk ash; SF = silica fume
 10, 15 and 20 = percentages of cement replacement
 22 and 25 = percentages of w/b

Table 4.41 show fresh properties of all concrete mixtures. Figure 4.64 shows relationship between percentage replacements of concrete with RHA with ratio of SP dosage in concrete mix to OPC control mix. As can be seen in this figure for both w/b

ratio, when the RHA content increased the Sp dosage also increased. Similar observation also was reported by (Chao-Lung, 2011 #45). In general, smaller the particle size and higher the specific surface of mineral admixture increases the water demands of concrete (Khan et al., 2014). RHA is a fine material and also has nature porous on its particles and both conditions make higher surface area compared to silica fume which only the finest material, even though the particle size of SF is almost 1/100 less times than that of RHA. As previous explanation, the surface area of RHA is 35250 m²/kg compared to that of OPC and SF which are 308 m²/kg and 25000 m²/kg respectively. The surface area of RHA is almost 93 times to that of OPC and 1.5 times to that of SF. As consequences, more mixing water is needed to cover RHA compared to SF and cement particles. To achieve similar workability with OPC concrete, the RHA and SF mixes need more mixing water available or increasing more dosages of Sp to make the paste covering the particle can act as lubrication. The type of superplasticizer used was a polycarboxylate (PCE) which is better performance compared to previous type of superplasticizer, sulphonated naphthalene formaldehyde. Superplasticizer greatly reduced water demand and improved cement dispersion. The nature of cement grain is to agglomerate with water and therefore it cause less free available mixing water. When superplasticizer is applied, it is absorbed at the surface of cement particle and change the charge of electrostatic of cement particle. It creates electrostatic dispersion and improves the ability of the cement particles to keep a distance from each other. The results of this process are increasing available mixing water and improve workability. In RHA mixes, the Sp dosage for w/b of 0.22 is increased around 10% compared that of 0.25. The Sp dosage is increased around 35% for RHA10% to RHA20%. All mixes in Table 4.41 confirm that there is no bleeding in fresh concrete, which could be a sign that the dosage of Sp is no over dosage.

Table 4.41: The properties of fresh concrete

Mix ID	W/b	RHA (%)	SF (%r)	Sp (%)	Slump (mm)	Fresh Density (kg/m ³)	Air content (%)
OPC-22	0.22	0	0	0.44	205	2506	1.7
RHA10-22	0.22	10	0	0.79	205	2458	1.6
RHA15-22	0.22	15	0	0.93	207	2448	1.6
RHA20-22	0.22	20	0	1.09	205	2441	1.5
SF10-22	0.22	0	10	0.71	203	2452	1.6
OPC-25	0.25	0	0	0.43	210	2478	1.8
RHA10-25	0.25	10	0	0.71	210	2444	1.7
RHA15-25	0.25	15	0	0.84	213	2425	1.7
RHA20-25	0.25	20	0	0.94	212	2392	1.6
SF10-25	0.25	0	10	0.63	211	2435	1.7

OPC = ordinary Portland cement; RHA = rice husk ash; SF = silica fume
 10, 15 and 20 = percentages of cement replacement
 22 and 25 = percentages of w/b

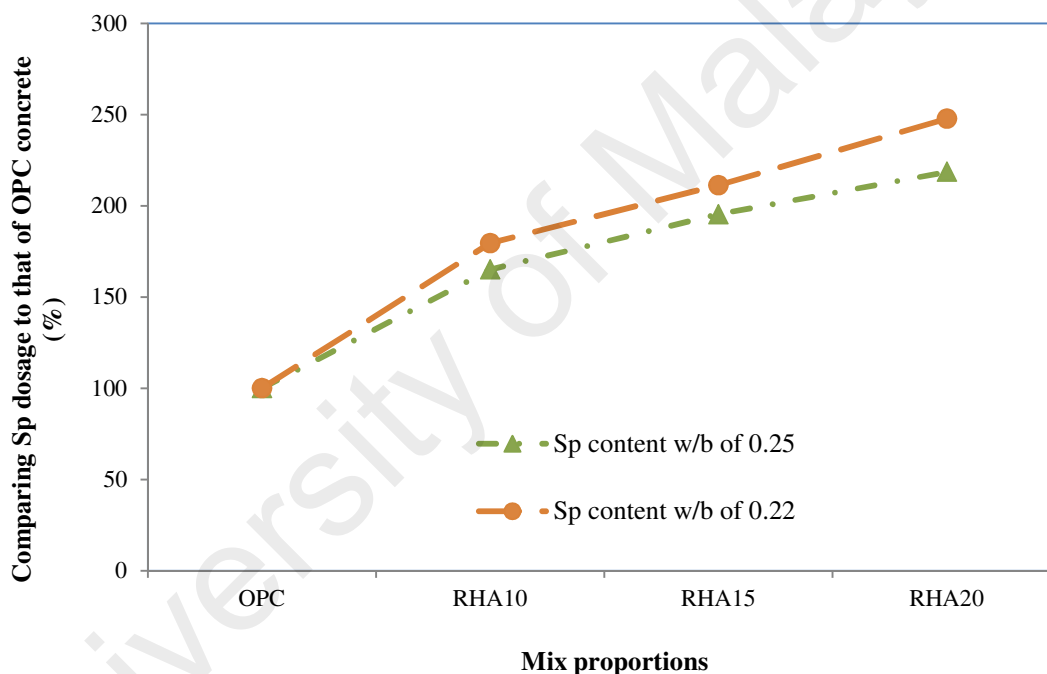


Figure 4.64: Comparing superplasticizer dosage of RHA and SF concrete to that of OPC concrete

Figure 4.65 shows the effect of incorporating RHA and SF in fresh concrete properties such as slump, air content and fresh density. The different fresh properties between RHA concrete are no significant but air content on RHA concrete is significantly different compared to OPC concrete. The slump of RHA and SF mixes are kept relatively similar due to adjustment of Sp dosage. The air content of RHA and SF

mix are reduced as increased of percentages of RHA in the mix even they have similar slump. The air content of RHA fresh concrete is decreased due to increase of fine particle in mixture. The RHA particle could easily fill in the void between fine aggregate and coarse aggregate and make it denser. The density of fresh RHA concrete is decreased compared to that of OPC concrete. It is due to the specific gravity of RHA is less than that of cement. In this study the replacement is based on weight method and it increased the total volume of RHA concrete. To keep in a unity volume, the fine aggregate was adjusted and it affected to fresh density of concrete.

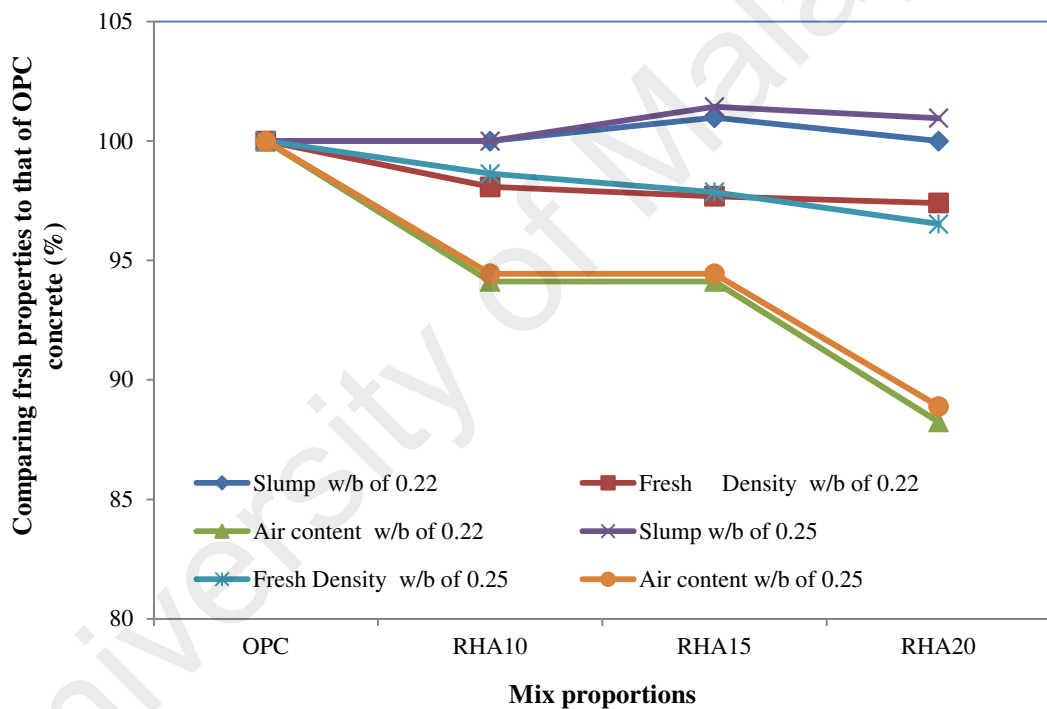


Figure 4.65: Comparing fresh properties of RHA and SF concrete to that of OPC concrete

4.6.2 Compressive strength of HPC

The strength of concrete depends on internal and external factors. The internal factor is the properties and proportions of the constituent materials, degree of hydration and external factors include the rate of loading, method of testing, method of curing and

specimen geometry. If concrete specimen is isolated from external factors then the strength of concrete is governed by the proportioning of cement, fine and coarse aggregates, water, and various admixtures applied. One of sensitive factors in determining concrete strength is the ratio of the water to cement as mentioned by Abrams law, the lower water-cement ratio the higher compressive strength. However according to Aitcin and Neville (1993) it is necessary to provide a certain minimum amount of water for the proper chemical action in the hardening of concrete. Extra water affects in increasing the workability of fresh concrete but also reduces the compressive strength of harden concrete (Poon et al., 2004).

Figure 4.66 and 4.67 show the compressive strength development for RHA, SF and OPC concrete with w/b of 0.22 and 0.25 at different ages up to 180 days. The specimens were cured in water and air drying. The temperature of water in the water tank was recorded at 22 ± 2 °C while the laboratory temperature was 30 ± 1 °C and relative humidity was 75 ± 2 %. For All tests, three specimens were tested each of the ages to get the mean of compressive strength of concrete. From the results, it can be seen that in two series, compressive strength increased with ages. The compressive strength of concrete tends to plateau after 28 days which is around 108-115 MPa. It could be the concrete reached the optimum strength of coarse aggregate as the strength of coarse aggregate is mostly fixed. Also it is important to note that the maximum size of coarse aggregate used in this study was 19 mm. Furthermore, (Baalbaki et al., 1991) mentioned that coarse aggregate could be the weakest part of high strength concrete. At mortar side, as long as water available, it is possible mortar gain more strength due to the hydration of cement and pozzolanic reaction can continue up to years. Figures 4.67 and 4.68 show that all the mixes, except RHA20 concrete, can achieve the compressive strength of 100 MPa on certain days depended on percentages of RHA and SF and curing method.

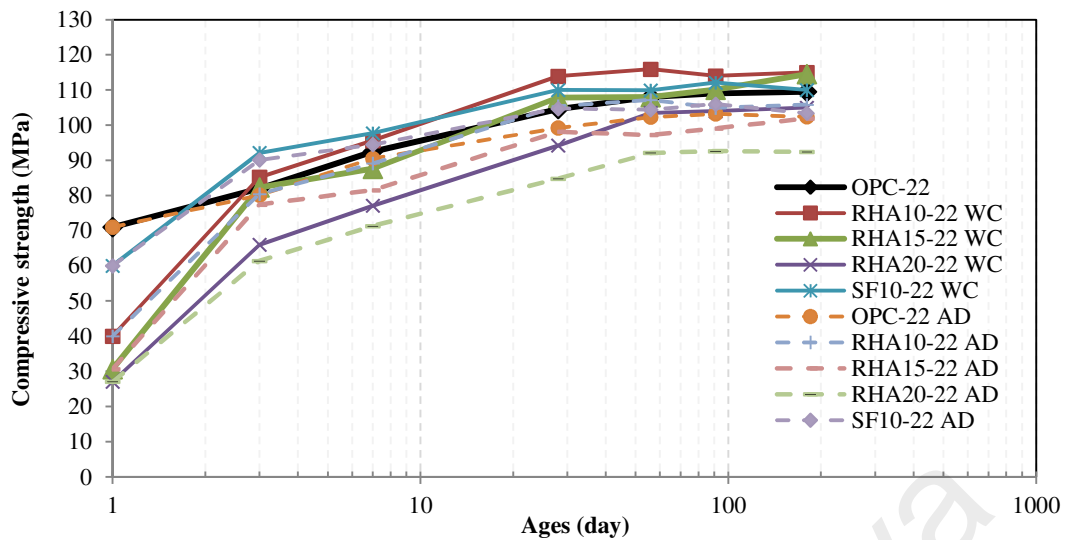


Figure 4.66: Compressive strength development of concrete for w/b of 0.22 subjected to water curing and air drying condition

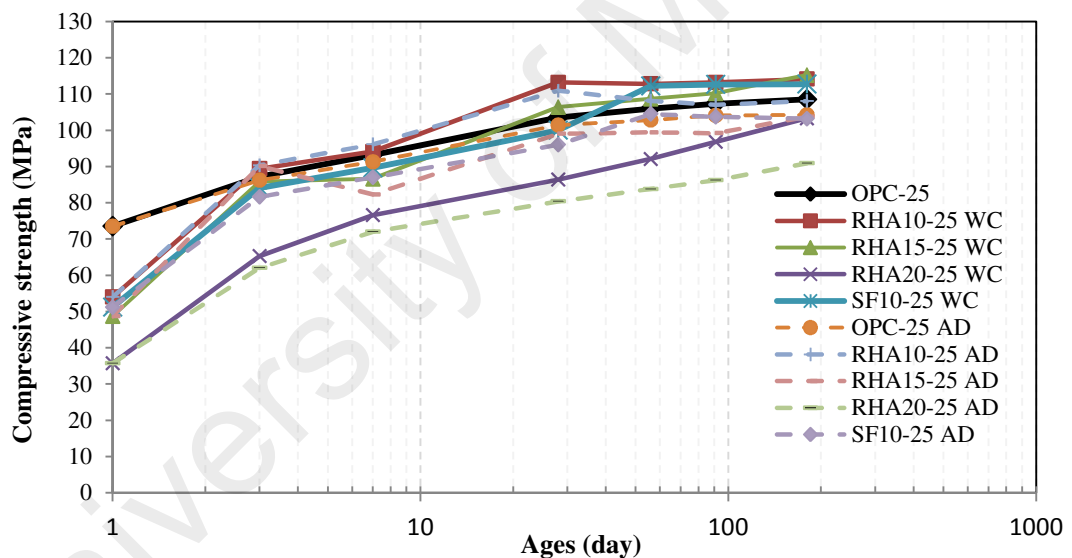


Figure 4.67: Compressive strength development of concrete for w/b of 0.25 subjected to water curing and air drying condition

4.6.2.1 Effect of RHA and w/b on the compressive strength

A lot of researches related to the application of rice husk ash in concrete were conducted and the results show that RHA could improve mechanical properties of concretes which mostly in normal and high strength concrete (Ganesan et al., 2008; Mahmud, H.B. et al., 2005) (Chao-Lung et al., 2011). In addition, it is possible that RHA can function as filler and pozzolanic material if the median particle of RHA

below that of size of cement (Rukzon et al., 2009). In this study the particle size of RHA was 13.50 μm which was less than particle size of cement (22.1 μm).

It can be seen in Table 4.42 that the compressive strength of RHA concrete regardless of w/b and percentages of replacement of RHA in mixture shows that the compressive strength are lower at early age compared to that of OPC concrete. This phenomena also observed by (Habeeb & Mahmud, 2010). However, the compressive strength of RHA concrete at early age could be higher than control concrete if the cement used was finest and higher compressive strength of cement (Bui et al., 2005). It was mentioned previously that the Blaine specific surface and compressive strength of cement used in this research were 351 m^2/kg and 42.5 MPa, which less than Bui (2005) used. Another opinion, Chao-Lung et al. (2011) explained that in the early age, the replacement 10-20% of cement with RHA reduced the amount of cement by 10-20% and it caused increasing the volume of capillary pores in concrete then CH occurring accumulated on the interface. As a result, the structures of micro structure were less compact, causing the strength to be lower than that of the specimen without RHA. Meanwhile, in replacement 10% of cement with SF, the early strength of SF concrete was better in compressive strength than that of RHA concrete. It could be due to the surface area of SF need less mixing water to cover its surface compared to that of RHA and having more available mixing water for hydration on early age. However, in RHA concrete, the porous of RHA can function as a reservoir and internal water curing as reported by (Van Tuan et al., 2011). With the progress of cement hydration process, the relative humidity in the bulk cement paste drops and the absorbed water in RHA will be released from these reservoirs to promote the hydration of cement and thus the degree of cement hydration increases further at the later stages. As it can be seen in Figure 4.66 and 4.67, the compressive strength of RHA is increased at later age and get higher than the specimen without RHA.

The 10% replacement of cement with RHA achieved 100 MPa at 28 days in w/b ratio of 0.22 and 0.25. Previous research also indicated the optimum level of cement replacement with RHA was found to be between 10% and 30% to produce concrete with high strength as much as 90 (Safiuddin, M. et al., 2010). The compressive strength of RHA concrete w/b ratio of 0.22 got higher than that of w/b ratio of 0.25. The mixes that have optimum packing density can increase the compressive strength with similar cement content by reducing w/b or reduce cement content with similar compressive strength. The 15% replacement with RHA achieved 100 MPa at 56 days in w/b ratio of 0.22 and 0.25 and the 20% RHA could reach 100 MPa at 180 days but only in w/b of 0.25 and w/b of 0.22 reaching 96 MPa. Comparing RHA to SF in replacement mixes, the different strength at 10% replacement was 1.5 % at 180 days, which is insignificant. This result shows that the RHA can be an alternative binder to SF to produce HPC with 28 days compressive strength of 100 MPa.

From Table 4.42, it can be summarized that at low w/b ratio of 0.22 to 0.25 and water curing condition the concrete mixes containing 10 to 15%RHA can achieve compressive strength of 100 MPa at 28 days. While concrete containing 15% RHA similar compressive strength could be achieved at 180 days. However, under air drying, the concrete containing 10% RHA still achieve the compressive strength of 100 MPa at 28 days while at 15% RHA replacement level this strength could be achieved at 180 days. These results show that irrespective the w/b ratio (at low level) and curing method concrete containing 10%RHA can gain the compressive strength of 100 MPa at 28 days. Usually, most of codes specified the strength of concrete based on 28 day test results. However, in high-rise concrete structures, the process of construction takes a long duration that the structural elements in lower floors, which are not fully loaded for periods of a year or more. For this reason, compressive strengths of concrete

incorporating RHA can be suggested that the test based on results of 56 or 91 days in order to achieve significant economy in material costs.

Table 4.42: Compressive strength of concrete

Mix ID	Compressive strength (MPa)						
	1 d	3 d	7 d	28 d	56 d	91 d	180 d
Water curing							
OPC-22	71.0	82.0	92.5	104.6	108.0	109.0	109.5
RHA10-22	40.0	85.2	95.6	113.9	115.9	114.0	115.0
RHA15-22	30.6	82.3	87.6	107.8	108.0	110.1	114.5
RHA20-22	27.0	66.0	77.1	94.2	103.5	104.0	105.0
SF10-22	60.0	92.1	97.7	110.0	109.9	112.1	110.0
OPC-25	73.5	87.2	93.2	103.5	106.0	107.3	108.5
RHA10-25	54.0	89.4	94.1	113.2	112.8	113.2	114.1
RHA15-25	48.7	85.8	86.6	106.4	108.7	110.2	115.2
RHA20-25	35.7	65.3	76.6	86.4	92.1	96.8	103.3
SF10-25	51.2	84.1	89.6	100.0	112.2	112.6	112.7
Air drying							
OPC-22	71.0	80.1	90.5	99.2	102.3	103.2	102.4
RHA10-22	40.0	80.4	89.1	105.4	107.2	104.9	105.8
RHA15-22	30.6	77.4	81.5	98.1	97.2	99.1	101.9
RHA20-22	27.0	61.4	71.3	84.8	92.1	92.6	92.4
SF10-22	60.0	90.1	94.5	104.7	104.4	106.0	103.4
OPC-25	73.5	86.2	91.3	101.4	102.8	104.1	104.2
RHA10-25	54.0	90.3	96.1	110.9	108.1	107.0	108.0
RHA15-25	48.7	90.1	82.3	99.0	99.4	99.2	103.7
RHA20-25	35.7	62.0	72.0	80.4	83.8	86.2	90.9
SF10-25	51.2	81.6	87.0	96.0	104.5	103.7	103.2

OPC = ordinary Portland cement; RHA = rice husk ash; SF = silica fume
 10, 15 and 20 = percentages of cement replacement
 22 and 25 = percentages of w/b

4.6.2.2 Rate of strength development of RHA concrete

The concrete is a unique construction material in the way it developing its strength. The process of strength is growing and may continue for weeks or months after the concrete mixtures have been mixed and placed. As long as mixing water is available, the hydration of cement and water can occur and the concrete can possible gain more strength. One of the objectives of the RHA concrete mix proportioning was to ensure the strength of concrete is developed compared to that of the OPC concrete. Table 4.43 present the rate of strength development at 1, 7, 28, 56, 91 and 180 days in relation to the compressive strength of OPC concrete at 28 days.

Table 4.43: Rate of compressive strength development

Mix ID	W/B	Curing method	Relative compressive strength to 28 day compressive strength (%)						
			1 d	3 d	7 d	28 d	56 d	91 d	180 d
OPC-22	0.22	WC	67.9	78.4	88.5	100.0	103.3	104.2	104.7
RHA10-22	0.22	WC	35.1	74.7	83.9	100.0	101.7	100.1	100.9
RHA15-22	0.22	WC	28.4	76.4	81.3	100.0	100.2	102.1	106.2
RHA20-22	0.22	WC	28.6	70.0	81.8	100.0	109.9	110.4	111.4
SF10-22	0.22	WC	54.6	83.7	88.8	100.0	99.9	101.9	100.0
OPC-22	0.22	AD	71.6	80.7	91.2	100.0	103.1	104.0	103.2
RHA10-22	0.22	AD	38.0	76.3	84.5	100.0	101.7	99.5	100.4
RHA15-22	0.22	AD	31.2	78.9	83.1	100.0	99.1	101.0	103.9
RHA20-22	0.22	AD	31.8	72.4	84.1	100.0	108.6	109.2	109.0
SF10-22	0.22	AD	57.3	86.1	90.3	100.0	99.7	101.2	98.7
OPC-25	0.25	WC	71.0	84.3	90.0	100.0	102.4	103.7	104.8
RHA10-25	0.25	WC	47.7	79.0	83.1	100.0	99.6	100.0	100.8
RHA15-25	0.25	WC	45.8	80.6	81.4	100.0	102.2	103.6	108.3
RHA20-25	0.25	WC	41.3	75.6	88.7	100.0	106.6	112.0	119.6
SF10-25	0.25	WC	51.2	84.1	89.6	100.0	112.2	112.6	112.7
OPC-25	0.25	AD	72.5	85.0	90.0	100.0	101.4	102.6	102.7
RHA10-25	0.25	AD	48.7	81.4	86.6	100.0	97.4	96.5	97.4
RHA15-25	0.25	AD	49.2	91.0	83.1	100.0	100.5	100.2	104.8
RHA20-25	0.25	AD	44.4	77.2	89.6	100.0	104.3	107.2	113.1
SF10-25	0.25	AD	53.3	85.0	90.6	100.0	108.9	108.0	107.5

*WC = Water curing; AD = Air drying

OPC = ordinary Portland cement; RHA = rice husk ash; SF = silica fume

10, 15 and 20 = percentages of cement replacement

22 and 25 = percentages of w/b

The initial rate of strength development of RHA concrete in w/b of 0.22 and 0.25 was slower than OPC concrete but almost all mixes achieved 80% of its 28 day strength in 7 days except RHA20-22, 76.5%. It can be seen the gain strength of RHA concrete is almost double from 1 day to 7 days. This increment is possible due to the reactive silica and also high silica content in the RHA. The product of hydration, calcium hydroxide CaOH reacts with silica oxide SiO₃ from RHA in the presence of water and appropriate temperature produce calcium silicate hydrate (C-S-H), which affects the RHA concrete more dense and increase the strength. The early strength of concrete has a practical and economic implication on construction industry. The form work can be turned over very fast and the construction need to sustain load on early age as well.

4.6.2.3 Effect of curing on the compressive strength

Concrete is aggregates bounding with product of hydration cement and water. Once the fresh concrete was placed, excess water was squeezed out of paste by weight of aggregate and cement. Then it creates micro channels and passages inside the concrete. Later, the water that not yet reacted with cement bleeds out onto the surface and evaporates. Furthermore, the water that reacted in hydration process left its space to be a porous. The porous is on mortar side but tends to reduce as age of concrete increased. The porous on normal concrete can be a continue process to make capillary to the surface of concrete. Evaporation can be very fast processing and depends on humidity outside and the wind speed on the surface of concrete. To avoid the detrimental effect to harden concrete, curing of harden concrete after discharging from mixer is a necessary practice in concrete. The study of curing on normal concrete conducted by Hayri and Baradan (2011) showed that there is a positive correlation on the detrimental compressive strength of concrete with inadequate curing of concrete and the rate of strength development. Furthermore, such correlation was much more in concrete incorporating pozzolan (Wada et al., 2000).

The fresh concrete after discharging from mixer to molds need to pay attention as fresh concrete to transform to plastic concrete and to solid concrete through hydration process. The main factor to this process is mixing water. The loss of mixing water due to evaporation as reflected less maintenance is a real problem in concrete technology. In normal concrete, the effect of dry curing to water curing can reduce 40 % compressive strength of concrete (Mamlouk et al., 2006).

Table 4.44 shows the ratio compressive strength between air drying and water curing. It can be seen that, in general, the difference between compressive strength specimens under air drying and water curing conditions is not significant. The ratio

varied between 0.88 and 1.05, the lowest ratio (ratio less than 0.9) is for concrete containing 20% RHA in both w/b ratios at later ages. The data showed that by increasing the RHA content the compressive strength is more sensitive to curing condition.

RHA concrete is more sensible to the curing compare to SF concrete at w/b of 0.22 as the ratio at 28 days is 0.93 for RHA concrete and 0.95 for SF concrete but it is 0.98 and 0.96 in w/b of 0.25, respectively. It could be related to early age of concrete as RHA concrete is less hydration compared to SF concrete. The porous of concrete surface is not well disconnected and the mixing water is evaporated. It can be seen in 3 days the loss of compressive strength is 0.94 % and 0.98% for RHA and SF concrete, respectively. Based on these results, it can be concluded that air drying in relative humidity of 70-80% does not affect significantly reduction in compressive strength of RHA concrete compared to SF concrete. Other possibility, the reason that the concrete was less sensitive to air curing was it could be both series of concrete got better cover after placing concrete before demolding. As reported by (Aitcin, 2003), the critical time for curing of HPC concrete was a few hours after placing. Table 4.44 also shows that there is a limited effect of curing to compressive strength of pozzolan concrete in w/b of 0.22 and 0.25. The difference between air curing and water curing at lower than 28 days and up to 180 days was around 10 %. However, there are slightly different the effect of curing on RHA concrete in w/b of 0.22, which is more prone compared to w/b of 0.25. The ratio of 7 to 28 days for normal compressive strength of RHA mixes under both curing regimes from 0.84 to 0.89 and for high strength concrete from 0.8 to 0.9 as reported by (Carrasquilio & Nilson, 1981). It means the results obtained in this study are better than previous observation and it could be HPC is the one of the reasons.

Table 4.44: Compressive strength ratio under air drying and water curing

Mix ID	Compressive strength ratio						
	1d	3d	7d	28d	56 d	91 d	180 d
OPC-22	1.00	0.98	0.98	0.95	0.95	0.95	0.94
RHA10-22	1.00	0.94	0.93	0.93	0.92	0.92	0.92
RHA15-22	1.00	0.94	0.93	0.91	0.90	0.90	0.89
RHA20-22	1.00	0.93	0.93	0.90	0.89	0.89	0.88
SF10-22	1.00	0.98	0.97	0.95	0.95	0.95	0.94
OPC-25	1.00	0.99	0.98	0.98	0.97	0.97	0.96
RHA10-25	1.00	1.01	1.02	0.98	0.96	0.95	0.95
RHA15-25	1.00	1.05	0.95	0.93	0.91	0.90	0.90
RHA20-25	1.00	0.95	0.94	0.93	0.91	0.89	0.88
SF10-25	1.00	0.97	0.97	0.96	0.93	0.92	0.92

OPC = ordinary Portland cement; RHA = rice husk ash; SF = silica fume
 10, 15 and 20 = percentages of cement replacement
 22 and 25 = percentages of w/b

The effect of pozzolanic material and curing method on strength gain of HSC based on previous observations are presented in following formula. The ACI Committee 209 proposed the relationship.

$$f_{cm}(t) = \left(\frac{t}{4+0.65t} \right) f_{c28} \quad \text{Eq. 1.}$$

Where, $f_{cm}(t)$ is the mean compressive strength at age of t days and f_{c28} is the cylinder compressive strength at 28 days. With similar formula, it was applied to these mixes. The prediction of compressive strength up to 180 days by using Eq. 1 based on actual compressive strength of cube 100x100x100 at 28 days are presented in Figure 4.68. The result of prediction base on equation is quite accepted as the IAE value is 16.5% which is larger than 10%. By utilizing similar model as Eq. 1, from simulation, the constant and the coefficient of Eq. 2 that show lower IAE value is shown in Table 4.45. The Eq. 1 which is proposed by ACI probably not intent to be use for RHA concrete as can be seen at early age the compressive strength of RHA concrete is lower than OPC concrete.

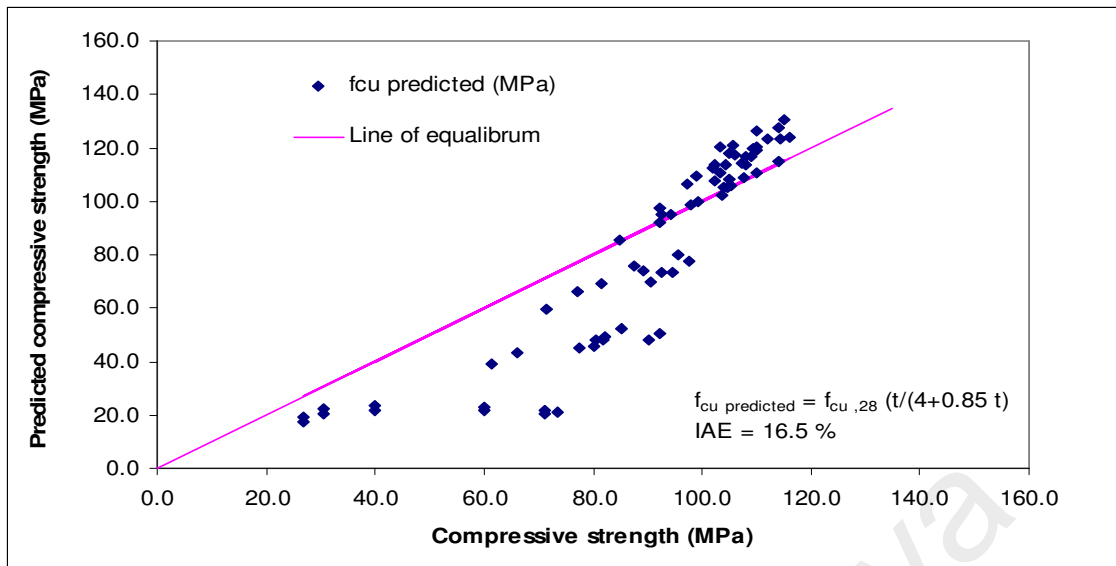


Figure 4.68: The predicted compressive strength using equation 1 base on compressive strength of HPC concrete at 28 days

$$f_{cm}(t) = \left(\frac{t}{c + \beta t} \right) f_{c28} \quad \text{Eq. 2}$$

Results on simulation for finding constant and coefficient for Eq.2 are shown in Table 4.45. Constant and coefficient were chosen based on the lowest IAE values was applied for the Eq.3. The result is shown in Figure 4.69.

$$f_{cm}(t) = \left(\frac{t}{1.1 + 0.95 t} \right) f_{c28} \quad \text{Eq. 3}$$

Table 4.45: Coefficient and constant explored to find $f_{cm}(t)$

Constant (c)	Coefficient (β)	IAE(%)
1.8	0.99	9.5
1.1	0.99	6
0.8	0.99	5.8
1.8	0.95	7.4
1.1	0.95	5.1
0.8	0.95	6.3
1.8	0.9	8.4
1.1	0.9	7.9
0.8	0.9	9.8
4	0.85	16.5

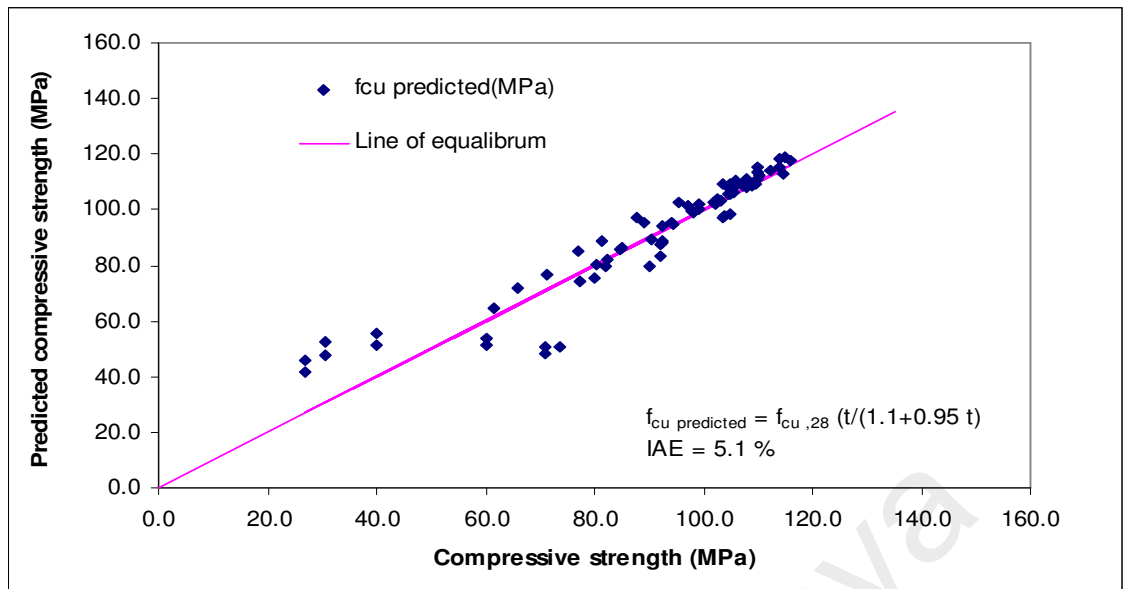


Figure 4.69: The predicted compressive strength using equation 2 base on compressive strength of HPC concrete at 28 days

By changing the constant and coefficient of model, Eq. 3 is suitable to be used in pozzolan concrete and high strength as the IAE value is 5.1 %. Furthermore, the Eq. 3 can be used to assess the strength development of RHA replacement up to 180 days based on compressive strength at 28 days.

4.6.2.4 Relationship between compressive strength of RHA and OPC concrete

Figures 4.70 and 4.71 show the relationship between compressive strength of RHA and OPC concrete from any age of compressive strength of OPC subjected to curing regime. It can be seen that at early age test some data are out of regression line due to low compressive strength of RHA concrete. However at later age the hydration of RHA concrete could achieve more as shown on 10% RHA that its compressive strength at 28 days is higher than OPC concrete. The 15% and 20% replacement show slightly lower development of strength rate than OPC. Those approaches not show a good real correlation between OPC concrete and RHA concrete, as R^2 of RHA concrete are less than 0.9. However, it works for SF concrete as R^2 is greater than 0.9.

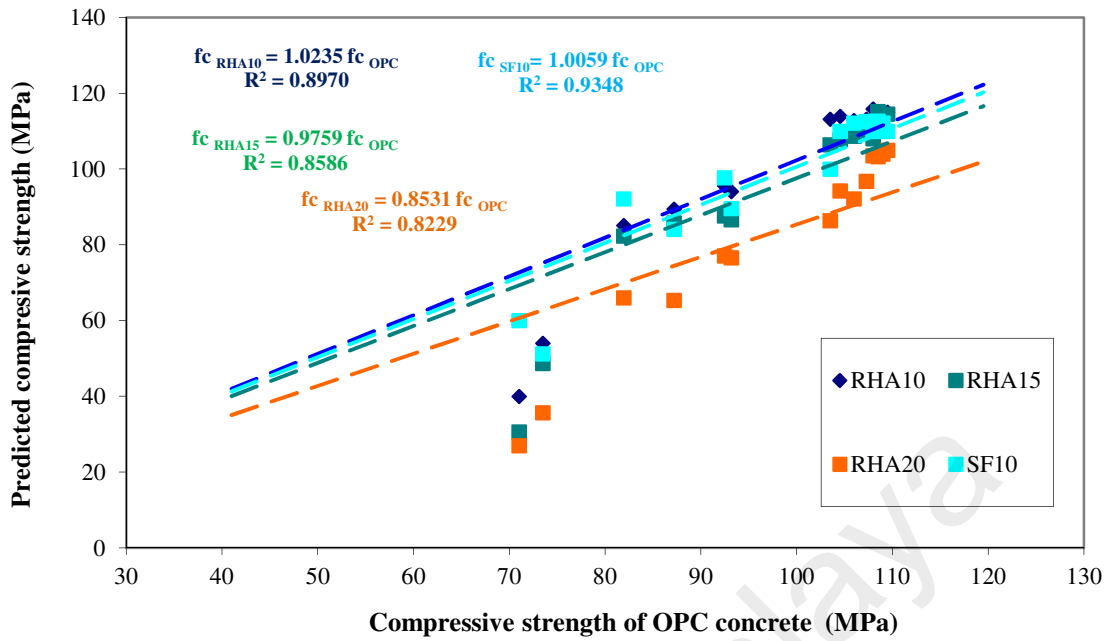


Figure 4.70: The compressive strength relation between OPC concrete and blended concrete subjected water curing

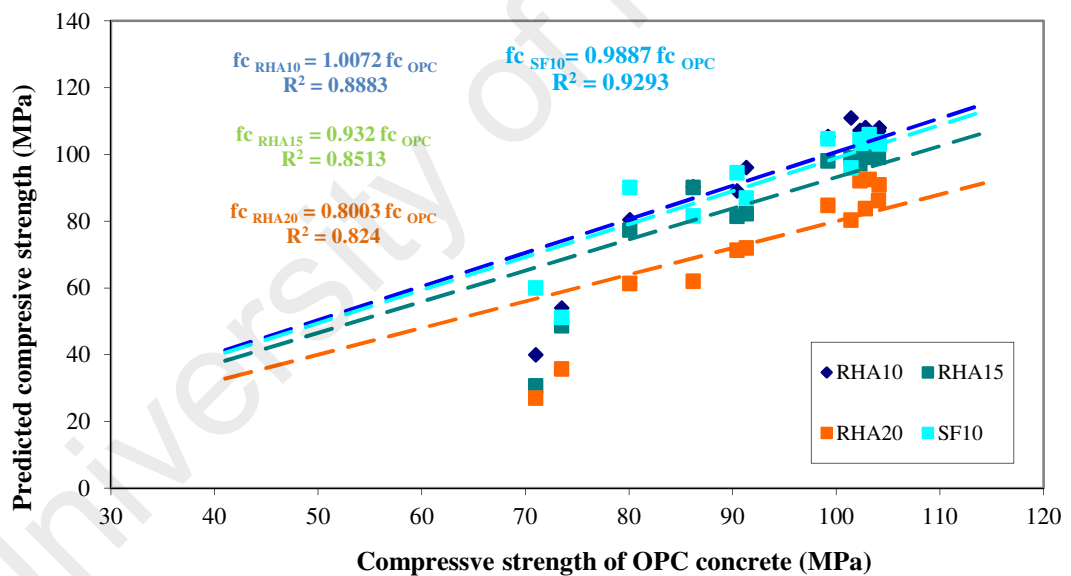


Figure 4.71: The compressive strength relation between OPC concrete and blended concrete subjected air curing

4.6.2.5 Relationship between Early Ages of 3 and 7 days compressive strength with 28 days compressive strength of OPC and RHA concrete

In the construction site there is a lot of sequence task having to wait to prove the concrete full fill the requirement. To cope with these problems, there is a need to

predict the compressive strength of concrete at 28 days based on early age concrete, such as 3 or 7 days. 7-day compressive strength test results are often used to monitor the gain of early strength and they are estimated to be about 64% to 70% of the 28-day strength for normal concrete. Until now, there are no such correlations for high performance concrete incorporating RHA. This section part will discuss the relation of compressive strength at 3 and 7 days to that of 28 days.

From previous section, the approach was trying to predict relationship between compressive strength of OPC and RHA concrete at any age but it was not satisfied. Now, the approach proposed is by eliminating the first day compressive strength of RHA concrete. The approach is by utilizing the compressive strength of RHA concrete at 3 and 7 days to predict compressive strength of RHA concrete at 28 days, which one of the criteria for strength design in concrete structure as stated on most codes. .

As shown in Figure 4.34 and 4.35, the 3 and 7 days of compressive strength are used to predict the 28 days of compressive strength. From previous discussion, the compressive strength of 20% replacement of RHA with cement in concrete at 28 days is lower than that of OPC concrete. However, if it is seen on strength development rate as shown in Figure 4.34 and 4.35, the higher percentage of RHA in concrete process higher rate than others. It could be the pozzolanic reaction occurs on those concretes. The relationship between compressive strength of OPC and RHA concrete at 28 days on 3 days and 7 days strength are excellent as R^2 are higher than 0.9.

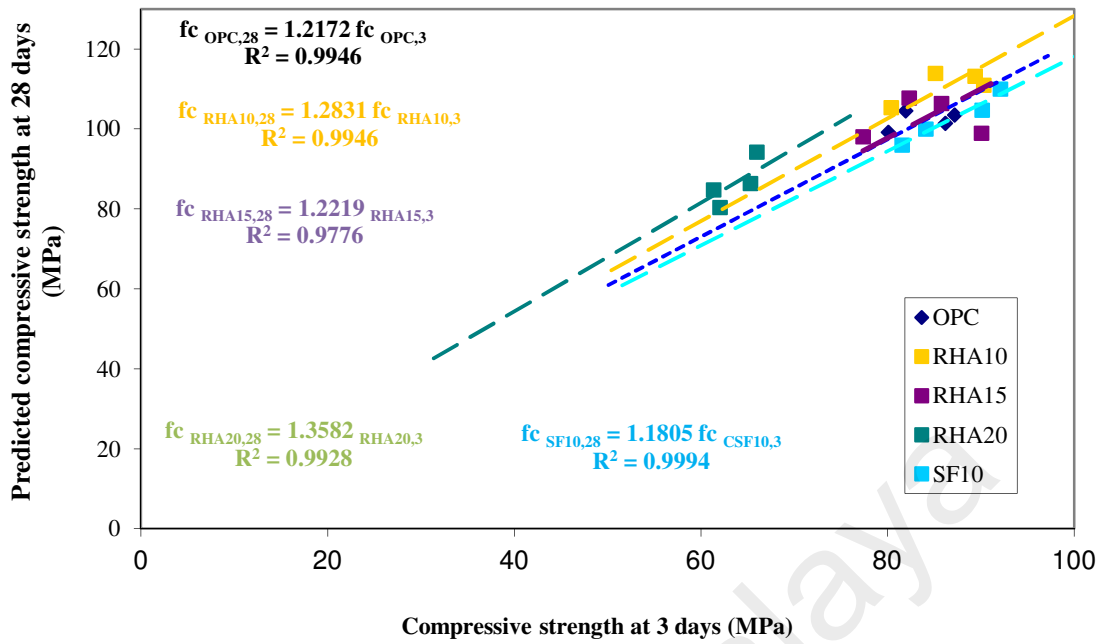


Figure 4.72: The compressive strength relation between 3rd day and 28th day concrete subjected water curing

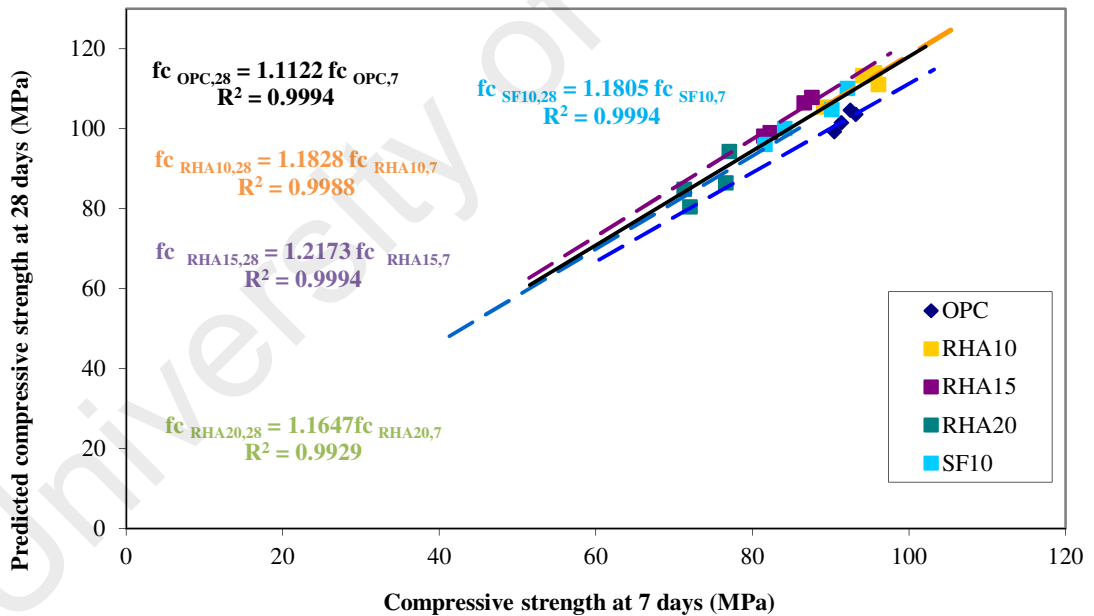


Figure 4.73: The compressive strength relation between 7th day and 28th day concrete subjected air curing

4.6.2.6 Compressive strength efficiency of cement

Figures 4.74 and 4.75 show the compressive strength efficiency of cement used on selected w/b mixtures, which are 0.22 and 0.25, and subjected to water curing. The

compressive strength of efficiency of cement is denoted as MPa/(kg cement). These figures show that the strength of efficiency values of RHA and SF concrete are higher than that of OPC concrete after 3 days. At 180 days, all mixes regardless w/b ratio and percentages of replacement achieved above 0.2 except OPC mixes, which only achieved 0.2. For w/b of 0.22 and 0.25 compressive strength efficiency of cement rises to up to 0.25 for 15% replacement of RHA with cement. The values w/b of 0.2 and 0.25 of efficiency coefficient are similar with 5 and 4 kg of cement/m³ to produce 1 MPa of compressive strength. It is clearly that by using RHA and SF in HPC reduced 20% of cement consumption to get similar compressive strength of control concrete. Similar results also reported by (Chao-Lung et al., 2011) that inclusion RHA on concrete mixture affected the increase of the strength efficiency of cement. The energy consumption and the detrimental CO₂ emission for the environment during the production of cement can significantly be reduced and it is the advantages of RHA as cement replacement to the environment.

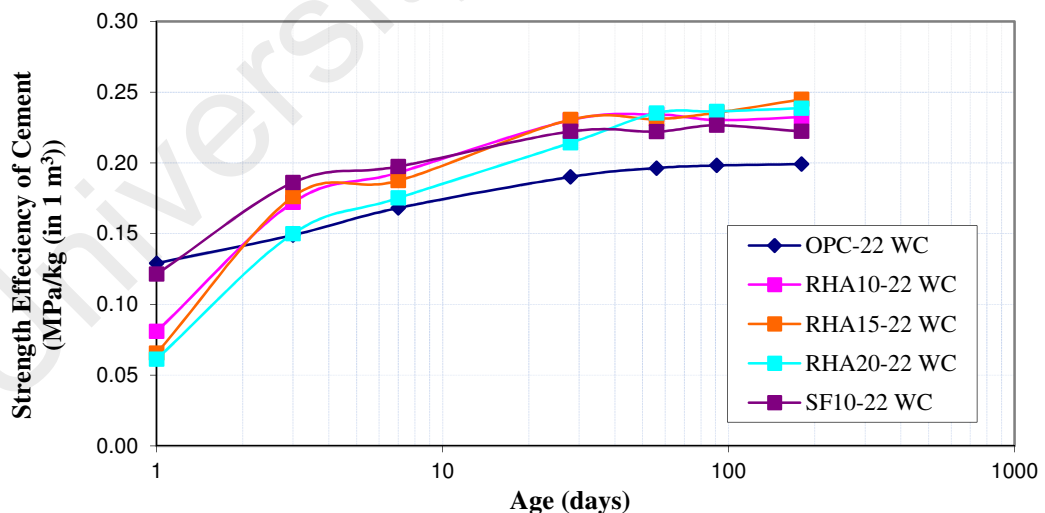


Figure 4.74: The strength efficiency of cement on selected mixes at W/b ratio of 0.22

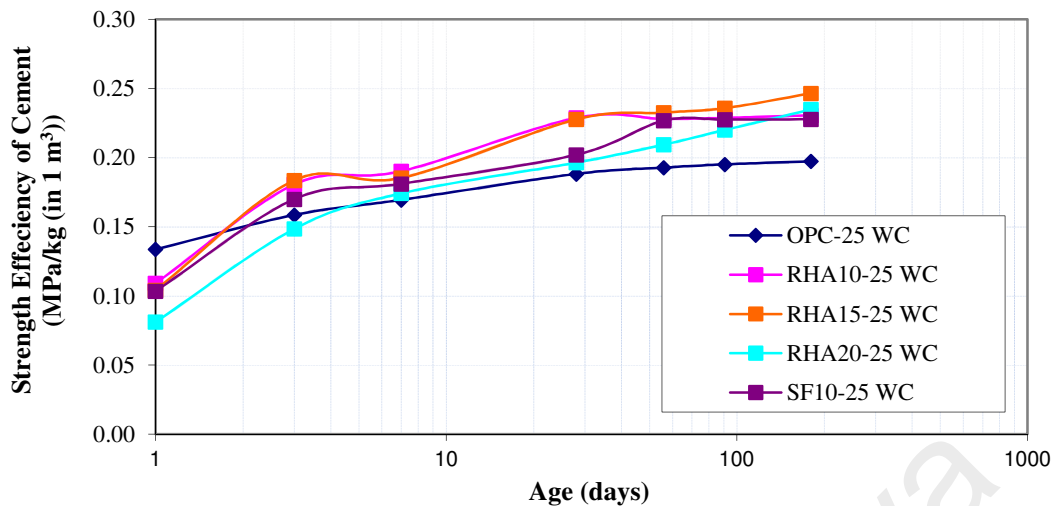


Figure 4.75: The strength efficiency of cement on selected mixes W/b ratio of 0.25

4.6.3 Flexural strength

The modulus of rupture is the theoretical maximum tensile stress that can be achieved at the bottom fiber of a test beam through flexural test. It is also known as modulus of rupture. The value is relevant for designing highway and aircraft pavements. The test was proposed as a compliance test by BS 5328: 1991, but in the US it was thought to be unsuitable for compliance purposes because of its relative complexity (Mazloom & Hassanloo, 2009). The dimensions of the beam and the arrangement of loading affect to the value of the modulus of rupture. There are some varieties in how the load applied. In this study the two-point loading is used as stated by BS 5328: 1991. This produces a constant bending moment between the load points so that one third of the span is subjected to the maximum stress which cracking is likely to take place.

4.6.3.1 Effect of RHA and w/b on the flexural strength

The development strength of flexure strength is shown Figure 4.76 and 4.77 for w/b ratios of 0.22 and 0.25, respectively. It can be seen from the figures that there is not

significant increase in the flexural strength after 7 days. The difference between 7 days and later ages of 28 and 90 days of flexural strength is less than 10%. It could be the outer fiber of beam had achieved such maturity compare to inside one. When the optimum load achieved, it produce high tensile stress, which possible excided tensile strength of inside concrete and the cracks occur and propagates very fast. Then the sudden failure could be take place. Table 4.46 shows the variation of modulus of rupture strength with RHA replacement percentages at W/b of 0.22 and 0.25 subjected to water curing and air drying conditions. The increasing flexural strength of high replacement of cement with RHA in concrete is higher than that of OPC and lower replacement of cement with RHA. At 90 days and w/b of 0.22, the increasing flexural strengths of OPC, RHA10, RHA15, RHA20 and SF10 concrete to 28 days were 5 %, 8%, 9.1%, 8.2%, and 6.3 %, respectively. For w/b of 0.25 the increasing flexural strengths of OPC, RHA10, RHA15, RHA20 and SF10 concrete to 28 days were 4.4 %, 8.6%, 9.3%, 11.1%, and 5.4 %, respectively

The 10% replacement of cement with RHA produced higher flexure strength at 28 and 90 days regardless of w/b. The strength increase 5 % and 6% at w/b of 0.22 and 0.25, respectively. For other replacement level, the strength was slightly lower than that of OPC concrete. The increments of flexural strength due to reduce w/b from 0.25 to 0.22 were around 5 up to 10%. The flexure strength of 10% RHA concrete was higher than that of OPC concrete regardless of w/b due to the additional strength from CSH produced by second hydration of RHA concrete at early age. The effect of pozzolanic was more influenced to flexure strength compared to the effect of filler. On the other side, more replacement of RHA did not automatically affect to increasing flexural strength higher than that of OPC concrete. It could be at higher replacement of cement with RHA and the cement content also reduced. It could be there was not enough

CaOH as hydration product of cement to react with SiO₃ from RHA to produce CSH.

As known, CSH is a strong crystal compared to CaOH.

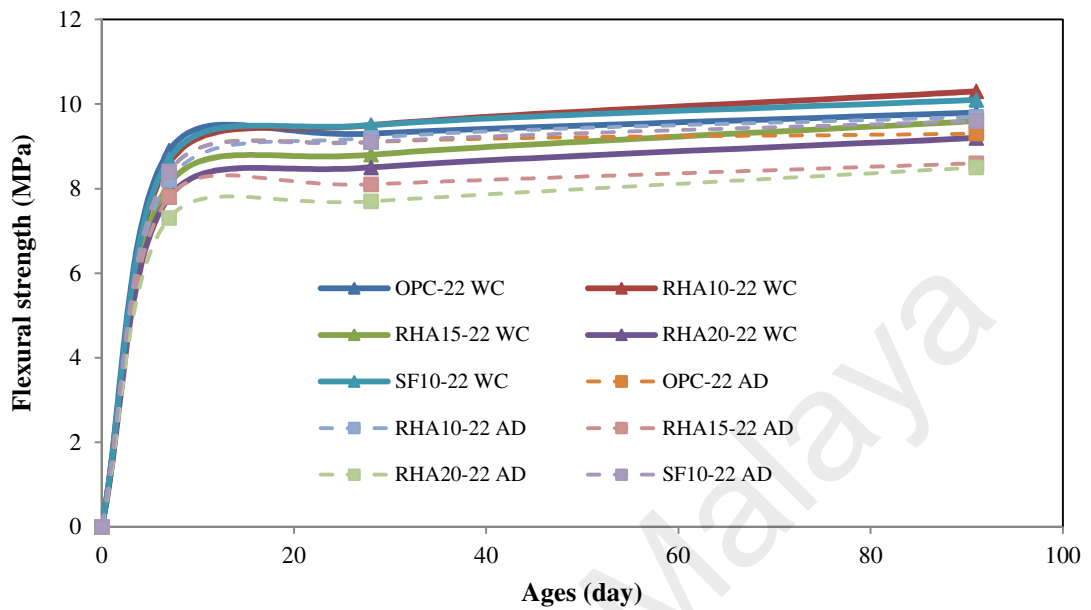


Figure 4.76 The development strength of flexure strength w/b of 0.22

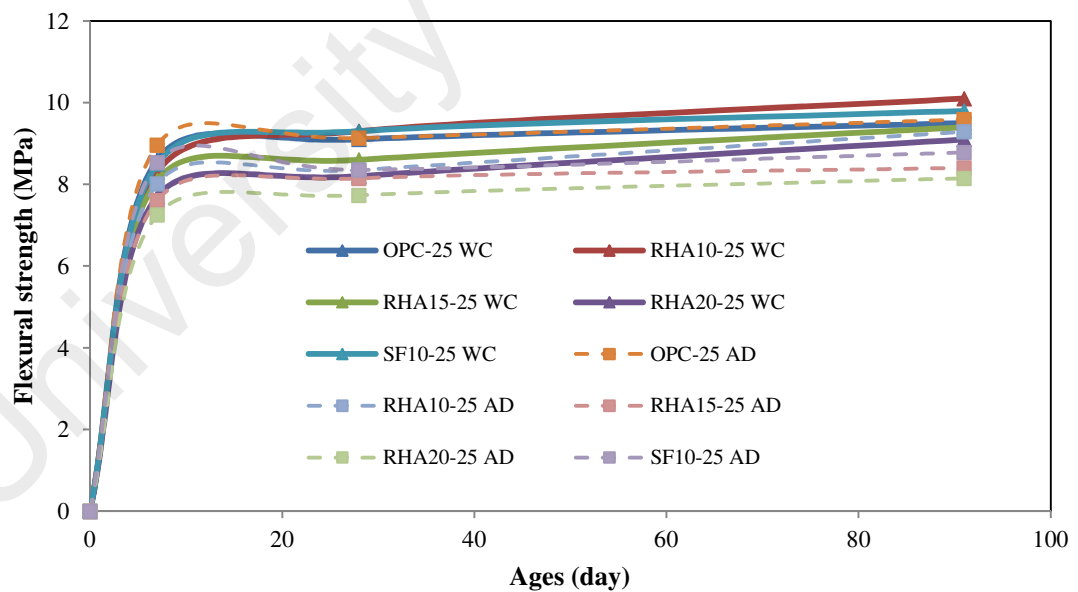


Figure 4.77 The development of flexure strength w/b of 0.25

Table 4.46: The flexural strength

Mix ID	flexural strength (MPa)			Strength as % of 28 day strength (%)		
	Water curing					
	7d	28d	90 d	7d	28d	90 d
OPC-22	8.9	9.3	9.8	95.7	100.0	105.4
RHA10-22	8.6	9.5	10.3	90.1	100.0	108.0
RHA15-22	8.1	8.8	9.6	92.0	100.0	109.1
RHA20-22	7.8	8.5	9.2	91.8	100.0	108.2
SF10-22	8.7	9.5	10.1	91.6	100.0	106.3
	Air drying curing					
OPC-22	8.7	9.1	9.4	95.6	100.0	103.3
RHA10-22	8.3	9.2	9.7	90.2	100.0	105.4
RHA15-22	7.7	8.3	8.8	92.7	100.0	106.0
RHA20-22	7.5	7.8	8.4	96.2	100.0	107.8
SF10-22	8.6	8.9	9.3	98.9	100.0	104.5
	Water curing					
OPC-25	8.6	9.1	9.5	94.5	100.0	104.4
RHA10-25	8.3	9.3	10.1	89.2	100.0	108.6
RHA15-25	8.1	8.6	9.4	94.2	100.0	109.3
RHA20-25	7.7	8.2	9.1	93.9	100.0	111.0
SF10-25	8.5	9.3	9.8	91.4	100.0	105.4
	Air drying curing					
OPC-25	8.4	8.9	9.3	93.3	100.0	103.3
RHA10-25	8.2	9.2	9.7	89.1	100.0	105.4
RHA15-25	7.8	8.1	8.6	96.3	100.0	106.2
RHA20-25	7.3	7.7	8.5	94.8	100.0	110.4
SF10-25	8.4	9.1	9.6	92.3	100.0	105.5

OPC = ordinary Portland cement; RHA = rice husk ash; SF = silica fume
 10, 15 and 20 = percentages of cement replacement
 22 and 25 = percentages of w/b

4.6.3.2 Effect of curing on the flexural strength

Table 4.47 shows the ratios of flexure strength concrete subjected air drying and water curing. The results suggest that the moduli of rupture are significantly affected by curing conditions. The trend indicated that removal of beam specimen after 7-day from the curing tank showed insignificant reduction of the modulus of rupture. In both cases, the reduced modulus of rupture was believed to be the result of micro-cracks initiated by drying shrinkage. The low permeability of the HPC caused internal differential shrinkage strains due to the fact that the moisture trapped in the interior part of the specimens could not evaporate as quickly as moisture at the surface. This relative shrinkage difference caused micro-cracking of concrete (Neville, A.M. , 1996).

Therefore, the specimens that were moist-cured up to the time of testing showed much higher modulus of rupture than those cured for only 7 days.

Table 4.47: The curing ratio of Air drying and Water curing

Mix ID	Flexural strength ratio (Air drying /Water curing)		
	7d	28d	90 d
OPC-22	0.98	0.98	0.96
RHA10-22	0.97	0.97	0.94
RHA15-22	0.95	0.94	0.92
RHA20-22	0.96	0.92	0.91
SF10-22	0.99	0.94	0.92
OPC-25	0.98	0.98	0.98
RHA10-25	0.99	0.99	0.96
RHA15-25	0.96	0.94	0.94
RHA20-25	0.95	0.94	0.93
SF10-25	0.99	0.98	0.98

OPC = ordinary Portland cement; RHA = rice husk ash; SF = silica fume
 10, 15 and 20 = percentages of cement replacement
 22 and 25 = percentages of w/b

4.6.3.3 The relationship between compressive and flexural strength

Table 4.48 provides the model used to predict relationship between the compressive strength and predicting modulus of rupture. Figure 4.78 shows the curve based on the ACI 363R-08, EC-2, NZS 3101:2006 and CSA A23.3-04. Meanwhile, Figure 4.79 shows the curves based on the current study. The differences of those models are the type of regression utilized. The previous one utilized the parabolic regression and the r of those regressions was weak due to less than 0.85. However, the current study utilized a linear regression model and the results showed that the r of those regressions is good due to greater than 0.9. In Table 4.48, the mean of the integral absolute error (IAE) values of current study models also shows lower than that of the current models. It could be the previous models were proposed not for pozzolanic concrete and compressive strength of concrete less than 100 MPa.

Table 4.48: Estimating equations of the different models

Code	Estimate model	R ²	IAE (%)
ACI 363R-08	$f_r = 0.94 f_{cm}^{1/2}$	0.6073	5.39
EC-2	$f_r = 0.43 (f_{cm-8})^{2/3}$	0.8388	3.10
NZS 3101:2006	$f_r = 0.8 f_{cm}^{1/2}$	n/a	10.50
CSA A23.3-04	$f_r = 0.6 f_{cm}^{1/2}$	n/a	32.87
Current study	$f_r = 0.7805 f_c^{0.5273}$	0.8798	3.01
Current study	$f_r_{OPC} = 0.0909 f_{c_{OPC}}$	0.9951	2.25
Current study	$f_r_{RHA10} = 0.0877 f_{c_{RHA10}}$	0.9896	3.59
Current study	$f_r_{RHA15} = 0.0869 f_{c_{RHA15}}$	0.9822	4.60
Current study	$f_r_{RHA20} = 0.0951 f_{c_{RHA20}}$	0.9834	4.47
Current study	$f_r_{CSF10} = 0.0904 f_{c_{SF10}}$	0.9902	3.58
Current study	$f_r_{HPC} = 0.0899 f_{c_{HPC}}$	0.9371	4.14

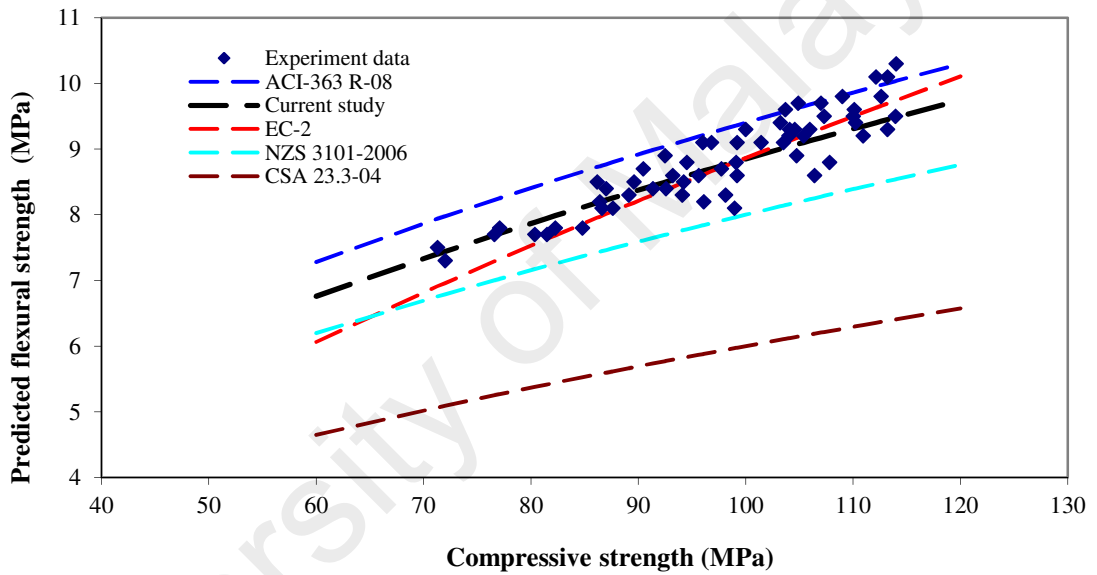


Figure 4.78: Relationship between compressive strength and predicting modulus of rupture from available models

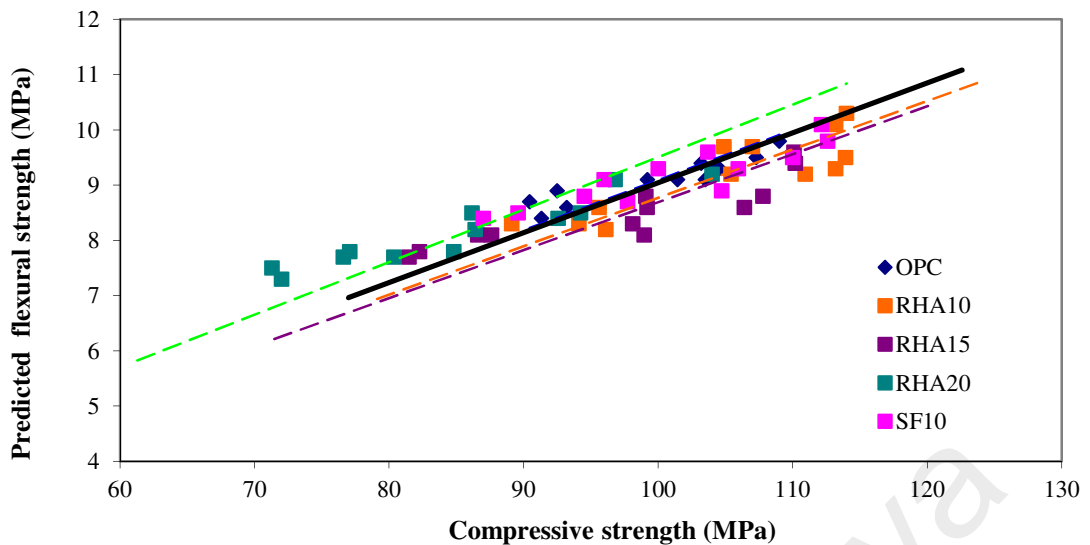


Figure 4.79: Relationship between compressive strength and predicting modulus of rupture for OPC, RHA and SF concrete

4.6.4 Splitting tensile strength

One of the main ideas in producing HPC is to increase durability of concrete. This objective can be achieved by utilizing pozzolan to reduce permeability of concrete through reducing porous and capillaries to the surface of concrete. However, cracking in concrete also reduces serviceability and increases durability problems. Cracks can occur due to its tensile stress exceeding its tensile strength and can propagate easily in tension zones. High strength high-performance concrete (HPC) requires, along with improved compressive strengths, high tensile strength, less porosity and very high durability. For getting the tensile strength of concrete, there are three types of tests available to measure it: indirect tension, mostly known as splitting tensile tension, flexure, and direct tension.

The method for splitting tensile test is an established method, simplest and reliable. For tensile strength it is often assumed that the cylinder splitting strength is a constant proportion of the direct tensile strength (Hannant et al., 1973). CEB-FIB-1990 allow to

predict direct tensile strength from splitting tensile strength by multiplying by conversion factors of $\lambda = 0.9$.

4.6.4.1 Effect of RHA on splitting tensile strength

Table 4.49 shows the variation of splitting tensile strength with different replacement percentages of RHA and SF at W/b of 0.22 and 0.25. It is observed that the inclusion of RHA in concrete did not much increase the splitting tensile strength of OPC. A close observation of Table 4.49 exhibits that any percentages of RHA and w/b do not increase the splitting tensile strengths compared to OPC concrete until 28 days. Similar finding also reported by (De Sensale, Gemma Rodríguez, 2006) that splitting tensile strength of concrete with replacements of 10%, 15% and 20% at 28 days did not increase at w/b of 0.32 but at w/b of 0.5 the splitting tensile strength was increased. The increasing of splitting tensile strength also depended on the sources of RHA. Habeeb, G.A and M.M Fayyadh (2009) also reported that at later age, 90 and 180 days, the splitting tensile strength of RHA concretes were higher compared to control concrete. However, in this study, at 28 days the splitting tensile strength of concrete with 10% of replacement of cement with RHA achieved higher than that of OPC concrete. The possibility reason that the replacement RHA higher than 10% has lower splitting strength at early age than OPC concrete was the pozzolanic reaction occurred slower than the concrete with 10% RHA. As increasing replacement of cement with RHA, the amount of cement also decreased and it means the rate of hydration process to produce CaOH also reduced. The filler effect was more dominant on early age than pozzolanic effect (De Sensale, Gemma Rodríguez, 2006; Sensale, 2006). It also can be seen in Table 4.49 that the ratio of tensile strength to 28th day of tensile strength of RHA concrete shows the increment. The more RHA replacement the higher increment percentage of its strength to 28th day of tensile strength. It means the pozzolanic effect is still processing.

Table 4.49: Splitting tensile strength of OPC and RHA concrete subjected to water curing and air drying conditions

Mix ID	Splitting tensile strength (MPa)			Strength as % of 28 days strength (%)		
	Water curing					
	7d	28d	90 d	7d	28d	90 d
OPC-22	6.4	6.6	6.7	97.3	100.0	102.0
RHA10-22	6.1	6.7	6.9	90.4	100.0	103.0
RHA15-22	6.0	6.4	6.6	94.3	100.0	103.4
RHA20-22	5.7	6.0	6.2	94.8	100.0	102.8
SF10-22	6.3	6.6	6.9	95.8	100.0	104.5
Mix ID	Air drying curing					
	7d	28d	90 d	7d	28d	90 d
	OPC-22	6.1	6.5	6.6	93.2	100.0
RHA10-22	6.1	6.3	6.5	96.9	100.0	103.9
RHA15-22	5.8	6.0	6.4	96.5	100.0	106.5
RHA20-22	5.5	5.9	6.1	93.3	100.0	102.8
SF10-22	6.1	6.5	6.7	95.2	100.0	103.8
Mix ID	Water curing					
	7d	28d	90 d	7d	28d	90 d
	OPC-25	6.1	6.5	6.6	94.2	100.0
RHA10-25	6.1	6.6	6.7	91.8	100.0	101.5
RHA15-25	5.8	6.3	6.6	92.1	100.0	104.6
RHA20-25	5.7	5.9	6.1	96.9	100.0	103.6
SF10-25	6.3	6.7	6.7	94.7	100.0	100.6
Mix ID	Air drying curing					
	7d	28d	90 d	7d	28d	90 d
	OPC-25	6.1	6.4	6.5	96.1	100.0
RHA10-25	6.0	6.2	6.6	97.4	100.0	107.1
RHA15-25	5.8	5.9	6.4	98.1	100.0	108.2
RHA20-25	5.6	5.8	6.0	96.6	100.0	103.3
SF10-25	6.1	6.5	6.6	94.5	100.0	101.5

OPC = ordinary Portland cement; RHA = rice husk ash; SF = silica fume
 10, 15 and 20 = percentages of cement replacement
 22 and 25 = percentages of w/b

4.6.4.2 Effect of curing on splitting tensile strength

Table 4.50 shows the ratio of splitting tensile strength under air drying and water curing conditions. It shows that there are insignificant losses of splitting tensile strength of HPC subjected to either air drying or water curing. This phenomenon was similar with specimen for compressive strength, which was insignificant due to subject of curing. Guneyisi et al. (2005) (Guneyisi et al., 2005; Güneysi et al., 2005) reported 10-20% of compressive strength of normal concrete were loss subjected to air drying.

Water curing was reported to be more effective in improving compressive strength at later ages for higher w/c ratio specimen than lower w/c ratio specimen. The reason that there was insignificant loss of strength in this research on subjecting curing method in low w/b ratio was due to well covering of specimens directly after casting. The critical curing age in low w/b was in few hours after placing of fresh concrete in molds. As mentioned by (Šelih et al., 1996) evaporation rates typically occurred within the first few hours of hydration and mostly was dominated by hydration of C3S and reactions involved calcium-sulfoaluminate phases. In this case, the samples had been covered by plastic sheet to minimize the effect of evaporating water from fresh concrete and the results showed that there was insignificant loss effect to strength subjected to curing method.

Table 4.50: Splitting tensile strength ratio of air drying and water curing

Mix ID	Splitting tensile strength ratio (Air drying curing /Water curing)		
	7d	28d	90 d
OPC-22	0.95	0.99	0.99
RHA10-22	1.01	0.94	0.95
RHA15-22	0.96	0.94	0.97
RHA20-22	0.96	0.98	0.98
SF10-22	0.97	0.98	0.97
OPC-25	1.00	0.98	0.98
RHA10-25	0.99	0.95	0.97
RHA15-25	1.00	0.94	0.97
RHA20-25	0.98	0.99	0.98
SF10-25	0.97	0.97	0.98

OPC = ordinary Portland cement; RHA = rice husk ash; SF = silica fume
 10, 15 and 20 = percentages of cement replacement
 22 and 25 = percentages of w/b

4.6.4.3 Relationship between compressive strength and splitting tensile strength

One of the most important fundamental properties of concrete other than compressive strength is tensile strength. In concrete design the concrete behavior is governed by compressive strength and tensile strength of concrete is used by designers to resist shear in unreinforced sections, and to resist shrinkage and temperature stresses

(Oluokun, 1991). Furthermore, an accurate prediction of tensile strength of concrete reduced cracking problems, improved shear strength prediction, and minimized failure of concrete in tension due to inadequate methods of tensile strength prediction. There are some formula offered by researchers and codes of practice but most of them are for predicting concrete with compressive strength up to 80 MPa, as shown in Table 4.51. ACI Building Code (ACI 318-11) provides the following an equation to predict the splitting tensile strength through the compressive strength:

$$f_t = 0.56f_c^{0.5} \quad \text{Eq. (1)}$$

The equation has a limitation which the empirical relationship between the splitting tensile strength and the cylinder compressive strength are for concrete with compressive strength between 21 and 83 MPa. Mokhtarzadeh and French (2000) proposed another formula which not uses 0.5 power as a classical formula used by ACI () as follow:

$$f_t = 0.30 f_c^{0.63} \quad \text{Eq. (5)}$$

Also, the equation has a limitation which the empirical relationship between the splitting tensile strength and the cylinder compressive strength are for concrete with strength between 48 and 103 MPa. Furthermore, (Arioglu et al., 2006) proposed the previous formula as:

$$f_t = 0.321f_c^{0.661} \quad \text{Eq. (6)}$$

Table 4.51: The relationship between compressive and splitting tensile strength formula

Source	Relationship	R ²	Range (MPa)	IAE (%)	Remark
Mokhtarzadeh and French	$f_t = 0.32f_c^{0.63}$	N/a	$48 \leq f_c \leq 103$	8.66	All mixes
Arioglu	$f_t = 0.321f_c^{0.661}$	N/a		5.88	All mixes
ACI 363R-08	$f_t = 0.59f_c^{0.5}$	N/a	$21 \leq f_c \leq 83$	7.18	All mixes
EC-2	$f_t = (1/3) (f_c - 8)^{2/3}$	N/a	$21 \leq f_c \leq 83$	6.74	All mixes
NZS 3101:2006	$f_t = 0.54f_c^{0.5}$	N/a	$48 \leq f_c \leq 103$	11.90	OPC concrete
CSA A23.3-04	$f_t = 0.67f_c^{0.5}$	N/a		5.40	
Current study	$f_t = 0.9290f_c^{0.4172}$	0.89	$70 \leq f_c \leq 115$	1.81	All mixes
Current study	$f_t = 1.0439f_c^{0.3892}$	0.92	$70 \leq f_c \leq 115$	1.7	RHA concrete
Current study	$f_t = 0.7819f_c^{0.457}$	0.89	$70 \leq f_c \leq 115$	1.22	OPC concrete
Current study	$f_t = 0.9679f_c^{0.4045}$	0.88	$70 \leq f_c \leq 115$	1.97	RHA15
Current study	$f_t = 1.6019f_c^{0.293}$	0.98	$70 \leq f_c \leq 115$	0.55	RHA20
Current study	$f_t = 1.1633f_c^{0.3729}$	0.85	$70 \leq f_c \leq 115$	1.61	SF10

However, all formula intent for the relationship of high strength concrete with compressive strength up to 83 MPa for cylinder, which is equivalent to 92 MPa of cube 100x100x100 mm (based on the conversion proposed by Del Viso et al. (2008) the ratio of cylinder to cube equals to 1.09. In this research, the compressive strength of concrete achieved more than 100 MPa and the concrete incorporating RHA and SF. As mention previously, the compressive strength of those concrete at early age was lower but at later age was higher.

In this study, the statistic mode use to predict the relation compressive strength and tensile strength still use the model:

$$f_t = k f_{cu}^n \quad \text{Eq. (7)}$$

The model is depicted in Table 4.51 and the all results of predicted is plotted in Figure 4.80. It can be seen that the ACI 318-08, CSA A23.3-04, and (Mokhtarzadeh & French, 2000) are conservative as the results show in lower estimation. In addition, the formula is proposed by others, (Arioglu et al., 2006) and EC-2 NZS 3101:2006, also over estimation. All of them, the IAE value are higher than 5 %. This study proposes

the formula to predict the splitting tensile strength through the compressive strength of concrete with the range of 70-115 MPa. The formula is

$$f_t = 0.9290 f_c^{0.4172} \quad \text{Eq (8)}$$

with the IAE value is 1.81%. The other formulas do not able to reach to this value, which probably the formulas are not prepared for pozzolanic concrete.

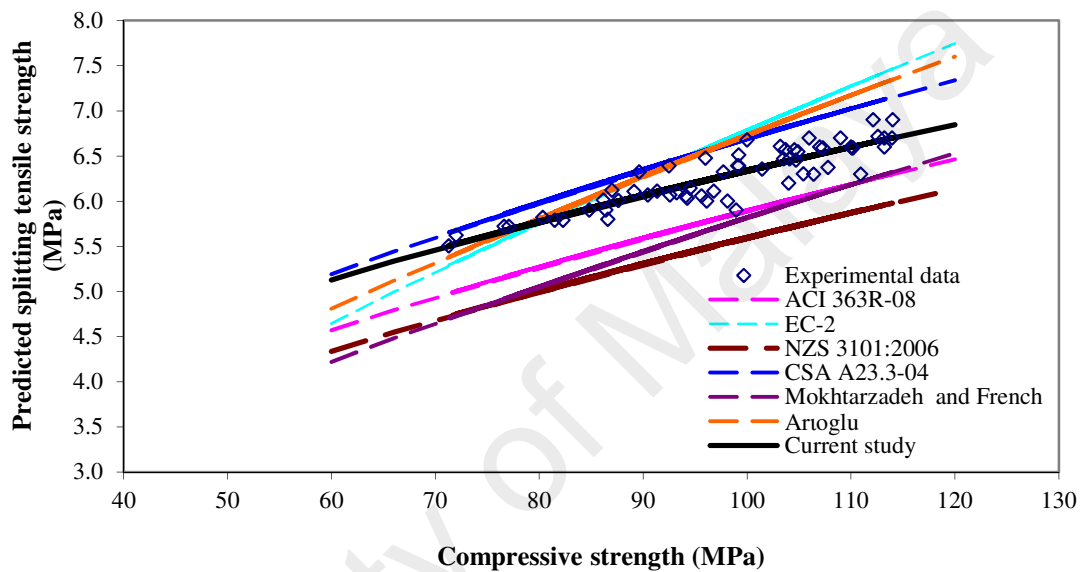


Figure 4.80: The curve of predicted splitting tensile strength by various formulas

Figure 4.82 show the relationship between the compressive strength to predicting splitting tensile strength of high performance concrete with generally having compressive strength in the range 70 up to 120 MPa. The regression analysis was performed and the following equations are provided:

$$f_t = 0.9264 f_c^{0.4174} \quad \text{with } R^2 = 0.8318 \quad \text{Eq. (9)}$$

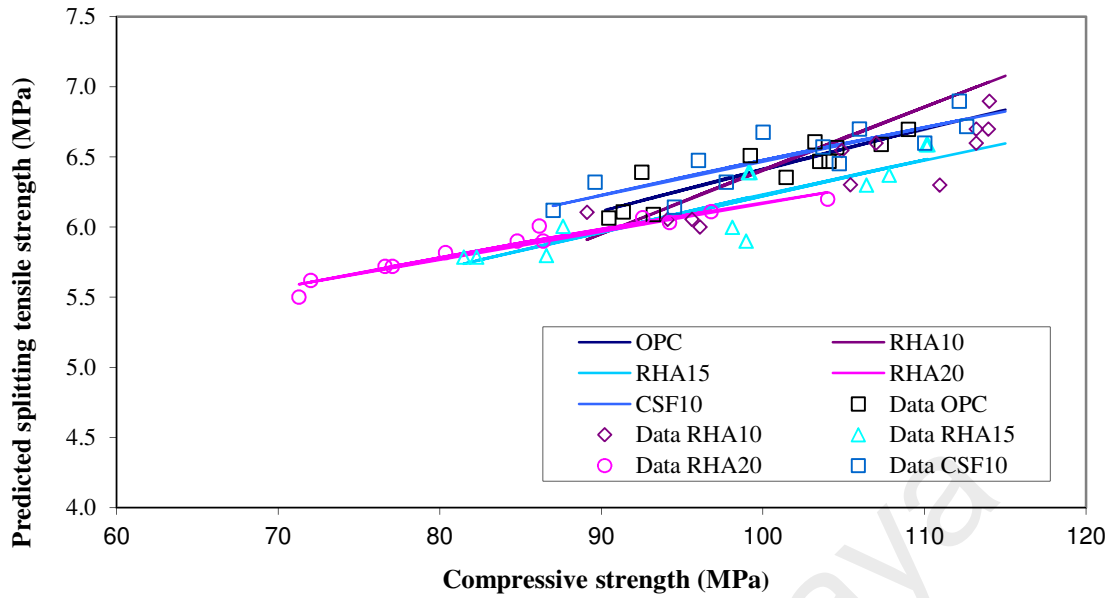


Figure 4.81: The curve of predicted splitting tensile strength by various formulas of concrete containing RHA

Figure 4.82 shows the relationship between the compressive strength to splitting tensile strength of HPC incorporating RHA generally having compressive strength in the range 70 up to 120 MPa the regression analysis was performed and the following equations are provided:

$$f_t = 0.7819 f_c^{0.457} \quad \text{for OPC concrete} \quad \text{Eq. (10)}$$

$$f_t = 1.0439 f_c^{0.3892} \quad \text{for RHA concrete} \quad \text{Eq. (11)}$$

$$f_t = 1.1633 f_c^{0.3729} \quad \text{for SF concrete} \quad \text{Eq. (12)}$$

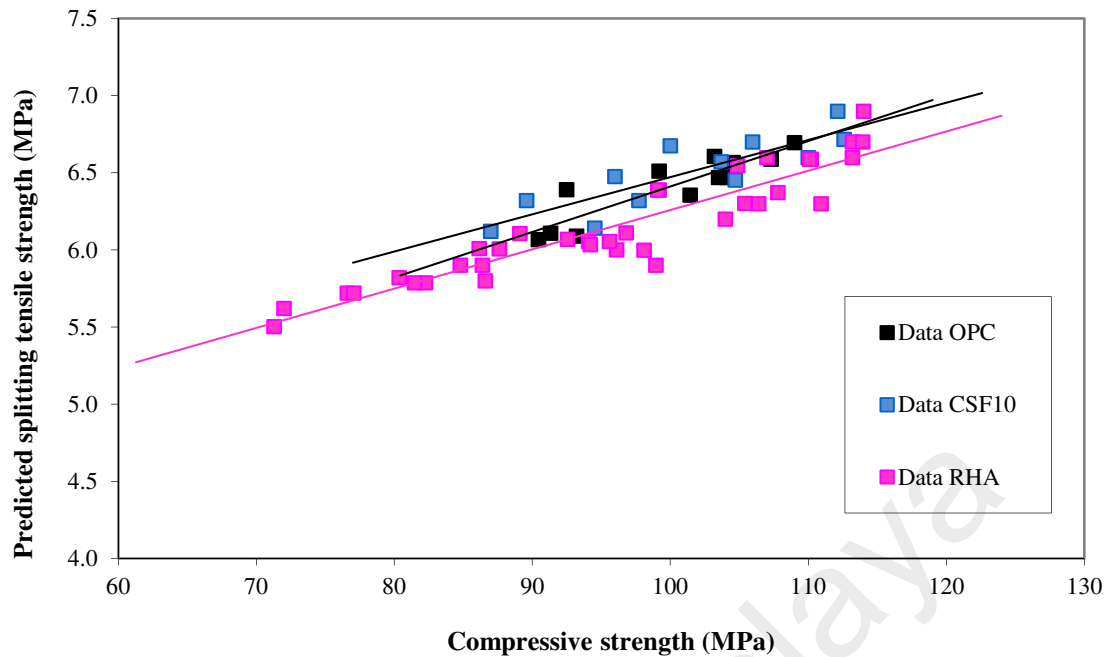


Figure 4.82: The curve of predicted splitting tensile strength by various formulas of concrete containing RHA

4.6.4.4 Relationship between the compressive strength and the ratio of splitting tensile and compressive strength

Table 4.52 provides the model to predict relationship between the compressive strength and the ratio of splitting tensile and compressive strength. Figure 4.83 and 4.84 shows the curve of the formula in Table 4.51. It shows the ratio tend to decrease when the compressive strength increased. It means that the rates of tensile strength development of concrete in this case are lower than that of rate compressive strength development. As mentioned previously, the filler and pozzolanic reaction affected to the compressive strength however, in the case of tensile strength pozzolanic material could have negligible effect as filler. It can be absented that the higher replacement of RHA in concretes the higher decreased tensile/compressive strength ratio. The average ratios of tensile and compressive strength are 0.064, 0.061, 0.062, 0.069 and 0.067 for OPC, RHA10, RHA15, RHA20 and SF concrete, respectively. From Figure 4.85 it can be

concluded that the ratio of tensile and compressive strength are significantly affected by the change of compressive strength.

Table 4.52: Statistical model used to predict the relationship between the compressive strength and the ratio of splitting tensile and compressive strength

Equation	Statistical model	A	B	R ²	IAE (%)	Remark
1	$\frac{ft}{fc} = \frac{Afc}{B + fc}$	0.0421	-33.364	0.9467	2.23	All mixes
2	$\frac{ft}{fc} = \ln(A + Bfc)$	1.1098	-0.0004	0.9395	6.19	All mixes
3	$\frac{ft}{fc} = \frac{1}{A + Bfc}$	6.1502	0.0960	0.9478	2.38	All mixes
4	$\frac{ft}{fc} = A fc^B$	0.9418	-0.5859	0.9444	1.79	All mixes
5	$\frac{ft}{fc} = A ft^B$	1.0770	-0.6177	0.9399	2.97	RHA
6	$\frac{ft}{fc} = \frac{Afc}{B + fc}$	0.0409	-34.445	0.9754	1.54	RHA

From Figure 4.83 and 4.84, it can be seen that the model of $\frac{ft}{fc} = \frac{Afc}{B + fc}$ is better than that of $\frac{ft}{fc} = A fc^B$ and also can be compared through its IAE value, which is the former is lower than the later one.

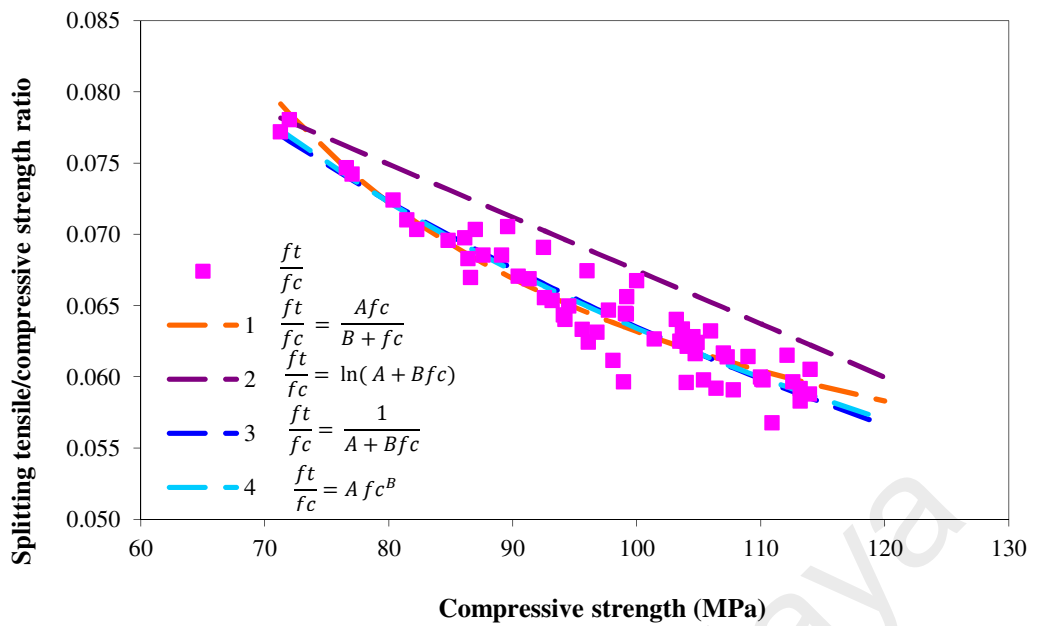


Figure 4.83: The curve of relationship between the compressive strength and the ratio of splitting tensile and compressive strength for all mixes

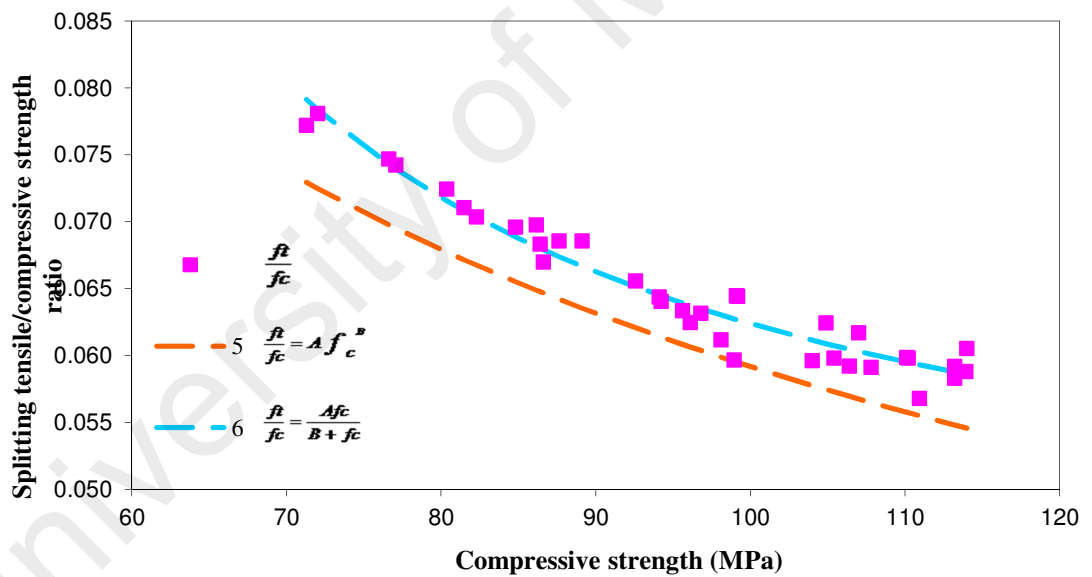


Figure 4.84: The curve of Relationship between the compressive strength and the ratio of splitting tensile and compressive strength for RHA concrete

4.6.4.5 Relationship between splitting tensile strength and modulus of rupture

The tensile strength of concrete mostly reported in splitting tensile strength and modulus of rupture rather than direct tensile strength. The ratio modulus of rupture and tensile splitting strength is around 1.53% (Ahmad & Shah, 1985). The assumption in

the flexure formula to calculate the modulus of rupture based on the linear assumption of strain through its section. However, concrete is not a homogeneous material as aggregate can increase the resistant of strain capacity in tension area. There is more tension stress that can still be hold after the first crack and it means that area is in the nonlinear area. As results, the modulus of rupture show higher tensile strength than its real tensile strength. It addition, the splitting tensile strength show close to tensile strength due to the splitting tensile strength could distribute the load on its area almost 85% of the tensile area..

Although, both the modulus of rupture and the splitting tensile strength are usually used to estimate the tensile strength of concrete, they do not yield equivalent results. Regression analyses were performed on the results obtained in this study using the following linear regression model:

$$f_t = a f_r \quad \text{Eq. (13)}$$

The Figure 4.85 shows the linear relationship of splitting tensile strength and modulus of rupture. All the curves have a good correlation as R^2 are higher than 0.9. The ratios of splitting tensile strength and modulus rupture are 0.68, 0.73, 0.73, 0.72 and 0.72 for OPC, RHA10, RHA15, RHA20 and SF concrete, respectively.

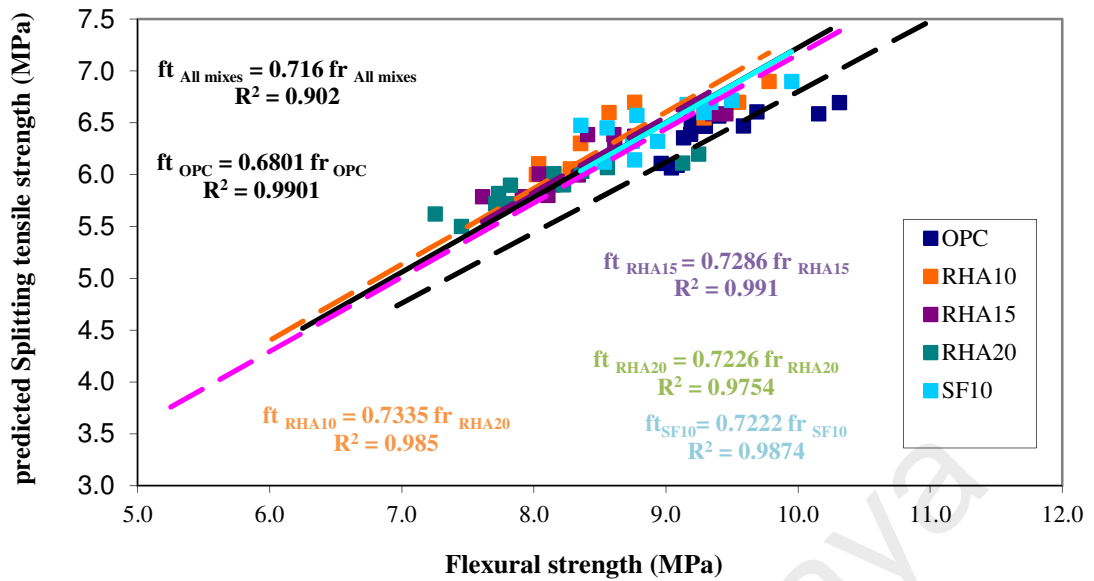


Figure 4.85: Relationship between Splitting tensile strength and modulus of rupture

4.6.5 Static modulus of elasticity

The static modulus of elasticity of the hardened cement paste and the aggregate in HPC is different than that in normal concrete. The behavior of HPC was more monolithic and the strength of the aggregate matrix interface was higher. Therefore, there is less bond micro cracking in HPC. The linear part of stress-strain curve could achieve as high as 85% of the failure stress in HPC concrete.

4.6.5.1 Effect of RHA on static modulus of elasticity

Table 4.53 shows the static modulus elasticity of concrete with w/b of 0.25, replacement percentages of RHA and ages of curing. Only this series will explain because there are not much different w/b 0.22 and 0.25 in this case. Generally, the results in Table 4.32 show that the static modulus of OPC concrete is less than RHA and SF concrete regarding replacement and ages in water curing; only 20% RHA replacement is lower than OPC concrete. This also was observed by xx that 20% RHA in normal concrete its static modulus was lower than OPC concrete. Less compressive

strength of concrete and more axial strain was the reason of less static modulus of elasticity. The 15% and 20% of RHA concrete show their static modulus of elasticity was lower than OPC concrete at any days of testing. The results of static modulus are shown in Figure 4.86. The values of the static modulus of elasticity were in the range of 36.0 – 47.2 GPa. It can be noted that the addition of RHA to concrete exhibited marginal increase on the elastic properties, the highest value was recorded for RHA20-25 mixture due to the increased reactivity of the RHA. Concretes incorporating pozzolanic materials usually show comparable values for the elastic modulus compared to the OPC concrete (Zhang & Malhotra, 1996) (Giaccio et al., 2007) (Vanchai et al., 2007).

Table 4.53: Static modulus of elasticity

Mix ID	W/b	Static modulus of elasticity E (GPa)		
		7 d	28 d	91 d
Water Curing				
OPC-25	0.25	36.0	39.6	45.8
RHA10-25	0.25	40.3	43.8	47.6
RHA15-25	0.25	39.4	42.9	46.2
RHA20-25	0.25	35.2	37.3	44.3
SF10-25	0.25	41.2	42.3	47.2
Air drying				
OPC-25	0.25	35.2	38.4	44.7
RHA10-25	0.25	36.5	41.3	46.1
RHA15-25	0.25	35.1	36.1	45.3
RHA20-25	0.25	34.3	35.5	41.6
SF10-25	0.25	38.7	41.2	46.5
Relative difference between water and air curing (%)				
OPC-25	0.25	2.27	3.13	2.46
RHA10-25	0.25	10.36	6.05	3.25
RHA15-25	0.25	12.14	18.84	1.99
RHA20-25	0.25	2.62	5.07	6.49
SF10-25	0.25	6.46	2.67	1.51

OPC = ordinary Portland cement; RHA = rice husk ash; SF = silica fume
 10, 15 and 20 = percentages of cement replacement
 22 and 25 = percentages of w/b

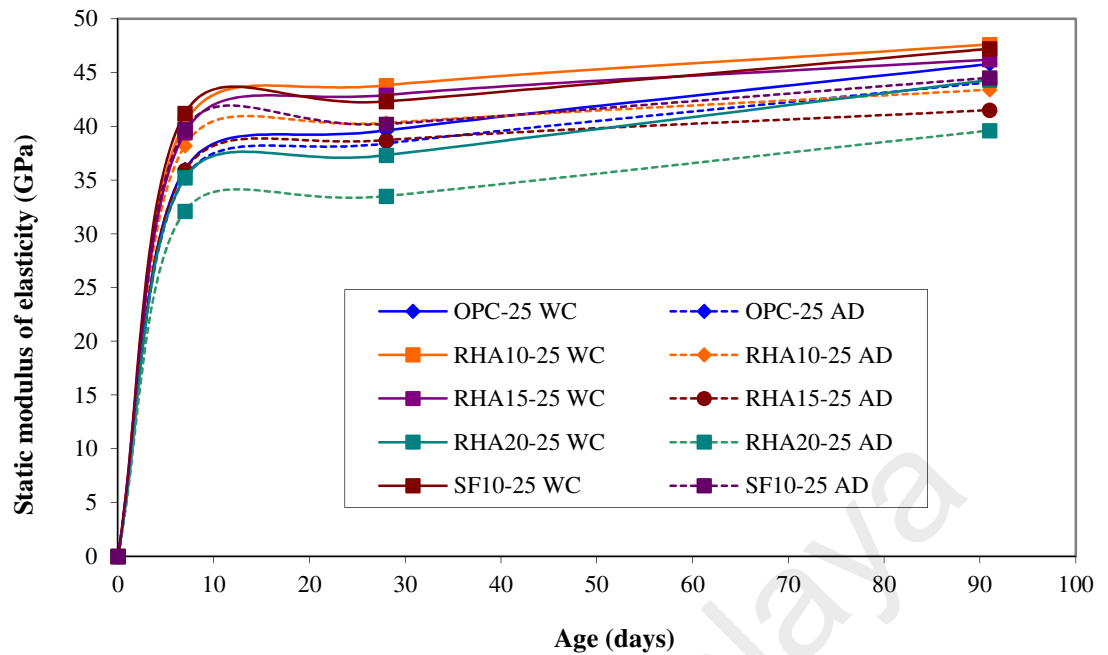


Figure 4.86: The development of static modulus of elasticity w/b 0.25 on water curing and air drying

4.6.5.2 Effect of curing on the static modulus of elasticity

In this study, the effect of curing on the static modulus of elasticity was also investigated. Test results showed in Table 4.53 that using water curing would result in slightly higher static modulus of elasticity of concrete compared to air-dry condition. This would be expected because of the increase of strength and the reduced shrinkage with water curing affected to the microstructure of concrete. The results showed that water curing the modulus of elasticity could get higher at later ages. At 90 days the static modulus of concrete was higher than that at 28 and 7 days. However, at air drying condition the improvement of static modulus of elasticity is slightly lower than that at water curing. It could be related to the compressive strength of the concrete which on both condition their compressive strength are almost similar.

Table 4.53 shows that the modulus of elasticity of concrete utilizing water curing in water tank continues to increase with age while with air-drying condition the increase is less. Khaloo and Kim (1999) studied the effect of curing condition of the modulus of

elasticity of lightweight of HSC i.e. compressive strength ranged from 71.5 to 86 N/mm² at 28 days. The various types of curing method include air drying condition at 13°C and 24°C, moist curing under polyethylene sheet at 13°C and 24°C, water curing at 13°C and submerged in water at 13°C and 24°C were used. The results showed that all curing method produce modulus of elasticity in the range of 22.3-26.52 kN/mm² and 23.7-29.1 kN/mm² at 7 and 28 days, respectively. There are a significant portion of the modulus of elasticity value could be achieved at 7 days of curing, but less than 10% strength gain was achieved from 7 to 28 days of curing.

4.6.5.3 Relationship between compressive strength and static modulus of elasticity

Table 4.54 provides the model to predict relationship between the compressive strength and predicting static modulus of elasticity. Figure 4.87 show the curve based on the ACI 318-08, EC-2, NZS 3101:2006 and CSA A23.3-04. Meanwhile, Figure 4.88 shows the curves based on the current study. The current study model is a little bit better than previous model due to the R² value is closed to 0.9. In Table 4.33, the IAE values of current study models also shows lower than that of the current models.

Table 4.54: Relationship models between static modulus of elasticity and compressive strength

Form of equation assumed	Correlation equation derived	R ²	Standard error of estimate (GPa)	IAE (%)
ACI 318-08	$E_c = 4.700 f_c^{0.5}$	0	5.9054	12.39
EC-2	$E_c = 22 (f_c/10)^{0.3}$			7.57
NZS 3101:2006	$E_c = 3.320 f_c^{0.5} + 6.900$	0.6336	3.2491	6.26
CSA A23.3-04	$E_c = 4.500 f_c^{0.5}$	0.1743	4.1355	7.80
Current study	$E_c = 1.8071 f_c^{0.6831}$	0.8230	2.3855	4.70
Current study	$E_{c_{OPC}} = 0.0367 f_{c_{OPC}}^{1.5175}$	0.9030		
Current study	$E_{c_{RHA10}} = 0.0693 f_{c_{RHA10}}^{1.3936}$	0.9321		
Current study	$E_{c_{RHA15}} = 0.0715 f_{c_{RHA15}}^{1.3773}$	0.7694		
Current study	$E_{c_{RHA20}} = 0.0945 f_{c_{RHA20}}^{1.3015}$	0.8218		
Current study	$E_{c_{CSF10}} = 0.4321 f_{c_{CSF10}}^{0.9977}$	0.8424		

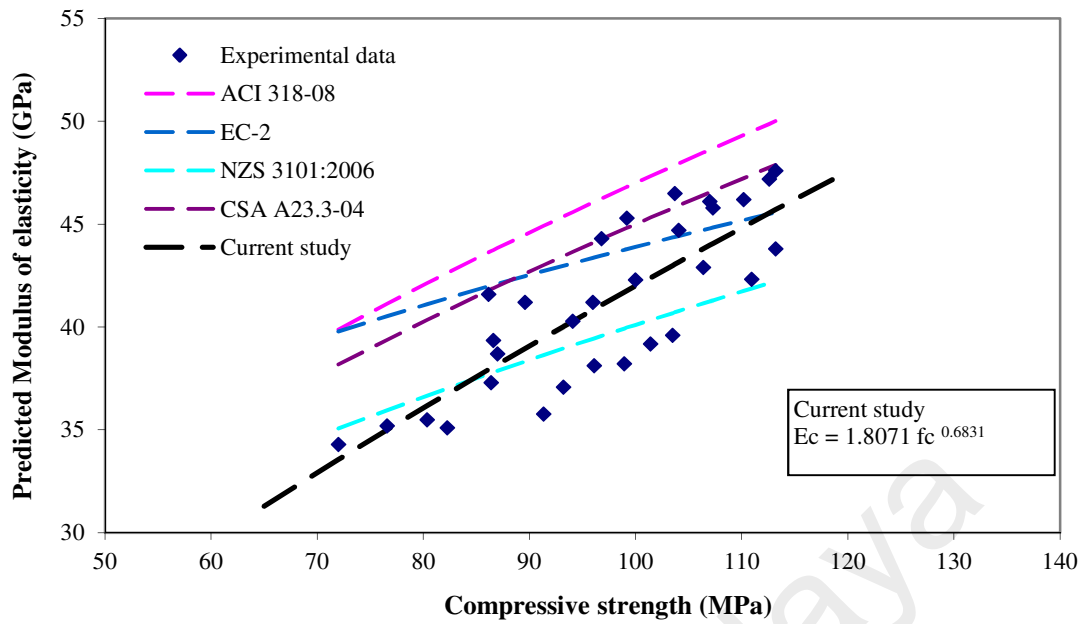


Figure 4.87: Relationship between compressive strength and predicting modulus of elasticity from available models

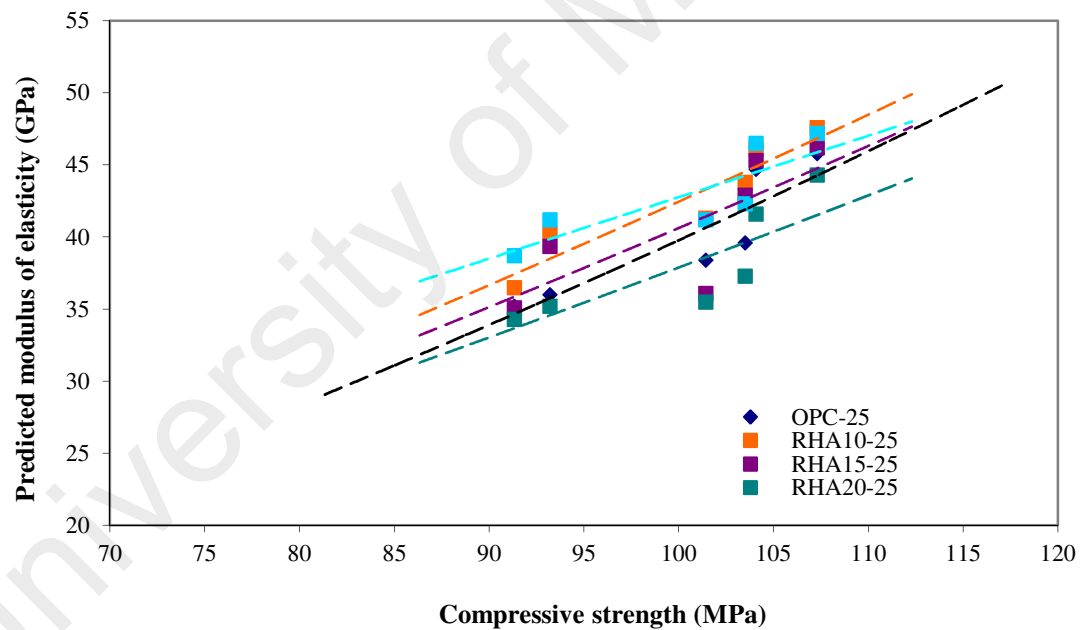


Figure 4.88: Relationship between compressive strength and predicting modulus of elasticity from OPC, RHA and SF concrete

4.6.6 Ultrasonic pulse velocity (UPV)

Non-destructive test is an analysis technique which conducts the test of a specimen without causing damage and the technique is widely use in science and industry to evaluate the properties of a material (Brauer et al., 2014). One of the popular non-destructive techniques used for evaluating quality of concrete is ultrasonic pulse

velocity (UPV). The UPV can often be used to assess the overall quality of a material, as well as to determine their elastic properties (Marfisi et al., 2005). In this study, UPV was used to predict the strength of concrete. As UPV wave could respond on the quality of concrete through the variation of its velocity when passing a certain distance of specimen. Hence, some researcher successfully utilized the UPV to determine the quality and uniformity of concrete, to estimate the static and dynamic modulus of elasticity of concrete (Castro & Carino, 1998) (Vipulanandan & Garas, 2008) and to measure the compressive strength of ground granulated blast furnace slag concrete (Shariq et al., 2013).

4.6.6.1 Effect of RHA replacement on W/b and UPV

Figures 4.89 and 4.90 show the effect of RHA, and SF content, w/b and curing method on UPV in concrete at any ages up to 180 days. As can be seen in the Figures, the replacement of cement with RHA tends to lower the value of UPV at early age. The value of OPC UPV is higher than that of RHA and SF due to the RHA and SF concrete at early age not as dense of OPC concrete. The hydration of OPC concrete in early age is higher than RHA and SF concrete due to OPC concrete having higher cement content than that of RHA and SF concrete. The difference of specific gravity and porous on RHA particles also could lower the density of concrete. At later age, starting after 7 days, RHA and SF concrete showed continue the increasing of UPV value. RHA and SF concrete reached higher the value of UPV than that of OPC concrete at 180 days, 5.46 and 5.40 km/sec for w/b 0.22 and 0.25. Malhotra (1976) and (IS-13311, 1992) has suggested that concrete has good durability when its pulse velocity value was in the range of 3.5–4.5 km/s. Since at first day all concrete mixes have reached UPV value above 3.660 m/s, therefore all concretes in this study could be considered as durable concrete.

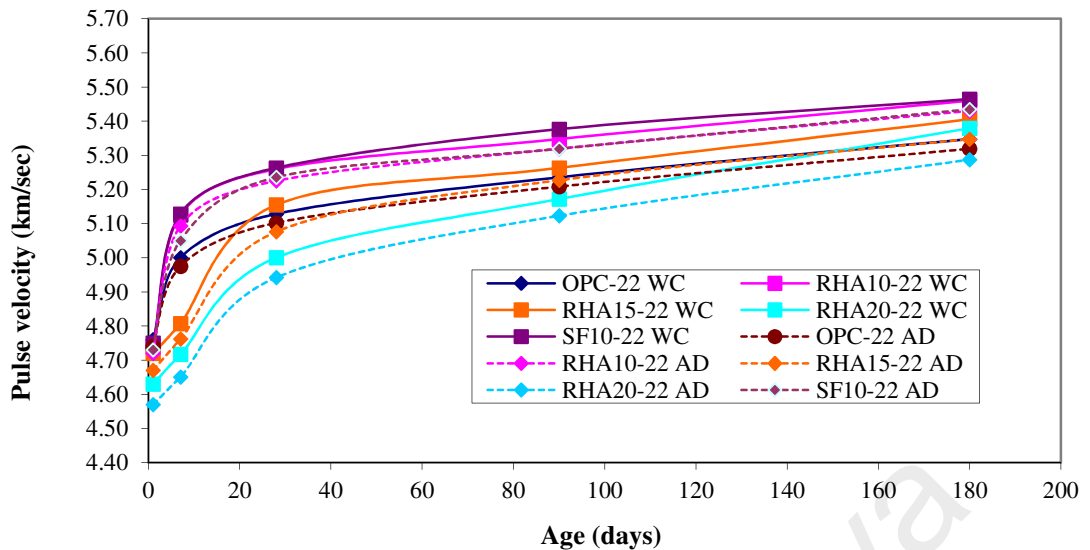


Figure 4.89: Evolution of UVP of concrete with age for w/b 0.22

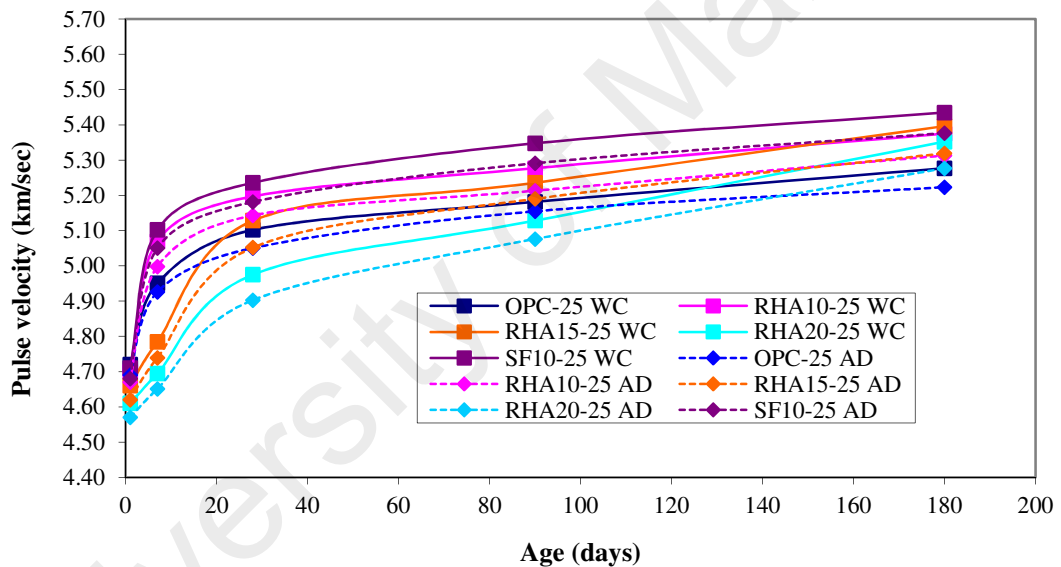


Figure 4.90: Evolution of UVP of concrete with age for w/b 0.25

4.6.6.2 Effect of curing on UPV

The wave of UPV can be interpreted as better density and high homogeneity of concrete if the value of UPV km/sec is higher compare with others. However, the moisture or empty pores in concrete due to curing also affects the value of UPV as shown in Table 4.55. The OPC concrete has the lower effect to curing regime compare to RHA and SF concrete regardless of w/b. On w/b 0.22 and w/b 0.25, the higher RHA content in concrete the more decrease the value of UPV at any ages. It means that RHA

and SF concrete are sensitive to curing. The percentages of the value of UPV air curing to water curing at 180 days on RHA 20% of w/b 0.22 above 96.75 % and 98.10%. The low w/b and high content RHA cause high loss of value of UPV.

Table 4.55: The results of UPV on various RHA and SF concrete up to 90 days

Mix ID	UVP air drying curing/water curing (%)				
	1 day	7days	28 days	90 days	180 days
OPC-22	99.58	99.60	99.42	99.24	99.10
RHA10-22	99.55	99.30	99.20	99.10	98.50
RHA15-22	98.94	98.71	98.64	98.40	98.21
RHA20-22	98.70	98.52	97.50	98.43	96.75
SF10-22	99.58	99.44	99.10	98.88	98.30

Table 4.55: Continue

Mix ID	UVP air drying curing/water curing (%)				
	1 day	7days	28 days	90 days	180 days
OPC-25	99.36	99.40	99.14	99.13	98.50
RHA10-25	99.51	99.20	99.05	98.20	98.10
RHA15-25	98.80	98.61	98.51	98.25	98.10
RHA20-25	98.48	98.30	98.13	97.81	97.42
SF10-25	98.98	98.85	98.57	98.29	98.12

OPC = ordinary Portland cement; RHA = rice husk ash; SF = silica fume
 10, 15 and 20 = percentages of cement replacement
 22 and 25 = percentages of w/b

4.6.6.3 Relationship between UPV and compressive strength

It was mentioned earlier that if the value of UPV get higher, it means that the concrete is more density and homogeneous. This character is similar with compressive strength of concrete, which get higher if the concrete is more dense and homogeneous. In forensic concrete, the NDT is an important test due to conducting the test of concrete without damage the structure. A linear model was adopted for their relation and the value of UPV can be used to predict the compressive strength of concrete. Figure 4.92 shows the relationship between compressive strength and UVP of OPC and concrete mixes containing 10%, 15% and 20% RHA, respectively and 10% SF, at all ages. The equation models proposed are:

$$f_c = 0.0036 v^{6.2166} \text{ for all mixes, } R^2 = 0.8604 \quad \text{Eq. (14)}$$

$$f_c = 0.1207 v^{4.1065} \text{ for OPC, } R^2 = 0.8872 \quad \text{Eq. (15)}$$

$$f_c = 0.0007 v^{7.2042} \text{ for RHA10, } R^2 = 0.8914 \quad \text{Eq. (16)}$$

$$f_c = 0.0008 v^{7.1836} \text{ for RHA15, } R^2 = 0.8902 \quad \text{Eq. (17)}$$

$$f_c = 0.0024 v^{6.4763} \text{ for RHA20, } R^2 = 0.9044 \quad \text{Eq. (18)}$$

$$f_c = 0.0107 v^{5.5150} \text{ for SF10, } R^2 = 0.9047 \quad \text{Eq. (19)}$$

Where, f_c is cube strength of concrete and v is ultrasonic pulse velocity of concrete.

Figures 4.91 show that the relationships between UVP and compressive strength are good as $r > 0.9$. The proposed formula is better than proposed by Turgut (Turgut, 2004), $f_c = 0.316e^{1.0269V}$. The formula was developed for concrete not incorporating pozzolanic material.

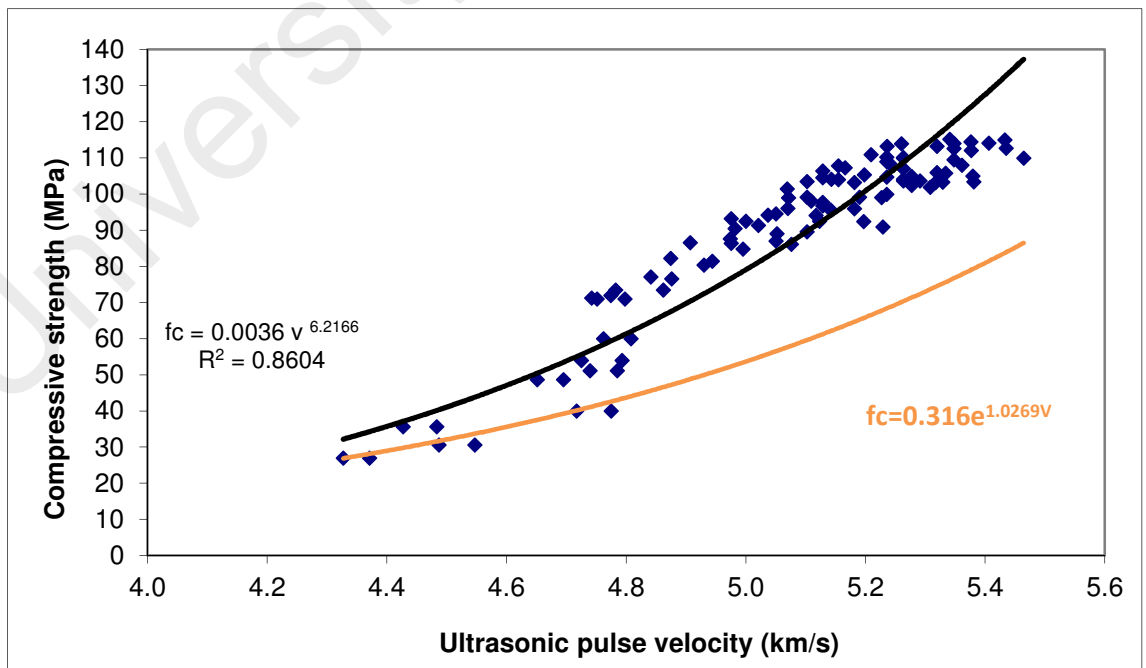


Figure 4.91: Relationship between compressive strength and UVP for all mixes

4.7 Durability of HPC

The durability test conducted on selected concrete such as OPC, RHA 10, RHA15 and SF10 with w/b =0.22 and 0.25. Each concrete specimen was subjected to air drying and water curing prior to test. The durability tests conducted were porosity, initial surface absorption test (ISAT), water absorption and sorptivity.

4.7.1 Porosity

4.7.1.1 Effect of RHA on porosity

The porosity test conducted based on RILEM suggestion and the values of porosity were found by using the formula explained in Chapter III through the water absorbed on the concrete specimen compared to oven dried concrete specimen. The values of porosity of concrete specimen taken at 7, 28, 90 days under at different w/b, age and percentages of RHA and SF concrete are given in the Table 4.56.

Table 4.56: The porosity at different w/b, age and in various percentages of RHA and SF concrete

Design mixture	W/B	Porosity		
		7 days (%)	28 days (%)	90 days (%)
Water curing				
OPC-22	0.22	8.64	6.75	6.20
RHA10-22	0.22	6.93	4.75	4.24
RHA15-22	0.22	7.34	5.48	4.52
SF10-22	0.22	5.46	4.36	3.49
Air drying				
OPC-22	0.22	9.00	7.00	6.33
RHA10-22	0.22	7.51	5.43	5.03
RHA15-22	0.22	7.93	6.23	5.40
SF10-22	0.22	5.43	4.30	4.00

Table 4.56 : Continue

Design mixture	W/B	Porosity		
		7 days (%)	28 days (%)	90 days (%)
Water curing				
OPC-25	0.25	8.84	7.54	6.90
RHA10-25	0.25	7.41	5.34	5.10
RHA15-25	0.25	8.20	6.20	5.68
SF10-25	0.25	6.16	5.26	4.60
Air drying				
OPC-25	0.25	9.30	7.90	7.00
RHA10-25	0.25	7.60	5.58	5.50
RHA15-25	0.25	8.53	6.60	5.83
SF10-25	0.25	6.84	5.61	4.91

OPC = ordinary Portland cement; RHA = rice husk ash; SF = silica fume
 10, 15 and 20 = percentages of cement replacement
 22 and 25 = percentages of w/b

4.7.1.2 Effect of w/b, RHA replacement and curing on Porosity

There is a contribution of w/b and % RHA replacement to porosity of concrete as it can be seen in Table 4.57. At 7, 28 and 90 days, the reducing porosities on OPC concrete in w/b 0.25 to w/b 0.22 is around 3%, 12% and 11% for water curing and air curing, respectively. It seems the curing is not critical for porosity value in OPC concrete. It could be the capillary from the surface to inner OPC concrete has disconnected since early age. However, effect of curing on 10% and 15% RHA concrete from w/b 0.25 to 0.22 is more sensitive in water curing compared to air drying. In air drying, it seems that water in RHA concrete is easy to evaporate compare to SF concrete. It can be seen in Table 4.36 that reduction of porosity value in SF concrete is still high until up to 90 days.

Table 4.57: Reducing porosity value from w/b 0.25 to w/b 0.22

Design mixture	% Reduce porosity value		
	7d	28d	90d
Water curing			
OPC-25 to OPC-22	-2.31	-11.70	-11.29
RHA10-25 to RHA10-22	-6.93	-12.42	-20.28
RHA15-25 to RHA15-22	-11.72	-13.14	-25.66
SF10-25 to SF10-22	-12.82	-20.64	-31.81
Air drying			
OPC-25 to OPC-22	-3.33	-12.86	-10.58
RHA10-25 to RHA10-22	-1.20	-2.76	-9.34
RHA15-25 to RHA15-22	-7.57	-5.94	-7.96
SF10-25 to SF10-22	-25.97	-30.47	-22.75

OPC = ordinary Portland cement; RHA = rice husk ash; SF = silica fume
 10, 15 and 20 = percentages of cement replacement
 22 and 25 = percentages of w/b

4.7.1.3 Effect of RHA and SF in concrete on porosity

Table 4.58 shows the reduced porosity values of RHA and SF concrete to OPC concrete after 7, 28 and 90 days curing. Generally, the specimens in water curing experience are high in reducing porosity value compared to air drying. The effect of replacement cement with 10% RHA gave more reducing porosity value than that of 15% RHA compared to OPC concrete. It could be related to the reaction of 15% RHA is not fully reacted up to 90 days. In this case, the SF is better performance compared to RHA concrete.

Table 4.58: Reducing porosity value from OPC concrete to various percentages of RHA and SF concrete

Design mixture	% Reduce porosity value		
	7d	28d	90d
Water curing			
RHA10-22 to OPC-22	-19.79	-29.63	-31.61
RHA15-22 to OPC-22	-15.05	-18.81	-27.10
SF10-22 to OPC-22	-36.81	-35.41	-43.71
RHA10-25 to OPC-25	-16.18	-29.18	-26.09
RHA15-25 to OPC-25	-7.24	-17.77	-17.68
SF10-25 to OPC-25	-30.32	-30.24	-33.33

Table 4.58: Continue

Design mixture	% Reduce porosity value		
	7d	28d	90d
	Air curing		
RHA10-22 to OPC-22	-16.56	-22.43	-20.54
RHA15-22 to OPC-22	-11.89	-11.00	-14.69
SF10-22 to OPC-22	-39.67	-38.57	-36.81
RHA10-25 to OPC-25	-18.28	-29.37	-21.43
RHA15-25 to OPC-25	-8.28	-16.46	-16.71
SF10-25 to OPC-25	-26.45	-28.99	-29.86

OPC = ordinary Portland cement; RHA = rice husk ash; SF = silica fume
 10, 15 and 20 = percentages of cement replacement
 22 and 25 = percentages of w/b

4.7.2 Initial surface absorption (ISA)

The ISAT was conducted to find the rate of flow of water into concrete per unit area at a stated interval from the start of the test at a constant applied head and temperature. Results were expressed as ml/ml²/s at a stated time from the start of test.

4.7.2.1 Effect of RHA replacement and W/b on initial surface absorption test

The results of the initial surface absorption test (ISAT) are shown in Table 4.59 and the Figures 4.92 and 4.93. For the RHA mixes, the ISA values were exhibited lower at 10% RHA than at 15% RHA but higher than 10% SF concrete. However, the ISA values are higher at control concrete. The incorporating RHA and SF have significant reduction on ISA value. This was expected since the RHA and SF act as micro filler and its extreme fineness allows it to fill the microscopic voids between cement particles, which greatly reduce the permeability. Figures 4.93 and 4.94 show than all ISA values are decreased as age of concrete increased. After 28 days, the rate of ISA value is decreased lower than that below at 28 days. It means that the process of pozzolanic reaction still continuing as reaction of cement is almost reaching the peak at 28 days. The incorporation of RHA is beneficial to reduce the permeability of concrete.

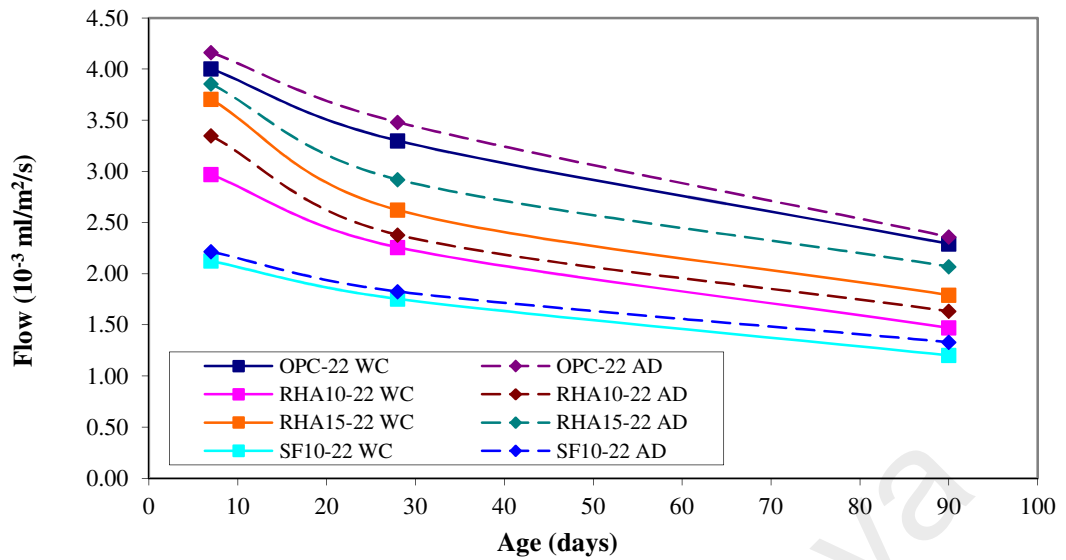


Figure 4.92: ISA value of concrete at 60 minutes at 7, 28 and 90 days for w/b 0.22

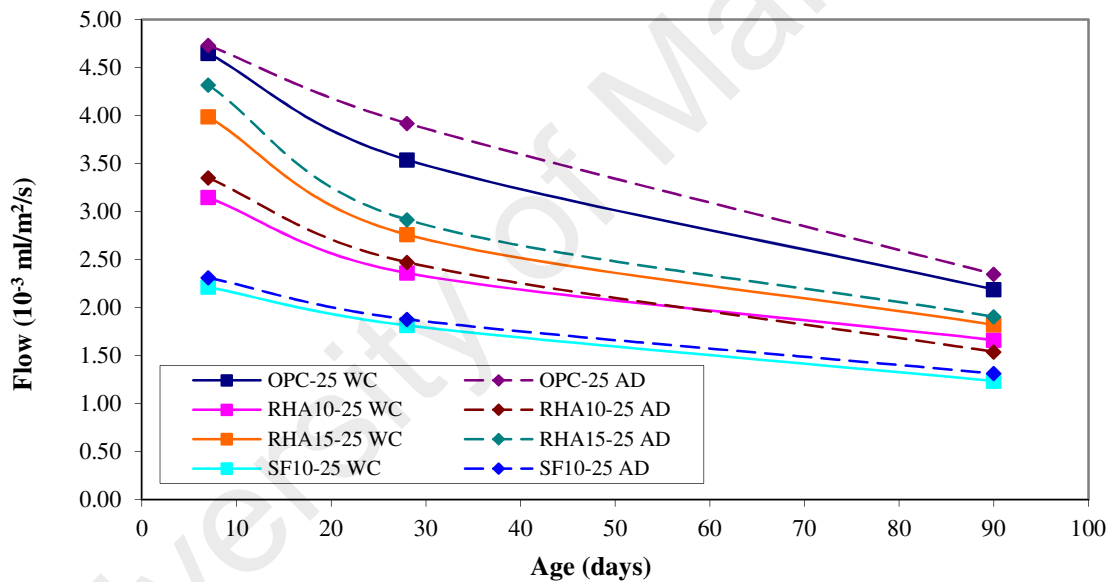


Figure 4.93: ISA value of concrete at 60 minutes at 7, 28 and 90 days for w/b 0.25

4.7.2.2 Effect of curing on initial surface absorption test

The specimens for ISAT were subjected to water curing and air drying curing. As it can be seen in Table 4.59 that curing was not so sensitive to these concrete, even the ISA value was lower at water curing compared with air drying curing. The different is around 5 % at any ages, which is not significant. It could be related to the treatment of

specimen after demolding that the specimen was covered by plastic sheet. The HPC concrete is critical a few hours after demolding.

Table 4.59: Initial surface absorption test for w/b 0.22 and 0.25 subjected water curing and air drying curing

Mix design	Flow (ml/m ² /s)			Flow (ml/m ² /s)			Flow (ml/m ² /s)		
	7 days			28 days			90 days		
	Elapsed time (minutes)			Elapsed time (minutes)			Elapsed time (minutes)		
	10	30	60	10	30	60	10	30	60
Water curing									
OPC-22	0.0087	0.0052	0.0040	0.0074	0.0043	0.0035	0.0052	0.0035	0.0023
RHA10-22	0.0062	0.0040	0.0030	0.0052	0.0029	0.0023	0.0035	0.0018	0.0015
RHA15-22	0.0071	0.0044	0.0037	0.0058	0.0034	0.0026	0.0046	0.0030	0.0019
SF10-22	0.0052	0.0028	0.0021	0.0041	0.0022	0.0018	0.0031	0.0016	0.0012
Air drying									
OPC-22	0.0095	0.0057	0.0042	0.0080	0.0049	0.0039	0.0045	0.0027	0.0024
RHA10-22	0.0069	0.0045	0.0034	0.0055	0.0030	0.0023	0.0038	0.0020	0.0016
RHA15-22	0.0080	0.0050	0.0039	0.0064	0.0037	0.0031	0.0042	0.0023	0.0020
SF10-22	0.0060	0.0030	0.0022	0.0045	0.0023	0.0018	0.0033	0.0016	0.0013
Water curing									
OPC-25	0.0100	0.0058	0.0047	0.0087	0.0052	0.0037	0.0046	0.0027	0.0024
RHA10-25	0.0070	0.0039	0.0031	0.0058	0.0031	0.0024	0.0038	0.0019	0.0015
RHA15-25	0.0082	0.0049	0.0040	0.0065	0.0036	0.0028	0.0042	0.0021	0.0018
SF10-25	0.0058	0.0026	0.0022	0.0045	0.0023	0.0018	0.0033	0.0016	0.0012
Air drying									
OPC-25	0.0130	0.0065	0.0047	0.0104	0.0052	0.0040	0.0052	0.0028	0.0025
RHA10-25	0.0081	0.0048	0.0034	0.0065	0.0033	0.0025	0.0042	0.0020	0.0017
RHA15-25	0.0098	0.0054	0.0043	0.0074	0.0039	0.0029	0.0046	0.0023	0.0019
SF10-25	0.0065	0.0027	0.0023	0.0049	0.0024	0.0019	0.0036	0.0017	0.0013

OPC = ordinary Portland cement; RHA = rice husk ash; SF = silica fume
 10, 15 and 20 = percentages of cement replacement
 22 and 25 = percentages of w/b

4.7.2.3 Relationship between initial surface absorption test (ISAT) and compressive strength

The results of the initial surface absorption test for selected HPC mixtures are presented in Table 4.60. Data show that at all ages, ISA values decreased with increasing age. The reasons are that the outer zone of the concrete surface became saturated as the capillaries were filled with water and made it more difficult for water to be absorbed by the inner pores (Long et al., 2001). Irrespective of the age of the specimen, compared to OPC concrete, there is a marked reduction in the ISA values for

RHA and SF concrete, indicating the importance of incorporating pozzolanic materials to reduce the permeability of concrete. The reduced pores in microstructure of concrete create denser of concrete and affect to compressive strength. Figure 4.94 shows the relationship between ISAT value and compressive strength concrete for selected HPC mixtures. It shows that the low of flow create the high strength and it is clear that low of water flow in concrete identic with a dense concrete. Table 4.39 shows the models proposed for OPC, RHA and SF concrete.

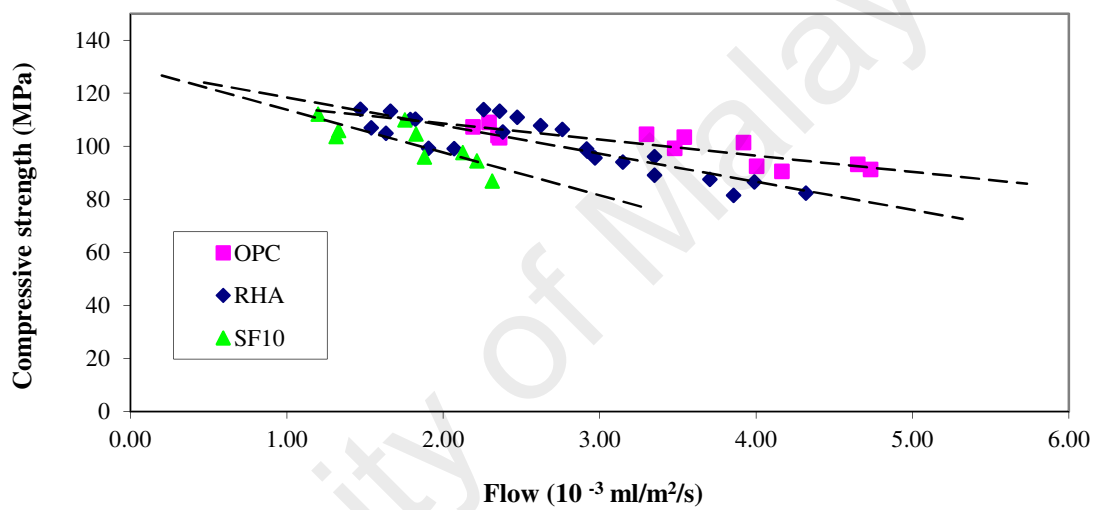


Figure 4.94: Relationship between ISA value and compressive strength

Table 4.60: Relationship model between ISA value and compressive strength

Mix	Model	R ²
OPC	$f_c = -6.0876 f + 120.77$	0.7530
RHA	$f_c = -10.585 f + 128.96$	0.7360
SF	$f_c = -16.119 f + 129.88$	0.6745

4.7.3 Sorptivity

Sorptivity is a kind of durability test that measure the characteristic of the material when absorb and transmit water through the capillary suction. Sorptivity is also as an indicator of the volume of the capillary pore space or open porosity. For above ground structure which water mostly not penetrates by pressures, sorptivity is important and suitable measurement (Sabir et al., 1998). It is important to note that in practice when

determining the slope of the graph, the readings at very early age are omitted. This is because there is an increase in the mass of the specimen caused by the filling of the open surface pores on the inflow face and the sides of the specimen when it is submerged (Sabir et al., 1998). Basheer et al.(Basheer et al., 2001) reported that the concrete degradation is mostly occur at near surface of concrete so that characteristic of surface zone is important and can be done through ASTM C 1585.

4.7.3.1 Effect of RHA on sorptivity

The sorptivity values calculated for RHA concrete after 7, 28 and 90 days of curing are presented in Table 4.61. It can be seen that at 7 days of water curing, the sorptivity value of 10% and 15% RHA concrete only 43% and 52% than that of OPC concrete. However, the sorptivity value of 10% SF concrete is 70% of that of OPC concrete. It means since the early age the RHA concrete can effectively reduce the pore space in concrete. At 28 and 90 days, the sorptivity values on 10% and 15% RHA are quite lower than that of OPC concrete, around 38% of the sorptivity value of OPC concrete. Ganesan, Rajagopal and Thangavel et al (Ganesan et al., 2008) observed that concrete with 10% RHA shows reduction on sorptivity value compared to control concrete. Umoh, 2016 #236] also found similar finding that 10% RHA content improve compressive strength with reducing sorptivity of the concrete. Furthermore, he mentioned that compressive strength of concrete can be predicted through its sorptivity characteristic. From the Table 4.61 it can be seen that the sorptivity value of RHA concrete tend to flat after 28 days and it could be related to the RHA reaction on concrete have almost fulfilled the pore space available. The performance of RHA concrete in term of sorptivity is better than SF concrete.

4.7.3.2 Effect of curing on sorptivity

As seen from Table 4.61, water curing on RHA concrete has great beneficial effect on its sorptivity when compared with that cured in air curing. At 7 days, the sorptivity of RHA concrete cured in water curing was much lower by about 119% compared to air drying RHA concrete. Meanwhile the sorptivity value of OPC concrete can only lower 42%. It demonstrates that curing is important for RHA concrete to keep the pore space reduce on RHA concrete. At 28 and 90 days, there is not much different on sorptivity value between the water curing and air drying. As stated earlier it could be the pore spaces is already reduced before concrete reaching 28 days.

Table 4.61: Effect of Rice husk ash and curing on sorptivity

Design mixture	Ages (days)					
	7 th		28 nd		90 th	
	Sorptivity coefficient ($\text{kg/m}^2/\text{min}^{0.5}$)	Normalizd (%)	Sorptivity coefficient ($\text{kg/m}^2/\text{min}^{0.5}$)	Normalizd (%)	Sorptivity coefficient ($\text{kg/m}^2/\text{min}^{0.5}$)	Normalizd (%)
Water curing						
OPC-25	0.0449	100.00	0.0412	100.00	0.0372	100.00
RHA10-25	0.0194	43.21	0.015	36.41	0.012	32.26
RHA15-25	0.0232	51.67	0.0178	43.20	0.0144	38.71
SF10-25	0.0313	69.71	0.0263	63.83	0.0255	68.55
Air drying						
OPC-25	0.0639	100.00	0.0574	100.00	0.0546	100.00
RHA10-25	0.0425	66.51	0.0381	66.38	0.0332	60.81
RHA15-25	0.0496	77.62	0.0435	75.78	0.0382	69.96
SF10-25	0.0397	62.13	0.0328	57.14	0.0297	54.40

OPC = ordinary Portland cement; RHA = rice husk ash; SF = silica fume
 10, 15 and 20 = percentages of cement replacement
 22 and 25 = percentages of w/b

4.7.4 Sulphate attack

Concrete in certain environment condition can experience degradation of strength. Degradation of concrete can be caused by various causes: fire, aggregate expansion and sea water degradation, etc. In this section, the sulphate attack on HPC containing RHA and SF will be elaborated. Sulphate is available in soil and sea water. In this study, the

sea water condition was stimulated by making dry and wet condition as tidal zone in sea water. Concrete that has contacted with sulphate can experience the chemical changes in cement. The deterioration mechanism is the chemical change in cement caused microstructural effect which the cement binder is weakening. It is worthy to note that sulphate solution caused damage through crystalline and re-crystalline in porous concrete.

4.7.4.1 Effect of RHA replacement on sulphate attack to compressive strength

Figure 4.95 shows the degradation of concrete after the concrete was exposed to Magnesium sulphate in three cycles. It can be seen that RHA, SF concrete and control concrete affected by magnesium sulphate after cycle 1. In cycle 1, the concrete experienced the improving compressive strength. It could be the process of crystalline was barely enough close to pores of concrete which caused concrete denser. However, in further cycling the concrete experience the degradation as compressive strength of concrete decreased. It could be the magnesium sulphate solution in concrete pores started to crystalline and re-crystalline due to wetting and drying cycling. It caused the concrete to expand and cause micro crack its surrounding. The control concrete experienced worst condition compared than the RHA and SF concrete. The 10% RHA concrete experienced less degradation than OPC, 15% RHA and 10%SF concrete. As mention earlier, it was related to the pores in concrete and 10% RHA having lower porosity than OPC, 15% RHA and 10%SF concrete

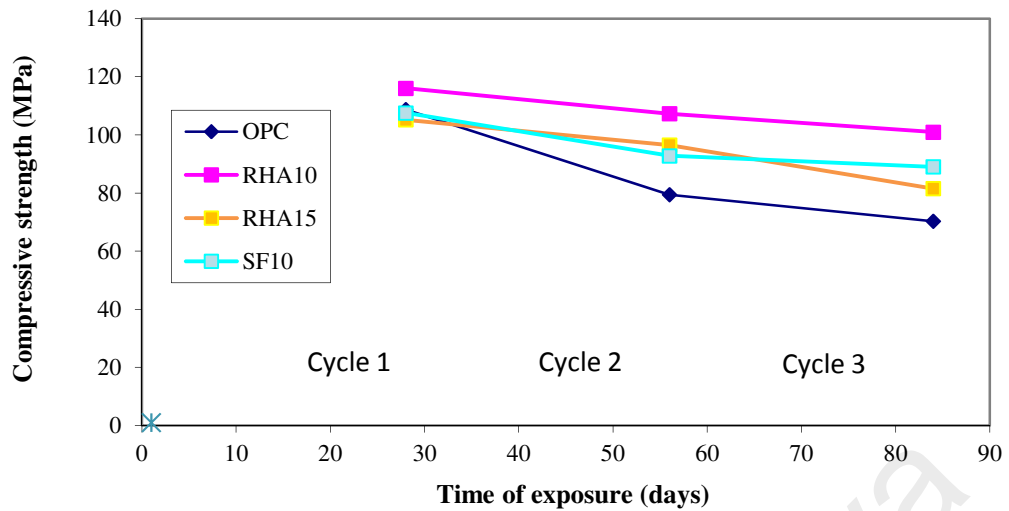


Figure 4.95: Development of compressive strength on sulphate condition

4.7.4.2 Effect of time exposure of sulphate on compressive strength

Figure 4.96 shows the reduction of compressive strength due to immerse the specimens in 5% Magnesium sulphate solution. The reduction was a comparison to the specimens without Magnesium sulphate experienced. The plain concrete is loss 28% and 36 % compressive strength at cycle 2 and 3 respectively. The 10% and 15% RHA concrete at cycle 2 almost similar loss which was 7.5% but at cycle 3, 10% RHA concrete was only loss 12% of its compressive strength and 15% RHA concrete was loss 21% of its compressive strength. Furthermore, the 10%SF concrete was loss 15% RHA concrete and 18% of its compressive strength at cycle 2 and 3 respectively. It is clearly showed that 10% RHA concrete was better performance than 10% SF concrete in sulphate attack.

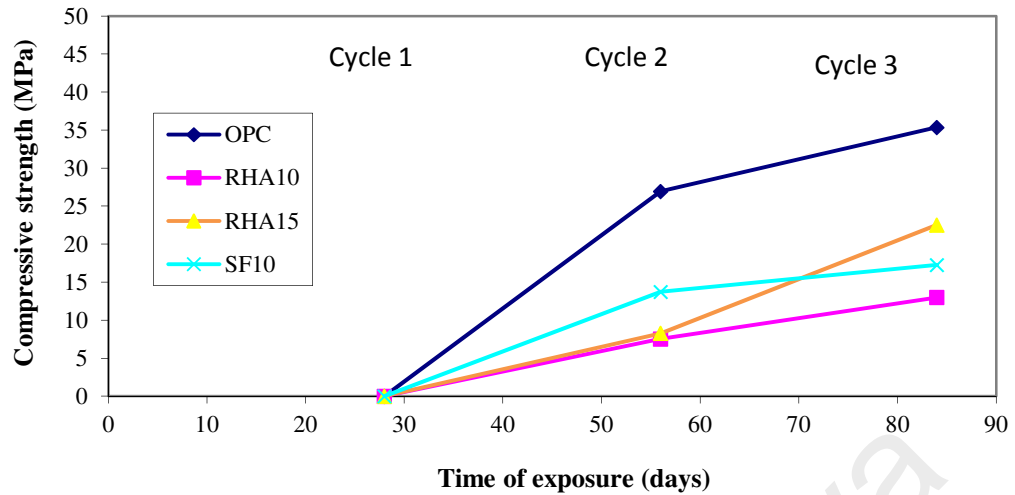


Figure 4.96: Development of compressive strength on sulphate condition

4.8 Time Dependent Deformation

The time-dependent deformations of concrete consist of shrinkage and creep. Shrinkage is the strain that occurs at zero stress, and creep is the strain produced by sustained stress (Bazant & Kim, 1991). Creep needs to be subdivided into two parts: the basic creep, which occurs at constant moisture content, and the drying creep, which represents an additional creep associated with moisture content variations. In this study only shrinkage was studied, especially drying shrinkage.

4.8.1 Shrinkage

During its service life, concrete experiences volume changes. One of the types of deformation experienced by concrete is shrinkage. The four main types of shrinkage associated with concrete are plastic, autogenous, carbonation and drying shrinkage (Mokarem, 2002). The volume changes in concrete due to shrinkage can lead to the cracking of the concrete. In the case of reinforced concrete, the cracking may produce a direct path for chloride ions to reach the reinforcing steel. Once chloride ions reach the steel surface, the steel will corrode, which itself can cause cracking, spalling, and delamination of the concrete.

4.8.1.1 Drying shrinkage

Shrinkage in concrete is classified as a time dependent phenomena, which the volume stability of concrete keeps change according time and without surcharge load. There are several types of shrinkage: autogenous, drying shrinkage, and plastic shrinkage. Drying shrinkage is considered one of the most important kinds of volume stability and it is a result of loss of water due to the humidity gradient between cement paste and atmosphere (Collins, 1989). It started to take place after the first day and a considerable portion of this length change was irreversible (Popovics, 1992). The drying shrinkage was influenced by various factors such as aggregate type and content, relative humidity, time of drying and the geometry of the test specimen (Hansen & Almudaiheem, 1987). It was generally agreed that 60% of the drying shrinkage would occur in the first three months (Hansen, 1987). Prediction of shrinkage was critical information due to shrinkage could cause cracks if it was restrained as it tensile stress exceeded its tensile strength (Altoubat & Lange, 2001). Then it could reduce the durability of concrete.

The shrinkage values at various ages under the two curing regimes are illustrated in Table 4.62. Drying shrinkage with time for the selected concrete mixes subjected to air-drying or 7 days water curing followed by air-drying (7W-D) are shown in Figure 4.59 and 4.60, respectively.

Table 4.62: Drying shrinkage values for selected mixtures

Ages (days)	Drying shrinkage ($\mu\epsilon$)							
	7 days initial water curing				Air drying			
	OPC 25	RHA10- 25	RHA15- 25	SF10-25	OPC 25	RHA10- 25	RHA15- 25	SF10-25
1	3	-15	-10	-50	-64	-67	-70	-99
3	-88	-103	-85	-135	-135	-140	-146	-220
7	-155	-184	-132	-195	-191	-213	-181	-235
28	-185	-210	-158	-233	-229	-240	-210	-310
56	-235	-260	-175	-313	-276	-296	-227	-360
90	-285	-328	-217	-365	-332	-360	-260	-410
180	-310	-346	-266	-384	-355	-394	-316	-438
242	-320	-366	-289	-410	-363	-407	-328	-454

OPC = ordinary Portland cement; RHA = rice husk ash; SF = silica fume
 10, 15 and 20 = percentages of cement replacement
 22 and 25 = percentages of w/b

4.8.1.2 Effect of RHA on drying shrinkage

Figure 4.97 and 4.98 show the total shrinkage results for the concrete mixes of OPC, RHA and SF concrete. These results correspond to the average micro strain ($\mu\epsilon$) of three measurements for each mix and curing method. The selected mixes are control concrete, 10% and 15% RHA concrete, and 10% SF concrete. The reason to choose those mixes was their compressive strength achieved above 100 MPa at 28 days. From Figure 4.97 and 4.98, the results show that incorporating RHA or SF to concrete mix increases the drying shrinkage compared to control concrete. The shrinkages of SF, RHA10, RHA15 and OPC concrete at 242 days were 410, 366, 289 and 320 $\mu\epsilon$, respectively. Those shrinkages fell within the typical range of value for concrete at advanced ages (200 and 800 $\mu\epsilon$). The shrinkage increased 41.99 %, 14.38% to 10%SF and 10% RHA concrete, but reduce 21.11 % to 15% RHA concrete compare to that of OPC concrete. However, the rates of shrinkage at 242 days showed all mixtures reached similar rate. At early age the shrinkage rate of 10% SF concrete showed the higher one, then 10% RHA, 15% RHA and OPC concrete. According to Li et al. (2010), the shrinkage occurred due to the pores less than 50 nm. In early age, the particles of RHA and SF reacted with CaOH to CSH through this reaction the capillary

pores reduced but increased fine pores. According to Mindess, Sidney et al. (2003) the small pores affected to compressive strength and fine pores affected to shrinkage. In the mix of 10% SF and RHA, the amounts of cement were higher than 15% RHA concrete. That cause in those mixes the amount of CaOH was higher and the possibility to react more with SiO₂ from SF and RHA. So that creates finer pores compare to 10%RHA concrete, which affected to higher shrinkage on those mixtures. Similar observation also reported by (Habeeb, G.A & M.M Fayyadh, 2009) and (Güneyisi et al., 2010) also reported similar trends for using silica fume.

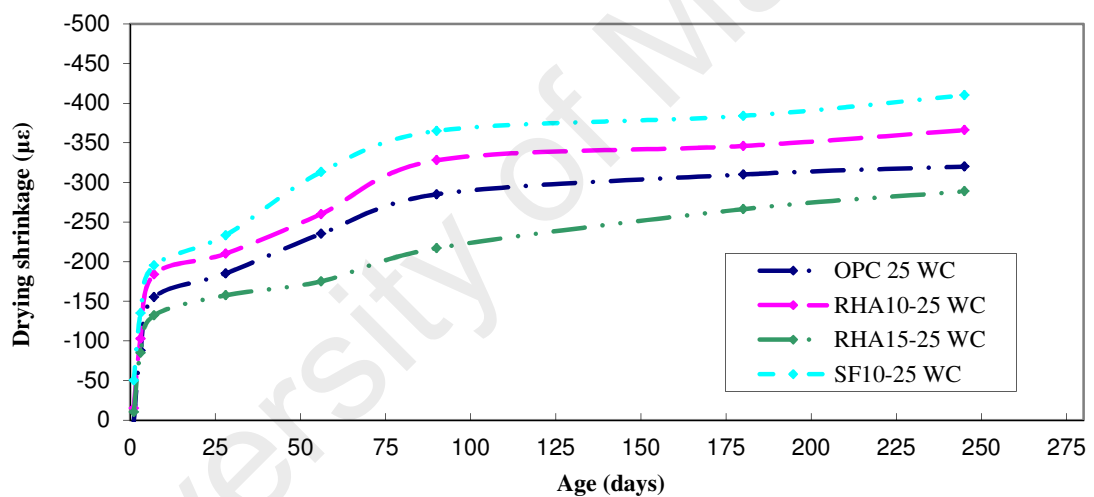


Figure 4.97: The shrinkage development of OPC, RHA10, RHA15 and SF10 at various ages (water curing)

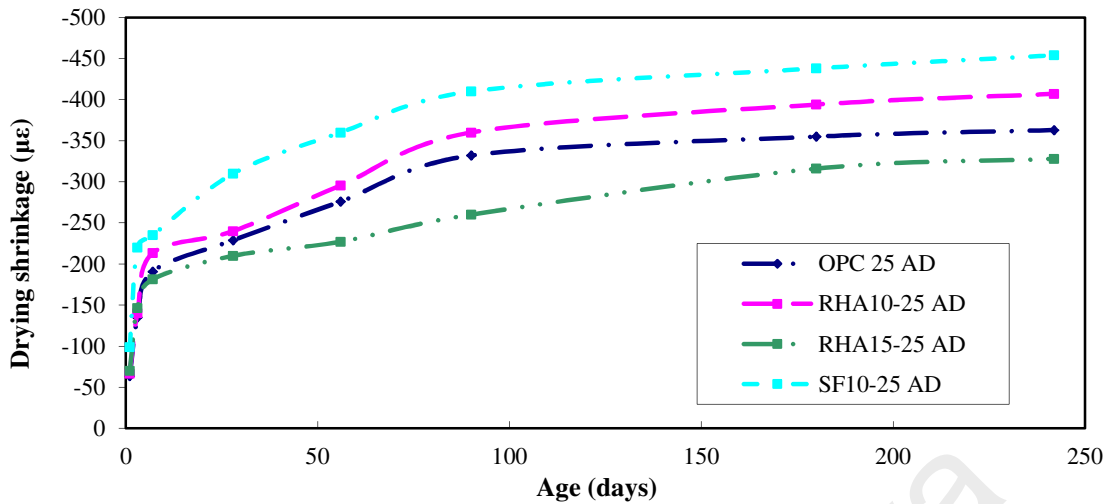


Figure 4.98: The shrinkage development of OPC, RHA10, RHA15 and SF10 at various ages (air drying curing)

4.8.1.3 Effect of curing on drying shrinkage

The purpose of curing on concrete is to protect the mixing water loss due to evaporation. As known, the mixing water is needed for the continuing hydration process. Water mixing evaporates through concrete capillary. So that the idea of curing is to minimize the mixing water loss through keeping the concrete close to relative humidity of 100% by fogging, wet burlap, water ponding, plastic sealing and compound painting. The concrete capillaries were different between concrete having low w/b and higher w/b. In high w/b, the concrete capillaries mostly were large pores and continuous. In low w/b, it was finer pores and discontinuous due to less water. Microspores, voids smaller than 50 nm, are related to drying shrinkage and creep phenomena (Mehta, P.K. & P. Monteiro, 1993).

The rate of drying shrinkage as shown in Figure 4.99 and Table 4.63 generally indicates that all the concrete mixes decreased with age. It is clearly shown in Figure 4.100 the rate of drying shrinkage decreases rapidly at early age and seem to be plate after 28 days. It was reported by (Neville, A.M. , 1996) that the rate of shrinkage decreased rapidly with time. In water curing, rate of shrinkage on OPC and RHA

concrete increase from first day and then decrease after third day meanwhile SF concrete was reduced from the first day. However, in air drying the rate of shrinkage decreased from the first day and increased again on the seventh day then decreased again except the silica fume concrete. The rate of shrinkage started to be plateau after 28 days regardless curing condition. Concretes experienced water curing showed high rate of shrinkage than air drying condition.

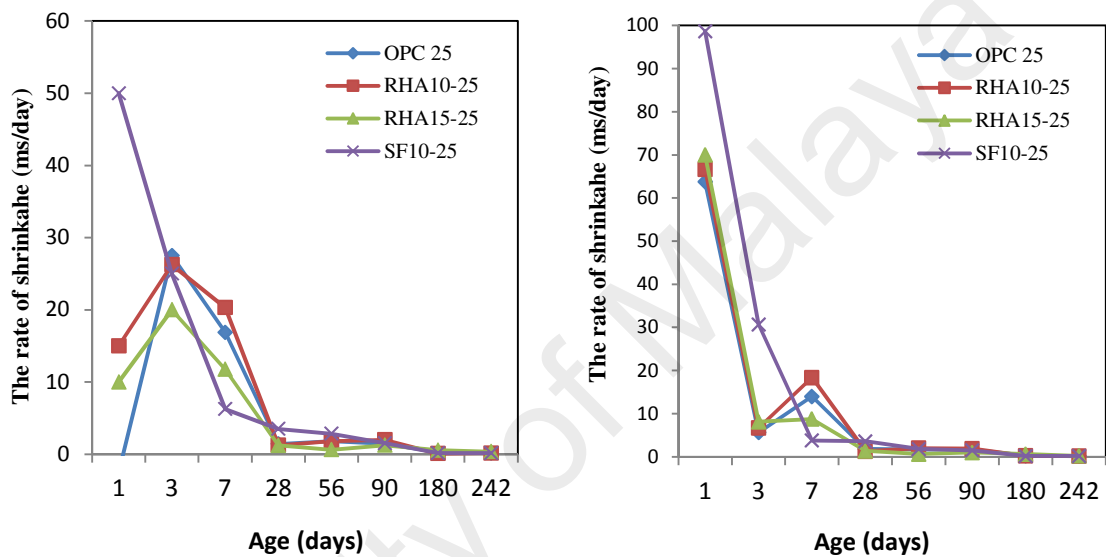


Figure 4.99: The rate of shrinkage due to water curing and air drying at w/b 0.25 up to 242 days

Table 4.63 shows the rate of shrinkage as percentages of 242 days shrinkage. It shows that OPC concrete subjected air drying produced about 63% of 242 days shrinkage at 28 days, while for concrete experienced 7 days water curing the value is 57%. It show that OPC concrete with initial water curing produced lower shrinkage. Similarly, at 28 days, RHA10, RHA 15 and SF10 concrete experienced initial water curing 7 days also showed lower shrinkage that that of air drying condition. Regardless of curing condition, 50% of 242 days shrinkage occurred within 28 days for all mixes and 90% of 242 days shrinkage occurred within 180 days for all mixes.

Table 4.63: The ratio of shrinkage strain percentage of 242 days

Ages (days)	Shrinkage strain percentage of 242 days ratio							
	7 days initial water curing				Air drying			
	OPC 25	RHA10-25	RHA15-25	SF10-25	OPC 25	RHA10-25	RHA15-25	SF10-25
1	-0.78	4.10	3.46	12.20	17.56	16.38	21.34	21.73
3	27.34	28.01	29.44	32.93	37.19	34.40	44.59	48.46
7	48.44	50.20	45.71	47.56	52.59	52.42	55.26	51.76
28	57.81	57.38	54.55	56.91	63.09	58.97	64.02	68.28
56	73.44	71.04	60.61	76.34	76.03	72.65	69.23	79.30
90	89.06	89.62	75.15	89.02	91.46	88.45	79.27	90.31
180	96.88	94.54	92.21	93.66	97.80	96.81	96.34	96.48
242	100.00	100.00	100.00	100.00	100.00	100.00	100.00	100.00

In predicting the ultimate shrinkage of present work, the equation for shrinkage after age 7 days for moist cured concrete xx is used.

$$(\varepsilon_{sh})_{t=} \frac{t}{35+t} (\varepsilon_{sh})_u \quad \text{Eq. (20)}$$

Where $(\varepsilon_{sh})_{t=}$ predicting shrinkage at t time

t = the time shrinkage considered

$(\varepsilon_{sh})_u$ = Ultimate shrinkage

The predicted ultimate shrinkage for OPC, RHA10, RHA15 and SF10 concrete taken based on shrinkage at 242 days for initial 7 days water curing are 279, 312, 252 and 357 $\mu\epsilon$ respectively. It seems the formula for predicting shrinkage by ACI 29 is underestimated.

4.8.2 Restrained shrinkage

At the beginning of using high performance concrete, there was a rising problem reported in this type of concrete, which early cracks always occurred. It could be due to the high usage of cement in HPC, which is more than that in normal concrete, and it could increase shrinkage of the concrete (Roberts, 2006). Shrinkage occurs in early age of concrete if restrained by adjacent element will generate tensile stress in the

element and cause cracks, which are possible to occur if stress exceeding the tensile strength of concrete. Cracks occurred in early age were against the purpose of developing HPC, which is high strength, workable and durability. It could be cracks in early age did not reduce the strength of the structure, but it could reduce the durability of the concrete. Through the cracks, the dangerous materials can ingress to concrete and create corrosion in reinforcement. Most reports available on cracks of concrete were in silica fume concrete (Whiting et al., 2000) (Altoubat & Lange, 2001). The crack itself is a complex phenomenon. It is important for any developing new HPC to check its mix design so that it should have a capability to resist cracks at an early age. To understand the behavior of concrete when it is restrained, in these study two samples were prepared in each OPC, 10%RHA, 15%RHA and 10%SF concrete on free shrinkage and restrained shrinkage conditions.

4.8.2.1 Free shrinkage before 24 hours

The restrained concrete sample was tested simultaneously with free shrinkage sample in a similar environment. The restrained concrete was designed to experience the effect of drying shrinkage after 24 hours of casting due to air drying. When the molds were demanded at 14 hours after casting, directly the samples were covered with aluminum foil to avoid evaporation. At 24 hours the aluminum foil was removed to let the samples exposed to ambient conditions to simulate air drying condition.

Figure 4.100 shows the free shrinkage of concretes at the age of one day. All samples of concretes experienced the expansion until up to 4 h after placing concrete on the molds, but the OPC showed higher expansion, up to 180 $\mu\epsilon$, and it is supported by Figure 4.101 that the OPC concrete experience higher temperature at that time. However the pozzolanic concrete showed similar behavior with OPC concrete, which on the peak temperature the concrete did not show shrinkage instead of expansion. This

behavior also agrees with the information from Figure 4.102 that shows the loss water in samples after 24 h.

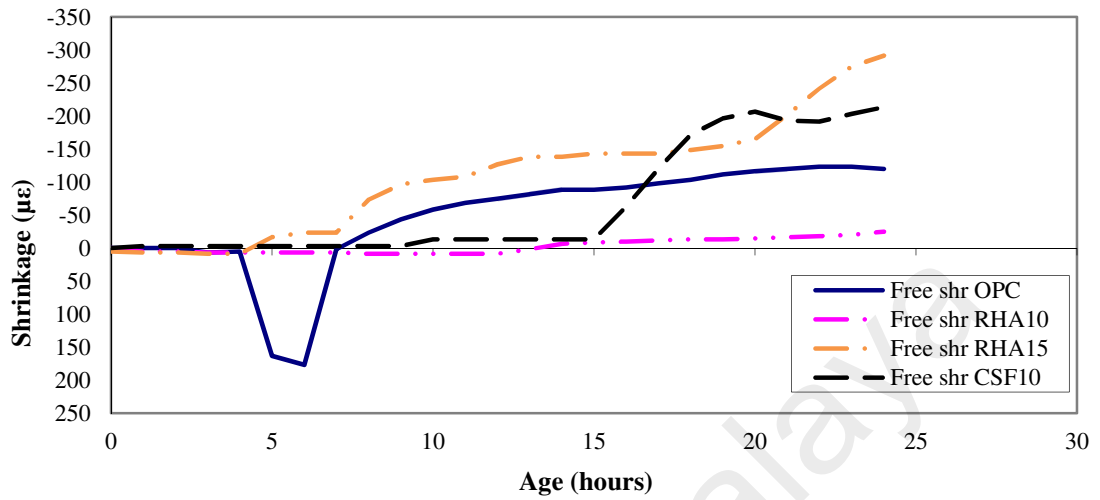


Figure 4.100: Free shrinkage during the age of one day

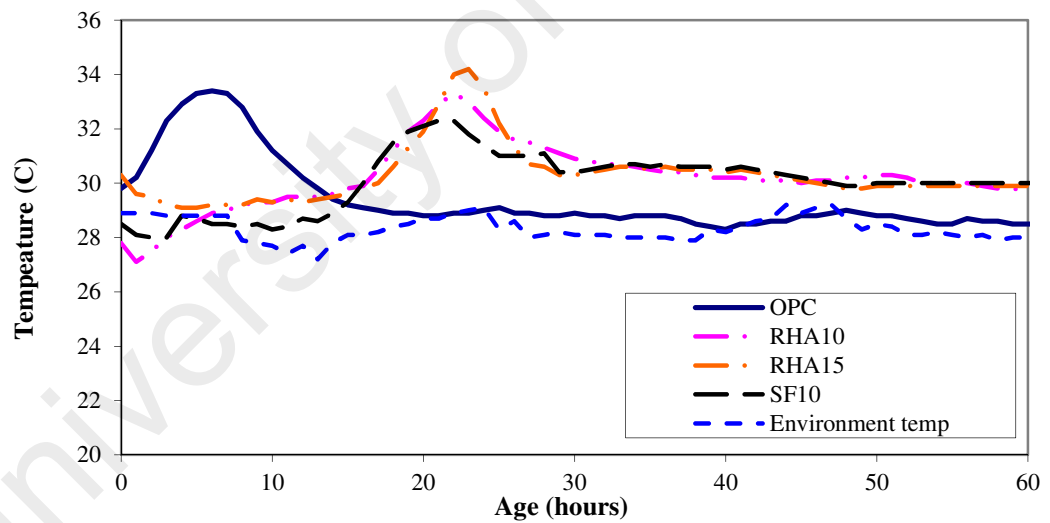


Figure 4.101: Temperature of concrete mixture after casting up to 60 hours

The loss water in samples was higher in pozzolanic concrete, which it means the drying shrinkage was more dominant than thermal shrinkage, see Figure 4.102. Higher rates of shrinkage by RHA15 concrete after this time may be explained by the pozzolanic reaction of RHA in concrete that consumes hydroxide crystals. Jensen and

Hansen (1996) explained that the calcium hydroxide crystals acted as internal restraints and the removal of these crystals induced additional shrinkage.

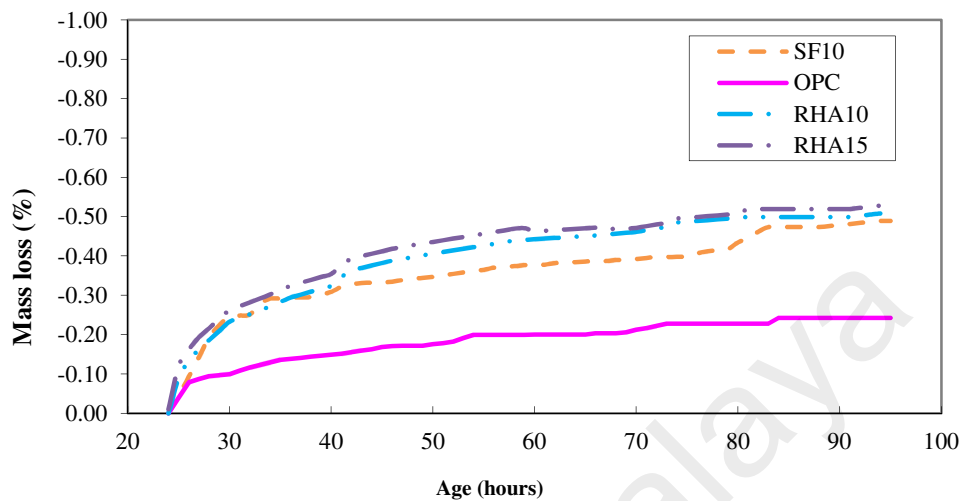


Figure 4.102 Mass losses after 24 hours

The OPC concrete showed the increase of temperature directly after placing and reached 33°C at 5 h. However, the RHA10, RHA15 and SF10 concrete start to increase temperature at 14 h and reach 32-34 °C at 25 h. The increase of temperature was related to the hydration process in concrete, which is an exothermic process. The OPC concrete start hydration process early compared to pozzolanic concretes could be due to its amount of cement was higher than pozzolanic concrete. It is clear evidence that pozzolanic material delayed hydration process as all pozzolanic concrete showed higher temperatures late compared to OPC concrete. All concrete showed their temperature after cooling down still above the ambient temperature, which means all concrete still continued in the hydration process.

4.8.2.2 Free shrinkage testing as a companion of restrained shrinkage

Figure 4.103 presents free shrinkages for concrete mixtures in this study. It is important to note that when the restrained shrinkage started to account, all the

measurements was reset to zero. At 24 hours, the aluminum foil sealed was removed and the samples were exposed to air drying condition. In the early hours of exposure, the concrete samples experienced either no shrinkage or minimal expansion in the period varied between 24 h and 27 h. It was probably related to hygrothermal disturbance during the first hours of exposure. The OPC concrete experienced the swelling at early age, more than other concrete. When the thermal effect dominated, slight expansion occurred. But if drying dominated the shrinkage occurred at a rapid rate until the age of 50 h and then the rate decreased afterward. The shrinkage strain of concrete reached 120, 145, and 170 $\mu\epsilon$ the age of 50 h for OPC, RHA10 and SF10 concrete, respectively. The RHA15 concrete was recorded only until 48 h due to the restrained samples was cracked at that time and shrinkage of RHA15 concrete reached 125 $\mu\epsilon$. However, according to Figure 4.105, the RHA15 concrete experienced the shrinkage was higher than other concrete up to 24 h. At 24 h, the shrinkage of RHA15 concrete reached 290 $\mu\epsilon$ and RHA10, OPC and SF10 concrete are 25, 105 and 205 $\mu\epsilon$ only.

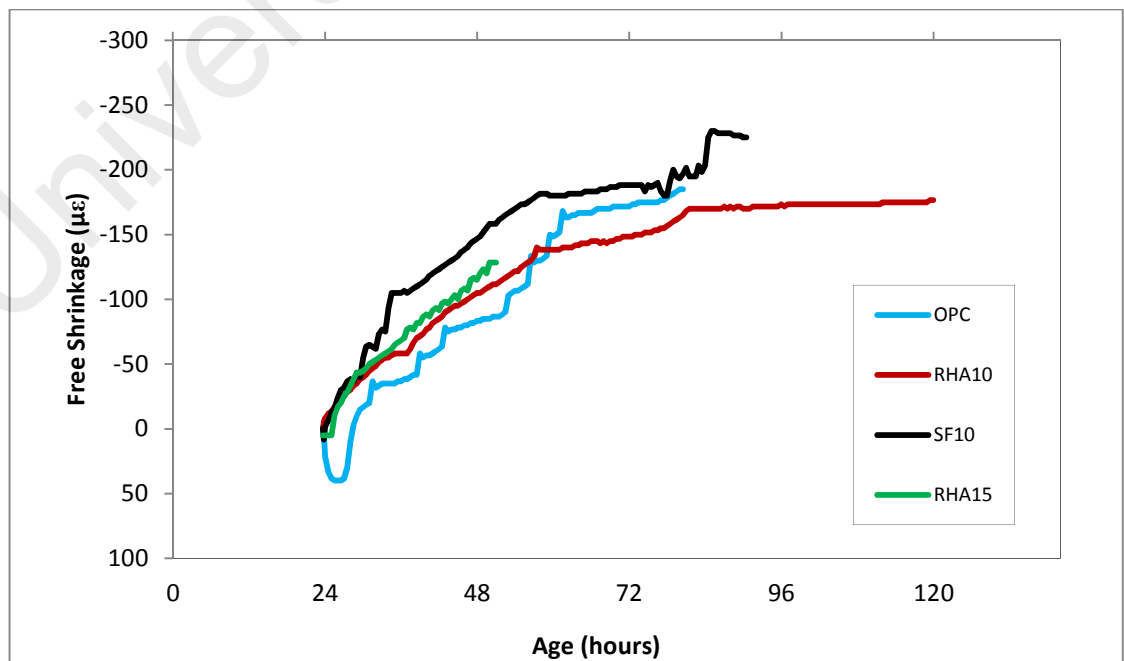


Figure 4.103: Free shrinkage of HPC

Figure 4.104 shows the elastic strain of HPC. The elastic strain was accumulated strain of each 5-10 $\mu\epsilon$ of restrained shrinkage samples before it was pushed back to original length. All samples showed the same trend up to 48 h.

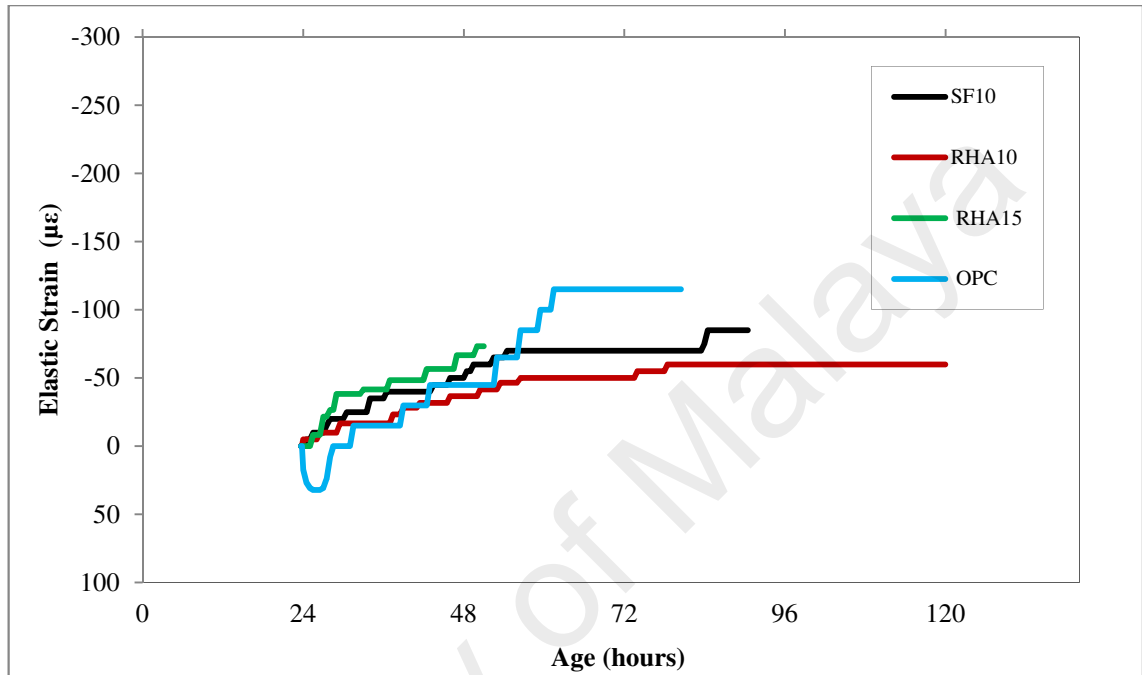


Figure 4.104: Elastic strain of HPC

Figure 4.106 shows the creep experience of HPC. The creep strain was calculated for each mix by subtracting the cumulative elastic strains imposed on restrained samples during the strain recovery from the total free shrinkage strains occurred at that time. The rate of creep evolution with time for SF10, RHA10, and RHA15 concrete started to develop at a high rate after the first 2 h of exposure to drying. Meanwhile the OPC concrete started to develop after 4 h at a lower rate than others. The RHA15, OPC and SF10 concrete were cracked at 48 h with 60 $\mu\epsilon$, at 115 $\mu\epsilon$ at 80 h and at 80 $\mu\epsilon$ at 90 h, respectively. The RHA10 concrete until 120 h did not show a crack. Figure 4.105 shows the shrinkage and creep on HPC. It is interesting to note that SF and OPC concrete experienced a constant shrinkage longer before it was crack more than 10

hours. For RHA 10, it showed the constant shrinkage after 72 hours. And it did not show crack until 120 hours.

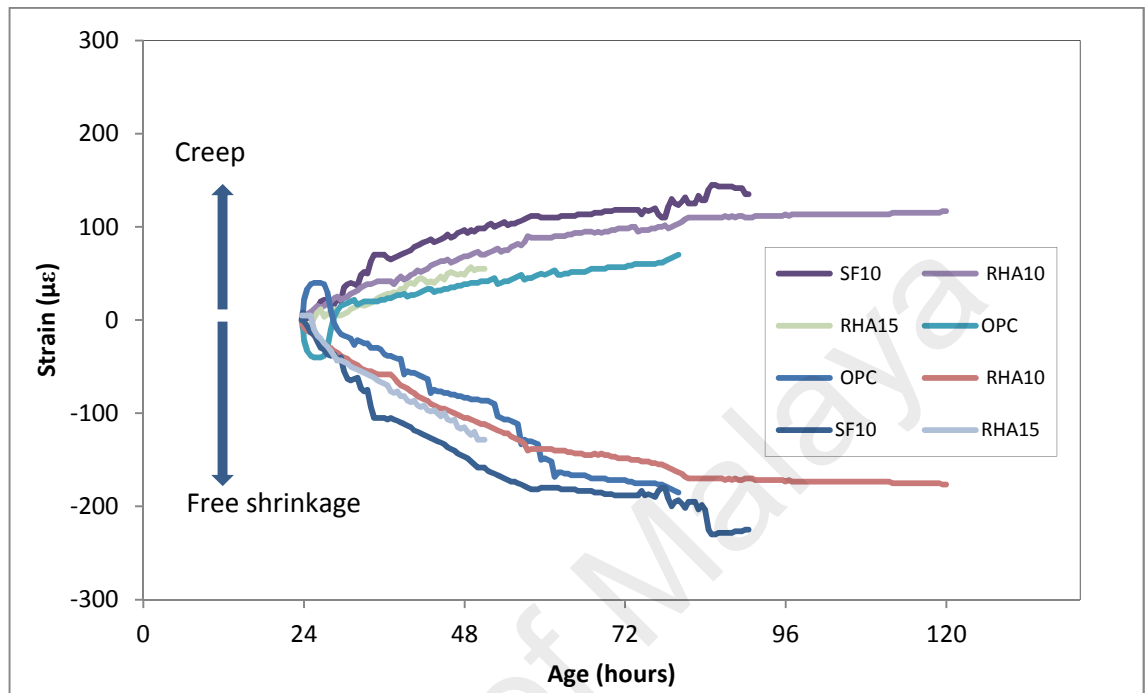


Figure 4.105: Shrinkage and creep strain of HPC

The degree of stress relaxation was characterized by the ratio of tensile creep strain to free shrinkage strain. In Figure 4.106, it is in order of 0.4-0.7 around the cracking time for all mixes. Tarek and Sanjayan (2008) found the ratio around 0.4-0.6 and Altoubat and Lange (2001) found around 0.5. Creep factor is a method of representing the creep in concrete, which is defined as the ratio of total creep strain to the total elastic strain at time considered (Altoubat & Lange, 2001).

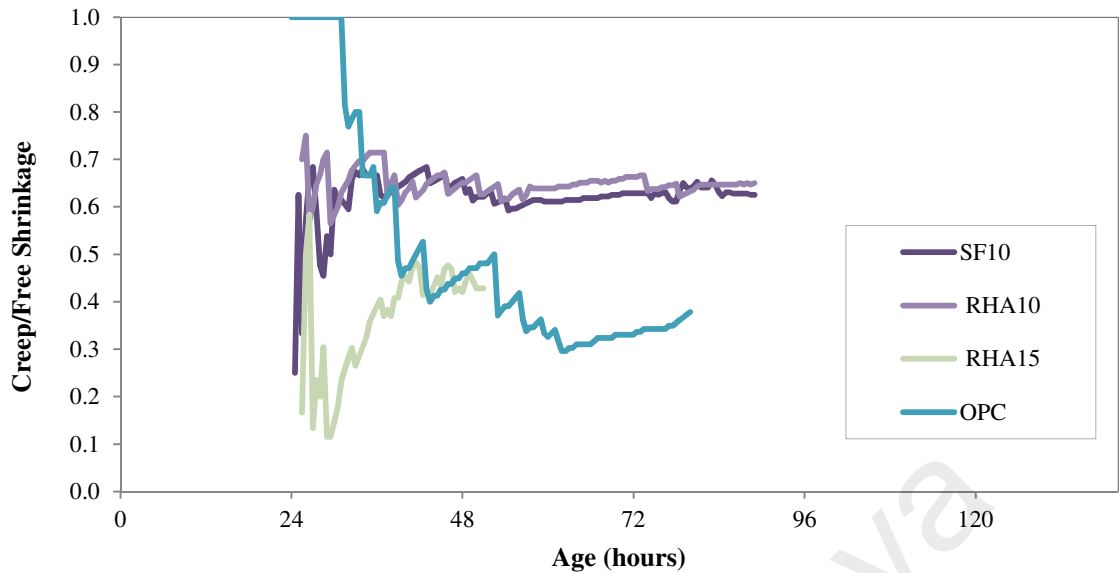


Figure 4.106: Early age creep/free shrinkage

The results in Figure 4.107 showed that the rate of creep factor in evolution with time for all concretes. The OPC and RHA15 concrete showed similar creep factors around 0.5 when it was cracked. The creep factor of SF10 concrete was 1.5 when it was cracked. However, the creep factor of RHA10 concrete was 1.95 and did crack yet until 144 hours. It can be seen that the lower creep factor tends to crack earlier. This shows that creep effects also played a significant role in time to cracking.

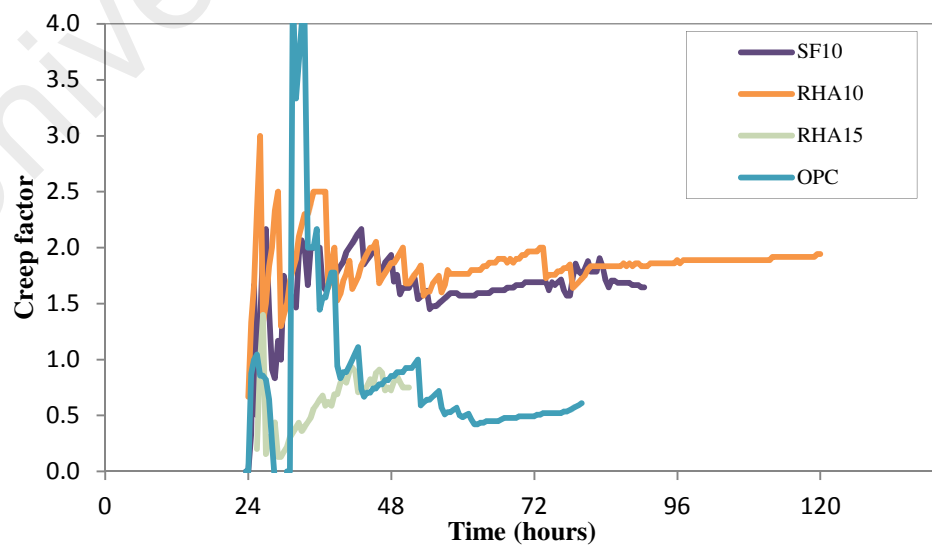


Figure 4.107: Early age creep factor

4.8.2.3 Effect of RHA on stress versus elastic strain

The results of induced tensile stress versus the cumulative elastic strain are presented in Figure 4.108. All concretes in this study showed the slope increasing almost constantly. The SF10 and OPC concrete showed the higher strain compared to RHA10 and RHA15 concrete. Even the RHA10 and the RHA15 concrete reached similar strain, the RHA15 occurred cracks earlier and RHA10 concrete did not showed cracks up to 144 h. The RHA 15 concrete experienced the cracks earlier than RHA10 concrete. It could be the RHA15 concrete experienced drying shrinkage up to 24 hours which mean concrete had residual stress. The lower stiffness of RHA10 and RHA15 concrete was likely due to slower reaction of RHA concrete than OPC concrete. The SF10 concrete showed higher stiffness than OPC and RHA concrete. However, after 50 hours, it increased strain from 60 $\mu\epsilon$ up to 120 $\mu\epsilon$ s but the tensile stresses were constant, which means the SF10 concrete experienced the creep. It could be the crack of SF10 concrete was delayed for a while.

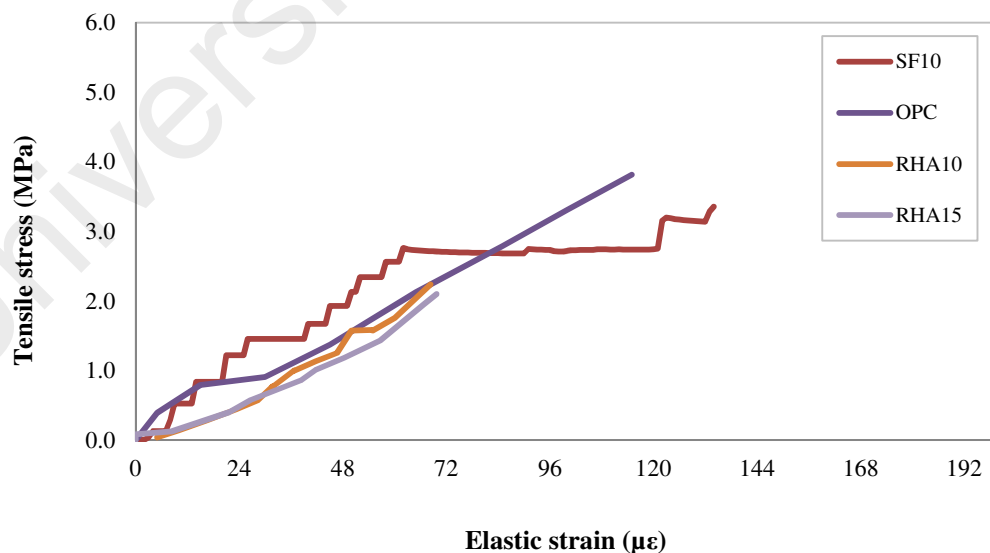


Figure 4.108: Stress versus strain in drying conditions

4.8.2.4 Effect of RHA on tensile strength

The tensile stresses developed in the restrained samples are shown in Figure 4.109. The tensile stress developed at early age was substantial, and led to fracture of all restrained specimens. The time to fracture varied from one mixture to another. The failure of RHA15 concrete occurred was earlier than RHA10 concrete and it means that the percentage of RHA in the mixture was affected to drying shrinkage. This behavior was primarily due to the high rate of shrinkage in the mixtures, which led to a rapid stress development. The indirect tensile strength development for the concrete mixes is also presented in Figure 4.110. To make easier to compare between the direct tensile stress and indirect tensile strength, the predicted tensile strength was modelled by regression analysis by utilizing the tensile strength of concrete at 1, 3 and 7 days. The following empirical relations were found reasonable to fit the data.

$$\text{OPC} \quad \sigma_{st} = 2.4435 t^{0.2080} \quad R^2 = 0.9952 \quad \text{Eq. (21)}$$

$$\text{RHA10} \quad \sigma_{st} = 2.1620 t^{0.2305} \quad R^2 = 0.9801 \quad \text{Eq. (22)}$$

$$\text{RHA15} \quad \sigma_{st} = 1.0370 t^{0.3502} \quad R^2 = 0.9877 \quad \text{Eq. (23)}$$

$$\text{SF10} \quad \sigma_{st} = 1.6607 t^{0.2762} \quad R^2 = 0.9989 \quad \text{Eq. (24)}$$

Where σ_{st} is the split tensile strength in MPa and t is the age in hours.

All RHA concretes showed lower tensile strength values compared to the control mix. The results showed that the tensile strength consistently reduced with increasing RHA content. As compared to the control mix at crack occurred, the 0 %, 10%, 15% RHA and 10% SF concrete resulted in 0.51%, 37%, 42%, 56% reductions in tensile strength, respectively. It seems that additions of 10% RHA into mixture cause

significant reductions to direct tensile strength of concrete. The restrained stress and age at cracking are presented in Table 4.64.

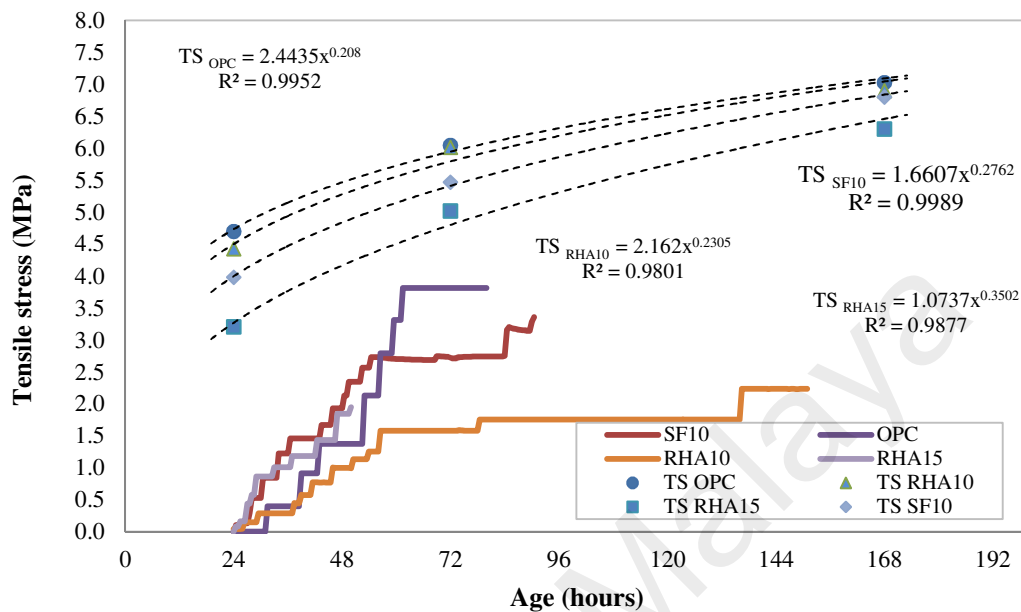


Figure 4.109: Tensile stress (σ_t) and tensile strength evolution with time

Table 4.64: Expansion and shrinkage stress and age of cracking

MixID	Maximum stress (MPa), σ_t^a	Age of cracking (hours)	f_t^b (MPa)	σ_t / f_t
OPC	3.12	80	6.15	0.51
RHA10	2.23	Did not fail after 160 h	6.0	0.37
RHA15	2.06	55	4.92	0.42
SF10	3.29	90	5.92	0.56

σ_t^a = Maximum tensile stress at failure ; f_t^b = Splitting tensile strength

Figure 4.110 presents the development of tensile stress and splitting tensile strength for each concrete. All RHA concretes showed lower splitting tensile strength development compared with the OPC concrete. The tensile stresses were expected to exceed the tensile strength at the time of cracking. As expected, the tensile stress measured at the time of cracking was found to be consistently smaller than the tensile strength measured from the split cylinder tests. The ratio of tensile stress at the time of cracking to the indirect tensile strength found from split strength test ranges between

0.45 and 0.55 as explained before. As, the ratio of the RHA10 showed below 0.45, it did not experience crack up to 144 hours. The OPC and SF10 and RHA15 concrete experienced the high stress ratio at early age. At 30 h, the ratios of tensile stress and tensile strength of the OPC, SF 10 and RHA15 concrete were 0.2, 0.22 and 0.25 meanwhile that ratio for RHA10 was 0.05. The high stress at early age suggested that permanent damage at micro level had occurred.

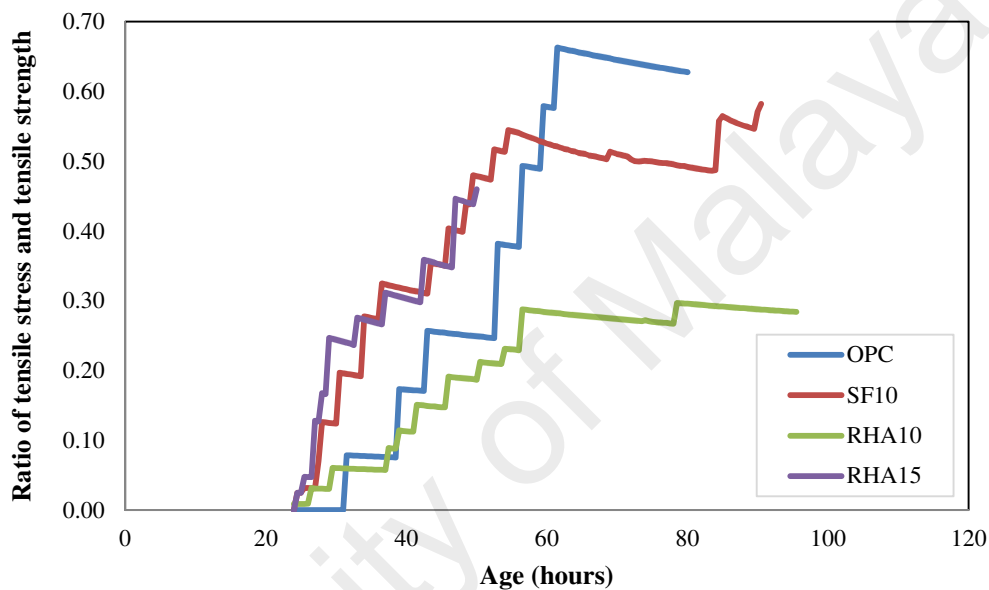


Figure 4.110: Ratio of tensile stress and tensile strength with time

4.8.2.5 Effect of RHA on modulus of elasticity of direct tensile

The development of elastic modulus for mixes related to ageing is presented in Figure 4.111. At the early age, the OPC concrete showed the elastic modulus measurement decrease after the initial measurement compared to RHA10, RHA15 and SF10 concrete. At beginning the OPC concrete experienced the swelling higher than other concretes. In this case the concrete was experiencing the compression and in this case it was avoided. The strain of OPC concrete at early age was relatively low and the stress was relatively higher than other concrete. The initial measurement represented the initial tangent modulus of elasticity, which expected higher than tangent or secant modulus. The RHA10, RHA15 and SF10 concrete experienced relatively lower

swelling than OPC concrete at early age. The initial modulus of those concrete tend to increase up to 48 hours and then level out or begin to increase slightly over 130 hours for RHA10 concrete. The other concrete did not record the strain due to having a crack below 100 hours.

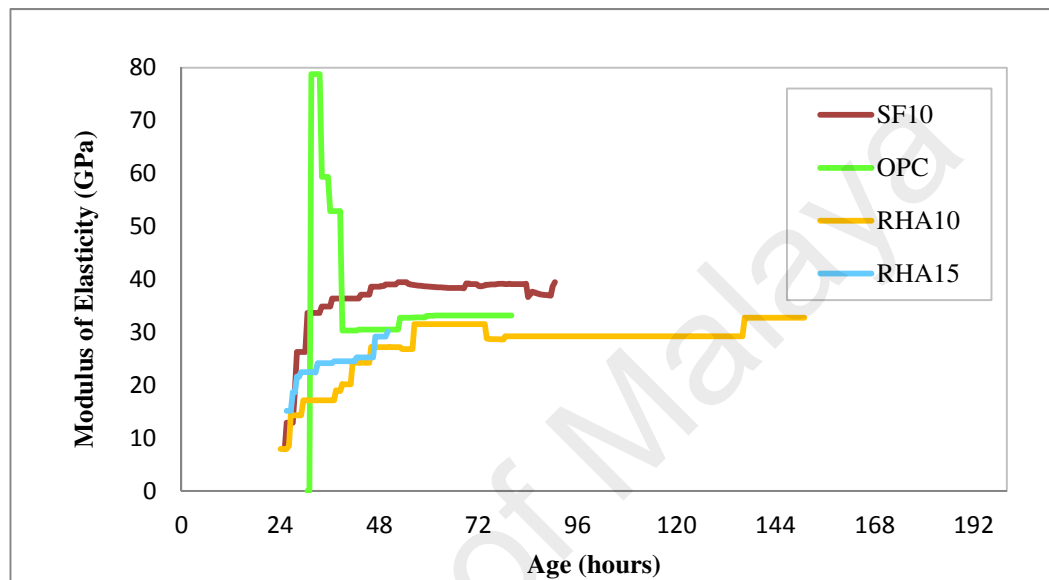


Figure 4.111: Modulus of elasticity of HPC at early age

4.9 Cost Analysis

As results from this study, it is found out that RHA can be used in producing HPC with compressive strength 100 MPa and the results is compatible with silica fume. The high price of silica fume is the reason that RHA is proposed as alternative replacement of silica fume. In this section the cost analysis for replacement silica fume with RHA is presented, see Table 4.65. The mix proportion used to compare the cost of 1 m³ concrete is similar. It was compared between 10% replacement of RHA and SF with cement in w/b of 0.25. Cost analysis of the materials used had been analyzed as per the purchased price from the market (as of February 2015).

Table 4.65: Comparison of cost analysis of OPC, RHA and Silica fume concrete

Ingredients	Unit cost (RM)	OPC concrete		RHA concrete		Silica fume concrete	
		Quantity	Amount (RM)	Quantity	Amount (RM)	Quantity	Amount (RM)
Water (l)	0.01	137.5	1.375	137.5	1.375	137.5	1.375
Cement (kg)	0.5	550	275	495	247.5	495	247.5
RHA (kg)	1	0	0	55	55	0	0
SF (kg)	3	0	0	0	0	55	165
Fine Agg. (kg)	0.05	690	34.5	690	34.5	690	34.5
Coarse Agg. (kg)	0.05	1050	52.5	1050	52.5	1050	52.5
Sp (l)	1	2.1	2.1	3.49	3.49	3.13	3.13
Total			365.5		394.4		504
Comp strength at 28 days (MPa)			103.5		113.2		100
Ratio Strength/Cost (MPa/RM)			0.28		0.29		0.20

The economic analysis reveals that the target mean strength of HPC is achieved in 28 days after replacing 10% of cement by RHA from the designed mix proportion of HPC. The ratio of strength to cost also show that RHA concrete has the highest ratio than that of control and silica fume concrete Thus, an obvious recommendation can be put forwarded to use HPC incorporating RHA as a supplement of SF. This is seen from the above cost analysis and which certainly confirms the reduction in the cost of construction of HPC grade 100 RHA concrete by about higher 8 % than that of the OPC and lower 27.8 % than that of the SF concrete.

CHAPTER 5: CONCLUSIONS AND RECOMMENDATIONS

5.1 Conclusions

5.1.1 Properties of RHA, aggregate blends and mixing method

1. The average particle size of RHA adopted in this study was 13 μm instead of 9.5 μm as they were insignificant difference in compressive strength of mortar.
2. The optimum fine aggregate/total aggregate (fa/ta) ratio was 0.45 and its packing density was 0.699 based on Modified Toufar Method.
3. Two steps mixing (TSM) is the suitable mixing method for producing HPC incorporating RHA compared to conventional mixing method.

5.1.2 Statistical models

1. Forty six (46) HPC mixes were prepared with varying water to binder (W/b) ratio, binder content, RHA content, the ratio of fa/ta and percentages of superplasticizer dosage.
2. Strong correlations were observed between variables adopted and the hardened properties of HPC. R^2 for predicting the slump, 1 day and 28 day-compressive strength are 0.9943, 0.9810 and 0.9858, respectively.

5.1.3 The mechanical properties of HPC

1. The hardened properties of HPC were improved with lower W/b ratio.
2. All hardened properties of HPC were improved in the presence of RHA up to 20% replacement.
3. In case of 10% RHA, the combined effect of the pozzolanic reaction and the micro filling ability resulted in higher UPV values compared to the 20% RHA concrete.
4. The compressive strength of the blended concrete with RHA was highest at 10% replacement for cement.

5. At 20% replacement and early age, RHA concrete provided lower values of compressive, splitting tensile and flexural strengths, modulus of elasticity and ultrasonic pulse velocity.
6. The compressive strength of the blended concrete with RHA was highest at 10% replacement of cement.
7. Replacing up to 20% would not adversely affect the strength and mechanical properties at later age.

5.1.4 The durability of RHA concrete

1. The porosity of RHA and SF concrete is influenced by age, w/b, RHA replacement and curing method.
2. The effect of curing on porosity of RHA concrete is significant at later age.
3. The RHA concrete is less porous than that of OPC but insignificant different that of SF10.
4. The initial surface absorption value of RHA concrete was lower than that of OPC concrete.
5. The relationship of ISA value and compressive strength of concrete is existed as the compressive strength increase as ISA value decrease, vice versa.
6. The sorptivity of RHA concrete was lower than that of OPC concrete and it reduces as the period of curing increase.
7. The effects of sulphate attack on compressive strength of RHA10 and RHA15 concrete show better than that of OPC concrete.

5.1.5 Time dependent properties

1. The drying shrinkage in term of deformation in length of RHA concrete was higher compared to that of OP concrete.

2. The effect of water curing for 7 days on drying shrinkage was significant as RHA concrete with initial water curing exhibited less shrinkage than that of air drying after casting.
3. The curing affected to shrinkage in RHA concrete.
4. Compared to other concretes, the crack of the RHA10 concrete due to restrained shrinkage at early age was delayed.

5.2 Recommendations for Future Studies

Research is a continuing process. Once any concept is developed, it does not necessarily mean that this will remain true for all the time. Furthermore, due to the unavailability of equipment, some tests were not possible to accomplish in this research. For this reason, the development of HPC including RHA cannot claim its completeness. Hence, further research should be carried out to confirm the beneficial effects of RHA on several concrete properties and durability issues of HPC, and thus to encourage the use of RHA in concrete. The following recommendations are given for further research on HPC including RHA.

- a. The slump loss of fresh concrete containing different percentages and fineness of RHA should be investigated.
- b. The effect of LOI percentages on RHA should be investigated on water absorption, workability, strength and durability of HPC.
- c. The effects of various curing conditions on the hardened properties and durability of HPC incorporating RHA should be investigated.
- d. The effect maximum size of aggregate in RHA concrete on workability, strength and durability should be investigated.

- e. The effects of RHA on the various time dependent properties of HPC such as autogenous shrinkage and creep should be examined.
- f. The effects of RHA on the durability performance of HPC regarding freezing and thawing, corrosion, alkali-aggregate reaction, acid attack, and carbonation should be investigated.
- g. The predicting model developed in this study was used for HPC including RHA for w/b of 0.22 up to 0.28; it should be employed to determine the mixture proportions of other w/b to wide range of its applicability.
- h. The effect of elevated temperature on RHA concrete should be investigated for future research.
- i. Restrained shrinkage at early age due to autogenous should be investigated.

REFERENCES

- ACI-363. (1984). State of the Art Report on High-Strength Concrete *Paper presented at the ACI Journal Proceedings*.
- ACI-363. (2002). High strength concrete: State-of-the art report *Manual of Concrete Practice-Part 5 (ACI 363R)*. Farmington Hills, USA.
- ACI-363R. (1992). State-of-the-art report on high strength concrete. Detroit: ACI Committee Report.
- Afiniwala, S., Patel, I., & Patel, N. (2013). Effect of High Volume Fly ash on Rheological Properties of Self Compacting Concrete. *International Journal of Emerging Technology and Advanced Engineering*, 3(7).
- Agullo, L., Toralles-Carbonari, B., Gettu, R., & Aguado, A. (1999). Fluidity of cement pastes with mineral admixtures and superplasticizer—a study based on the Marsh cone test. *Materials and Structures*, 32(7), 479-485.
- Ahmad, S. H., & Shah, S. P. (1985). Structural properties of high strength concrete and Its Implications for precast prestressed concrete. *PCI Journal*, 30(6).
- Aïtcin, P. C. (2003). The durability characteristics of high performance concrete: a review. *Cement and Concrete Composites*, 25(4), 409-420.
- Aïtcin, P. C. (1992). *The use of superplasticizers in high performance concrete*. Paper presented at the High Performance Concrete: From material to structure, London.
- Aïtcin, P. C. (1997). *Sherbrooke mix design method*. Paper presented at the One Day Short Course on Concrete Technology/High Performance: Properties and Durability, Kuala Lumpur.
- Aïtcin, P. C. (1998). *High-Performance Concrete*. New York: E & FN Spon.
- Aïtcin, P. C. (2000). Cements of yesterday and today concrete of tomorrow - Review. *Cement and Concrete Research*, 30, 1349-1359.
- Aïtcin, P. C. (2001). The ingredients of high-performance concrete. *Concrete international*, 23, 20-21.

- Aitcin, P. C., & Neville, A. (1993). High-performance concrete demystified. *Concrete international*, 15(1), 21-26.
- Akasaki, J. L., Tashima, M. M., da-Silva, C. A. R., da-Silva, E. J., Barbosa, M. B., & Paya, J. (2005). Comparative Studies between the RHA amorphous and crystalline. *Materiales Compuestos*, 8, 1-8.
- Al-Amoudi, O. S. B., Al-Kutti, W. A., Ahmad, S., & Maslehuddin, M. (2009). Correlation between compressive strength and certain durability indices of plain and blended cement concretes. *Cement and Concrete Composites*, 31(9), 672-676.
- Al-Khalaf, M. N., & Yousif, H. A. (1984). Use of rice husk ash in concrete. *The International Journal of Cement Composites and Lightweight Concrete*, 6(4), 241-248.
- Aldahdooh, M., Bunnori, N. M., & Johari, M. M. (2013). Evaluation of ultra-high-performance-fiber reinforced concrete binder content using the response surface method. *Materials & Design*, 52, 957-965.
- Alqadia, A. N. S., Mustapha, K. N. B., Naganathan, S., & Al-Kadi, Q. N. S. (2013). Development of self-compacting concrete using contrast constant factorial design. *Journal of King Saud University - Engineering Sciences*, 25(2), 105-112.
- Alsadey, S. (2012). Influence of superplasticizer on strength of concrete. *IJRET*, 1, 2277-4378.
- Altoubat, S. A., & Lange, D. A. (2001). Creep, shrinkage, and cracking of restrained concrete at early age. *ACI Materials Journal*, 98(4).
- Aly, T., Sanjayan, J., & Collins, F. (2008). Effect of polypropylene fibers on shrinkage and cracking of concretes. *Materials and Structures*, 41(10), 1741-1753.
- Arioglu, N., Girgin, Z. C., & Arioglu, E. (2006). Evaluation of ratio between splitting tensile strength and compressive strength for concretes up to 120 MPa and its application in strength criterion. *ACI Materials Journal*, 103(1).
- ASTM-C29/C29M. (2004). Standard test method for bulk density ("unit weight") and voids in aggregate *Annual Book of ASTM Standards*. Philadelphia, USA: American Society for Testing and Materials.
- ASTM-C109. (2007). Standard Specification for Compressive Strength of Mortars *Annual Book of ASTM Standards*. Philadelphia, USA: American Society for Testing and Materials.

- ASTM-C127. (2004). Standard test method for density, relative density (specific gravity), and absorption of coarse aggregate *Annual Book of ASTM Standards*. Philadelphia, USA: American Society for Testing and Materials.
- ASTM-C128. (2004). Standard test method for density, relative density (specific gravity), and absorption of fine aggregate *Annual Book of ASTM Standards*. Philadelphia, USA: American Society for Testing and Materials.
- ASTM-C150. (2004). Standard Specification for Portland Cement. *Annual Book of ASTM Standards*. Philadelphia, USA: American Society for Testing and Materials.
- ASTM-C494. (2004). Standard specification for chemical admixtures for concrete. *Annual Book of ASTM Standards*. Philadelphia, USA: American Society for Testing and Materials.
- ASTM-C531. (1985). Standard Test Method for Linear Shrinkage and Coefficient of Thermal Expansion of Chemical-Resistant Mortars, Grouts, Monolithic Surfacing, and Polymer Concretes. Philadelphia, USA: American Society for Testing and Materials.
- Auta, M., & Hameed, B. (2011). Optimized waste tea activated carbon for adsorption of Methylene Blue and Acid Blue 29 dyes using response surface methodology. *Chemical Engineering Journal*, 175, 233-243.
- Baalbaki, W., Benmokrane, B., Chaallal, O., & Aitcin, P.-C. (1991). Influence of coarse aggregate on elastic properties of high-performance concrete. *ACI Materials Journal*, 88(5).
- Basheer, L., Kropp, J., & Cleland, D. J. (2001). Assessment of the durability of concrete from its permeation properties: a review. *Construction and Building Materials*, 15(2), 93-103.
- Bazant, Z. P., & Kim, J. K. (1991). Improved prediction model for time-dependent deformations of concrete: Part 2-Basic creep. *Materials and Structures*, 24(144), 409-421.
- Bektas, F., & Bektas, B. A. (2014). Analyzing mix parameters in ASR concrete using response surface methodology. *Construction and Building Materials*, 66, 299-305.
- Bentz, D. P. (2010). Blending different fineness cements to engineer the properties of cement-based materials. *Magazine of concrete research*, 62, 327-338.

- Bonikowsky, D. A., Cumming, N. A., Dolen, T. P., Ford, J. H., Fratianni, J. J., Reading, T. J., . . . Miller Jr, R. E. (1992). Guide to Consolidation of Concrete in Congested Areas. *ACI Structural Journal*, 89(5), 577-586.
- Bozkurt, N., & Yazicioglu, S. (2010). Strength and capillary water absorption of lightweight concrete under different curing conditions. *Indian Journal of Engineering and Material Sciences*, 17, 145-151.
- Brandt, A. M., & Kucharska, L. (1999). *Development in cement based composite*. Paper presented at the Int. Seminar on Extending Performance Concrete, Dundee, UK.
- Brauer, H., Ziolkowski, M., & Toepfer, H. (2014). Defect detection in conducting materials using eddy current testing techniques. *Serbian Journal of Electrical Engineering*, 11(4), 535-549.
- BS-882. (1992). Specification for aggregates from natural sources for concrete. London: British Standards Institution.
- BS-1881-5. (1970). Methods of testing hardened concrete for other than strength. London: British Standard Institution.
- BS-1881-111. (1983). Method of Normal Curing of Test Specimens (20 C Method) *British Standards Institution* (pp. 4). London.
- BS-1881-116. (1983). Testing concrete. Method for determination of compressive strength of concrete cubes. London: British Standards Institution.
- BS-1881-117. (1983). Method for determination of tensile splitting strength. London: British Standard Institution.
- BS-1881-118. (1983). Method for determination of flexural strength. London: British Standard Institution.
- BS-1881-121. (1983). Method of F determination of static modulus of elasticity in compression London: British Standard Institution.
- BS-1881-1377. (1990). Methods of test for soils for civil engineering purposes *British Standards Institution, London*.
- BS-3892. (1982). Part 1: Pulverised fuel ash for use as a cementitious component in structural concrete: British Standards Institution: London.

- Bui, D. D., Hu, J., & Stroeven, P. (2005). Particle size effect on the strength of rice husk ash blended gap-graded Portland cement concrete. *Cement and Concrete Composites*, 27(3), 357-366.
- Carrasquilio, R. L., & Nilson, A. H. (1981). *Properties of high strength concrete subject to short-term loads*. Paper presented at the ACI Journal Proceedings.
- Castro, P. F., & Carino, N. J. (1998). Tensile and nondestructive testing of FRP bars. *Journal of composites for construction*, 2(1), 17-27.
- Chandrasekhar, S., Satyanarayana, K. G., Pramada, P. N., & Raghavan, P. (2003). Review: Processing, Properties and Applications of Reactive Silica from Rice Husk- an Overview. *Journal of Materials Science*, 38, 3159 - 3168.
- Chang, P.-K. (2004). An approach to optimizing mix design for properties of high-performance concrete. *Cement and Concrete Research*, 34(4), 623-629.
- Chao-Lung, H., Le Anh-Tuan, B., & Chun-Tsun, C. (2011). Effect of rice husk ash on the strength and durability characteristics of concrete. *Construction and Building Materials*, 25(9), 3768-3772.
- Chen, C. T., & Struble. (2009). Influence of Mixing Sequence on Cement-Admixture Interaction. *ACI Materials Journal*, 106(6), 503-508.
- Chen, W., & Brouwers, H. J. H. (2008). Mitigating the effects of system resolution on computer simulation of Portland cement hydration. *Cement & Concrete Composites*, 30, 779-787.
- Chindaprasirt, P., & Rukzon, S. (2008). Strength, porosity and corrosion resistance of ternary blend Portland cement, rice husk ash and fly ash mortar. *Construction and Building Materials*, 22(8), 1601-1606.
- Chopra, D., & Siddique, R. (2015). Strength, permeability and microstructure of self-compacting concrete containing rice husk ash. *Biosystems Engineering*, 130, 72-80.
- Chopra, S. K., Ahluwalia, S. C., & Delhi, S. L. N. (1981). *Technology and manufacture of rice-husk ash masonry (RHAM) cement*. Paper presented at the Proceedings of ESCAP/RCTT Workshop on Rice-Husk Ash Cement.
- Cisse, I. K., & Laquerbe, M. (2000). Mechanical characterisation of filler sandcretes with rice husk ash additions: Study applied to Senegal. *Cement and Concrete Research*, 30, 13-18.

- Cochet, G., & Sorrentino, F. (Eds.). (1993). *Limestone filled cements: properties and uses* (Vol. 4). New Delhi, India: AB1 Book Pvt. Ltd.
- Collins, T. M. (1989). Proportioning high-strength concrete to control creep and shrinkage. *ACI Materials Journal*, 86(6).
- Cook, D. J., Hinczak, I., Jedy, M., & Cao, H. T. (1989). *The behavior of Slag Cement Concretes in Marine Environment- Chloride Ion Penetration*. Paper presented at the SP-114: Fly Ash, Silica Fume, Slag, and Natural Pozzolans in Concrete: Proceedings of the Third International Conference, Trondheim, Norway.
- Cordeiro, G. C., Filho, R. D. T., & Fairbairn, E. M. R. (2009). Use of ultrafine rice husk ash with high-carbon content as pozzolan in high performance concrete. *Materials and Structures*, 42, 983-992.
- Cordeiro, G. C., Filho, R. D. T., Tavares, L. M., & Fairbairn, E. (2008). Pozzolanic activity and fillers effect of sugar cane bagasse ash on Portland cement and lime mortars. *Cement and Concrete Composites*, 30(5), 410-418.
- Cordeiro, G. C., Filho, R. D. T., Tavares, L. M., Fairbairn, E. M. R., & Hempel, S. (2011). Influence of particle size and specific surface area on the pozzolanic activity of residual rice husk ash. *Cement & Concrete Composites*, 33, 529-534.
- Coutinho, J. S. (2003). The combined benefits of CPF and RHA in improving the durability of concrete structure. *Cement and Concrete Composites*, 25, 51-59.
- Cusson, D., & Hoogeveen, T. (2007). An experimental approach for the analysis of early-age behavior of high performance concrete structures under restrained shrinkage. *Cement Concrete Research*, 37, 200-209.
- Damtoft, J. S., Herfort, D., & Yde, E. (1999). *Concrete binders, mineral addition and chemical admixture: State of the art and challenges for the 21st century*. Paper presented at the Extending Performance of Concrete Structures, Dundee, UK.
- De Schutter, G., & Audenaert, K. (2004). Evaluation of water absorption of concrete as a measure for resistance against carbonation and chloride migration. *Materials and Structures*, 37(9), 591-596.
- De Sensale, G. R. (2006). Strength development of concrete with rice-husk ash. *Cement and Concrete Composites*, 28(2), 158-160.
- De Sensale, G. R., Ribeiro, A. B., & Gonçalves, A. (2008). Effects of RHA on autogenous shrinkage of Portland cement pastes. *Cement and Concrete Composites*, 30(10), 892-897.

- Del Viso, J. R., Carmona, J. R., & Ruiz, G. (2008). Shape and size effects on the compressive strength of high-strength concrete. *Cement and Concrete Research*, 38(3), 386-395.
- Dingyuan, F., & Liqun, F. (1989). Main meteorological problems of rice production and protective measures in China. *Int. J. Biometeorol*, 1(3), 1-6.
- Domone, P. L. J., & Soutsos, M. N. (1994). An approach to the proportioning of high-strength concrete mixes. *Concrete international*, 16(10), 26-31.
- Duval, R., & Kadri, E. (1998). Influence of silica fume on the workability and the compressive strength of high-performance concretes. *Cement and Concrete Research*, 28(4), 533-547.
- El-Dakroury, A., & Gasser, M. (2008). Rice husk ash (RHA) as cement admixture for immobilization of liquid radioactive waste at different temperatures. *Journal of Nuclear Materials*, 381(3), 271-277.
- FAOSTAT. (2013). Rice production. from <http://faostat.fao.org/site/567/DesktopDefault.aspx?PageID=567#ancor>
- Fennis, S. A. A. M., Walraven, J. C., & Nijland, T. G. (2008). *Measuring the packing density to lower the cement content in concrete*. London: Taylor & Francis Group.
- Fook, P. W. (2004). *Engineering properties and durability of superplasticized metakaolin concrete with different water/binder ratios*. (Master Thesis), University of Malaya, Kuala Lumpur, Malaysia.
- Funk, J. E., & Dinger, D. (2013). *Predictive process control of crowded particulate suspensions: applied to ceramic manufacturing*: Springer Science & Business Media.
- Gagne, R., Aïtcin, P. C., Pigeon, M., & Pleau, R. (1992). *Frost durability of high performance concretes*. Paper presented at the High Performance Concrete: From material to structure, London.
- Gambhir, M. L. (2006). *Concrete technology* (3rd ed.). New Delhi, India: Tata McGraw-Hill Publishing.
- Ganesan, K., Rajagopal, K., & Thangavel, K. (2008). Rice husk ash blended cement: assessment of optimal level of replacement for strength and permeability properties of concrete. *Construction and Building Materials*, 22(8), 1675-1683.

- Giaccio, G., de Sensale, G. R., & Zerbino, R. (2007). Failure mechanism of normal and high-strength concrete with rice-husk ash. *Cement and Concrete Composites*, 29(7), 566-574.
- Givi, A. N., Rashid, S. A., Aziz, F. N. A., & Salleh, M. A. M. (2010). Assessment of the effects of rice husk ash particle size on strength, water permeability and workability of binary blended concrete *Construction and Building Materials*, 24, 2145-2150.
- Goltermann, P., Johansen, V., & Palbøl, L. (1997). Packing of aggregates: an alternative tool to determine the optimal aggregate mix. *ACI Materials Journal*, 94, 435-443.
- Güneyisi, E., Gesoğlu, M., & Özbay, E. (2010). Strength and drying shrinkage properties of self-compacting concretes incorporating multi-system blended mineral admixtures. *Construction and Building Materials*, 24(10), 1878-1887.
- Güneyisi, E., Özturan, T., & Gesoğlu, M. (2005). A study on reinforcement corrosion and related properties of plain and blended cement concretes under different curing conditions. *Cement and Concrete Composites*, 27, 449-461.
- Güneyisi, E., Özturan, T., & Gesoğlu, M. (2005). A study on reinforcement corrosion and related properties of plain and blended cement concretes under different curing conditions. *Cement and Concrete Composites*, 27(4), 449-461.
- Habeeb, G. A., & Fayyadh, M. M. (2009). Rice husk ash concrete: the effect of RHA average particle size on mechanical properties and drying shrinkage. *Australian Journal of Basic and Applied Sciences*, 3(3), 1616-1622.
- Habeeb, G. A., & Fayyadh, M. M. (2009). Rice husk ash concrete: the effect of RHA average particle size on mechanical properties and drying shrinkage. *Australian Journal of Basic and Applied Sciences*, 3(3), 1616-1622.
- Habeeb, G. A., & Mahmud, H. B. (2010). Study on properties of rice husk ash and its use as cement replacement material. *Materials Research*, 13(2), 185-190.
- Hall, C. (1989). Water sorptivity of mortars and concretes: a review. *Magazine of Concrete Res*, 41(14), 51-61.
- Hallal, A., Kadri, E. H., Ezziane, K., Kadri, A., & Khelafi, H. (2010). Combined effect of mineral admixtures with superplasticizers on the fluidity of the blended cement paste. *Construction and Building Materials*, 24(8), 1418-1423.

- Hannant, D. J., Buckley, K. J., & Croft, J. (1973). The effect of aggregate size on the use of the cylinder splitting test as a measure of tensile strength. *Matériaux et Construction*, 6(1), 15-21.
- Hansen, W. (1987). Drying shrinkage mechanisms in Portland cement paste. *Journal of the American Ceramic Society*, 70(5), 323-328.
- Hansen, W., & Almudaiheem, J. A. (1987). Ultimate drying shrinkage of concrete--influence of major parameters. *ACI Materials Journal*, 84(3).
- Hayri, U. N., & Baradan, B. (2011). The effect of curing temperature and relative humidity on the strength development of Portland cement mortar. *Scientific Research and Essays*, 6(12), 2504-2511.
- Hinds, W. C. (2012). *Aerosol technology: properties, behavior, and measurement of airborne particles*: John Wiley & Sons.
- Huo, X. S., & Wong, L. U. (2006). Experimental study of early-age behavior of high performance concrete deck slabs under different curing methods. *Construction and Building Materials*, 20(10), 1049-1056.
- Hussain, R. R., & Ishida, T. (2011). Investigation of Volumetric Effect of Coarse Aggregate on Corroding Steel Reinforcement at the Interfacial Transition Zone of Concrete. *KSCE Journal of Civil Engineering*, 15(1), 153-160.
- Hwang, C. L., & Chandra, S. (1996). *The use of rice husk ash in concrete* Westwood, NJ William Andrew Publishing.
- Ibragimov, A. M. (1989). Effect of the maximum size of coarse aggregate on the main parameters of concrete. *Hydrotechnical Construction*, 23(3), 141-144.
- IS-13311. (1992). Standard Code of Practice for Non-Destructive Testing of Concrete: Part 1-Ultrasonic Pulse Velocity *Part I*. New Delh: Bureau of Indian Standards.
- Islam, M. N., Zain, M. F. M., & Maslina Jamil, M. (2012). Prediction of Strength and Slump of Rice Husk Ash Incorporated High-Performance Concrete. *Journal of Civil Engineering and Management*, 18(3), 310-317.
- Ismail, M. S., and Waliuddin, A.M. (1996). Effect of rice husk ash on high strength concrete. *Construction and Building Material*, 10, 521-526.
- Ismail, M. S., & Waliuddin, A. M. (1996). Effect of rice husk ash on high strength concrete. *Construction and Building Material*, 10, 521-526.

- Jauberthie, R., Rendell, F., Tamba, S., & Cisse, I. (2000). Origin of the pozzolanic effect of rice husks. *Construction and Building Materials*, 14(8), 419-423.
- Jeenu, G., Vinod, P., & Mangal, L. (2012). Packing characteristics of aggregates for High Performance Concrete. *International Journal of earth sciences and engineering*, 1424-1431.
- Jensen, M., & Hansen, P. F. (1996). Autogenous deformation and change of the relative humidity in silica fume-modified cement paste. *ACI Materials Journal*, 93(6).
- Juliano, B. O. (1985). Rice hull and Rice straw. St. Paul, Minesota: American Association of cereal Chemist
- Kala, F. (2013). Effect of Granite Powder on Strength Properties of Concrete *Research Inveny: International Journal Of Engineering And Science*, 2(12), 36-50.
- Kartini, & Mahmud, H. (2010). Absorption and permeability performance of Selangor rice husk ash blended grade 30 concrete. *Journal of engineering science and technology*, 5(1), 1-16.
- Khalaf, R. S. (1995). Technique of multi-step concrete mixing. *Material Structure*, 12 230- 234.
- Khaloo, R. A., & Kim, N. (1999). Effect of curing condition on strength and elastic modulus of lightweight high-strength concrete. *ACI Materials Journal*, 96, 485-490.
- Khan, S. U., Nuruddin, M. F., Ayub, T., & Shafiq, N. (2014). Effects of different mineral admixtures on the properties of fresh concrete. *The Scientific World Journal*, 2014.
- Kishore, R., Bhikshma, V., & Prakash, P. J. (2011). Study on strength characteristics of high strength rice husk ash concrete. *Procedia Engineering*, 14, 2666-2672.
- Kosmatka, S. H., Kerkhoff, B., & Panarese, W. C. (2002). *Design and control of concrete mixtures*. Skokie, IL, USA: Portland Cement Association.
- Kosmatka, S. H., & Panarese, W. C. (2002). *Design and control of concrete mixtures: Portland Cement Association*.
- Larrard, F. D. (1992). *Ultrafine particles for making very high strength concrete*. Paper presented at the High Performance Concrete: From material to structure, London.

- Laskar, A. I., & Talukdar, S. (2008). Rheological behavior of high performance concrete with mineral admixtures and their blending. *Construction and Building Materials*, 22, 2345-2354.
- Lawler, J. S., Connolly, J. D., Krauss, P. D., Tracy, S. L., Janney, W., & Ankenman, B. (2005). Supplementary Cementitious Materials to Enhance Durability of Concrete Bridge Decks *NCHRP Report for Project 18-08A* (pp. 1-90). Washington, DC: National Cooperative Highway Research Program.
- Le, H. T., Kraus, M., Siewert, K., & Ludwig, H.-M. (2015). Effect of macro-mesoporous rice husk ash on rheological properties of mortar formulated from self-compacting high performance concrete. *Construction and Building Materials*, 80, 225-235.
- Li, Y., Bao, J., & Guo, Y. (2010). The relationship between autogenous shrinkage and pore structure of cement paste with mineral admixtures. *Construction and Building Materials*, 24(10), 1855-1860.
- Long, A. E., Henderson, G., D., & Montgomery, F., R. (2001). Why assess the properties of near-surface concrete? *Construction and Building Materials*, 15(2), 65-79.
- Maeda, N., Wada, I., Kawakami, M., Ueda, T., & Pushpalal, G. K. D. (2001). *Chloride diffusivity of concrete incorporating rice husk ash*. Paper presented at the Fifth CANMET/ACI Int. Conf. Recent Advances in Concrete Technology, SP-200, Singapore.
- Mahmud, H. B., Chia, B. S., & Hamid, N. B. A. A. (1997). *Rice husk ash-an alternative material in producing high strength concrete*. Paper presented at the Int. Conf. on Engineering Material, Ottawa, Canada.
- Mahmud, H. B., Kaoy, Y. C., Hamid, N. B. A. A., & Zain, M. F. M. (2002). *Use of rice husk ash to produce high strength/high performance G80 concrete*. Paper presented at the 6th Int. Symp. On Utilization of High Strength/High Performance Concrete, Leipzig, Germany.
- Mahmud, H. B., Majuar, E., & Hamid, N. B. A. A. (2003). *Evaluation on the use of rice husk ash to produce Grade 80 concrete*. Paper presented at the Int. Conf. 5th Asia Pacific Structural Engineering and Construction (APSEC 2003), Johor Bahru, Malaysia.
- Mahmud, H. B., Majuar, E., Zain, M. F. M., & Hamid, N. B. A. A. (2005). Strength, durability and shrinkage of high-strength rice husk ash concrete. *ACI Special Publication*, 228.

- Mahmud, H. B., Malik, M. F., Kahar, R. A., Zain, M. F. M., & Raman, S. N. (2009). Mechanical Properties and Durability of Normal and Water Reduced High Strength Grade 60 Concrete Containing Rice Husk Ash. *Journal of Advanced Concrete Technology*, 7(1), 21-30.
- Makani, A., Vidal, T., Pons, G., & Escadeillas, G. (2010). *Time-dependent behaviour of high performance concrete: influence of coarse aggregate characteristics*. Paper presented at the EPJ Web of Conferences.
- Malhotra, V. M. (1976). *Testing hardened concrete: nondestructure methods*: American Concrete Institute Monograph Series.
- Mamlouk, M. S., Zaniewski, J. P., & Peng, X. (2006). *Materials for civil and construction engineers*. New Jersey: Pearson Prentice Hall.
- Marfisi, E., Burgoyne, C., Amin, M., & Hall, L. (2005). The use of MRI to observe the structure of concrete. *Magazine of concrete research*, 57(2), 101-109.
- Mazloom, M., & Hassanloo, A. (2009). *Effect of silica fume and superplasticizers on tensile strength of concrete* Paper presented at the 34th Conference on Our world in concrete and structures, Singapore.
- Mazloom, M., Ramezani-pour, A. A., & Brooks, J. J. (2004). Effect of silica fume on mechanical properties of high-strength concrete. *Cement & Concrete Composites*, 26(4), 347-357.
- Mazlum, S., & Uyan, M. (1992). *Strength of mortar made with cement containing rice husk ash and cured in sodium sulphate solution*. Paper presented at the 4th Int. Conf. On Fly Ash, Silica Fume, Slag and Natural Pozzolans in Concrete, SP-132, Istanbul, Turkey.
- Mbessa, M., & Péra, J. (2001). Durability of high-strength concrete in ammonium sulfate solution. *Cement and Concrete Research*, 31, 1227-1231.
- Meddah, M. S., & Tagnit-Hamou, A. (2009). Pore structure of concrete with mineral admixtures and its effect on self-desiccation shrinkage. *ACI Materials Journal*, 106(3).
- Meddah, M. S., Zitouni, S., & Belâabes, S. (2010). Effect of content and particle size distribution of coarse aggregate on the compressive strength of concrete. *Construction and Building Materials*, 24(4), 505-512.
- Meeks, K. W., & Carino, N. J. (1999). Curing of high-performance concrete: Report of the State-of-the-Art (pp. 181). Gaithersburg, Maryland: Building and Fire

Research Laboratory, National Institute of Standards and Technology (NISTIR 6295).

- Mehta, P. K. (1979). *The chemistry and technology of cement made from rice husk ash*. Paper presented at the Proc UNIDO/ESCAP/RCTT workshop on rice husk ash cements, Peshamar, Pakistan.
- Mehta, P. K. (1992). *Rice husk ash-a unique supplementary cementing material*. Paper presented at the Proceedings of the International Symposium on Advances in Concrete Technology, Athens, Greece.
- Mehta, P. K. (2002). Greening of the concrete industry for sustainable development. *Concrete international*, 24, 23-28.
- Mehta, P. K., & Aïtcin, P. C. (1990). Principles underlying production of high-performance concrete. *Cement, concrete and aggregates*, 12(2), 70-78.
- Mehta, P. K., & Aïtcin, P. C. (1997). *Microstructural basis of selection of material and mix proportion for high strength concrete*. Paper presented at the One Day Short Course on Concrete Technology/High Performance: Properties and Durability, Kuala Lumpur.
- Mehta, P. K., & Monteiro, P. (1993). Concrete: Structure, Properties and Materials. *Unpublished manuscript for revision of Mehta, PK and Monteiro, PJM Concrete: Structure, Properties, and Materials*.
- Mehta, P. K., & Monteiro, P. J. M. (1993). *Concrete: Structure, properties and material*. Englewood Cliffs, N.J: Practice Hall Inc., .
- Memeon, A. H., Radin, S. S., Zain, M. F. M., & Trottier, J. F. (2002). Effect of mineral and chemical admixtures on high-strength concrete in seawater. *Cement and Concrete Research*, 32, 373-377.
- Mindess, S., Young, F., & Darwin, D. (2003). *Concrete (2nd ed.)*. New Jersey, USA: Prentice-Hall.
- Mindess, S., Young, J. F., & Darwin, D. (2003). *Concrete*. New Jersey: Prentice Hall.
- Mohammed, M. H., Emborg, M., Pusch, R., & Knutsson, S. (2012). *Packing theory for natural and crushed aggregate to obtain the best mix of aggregate: Research and development*. Paper presented at the Proceedings of WASET International Conference on Civil and Construction Engineering, Stockholm, Sweden.

- Mokarem, D. W. (2002). *Development of concrete shrinkage performance specifications*. Virginia Polytechnic Institute and State University.
- Mokhtarzadeh, A., & French, C. (2000). Mechanical properties of high-strength concrete with consideration for precast applications. *ACI Materials Journal*, 97(2).
- Montgomery, D. C. (2005). *Design and Analysis of Experiments: Response surface method and designs*. New Jersey: John Wiley and Sons, Inc.
- Muga, H., Betz, K., Walker, J., Pranger, C., & Vidor, A. (2005). *Development of Appropriate and Sustainable Construction Materials*. Michigan, USA: Sustainable Futures Institute, Michigan Technological University.
- Myers, R. H., Montgomery, D. C., Vining, G. G., Borror, C. M., & Kowalski, S. M. (2004). Response surface methodology: a retrospective and literature survey. *Journal of quality technology*, 36(1), 53.
- Nehdi, M., Duquette, J., & Damatty, A. (2003). Performance of rice husk ash produced using a new technology as a mineral admixture in concrete. *Cement and Concrete Research*, 33, 1203-1210.
- Nehdi, M. L., & Sumner, J. (2002). Optimization of ternary cementitious mortar blends using factorial experimental plans *Materials and Structures*, 35, 495-503.
- Neville, A. M. (1995). *Properties of concrete*. England: Pitman Books Limited.
- Neville, A. M. (1996). *Properties of Concrete* (Vol. Fourth and Final Edition). New York: New York: J. Wiley.
- Neville, A. M., & Brooks, J. J. (1987). *Concrete technology*. England: Longman Scientific & Technical.
- Nili, M., Ehsani, A., & Shabani, K. (2010). *Influence of nano-SiO₂ and micro-silica on concrete performance*. Paper presented at the Proceedings Second International Conference on Sustainable Construction Materials and Technologies.
- Oluokun, F. A. (1991). Prediction of Concrete Tensile Strength from Its Compressive Strength: Evaluation of Existing Relations for Normal Weight Concrete. *ACI Materials Journal*, 88(3).

- Osbaeck, B., & Johansen, V. (1989). Particle size distribution and rate of strength development of Portland cement. *Journal of the American Ceramic Society*, 72(2), 197-201.
- Paya, P., Monzó, J., Borrachero, M. V., Mellado, A., & Ordoñez, L. M. (2001). Determination of amorphous silica in rice husk ash by rapid analytical method. *Cement and Concrete Research*, 31, 227-231.
- Pliskin, L. (1992). *High performance concrete-engineering properties and code aspects*. Paper presented at the High Performance Concrete: From material to structure, London.
- Poon, C. S., Shui, Z. H., Lam, L., Fok, H., & Kou, S. C. (2004). Influence of moisture states of natural and recycled aggregates on the slump and compressive strength of concrete. *Cement and Concrete Research*, 34(1), 31-36.
- Popovics, S. (1992). *Concrete materials: properties, specifications, and testing*: William Andrew.
- Punkki, J., Golaszewski, J., & Gjorv, O. E. (1996). Workability loss of high-strength concrete. *ACI Materials Journal*, 93(5).
- Rahman, M. A., Hasegawa, H., Rahman, M. M., Miah, M. A. M., & Tasmin, A. (2008). Arsenic accumulation in rice (*Oryza sativa* L.): Human exposure through food chain. *Ecotoxicology and Environmental Safety*, 69(2), 317-324.
- Ramezaniapour, A. A., Khani, M. M., & Ahmadibeni, G. (2009). The effect of rice husk ash on mechanical properties and durability of sustainable concretes. *Int. J. Civil Eng*, 7(2), 83-91.
- Rashid, M. A., Mansur, M. A., & Paramasivam, P. (2002). Correlation between mechanical properties of high-strength concrete. *Journal of Materials of Civil Engineering, ASCE*, 14 (3), 527-542.
- Rejeb, S. K. (1996). Improving compressive strength of concrete by a two-step mixing method. *Cement and Concrete Research*, 26(4), 585-592.
- Roberts, J. (2006). High Performance Concrete Enhancement Through Internal Curing. *Northeast Solite Corporation*, 55-59.
- Rukzon, S., Chindapasirt, P., & Mahachai, R. (2009). Effect of grinding on chemical and physical properties of rice husk ash. *International Journal of Minerals, Metallurgy and Materials*, 16(2), 242-247.

- Rupnow, T. D., Schaefer, V. R., Wang, K., & Hermanson, B. L. (2007). Improving Portland Cement Concrete Mix Consistency and Production Rate Through Two-Stage Mixing.
- Sabir, B. B., Wild, S., & O'farrell, M. (1998). A water sorptivity test for martar and concrete. *Materials and Structures*, 31(8), 568-574.
- Safiuddin, M. (2008). *Development of self-consolidating high performance concrete incorporating rice husk ash*. University of Waterloo.
- Safiuddin, M. (2008). *Development of self-consolidating high performance concrete incorporating rice husk ash*. University of Waterloo.
- Safiuddin, M., Islam, M. N., Zain, M. F. M., & Mahmud, H. B. (2009). Material aspects for high-strength high performance concrete. *International Journal of Mechanical and Materials Engineering*, 4(1), 9-18.
- Safiuddin, M., West, J. S., & Soudki, K. A. (2010). Hardened properties of self-consolidating high performance concrete including rice husk ash. *Cement and Concrete Composites*, 32(9), 708-717.
- Safiuddin, M., West, J. S., & Soudki, K. A. (2011). Flowing ability of the mortars formulated from self-compacting concretes incorporating rice husk ash. *Construction and Building Materials*, 25, 973-978.
- Saraswathy, V., & Song, H. (2007). Corrosion performance of rice husk ash blended concrete. *Construction and Building Materials*, 21, 1779-1784.
- Sari, M., Prat, E., & Labastire, J.-F. (1999). High strength self-compacting concrete original solutions associating organic and inorganic admixtures. *Cement and Concrete Research*, 29(6), 813-818.
- Sastry, M. R. L., Rao, K. S., & Rao, P. S. (2012). Material Aspects Of High Performance Concrete. *RSM International Journal of Engineering, Technology & Managemen*, 2, 12-21.
- Šelih, J., Sousa, A. C., & Bremner, T. W. (1996). Moisture transport in initially fully saturated concrete during drying. *Transport in porous media*, 24(1), 81-106.
- Sensale, G. R. g. d. (2006). Strength development of concrete with rice-husk ash. *Cement & Concrete Composites*, 28 158-160.

- Sereshti, H., Eskandarpour, N., Samadi, S., & Aliakbarzadeh, G. (2014). Investigation on *Dracaena Sanderiana* Phytoremediation Ability for Hg and Cd using Multivariate Optimized Task Specific Ionic liquid-based Dispersive liquid-liquid Microextraction. *International Journal of Environmental Research*, 8(4), 1075-1084.
- Shariq, M., Prasad, J., & Masood, A. (2013). Studies in ultrasonic pulse velocity of concrete containing GGBFS. *Construction and Building Materials*, 40, 944-950.
- Siddique, R. (2008). *Rice Husk Ash Waste Materials and By-Products in Concrete* (pp. 235-264): Springer.
- Simon, M. J. (2003). *Concrete Mixture Optimization Using Statistical Methods: Final Report* (pp. 53). McLean, VA: FHWA Office of Infrastructure Research and Development.
- Sobolev, K. (2004a). The development of a new method for the proportioning of high-performance concrete mixtures. *Cement and Concrete Composites*, 26(7), 901-907.
- Sobolev, K. (2004b). The development of a new method for the proportioning of high-performance concrete mixtures. *Cement & Concrete Composites*, 26, 901-907.
- Sobolev, K., Flores, I., Torres-Martinez, L. M., Valdez, P. L., Zarazua, E., & Cuellar, E. L. (2009). Engineering of SiO₂ nanoparticles for optimal performance in nano cement-based materials *Nanotechnology in construction 3* (pp. 139-148): Springer.
- Speare, P. R. S., Eleftheriou, K., & Siludom, S. (1999). *Durability of concrete containing rice husk ash as an additive*. Paper presented at the Int. Seminar on Exploiting Wastes in Concrete, Dundee, UK.
- Stroeven, P., Bui, D. D., & Sabuni, E. (1999). Ash of vegetable waste used for economic production of low to high strength hydraulic binders. *Fuel*, 78, 153-159.
- Sugita, S., Shoya, M., & Tokuda, H. (1992). *Evaluation of pozzolanic activity of rice husk ash*. Paper presented at the 4th Int. Conf. On Fly Ash, Silica Fume, Slag and Natural Pozzolans in Concrete, Istanbul, Turkey.
- Survey, U. S. G. (2012). Mineral Commodity Summaries. from <http://minerals.usgs.gov/minerals/pubs/commodity/cement/mcs-2012-cemen.pdf>

- Swamy, R. N., & Mahmud, H. B. (1986). *Mix proportions and strength characteristics of concrete containing 50 percent low-calcium fly ash*. Paper presented at the The 2nd Int. Conf. on Fly Ash, Silica Fume, Slag and Natural Pozzolans in Concrete, ACI SP-91.
- Tam, C. T. (2003). *Constituents and Properties of Concrete Civil Engineering Handbook*, : CRC Press LLC.
- Tao , Z., & Weizu, Q. (2006). Tensile creep due to restraining stresses in high-strength concrete at early ages. *Cement Concrete Research*, 36, 584-591.
- Tarek, A., & Sanjayan, J. G. (2008). Factors contributing to early age shrinkage cracking of slag concretes subjected to 7-days moist curing. *Materials and Structures*, 41(4), 633-642.
- Taylor, H. F. W. (1997). *Cement chemistry*. London: Thomas Telford.
- Tongaroonsri, S., & Tangtermsirikul, S. (2009). Effect of mineral admixtures and curing periods on shrinkage and cracking age under restrained condition. *Construction and Building Materials*, 23, 1050-1056.
- Toufar, W., Born, M., & Klose, E. (1976). Contribution of optimisation of components of different density in polydispersed particles systems. *Freiberger Booklet A*, 558, 29-44.
- Tregger, N., Ferrara, L., & Shah, S. P. (2008). Identifying viscosity of cement paste from mini-slump-flow test. *ACI Materials Journal*, 105(6).
- Tuan, N. V., Ye, G., Breugel, K. v., Fraaij, A. L. A., & Bui, D. D. (2011). The study of using rice husk ash to produce ultra high performance concrete. *Construction and Building Materials*, 25(4), 2030-2035.
- Turgut, P. (2004). Research into the correlation between concrete strength and UPV values. *NDT. net*, 12(12), 1-9.
- Van Tuan, N., Ye, G., Van Breugel, K., & Copuroglu, O. (2011). Hydration and microstructure of ultra high performance concrete incorporating rice husk ash. *Cement and Concrete Research*, 41(11), 1104-1111.
- Van, V.-T.-A., Rößler, C., Bui, D.-D., & Ludwig, H.-M. (2013). Mesoporous structure and pozzolanic reactivity of rice husk ash in cementitious system. *Construction and Building Materials*, 43, 208-216.

- Van, V. T. A., Rößler, C., Bui, D.-D., & Ludwig, H.-M. (2014). Rice husk ash as both pozzolanic admixture and internal curing agent in ultra-high performance concrete. *Cement and Concrete Composites*, 53, 270-278.
- Vanchai, S., Jaturapitakkul, C., & Chaiyanunt, R. (2010). Compressive Strength and Heat Evolution of Concretes Containing Palm Oil Fuel Ash. *Journal of Materials in Civil Engineering*, 22(10), 1033-1038.
- Vanchai, S., Jaturapitakkul, C., & Kiattikomol, K. (2007). Influence of pozzolan from various by-product materials on mechanical properties of high-strength concrete. *Construction and Building Materials*, 21(7), 1589-1598.
- Venkatanarayanan, H. K., & Rangaraju, P. R. (2015). Effect of grinding of low-carbon rice husk ash on the microstructure and performance properties of blended cement concrete. *Cement and Concrete Composites*, 55, 348-363.
- Vipulanandan, C., & Garas, V. (2008). Electrical resistivity, pulse velocity, and compressive properties of carbon fiber-reinforced cement mortar. *Journal of Materials in Civil Engineering*, 20(2), 93-101.
- Wada, I., Kawano, T., Kawakami, M., & Maeda, N. (2000). Effect of highly reactive rice husk ash on durability of concrete and mortar. *ACI Special Publication*, 192.
- Wang, P. H., Lin, K. S., Huang, Y. J., Li, M. C., & Tsaur. (1998). Synthesis of zeolite ZSM-48 from rice husk ash. *Journal of Hazardous Material*, 58, 147-152.
- Whiting, D. A., Detwiler, R. J., & Lagergren, E. S. (2000). Cracking tendency and drying shrinkage of silica fume concrete for bridge deck applications. *ACI Materials Journal*, 97(1).
- Wiegrink, K., Marikunte, S., & Shah, P. S. (1993). Shrinkage cracking of high-strength concrete. *ACI Mater Journal*, 93(5), 409-415.
- Wong, L. C. Y., Emrus, S. A., Bashir, B. M., & Teng, J. Y. S. (2010). *Malaysian padi and rice industry: application of supply chain management approach*. Paper presented at the The national rice conference, Swiss garden golf resort, Lumut.
- Wu, D. S., & Peng, Y. N. (2003). The macro- and micro properties of cement pastes with silica-rich material cured by wet-mixed steaming injection. *Cement and Concrete Research*, 33, 1331-1345.
- Xu, W., Lo, T. Y., & Memon, S. A. (2012). Microstructure and reactivity of rich husk ash. *Construction and Building Materials*, 29, 541-547.

- Yaqub, M., & Bukhari, I. (2006). *Effect of size of coarse aggregate on compressive strength of high strength concrete*. Paper presented at the 31st Conference on Our World in Concrete & Structures.
- Yen, T., Lai, C. P., Tang, J. W., & Huang, Y. L. (2000). Optimizing mix-proportions for flowable high performance concrete via mortar rheology. *Journal of the Chinese Institute of Engineers*, 23(1), 41-51.
- Yu, Q., Sawayama, K., Sugita, S., Shoya, M., & Isojima, Y. (1999). The reaction between rice husk ash and $\text{Ca}(\text{OH})_2$ solution and the nature of its product. *Cement and Concrete Research*, 29, 37-43.
- Zhang, M.-H., & Malhotra, V. M. (1996). High-performance concrete incorporating rice husk ash as a supplementary cementing material. *ACI Materials Journal*, 93(6).
- Zhang, M., Lastra, R., & Malhotra, V. (1996). Rice-husk ash paste and concrete: some aspects of hydration and the microstructure of the interfacial zone between the aggregate and paste. *Cement and Concrete Research*, 26(6), 963-977.
- Zhang, M. H., Lastra, R., & Malhotra, V. M. (1996). Rice-hush ash paste and concrete: Some aspects of hydration and the microstructure of the interfacial zone between the aggregate and paste. *Cement and Concrete Research*, 26, 963-977.
- Zia, P., Ahmad, S., & Leming, M. (1991). High-performance concrete: State-of-the art report (1989-1994) (pp. 251). Washington, D.C: Strategic Highway Research Program, National Research Council.
- Zingga, A., Winnefeld, F., Holzer, L., Pakusch, J., Becker, S., Figi, R., & Gauckler, L. (2009). Interaction of polycarboxylate-based superplasticizers with cements containing different C3A amounts. *Cement and Concrete Composites*, 31(3), 153-162.

LIST OF PUBLICATIONS AND PAPERS PRESENTED

Hilmi Bin Mahmud and **Syamsul Bahri**, 2011, Development of Sustainable High Performance Grade 100 Concrete Incorporating Rice Husk Ash, Proceeding of the 4th ASEAN Civil Engineering Conference, Yogyakarta, Indonesia

Syamsul Bahri, 2011, Effect of initial particle surface moisture mixing method (IPSM) on the workability and compressive strength of mortar 100 MPa, 2nd Aceh Development International Conference, UKM Bangi, Malaysia

S. Bahri, H. B. Mahmud, 2013, Rice Husk Ash – An Alternative Material to Silica Fume For Production Of 100 MPa Mortar, Electronic Journal of Structural Engineering 13(1), 31-35

Hilmi Bin Mahmud and **Syamsul Bahri**, 2013, Comparison of Two Mixing Methods for Producing 100 MPa High Performance Rice Husk Ash Concrete, New Developments in Structural Engineering and Construction, Yazdani, S. and Singh, A. (Eds.), ISEC-7, Honolulu, Hawaii

Hilmi Bin Mahmud and **Syamsul Bahri**, 2015, Production of High Strength High Performance 100 MPa Rice Husk Ash Concrete, The Sixth Jordanian International Civil Engineering Conference (JICEC06), Amman, Jordan

Mahmud, H., **Bahri, S.**, Yee, Y., Yeap, Y. (2016). 'Effect of Rice Husk Ash on Strength and Durability of High Strength High Performance Concrete'. World Academy of Science, Engineering and Technology, International Journal of Civil, Environmental, Structural, Construction and Architectural Engineering, 10(3), 375 - 380.

Ahmmad, R., Jumaat, M. Z., **Bahri, S.**, & Islam, A. S. (2014). Ductility performance of lightweight concrete element containing massive palm shell clinker. *Construction and Building Materials*, 63, 234-241.

Aprianti, E., Shafigh, P., **Bahri, S.**, & Farahani, J. N. (2015). Supplementary cementitious materials origin from agricultural wastes–A review. *Construction and Building Materials*, 74, 176-187.